GEM TN-91-000002

GEM Muon Meeting
SSCL

July 17, 1991

Abstract:
Transparencies and contributions to the Second Muon Meeting held at the SSC Lab on July 17, 1991.

7/24/91-KM

REVISED AGENDA FOR SECOND MUON MEETING SSCL JULY 17,1991

The focus of this meeting will be to plan the efforts for the initial period leading to an LOI at the end of the year, to understand the resources (financial, technical and personnel) needed in support of this effort, and to organize a simulation effort capable of evaluating the iterative steps to optimization of the detector.

For each of the major detector efforts, for the support and alignment efforts, as well as for the magnet, we expect to hear reports on the current design status, the short (6 mo) term goals and critical issues, longer term goals (to Design Report at end of 92), the level of effort currently involved, and the resources needed to execute these plans. These reports should be concise and brief to allow time for discussion.

WE will also have discussions on test beam efforts, now and in the forseeable future. The trigger effort will be discussed with a view towards supplying requirements for the detector hardware.

AGENDA JULY 17 SSCL

8:30 AGENDA.....M.MARX
8:45 MAGNET.....LLNL,MITPFC,GD (Johnson,Marsden...)
Baseline,options,R&D needs
9:30 DETECTOR OPTIONS - Status,Goals,Needs.....15 min each
PDT/LST.....Zhou
LST.....Osborne
Pads.....Polychronakis
L*.....Fackler/Grinnell
PDT/Straws.....Bromberg
10:45 TRIGGER/ELECTRONICS.....Bolton
Scintillators.....Marlow
11:15 TEST BEAM.....Osborne,Weinstein,....
11:30 REPORT ON CERN MUON MEETING.....(Polychronakis,Mohammadi..
.....LUNCH.....
1:00 DETECTOR SUPPORT & ALIGNMENT - Status & Needs....Grinnell,JOhnson, Nimbleff
1:30 SIMULATION TOOLS.....10 min each
GEANT.....Bolton
3D Tracing.....diGiacomo
Resolution.....Rosenson
Cost/Performance Parametrization.....Deis
Magnetic Field.....(LLNL,MITPFC...?)
Punchthrough.....McNeil
3:00 DISCUSSION OF PLANS ...Magnet,Detectors,Trigger
Emphasis on design of forward (eta>1.5) regions
Effects of B field on Resolution.....Zhou

Momentum measurement

Consider multiple scattering + measurement error

- If measurement error dominates, then:

  1:2:1 is best solution for fixed no. of measurements

- If multiple scattering dominates, then this is not so!

- In 2nd Detector, which of these dominates depends on momentum

(Remainder is for $\eta = 0$).

<u>Geometry</u>

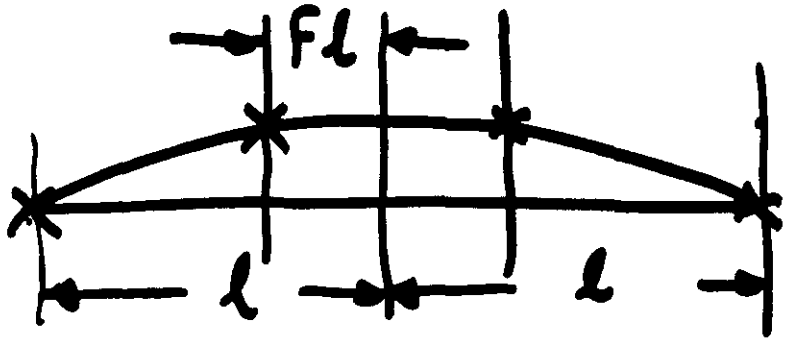

Measurement error per measurement $= \sigma$

Multiple scattering angle per measurement $= \epsilon$

$$\frac{dp}{p} = \frac{2\sqrt{\sigma^2 + \frac{\theta^2 l^2}{2}(1-f)^2}}{1-f^2} \cdot \frac{p}{0.3Bl^2}$$

There is an optimum value of f for a given $\frac{\theta^2 l^2}{2\sigma^2}$.

Compare with 'classical' 1:2:1

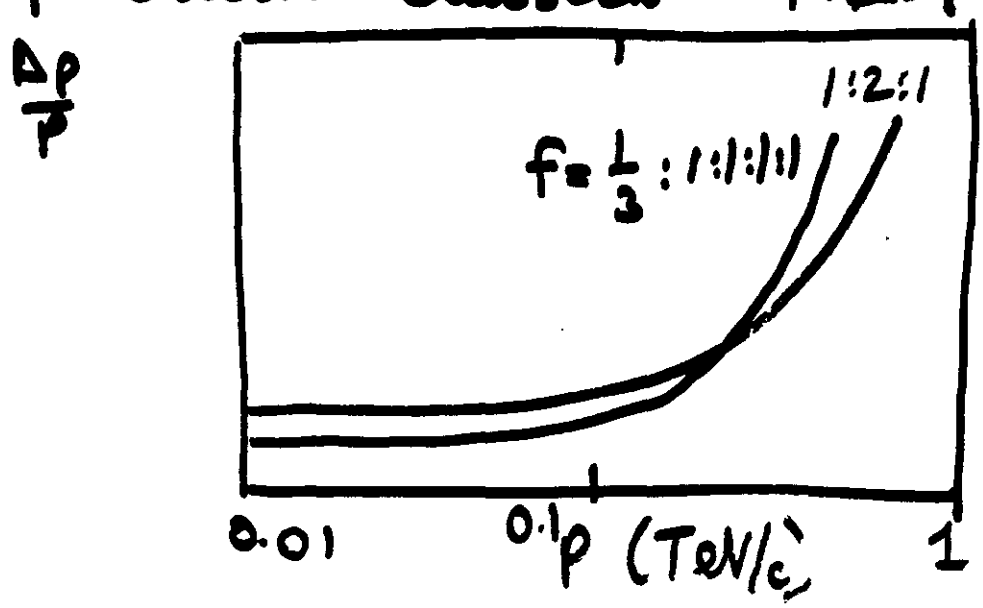

Describe in terms of 1. low-momentum rates

2. high- " "

3. Crossover momentum.

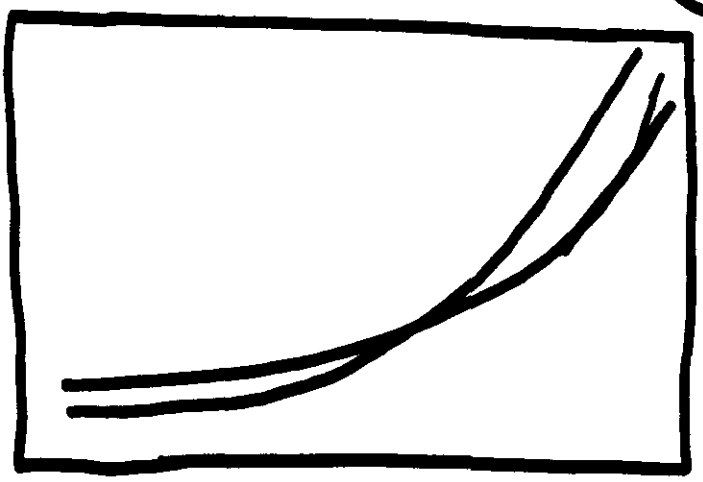

For Ahlen proposal

$\sigma = 50\mu m$, $L/X_0 = 0.07$, $l = 1.7m$

f	Crossover p GeV/c	low-p rates $1/1+f$	high-p rates $1/1-f^2$
→ 0.05	383	0.95	1.003
0.1	259	0.91	1.01
0.2	165	0.93	1.04
0.3	119	0.77	1.10
0.333	108.	0.75	1.13
0.4	89.1	0.71	1.19

May be pattern recognition advantage?

Multiple scatt. only

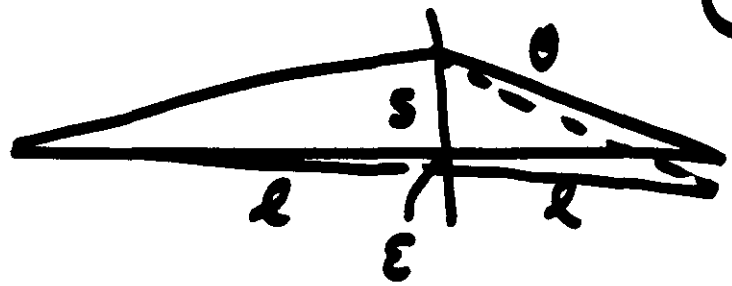

$$s = \frac{\ell^2}{2R}$$

$$\varepsilon = \frac{1}{2}\theta\ell$$

$$\frac{\Delta p}{p} \sim \frac{\varepsilon}{s} \propto \frac{\theta}{\ell} \quad \text{for fixed } p$$

Compare:

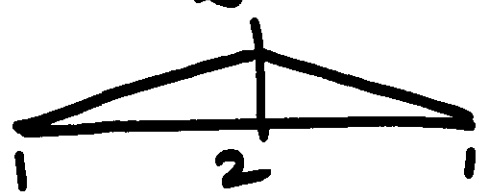

with:

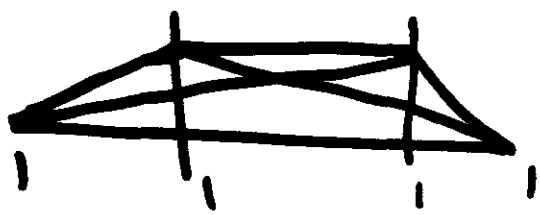

2nd case 2 measurements: $\times \frac{1}{\sqrt{2}}$

ℓ by $2/3$: $\times \frac{3}{2}$

θ by $1/\sqrt{2}$: $\frac{1}{\sqrt{2}}$

So factor is $3/4$

Alex Marin / B.U.
07/17/91
SSCL

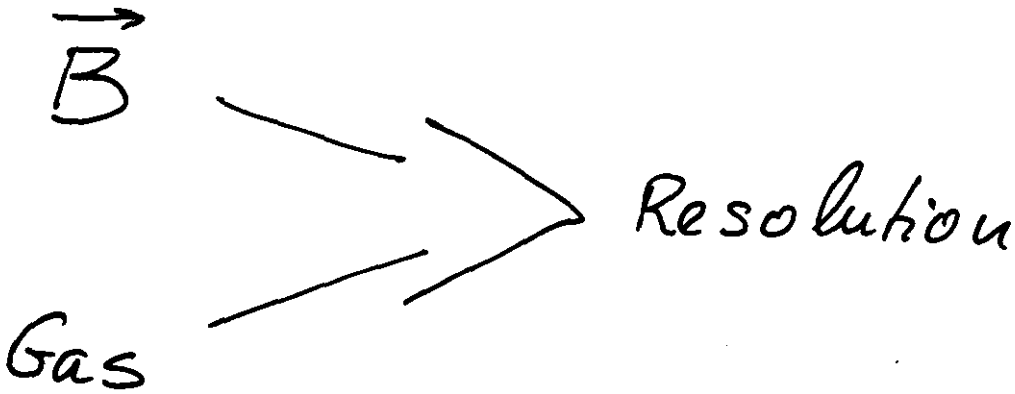

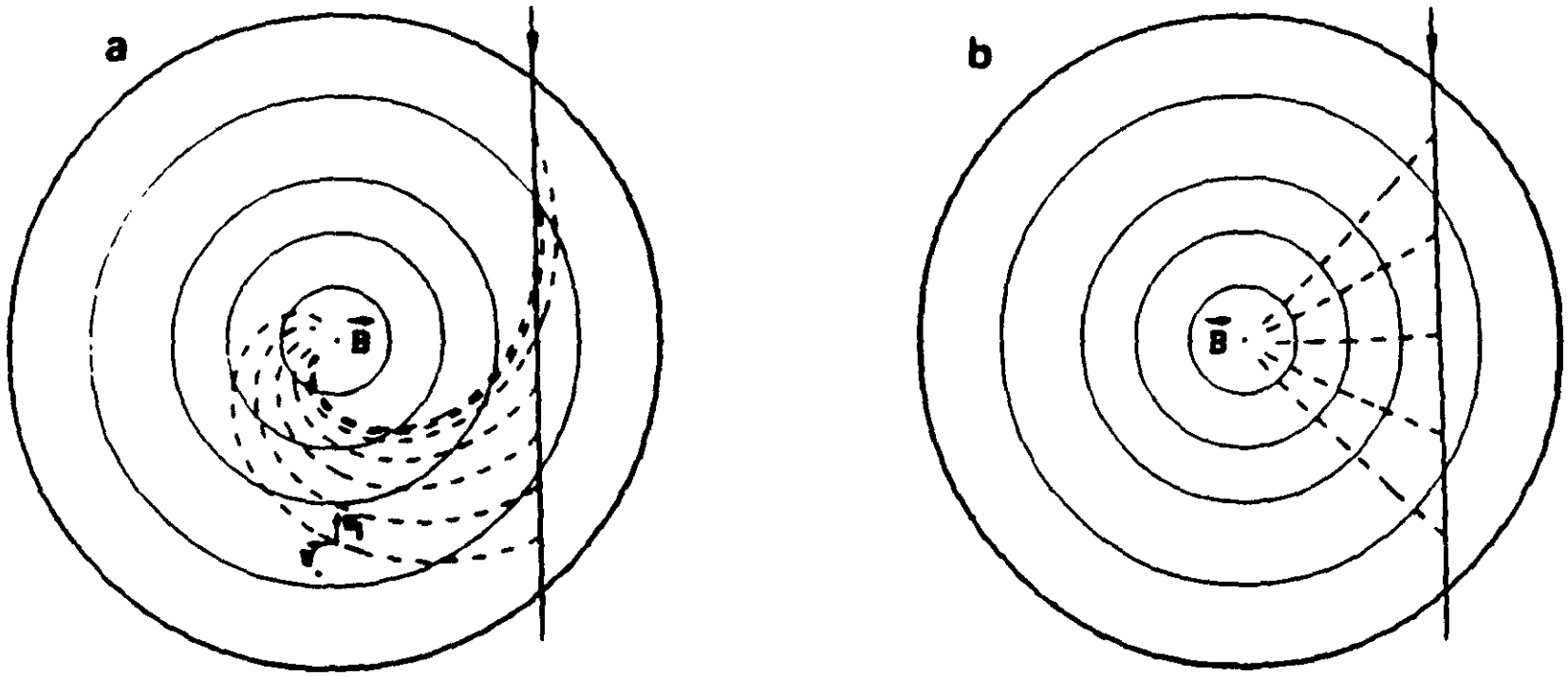

Fig. 8. Electron drift trajectories (dashed lines) in a 1 in. diameter drift tube at 15 kG B-field. The solid line with the arrow is the particle track and the thin solid circles inside the tube represent the E-field potentials. (a) for 50–50 argon–ethane gas. (b) for DME gas.

Basic Performance of drift tube in B-field:

Drift velocity and Lorentz angle :

$$E_{field} = HV_{wire}/r/Ln(b/a)$$
$$V_0 = k(eE/m)\tau \sim f(E,k,\tau)$$

$B=0$

$$V_r = V_0 \times (1+(\omega_r\tau)^2)/(1+(\omega\tau)^2)$$
$$V_T = V_0 \times (\omega_z\tau + \omega_r\omega_T\tau^2)/(1+(\omega\tau)^2)$$
$$V_z = V_0 \times (\omega_T\tau + \omega_r\omega_z\tau^2)/(1+(\omega\tau)^2)$$

$B \neq 0$

$$\omega_c(\omega_r,\omega_T,\omega_z) = eB/mc = e/mc \times (B_r, B_T, B_z)$$
$$tan\theta_{Lorentz} = \omega\tau$$

$$\text{Drifttime(r)} = \int_a^r dr'/V_r(r')$$

Experimental data needed for space-time function:

1) Accurate magnetic field map and wire high voltage;

2) Drift velocity vs. electric field for used drift gas;

3) Lorentz angle vs. E-field and B-field for used drift gas.

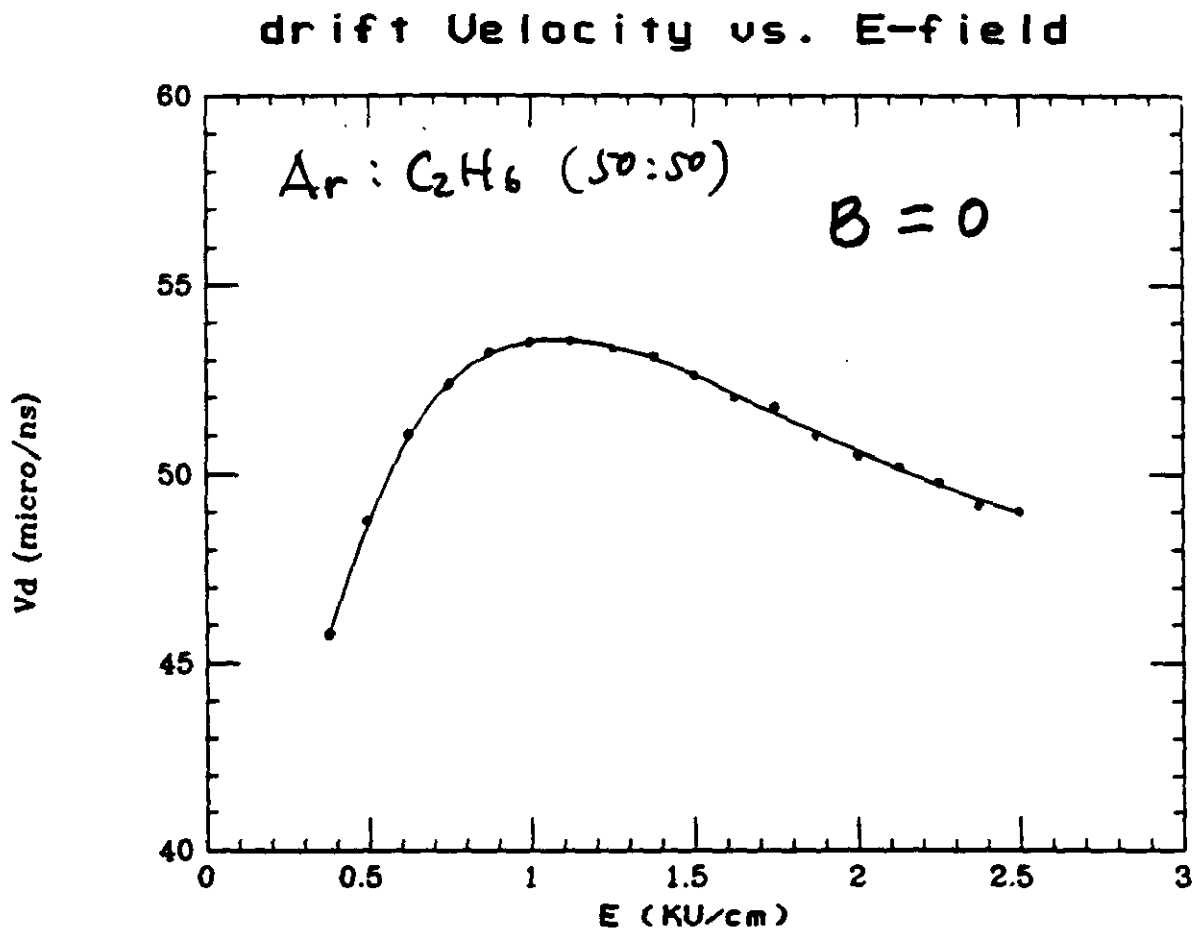
drift Velocity vs. E-field
Ar : C2H6 (50:50)
B = 0
Vd (micro/ns)
60
55
50
45
40
0
0.5
1
1.5
2
2.5
3
E (KU/cm)

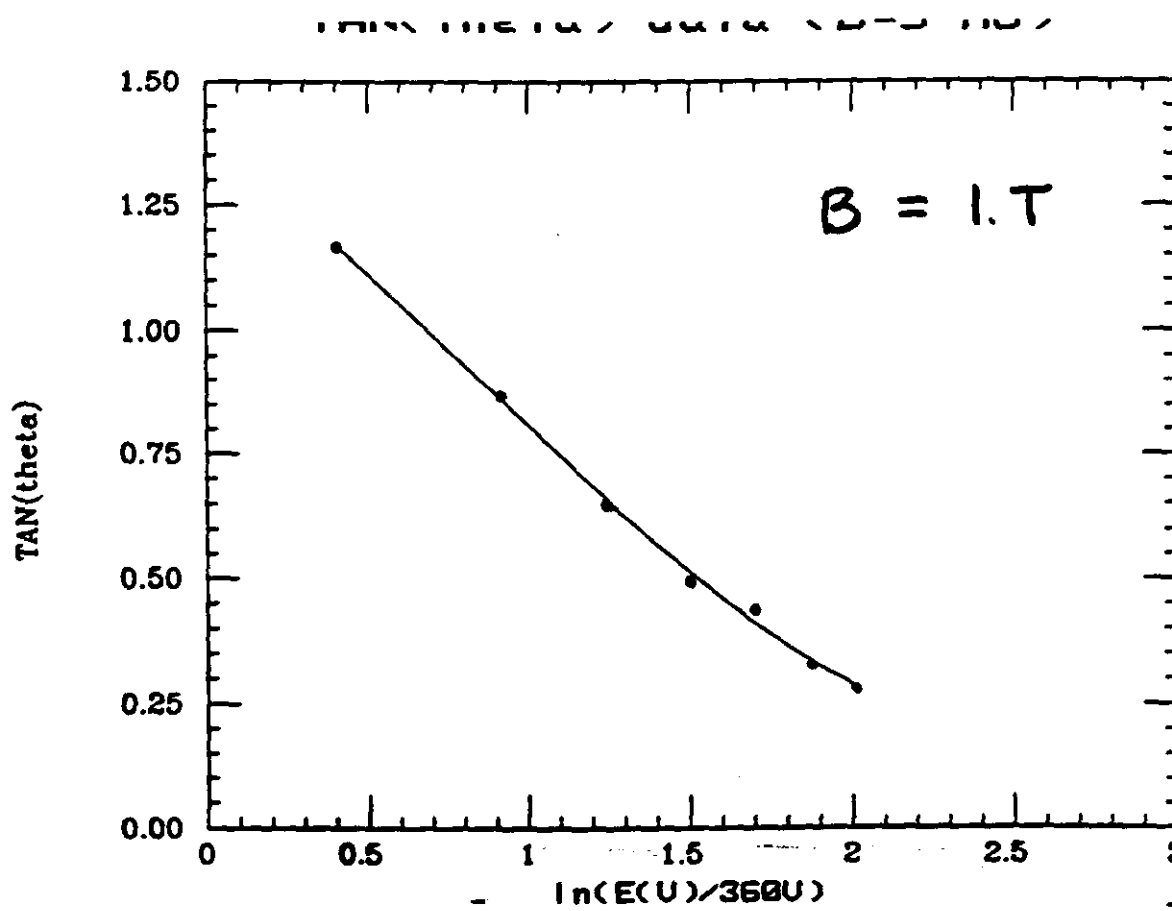
B = 1.T
TAN(theta)
1.50
1.25
1.00
0.75
0.50
0.25
0.00
0
0.5
1
1.5
2
2.5
3
ln(E(U)/360U)

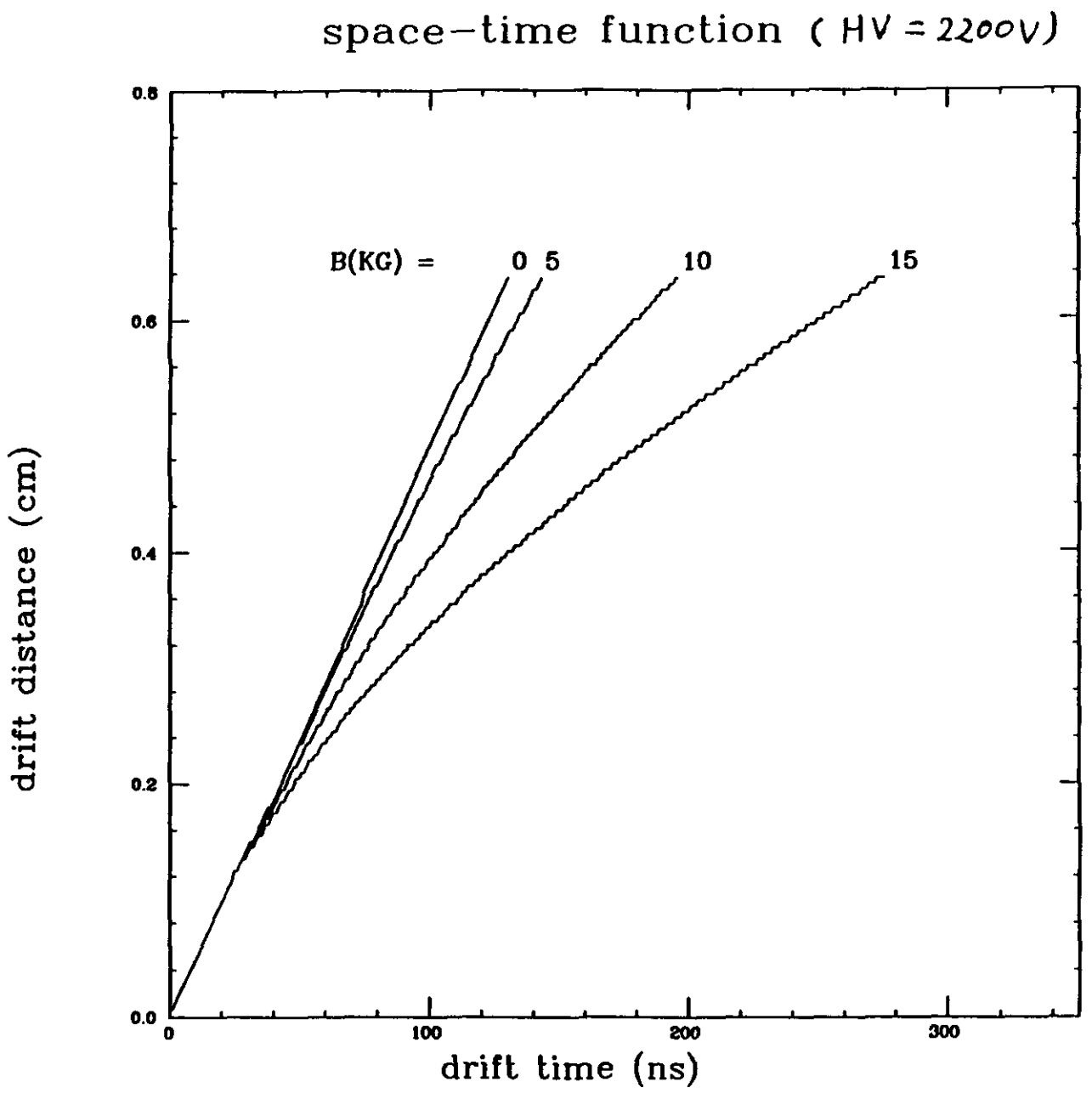
space-time function (HV = 2200V)
B(KG) =
0
5
10
15
0.0
0.2
0.4
0.6
0.8
0
100
200
300
drift distance (cm)
drift time (ns)

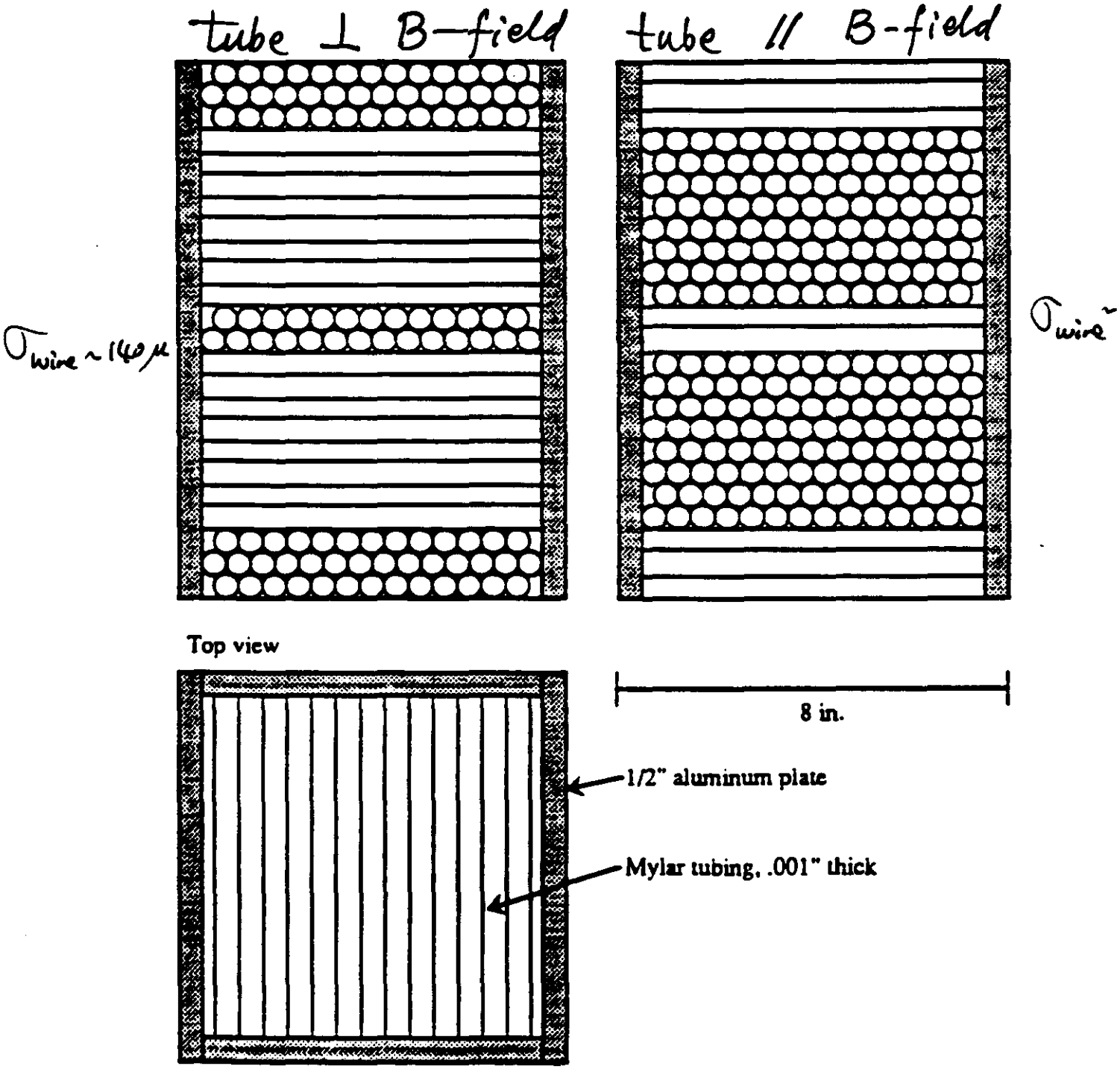

Drift tube array.

PBAR

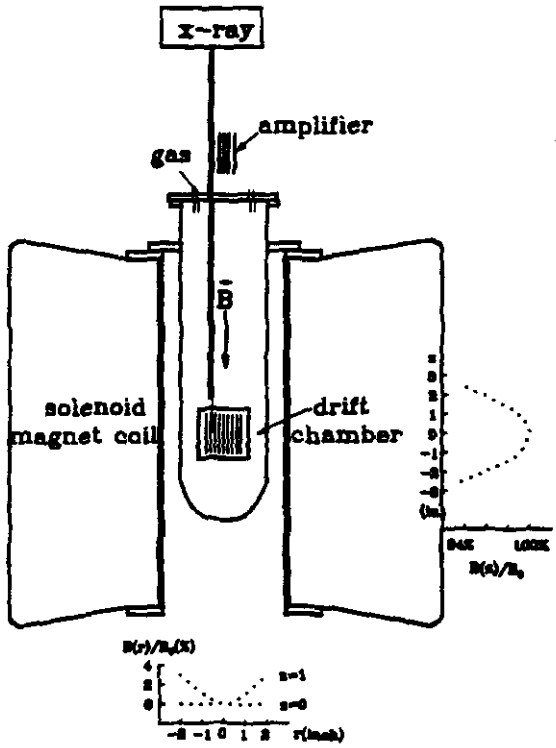
x-ray
amplifier
gas
B
solenoid
magnet coil
drift
chamber

(a)

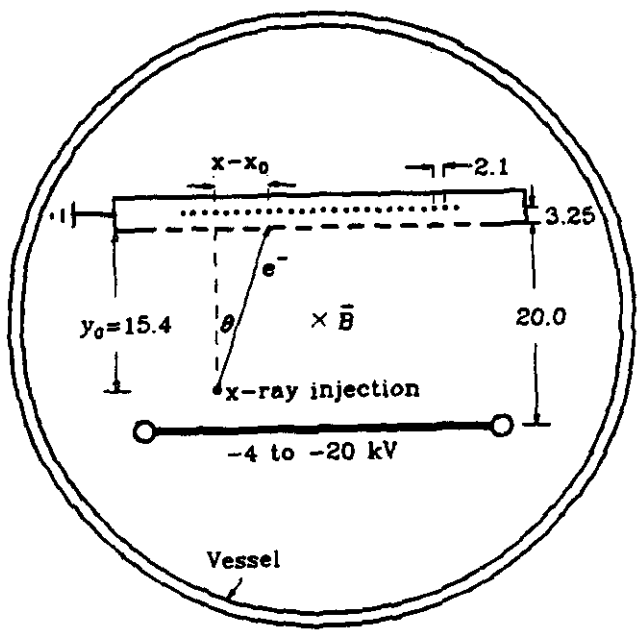
x−x0
2.1
3.25
e−
y0=15.4
θ
× B
20.0
x−ray injection
−4 to −20 kV
Vessel

(b)

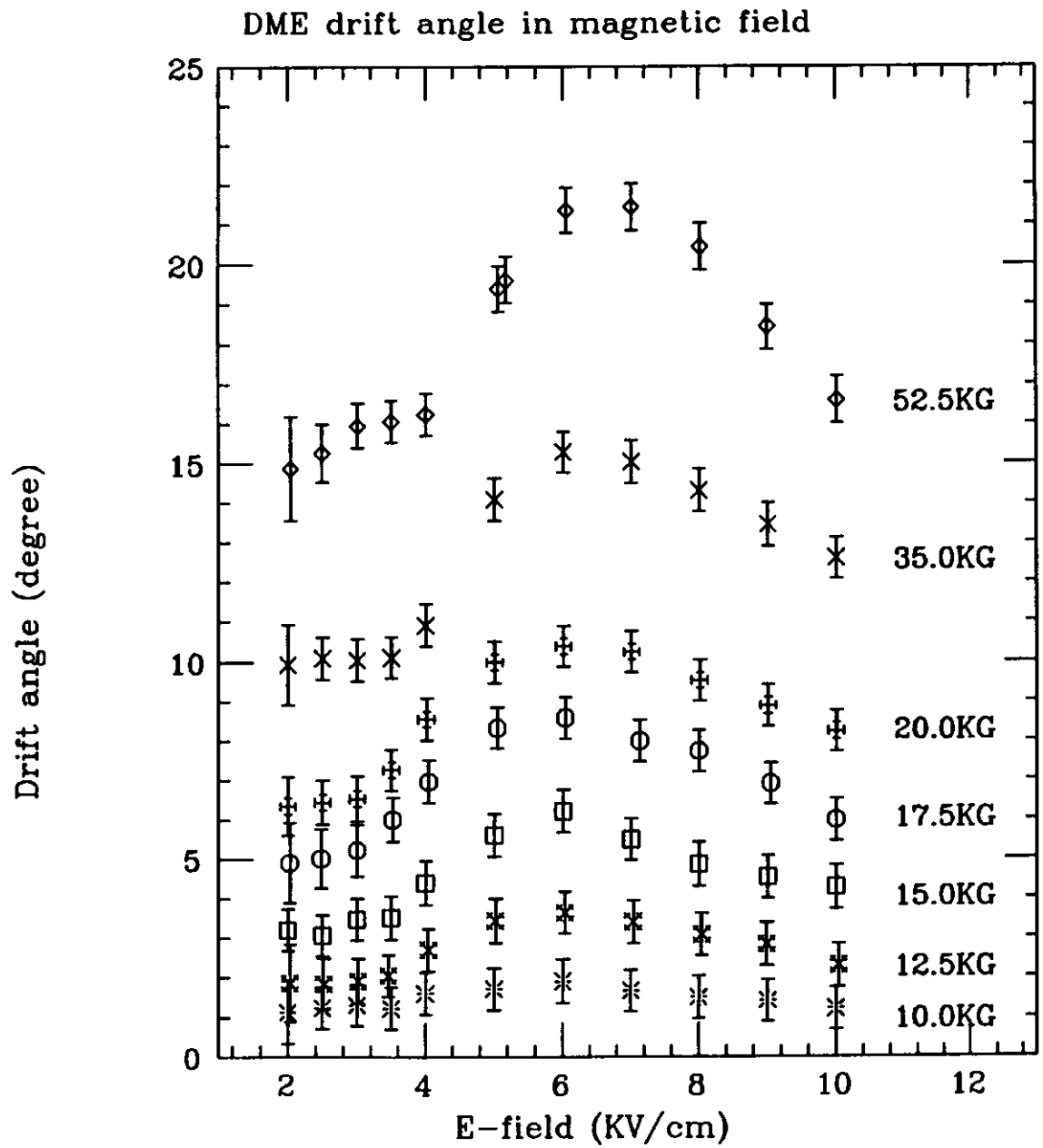
DME drift angle in magnetic field
Drift angle (degree)
E−field (KV/cm)
52.5KG
35.0KG
20.0KG
17.5KG
15.0KG
12.5KG
10.0KG
0
5
10
15
20
25
2
4
6
8
10
12

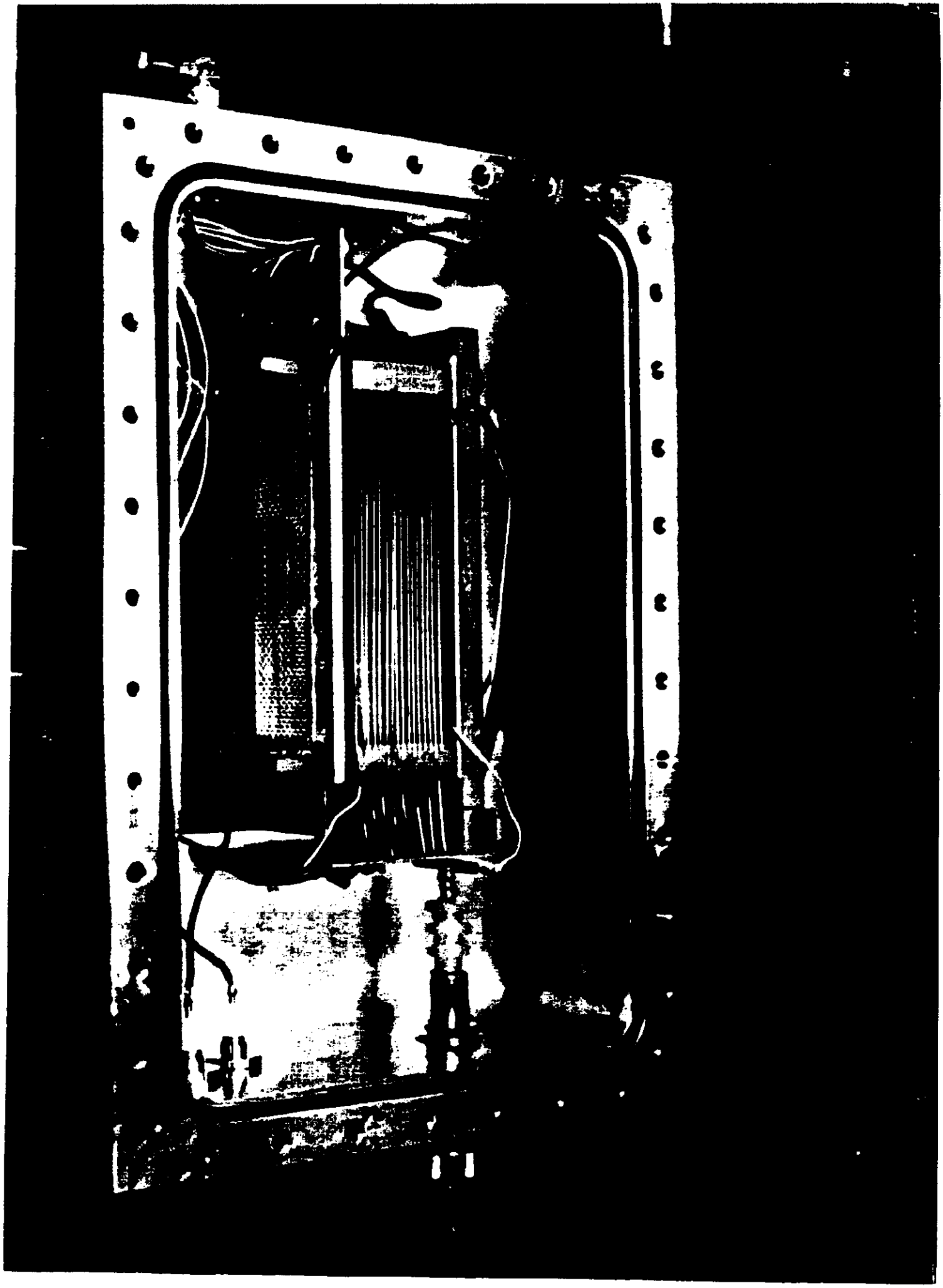

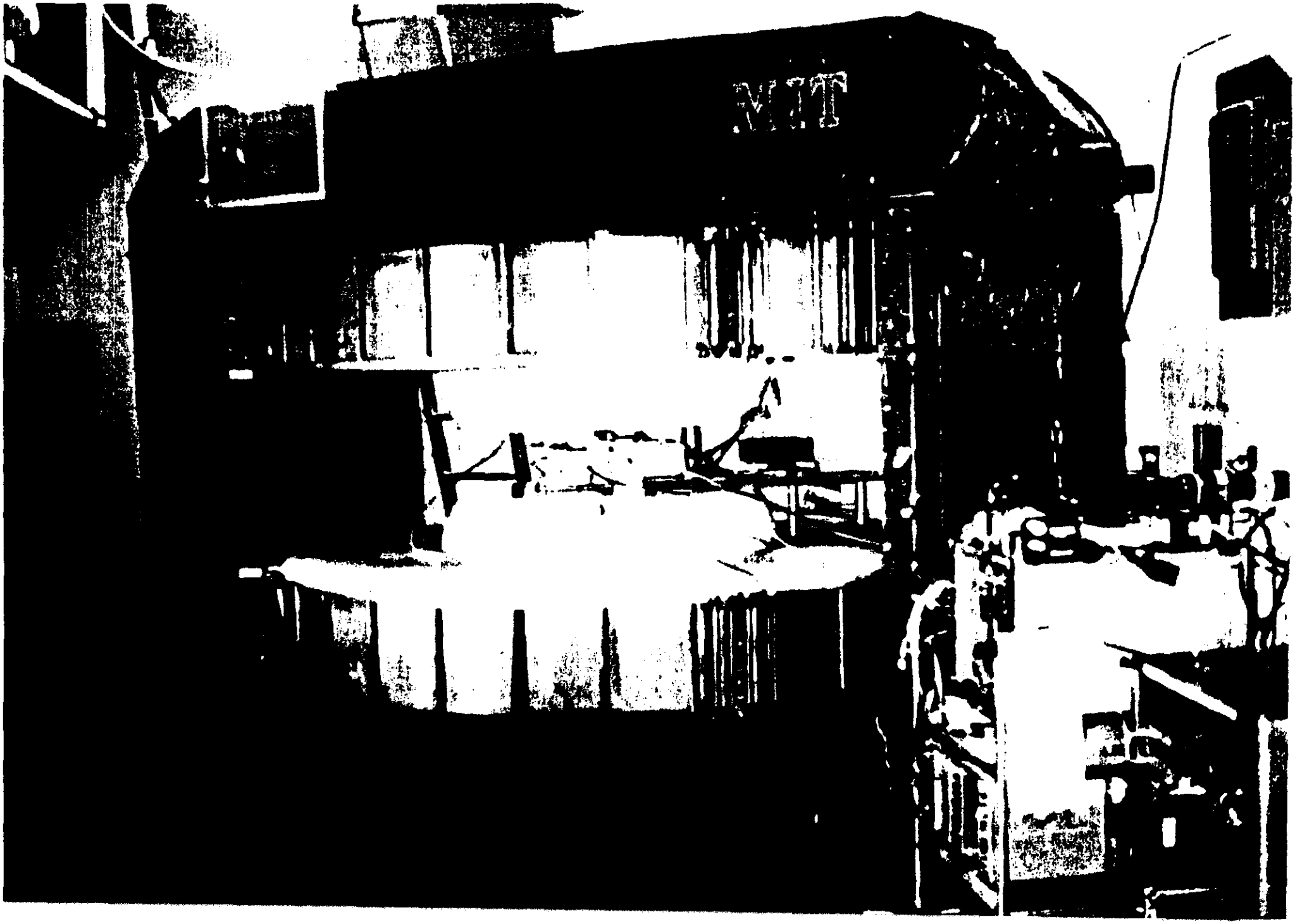
MIT

WIRE SIGNALS => V_D

13-May-91
21:26:28

LeCroy

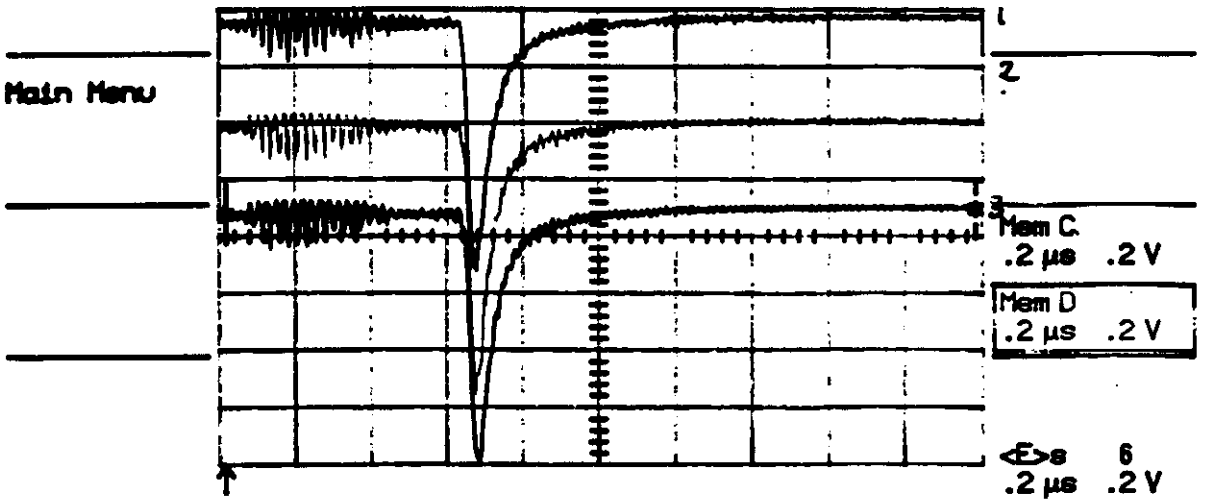

Parameters
Source

Function F [1.5 ns, 1.9615 µs] 784 pts

maximum	46.8 mV	period	- - -
minimum	-868.8 mV	width	62.1 ns
mean	-38.86 mV	rise	130.6 ns
sdev	138.90 mV	fall	23.6 ns
rms	138.03 mV	delay	644.0 ns

EXT -0.05 V AC

CH1 .1 V
CH2 .1 V
T/div .2 µs

PADS SIGNALS => θ_L

13-May-91
21:21:26

LeCroy

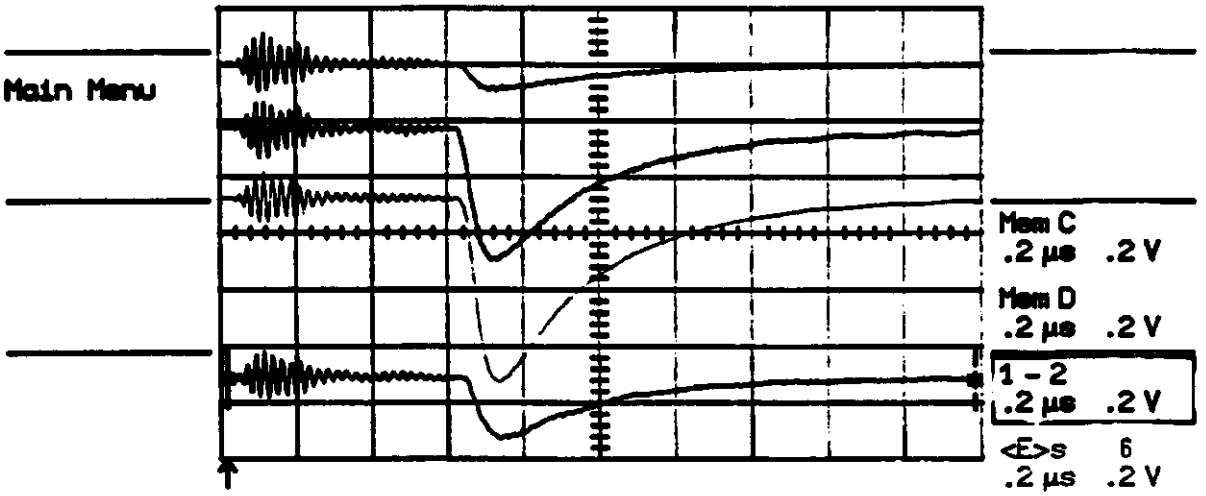

Parameters
Source

Function E [1.5 ns, 1.9615 µs] 784 pts

maximum	84 mV	period	- - -
minimum	-229 mV	width	278.9 ns
mean	-48.5 mV	rise	485.8 ns
sdev	80.6 mV	fall	58.4 ns
rms	77.6 mV	delay	882.5 ns

EXT -0.05 V AC

CH1 .1 V
CH2 .1 V

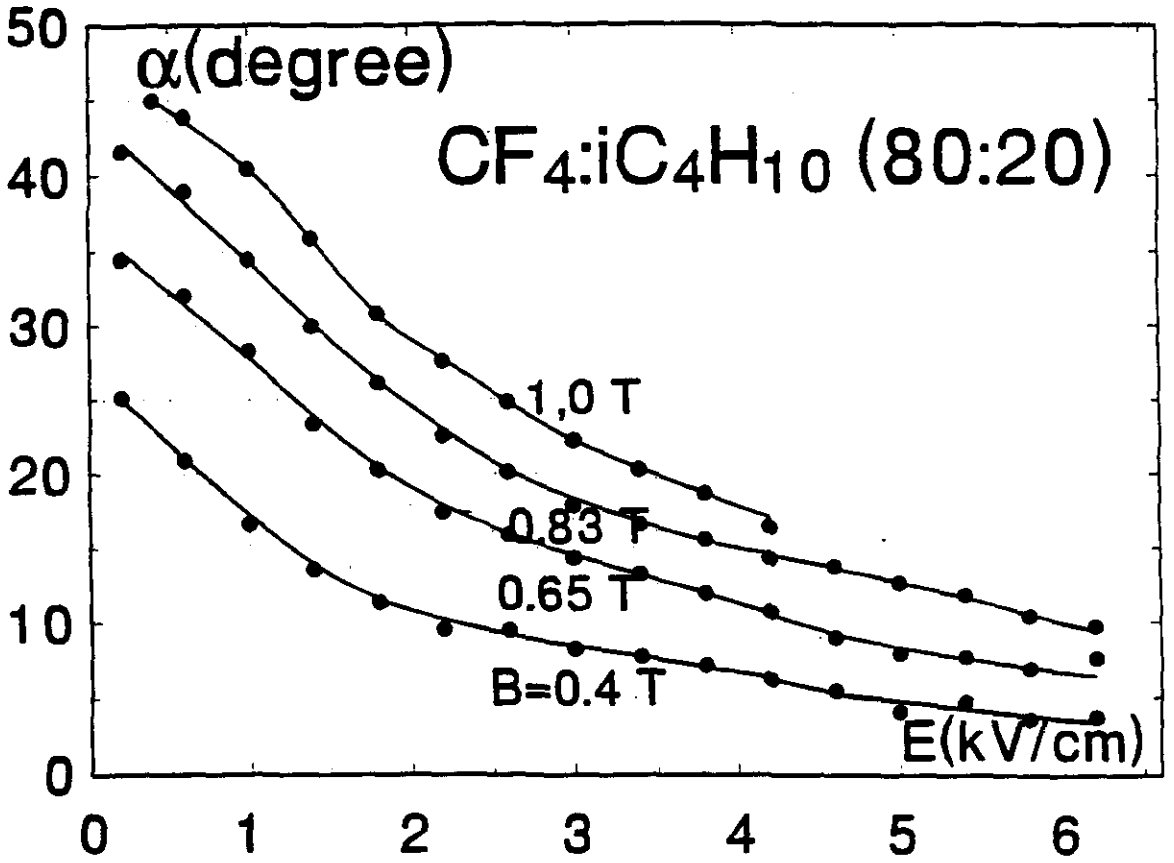

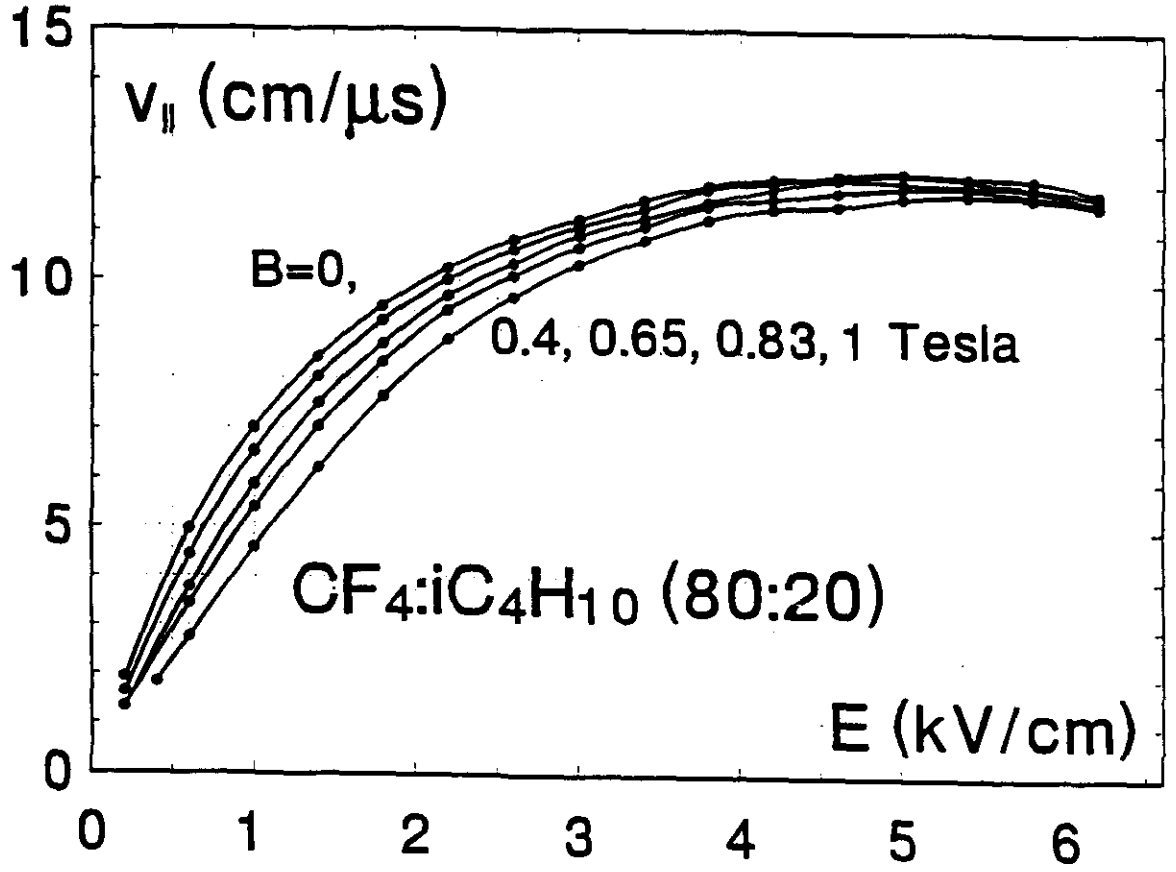

CENTRAL TRACKER CANDIDATE

GOALS :

(1) Find a suitable gas

- small Lorentz angle
- high drift velocity
- high efficiency

(2) Drift tube orientation in B field studies using our prototype

- compare prediction / exp. values
- resolution as a function of B, $\vec{B} \times \vec{z}$
- $\vec{B}$ nonuniformity effects on tube resolution

Pressurized Drift Tube Muon System

Bing Zhou, Boston University

- *Our Motivations*
- *Configuration & Expected Performance*
- *Crucial R&D Issues*
- *PDT Subsystem R&D Plans*

LIST OF COLLABORATORS

for the Pressurized Drift Tubes muon system

BOSTON UNIVERSITY

S. Ahlen, T. Johnson, D. Loomba, A. Marin, D. Osborne, J. Shank, D. Warner, S. Whitaker, B. Wilson, B. Zhou

BROWN UNIVERSITY

M. Wigdoff

INDIANA UNIVERSITY

D. Alyea, C. Bower, R. Heinz, J. Musser, J. Pitts, [redacted] S. Mufse

INSTITUTE FOR ATOMIC PHYSICS, BUCHAREST

A. Aculai, C. Blaj, H. Bozdoc, L. Butacu, M. Ciobanu, D. Ighicianu, D. Lazarovici, S. Miron, G. Pascovici, M. Pentia, D. Pop, V. Popa, G. Radulescu, D. Spanu, V. Valeanu

INSTITUTE OF HIGH ENERGY PHYSICS, BEIJING

W. Gu, Y. Gu, Y. Guo, Y. Huang, J. Li, C. Mao, H. Sheng, R. Xu, D. Zhang, B. Zhuang

JOINT INSTITUTE FOR NUCLEAR RESEARCH, DUBNA

G. Alekseev and others

LOS ALAMOS NATIONAL LABORATORY

R. Barber, M. Brooks, T. Coan, J. Hanlon, D. Lee, G. Sanders, B. Smith

MIT

I. Pless and others

WASHINGTON UNIVERSITY

J. Beatty, D. Ficenec

Other groups welcome !

C. Bromberg, R. Miller, C. Yosef, B. Pope

Michigan State University

Motivation for PDT

Precision and robust muon system in a large volume of magnetic field is the heart of the complementary SSC detector

1) High precision tracking in high magnetic field;

2) Most robust muon system in large scale;

3) Close to 100% acceptance in ϕ;

4) Modular construction – easy for international collaboration;

5) Easily configurable in non-uniform B-field;

6) Well understood technology;

7) Low cost.

PDT features and characteristics	
Features	**Achieved Characteristics**
Resolution/wire	1. Stainless steel DT EXAM $\sigma_{wire} = 165\mu m$ at 1Atm 2. StrawMAC $\sigma_{wire} = 45\mu m$ at 4Atm 3. Independent of the track angle
drift time	less than 400 ns at $B = 0$ for $\Phi = 3.8cm$ less than 520 ns at $B_{\parallel} = 1T$ for $\Phi = 3.8cm$
% Rad. Length for $150\mu m$ SS	1.7% per tube, i. e. $(\Delta P/P)_{MS} < 1\%$ for $\eta < 2$ at 100 Gev
PDT in magn.fields	Max. B used : 3T and 30% B nonuniformity
Robust structure	10g during balloon flights
Prec. mount, alligment	$\sigma_{position} \sim 25\mu m$; balloon and L3 experience

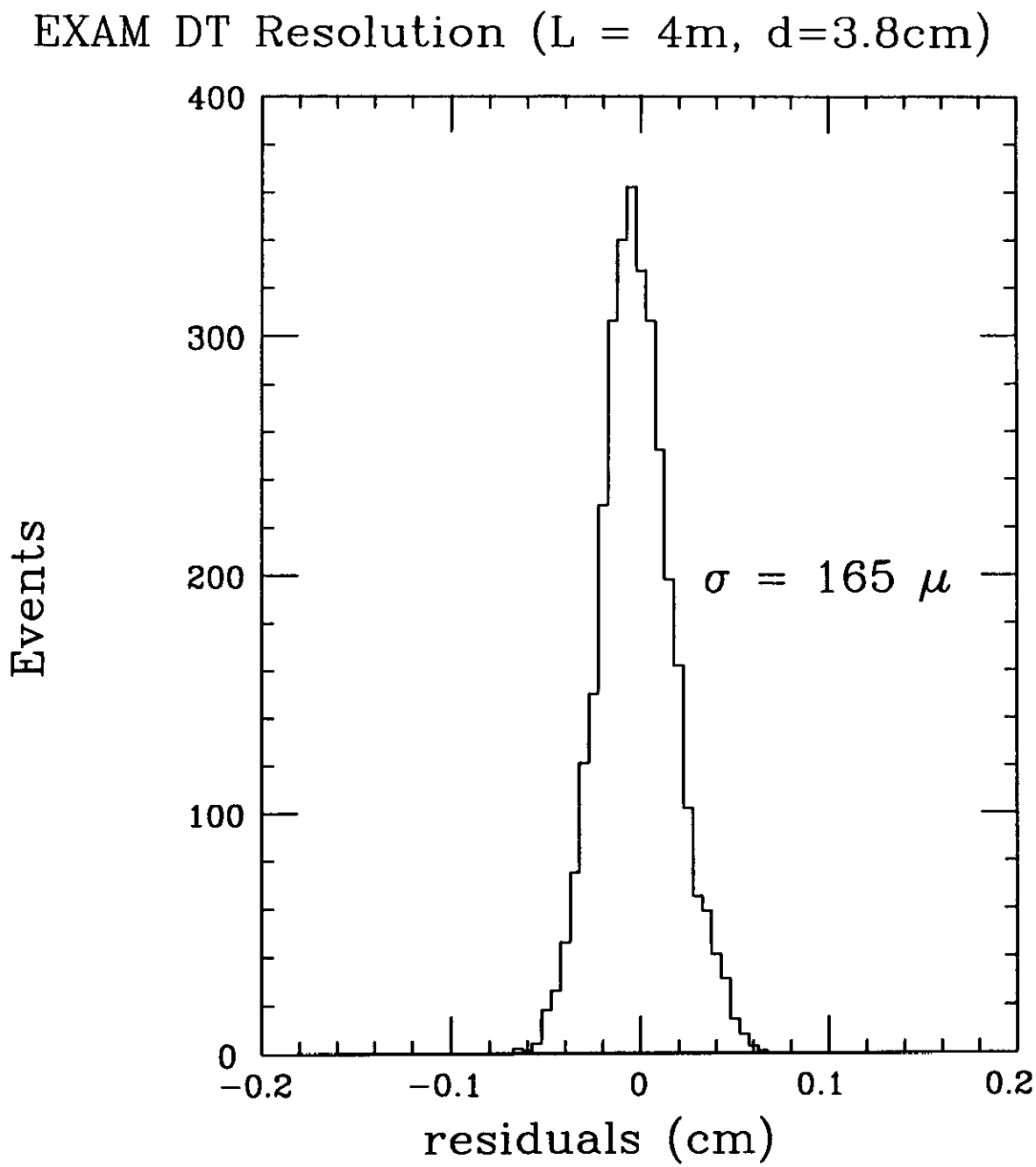
EXAM DT Resolution (L = 4m, d=3.8cm)
Events
400
300
200
100
0
−0.2
−0.1
0
0.1
0.2
residuals (cm)
σ = 165 μ

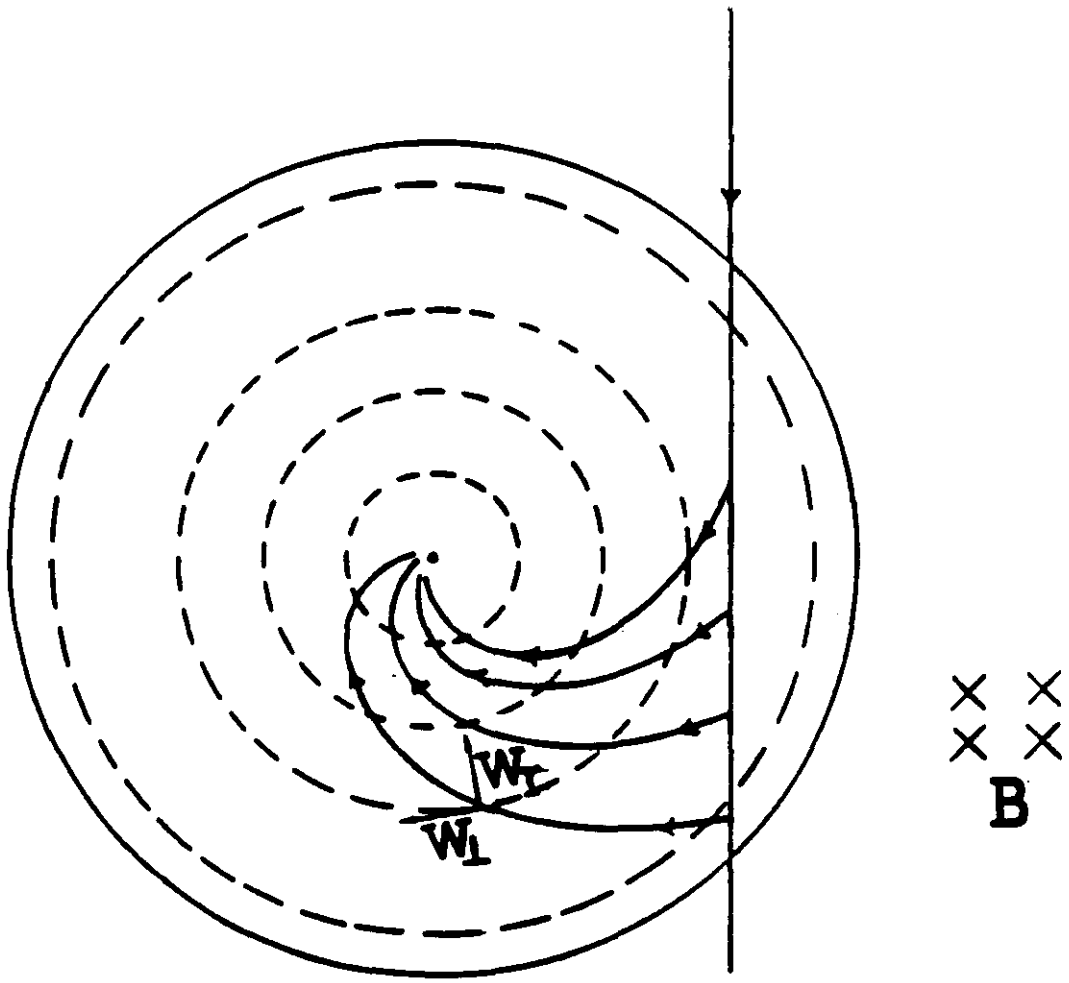

Drift Trajectories For
Electron Swarm
Centroids

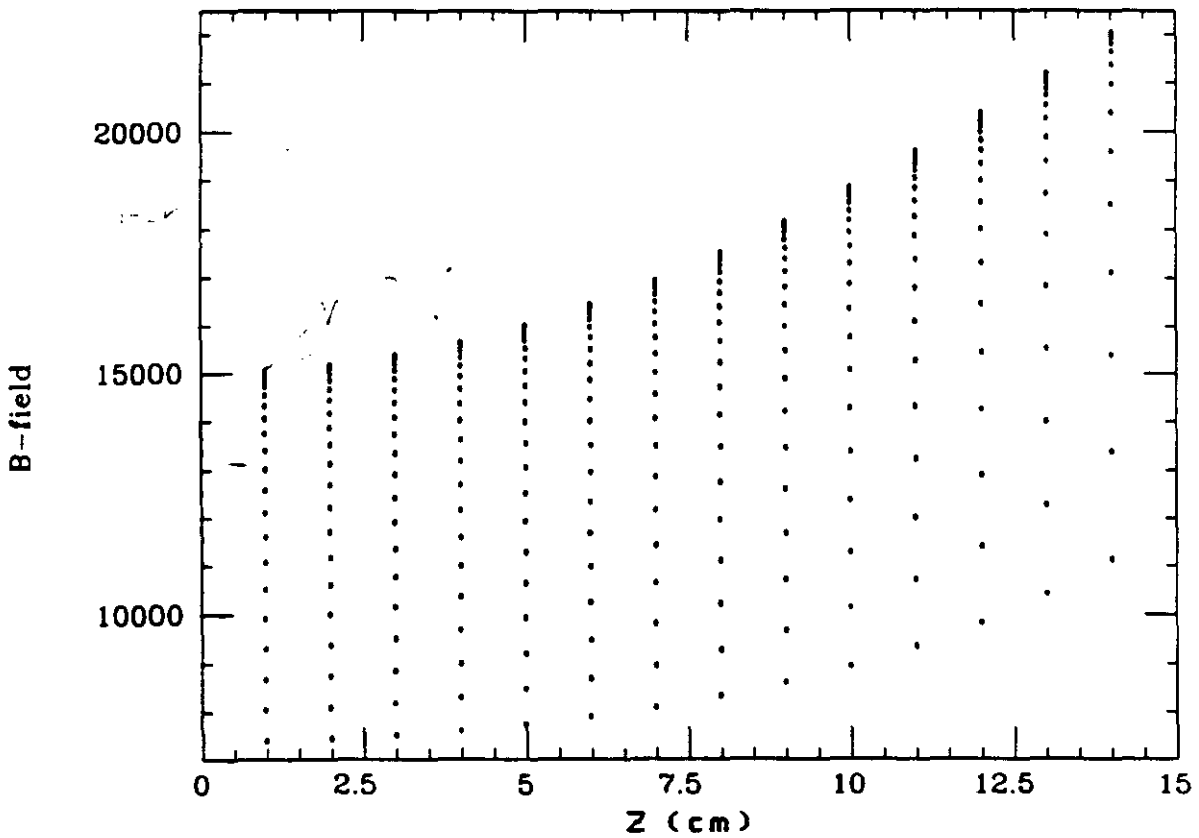

BR distribution

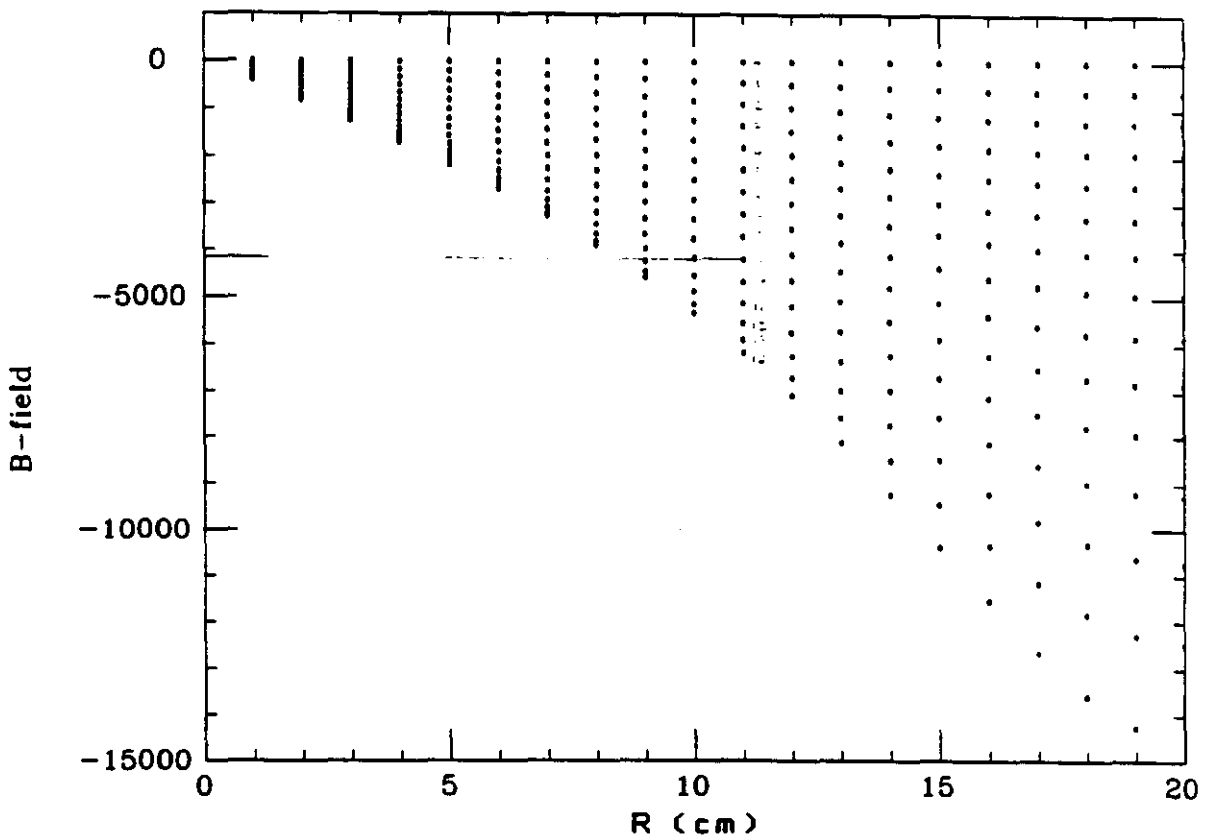

space-time function wire 99 // B-field

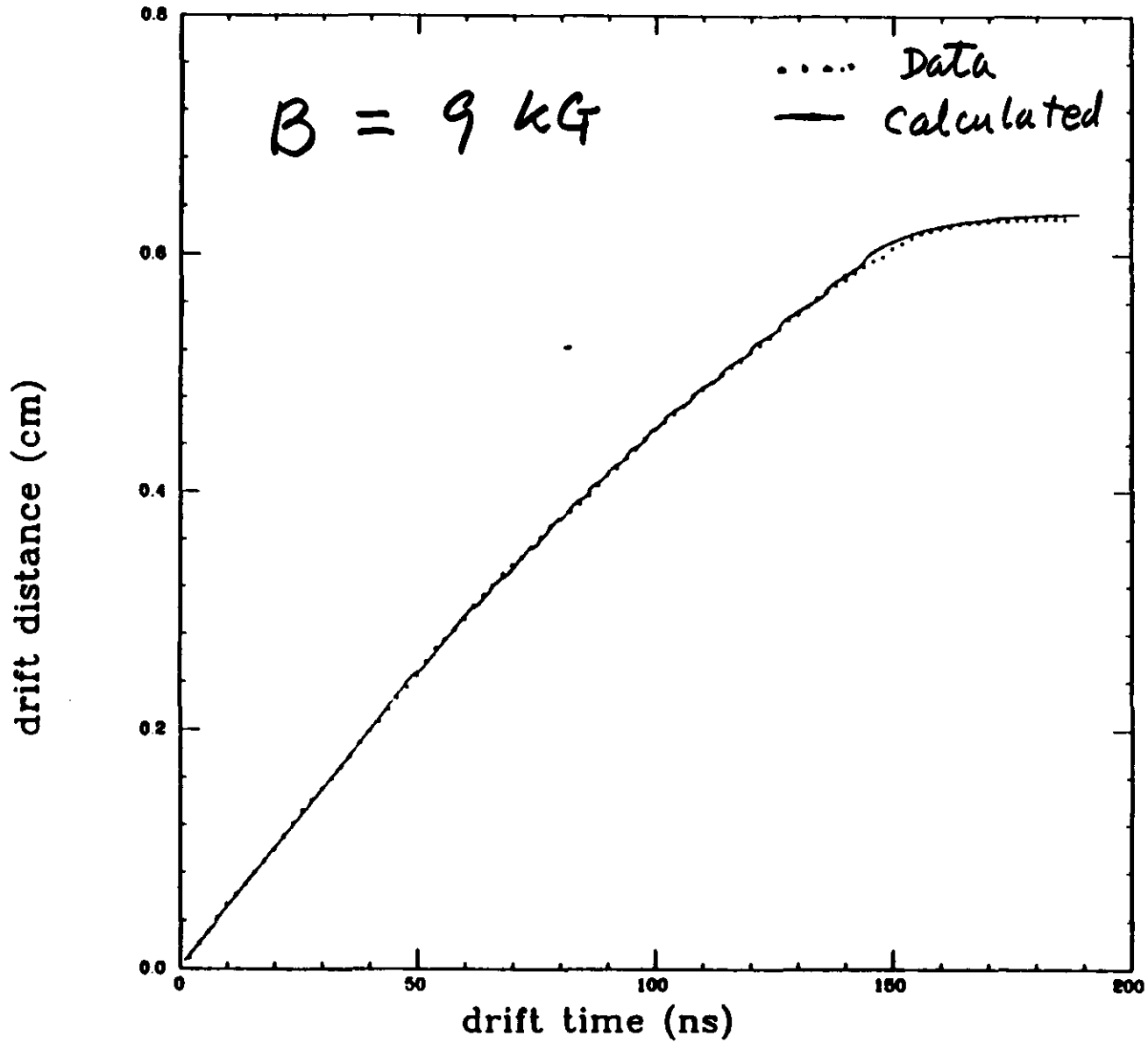

space-time function wire 221 ⊥ B-field

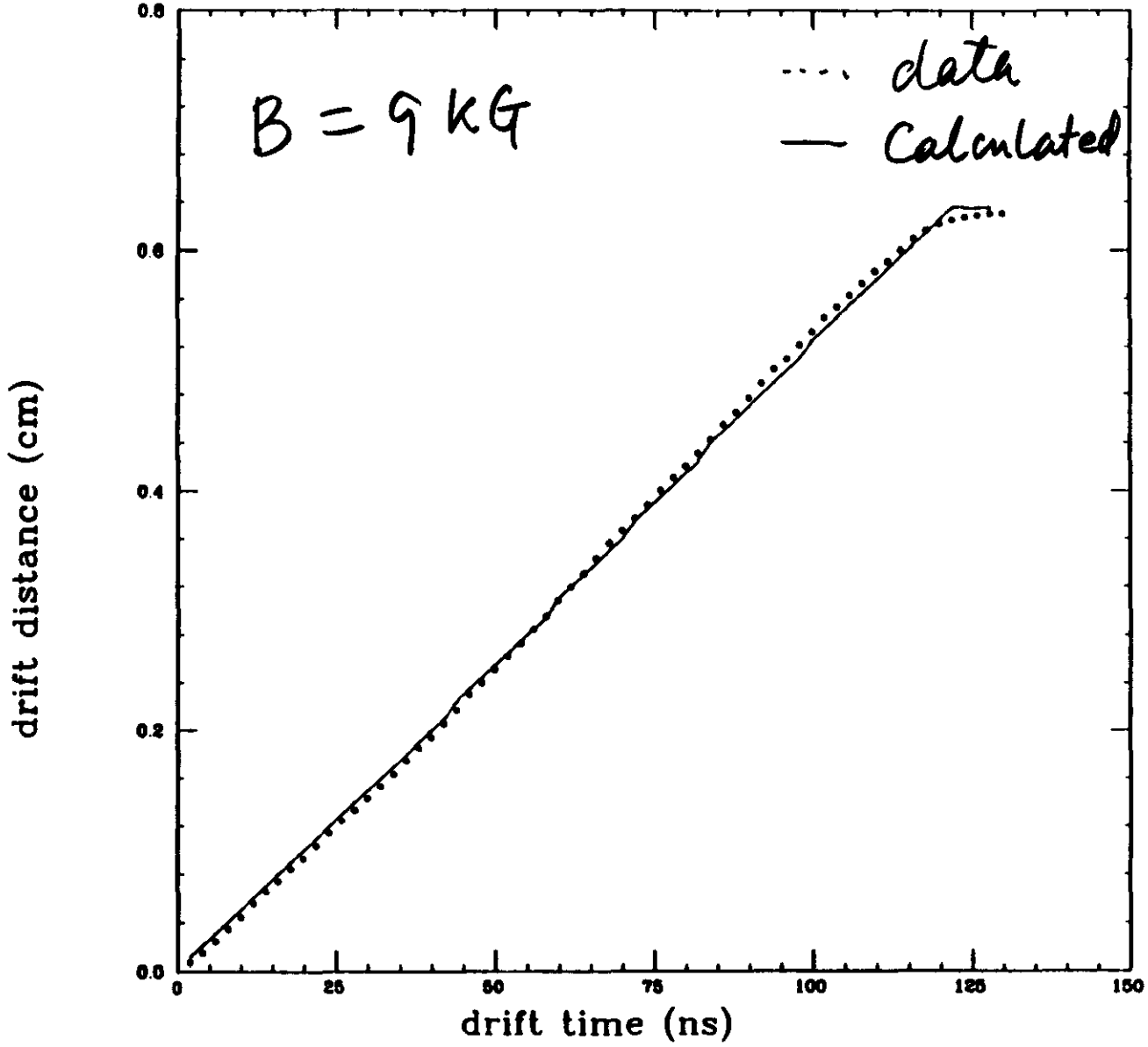

proton Test beam

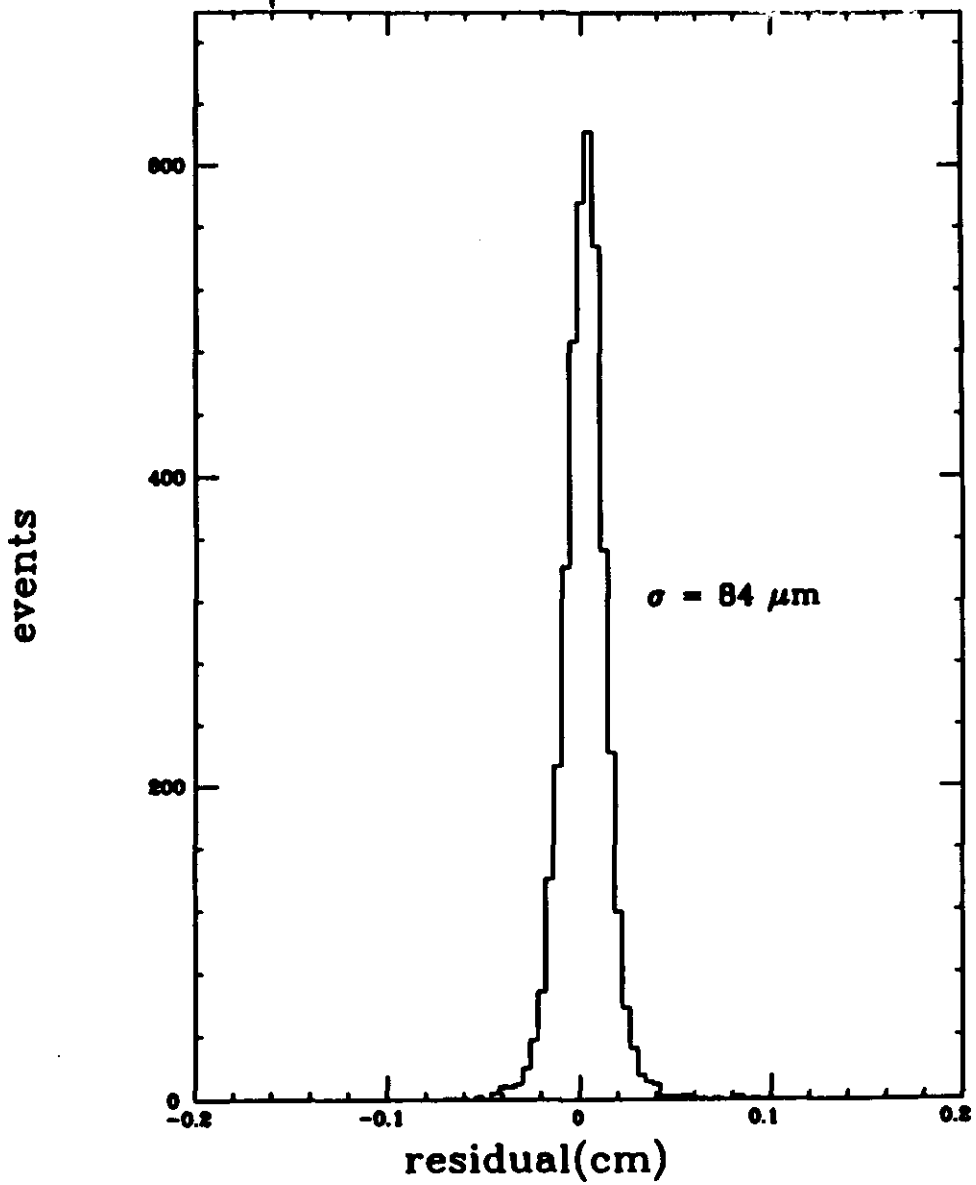

PRESSURIZED DRIFT TUBE OPTION FOR SECOND DETECTOR'S MUON SYSTEM

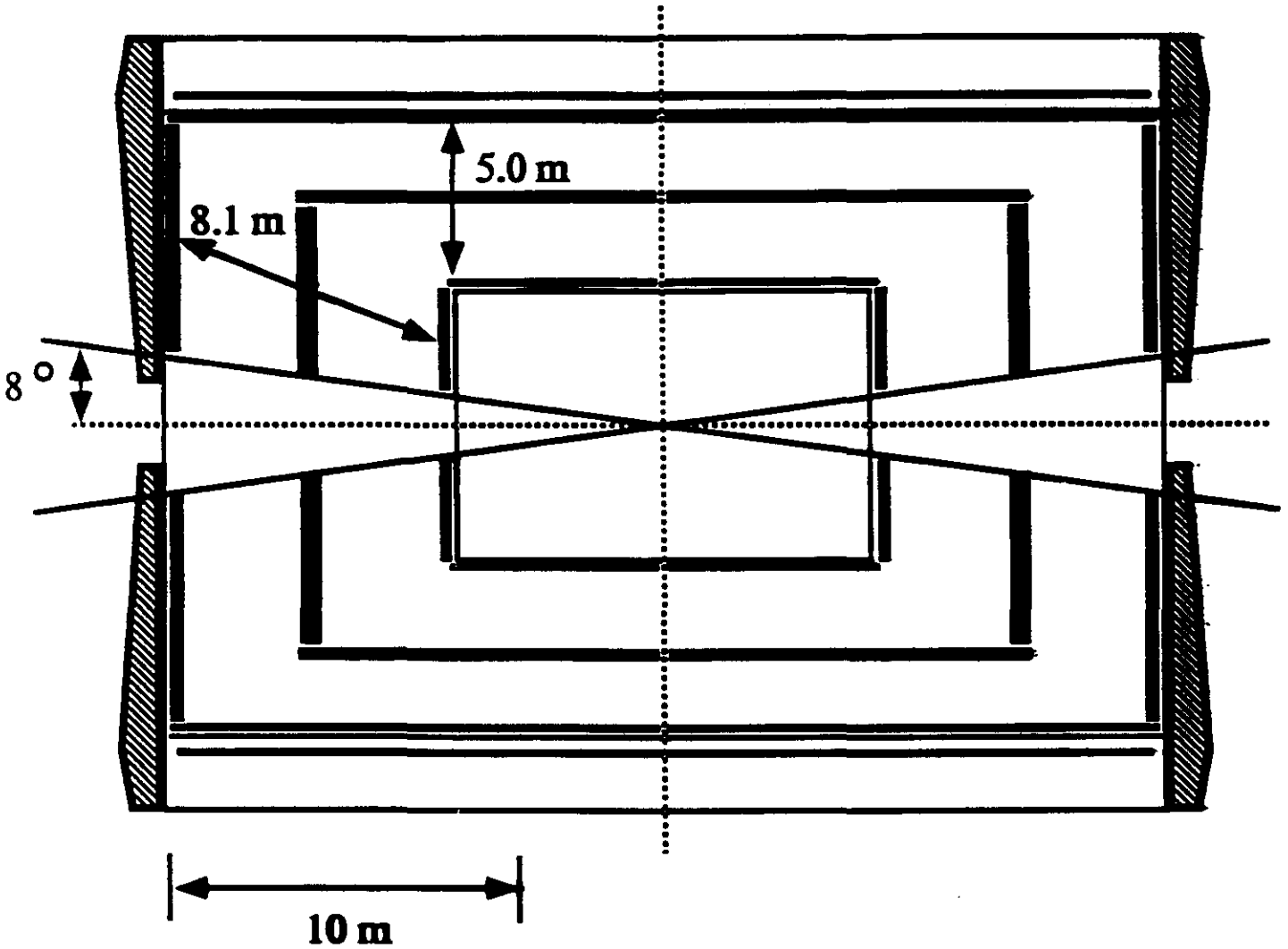

MUON CHAMBERS:

- 3.8 cm diameter stainless steel drift tubes (568 km, 90 tons)
- 16 layers (1:2:1 configuration)
- 14% of radiation length for central layer
- operated at 2 atm for 110 micron resolution
- 39,000 TDC's
- Resolution = 3.8 % at 90 degrees at 500 GeV for 1.4 Tesla
- Cost = $80M

END VIEW OF BARREL MUON DRIFT TUBES

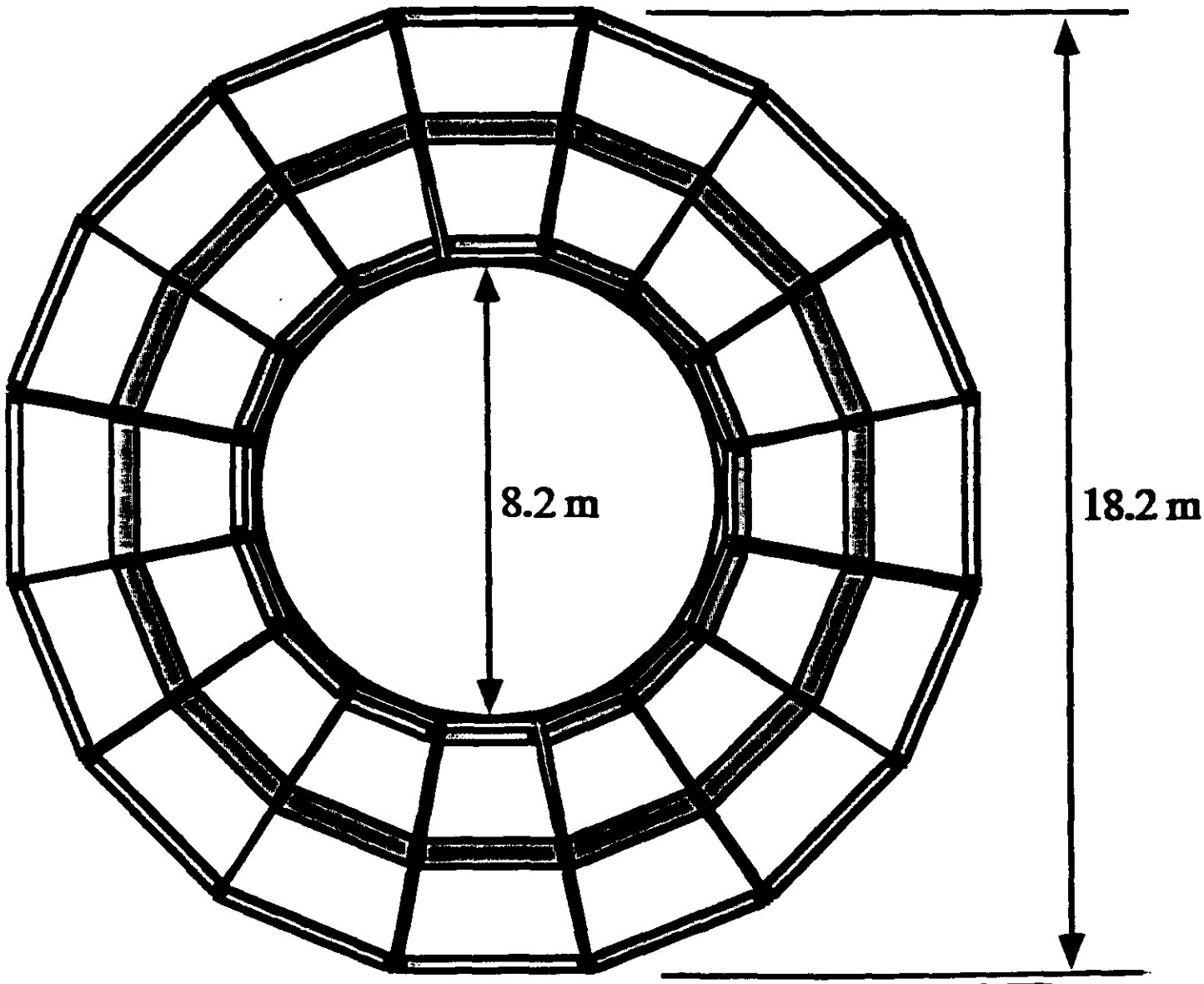

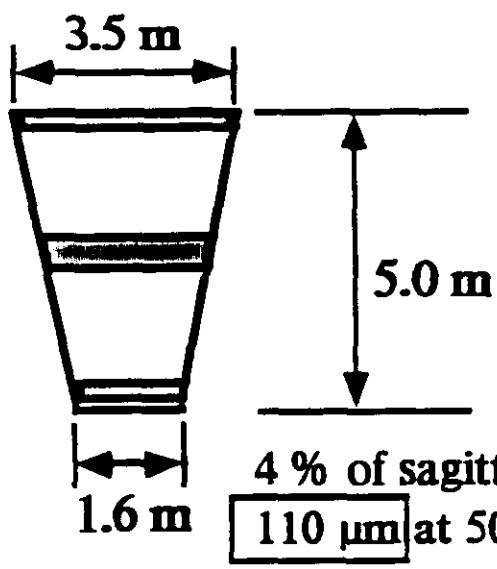

4 % of sagitta = 110 μm at 500 GeV

HRS (8 octants)

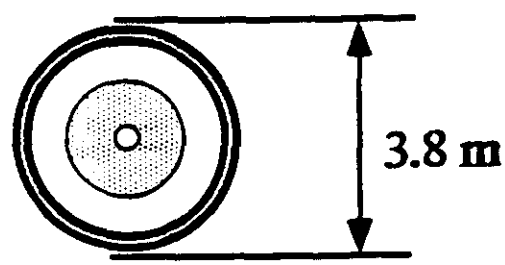

1.5% of sagitta = 170 μm at 15 GeV

End View of Barrel Drift Tubes and Limited Streamer Tubes

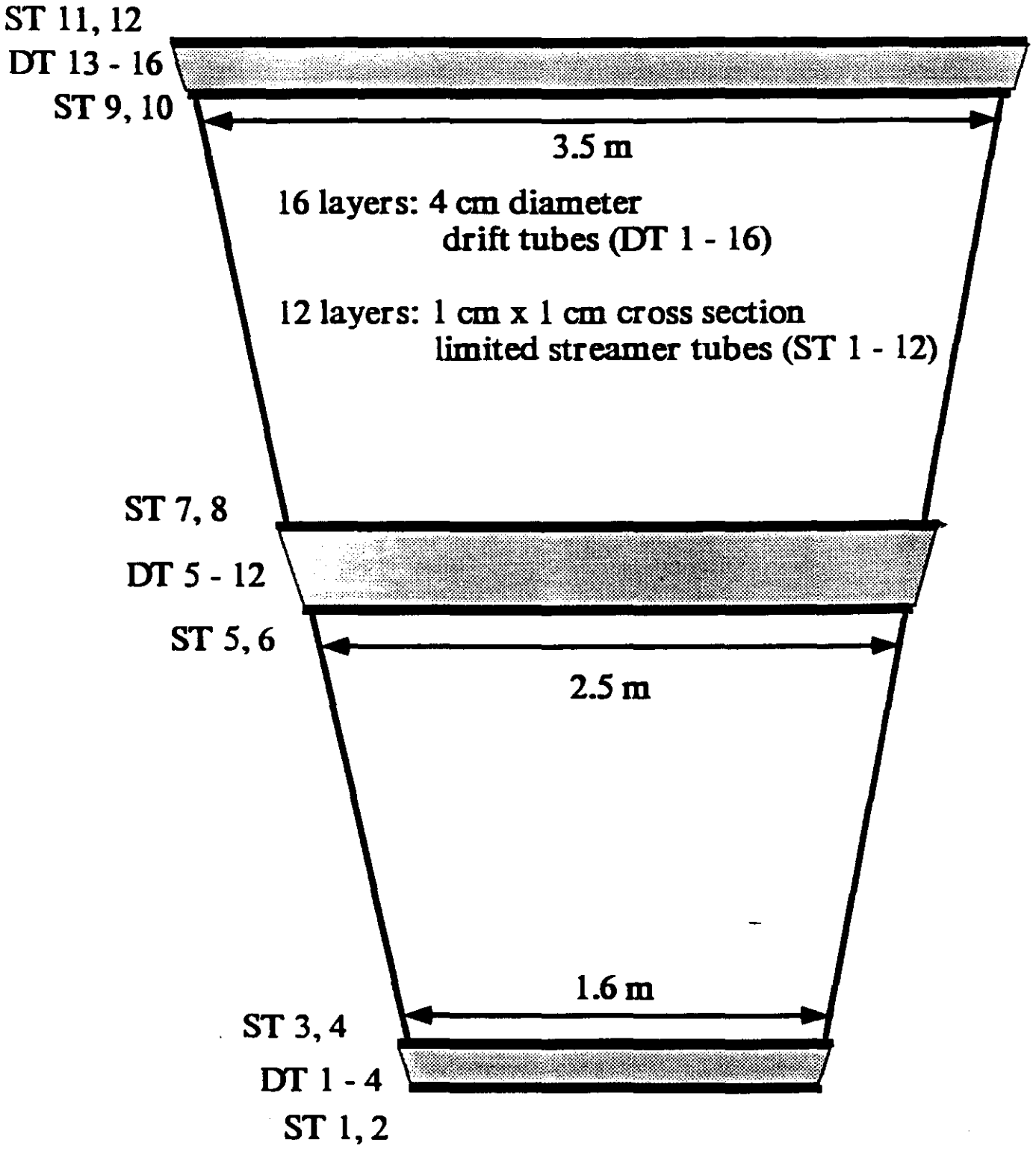

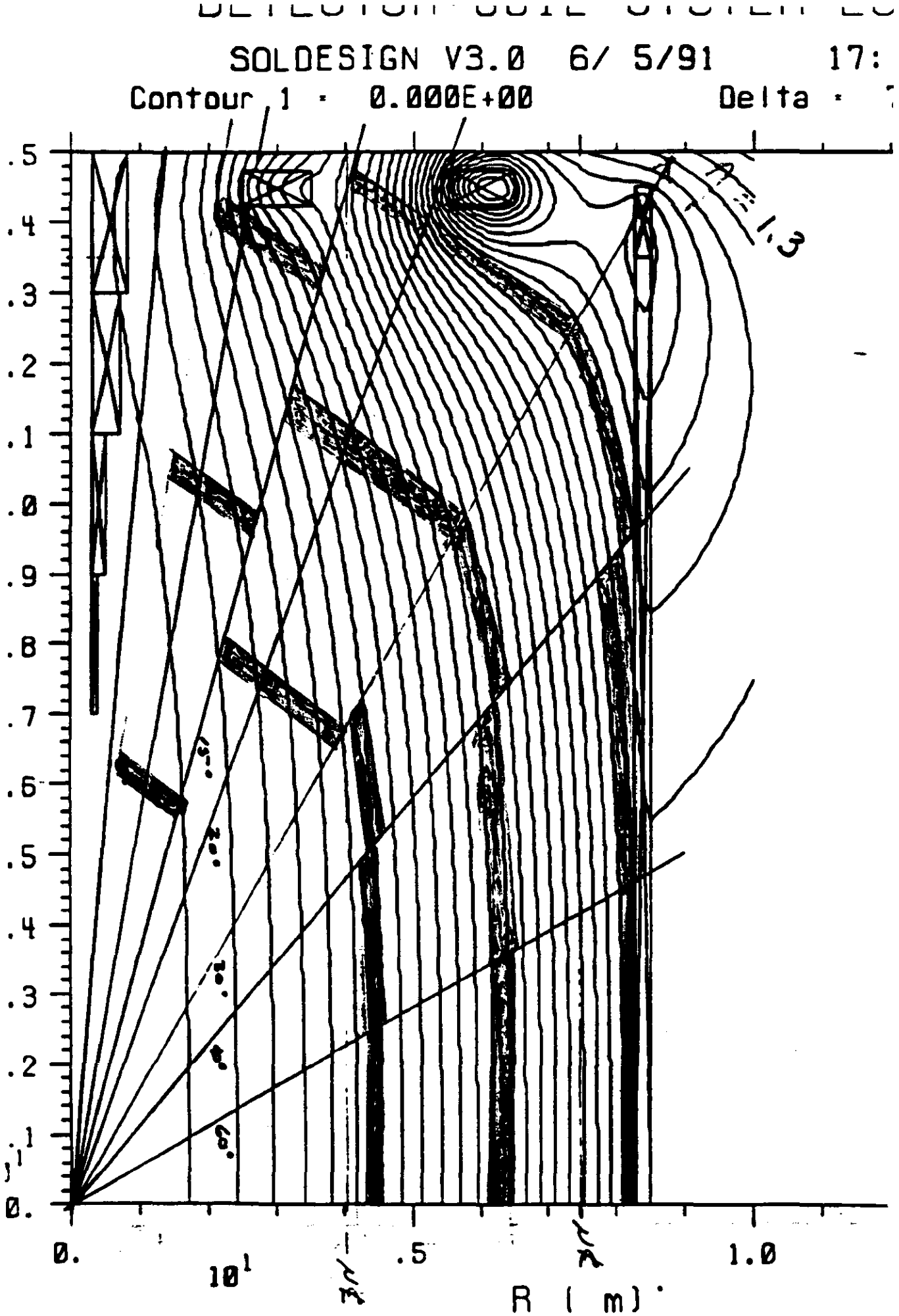
SOLDESIGN V3.0 6/ 5/91 17:
Contour 1 = 0.000E+00
Delta =
.5
.4
.3
.2
.1
.0
.9
.8
.7
.6
.5
.4
.3
.2
.1
0.
0.
.5
1.0
R (m)

Momentum Resolution of Pressurized Drift Tube Muon System for B = 1.4 T, sigma(sys) = 75 micron, 16 layers, 110 micron/ layer spatial resolution (2 atm), sigma(z) = 1 cm and assuming 90% efficiency per layer

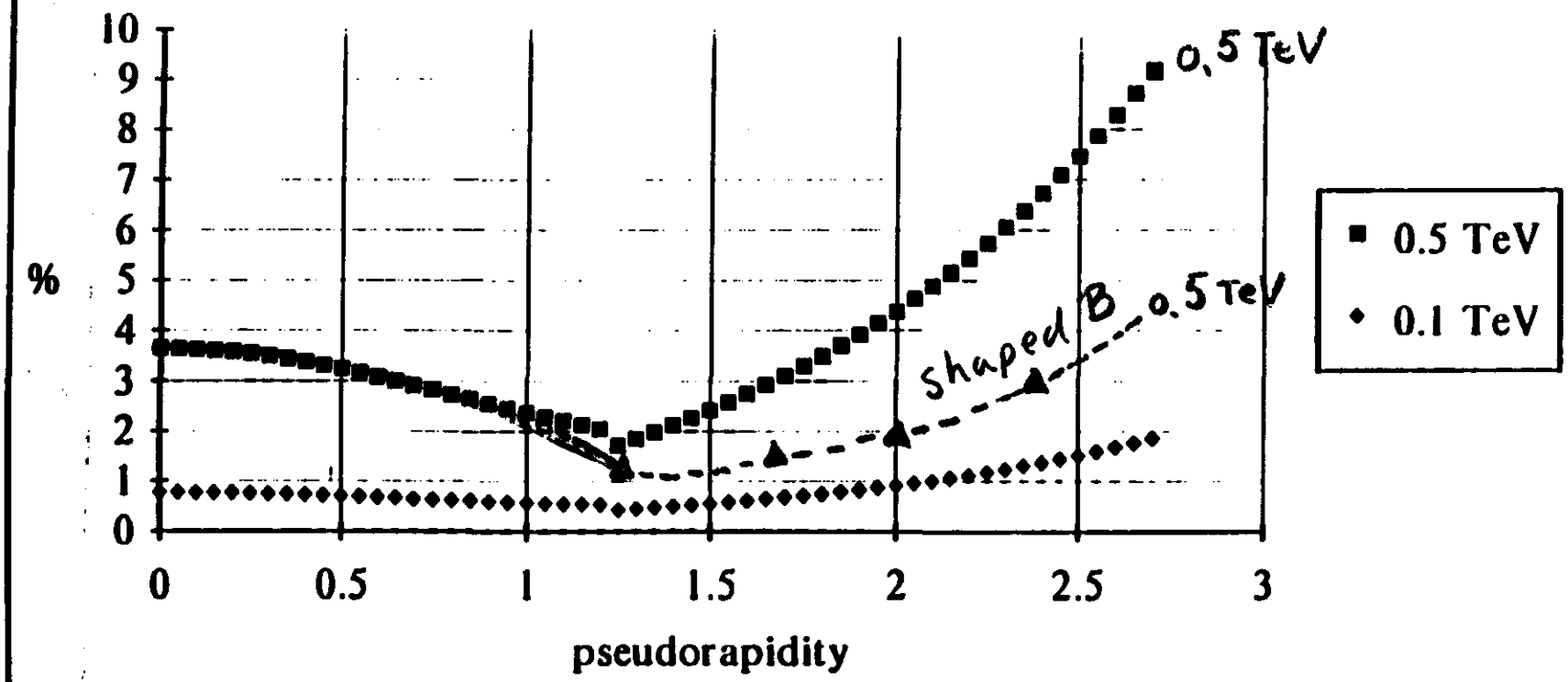

L3 AND L★
WIRE POSITIONING ACCURACY

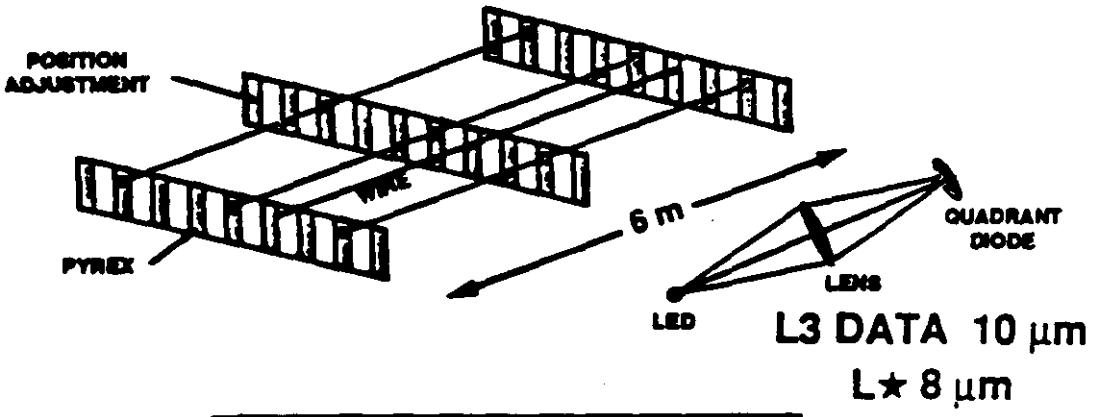

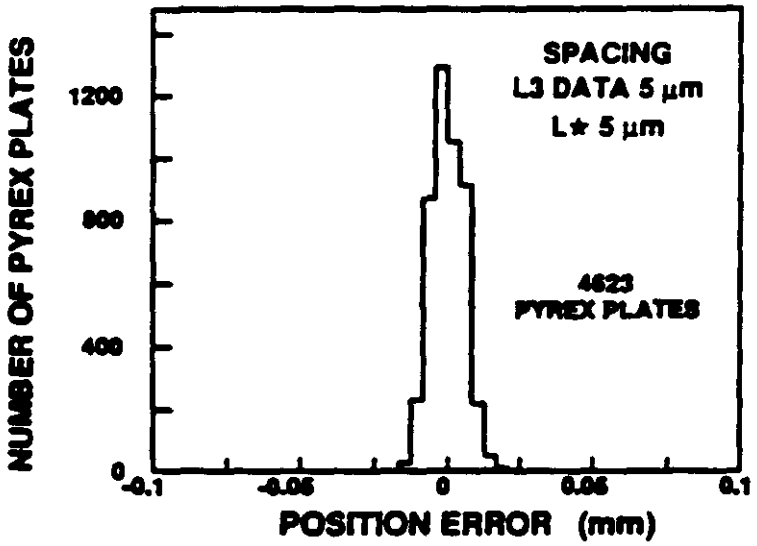

X STRAIGHTNESS MONITOR

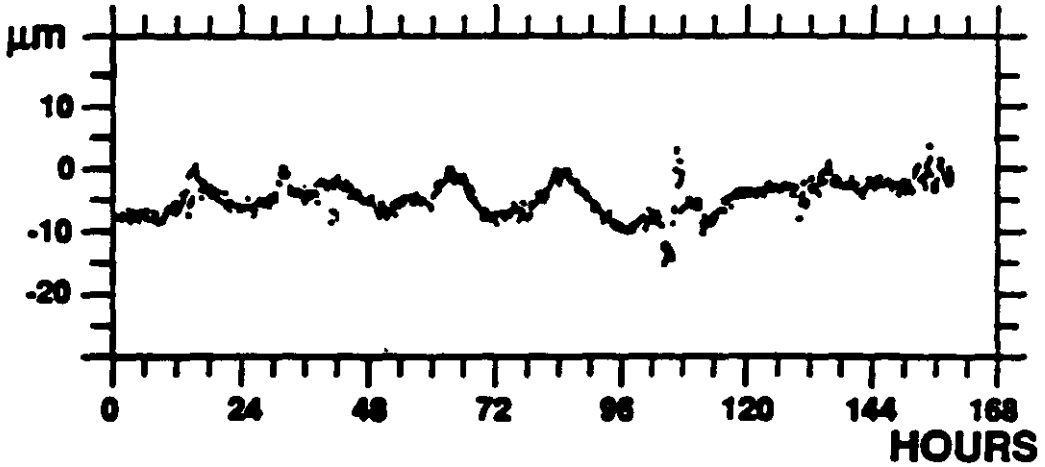

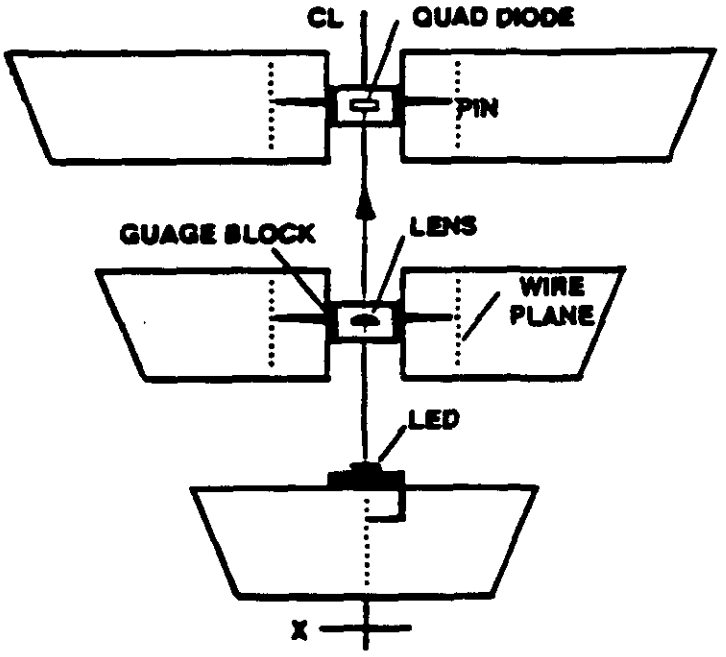

Stability of L3 Alignment for 3 Layers of Chambers

4μm

Reproduces after 1 Year

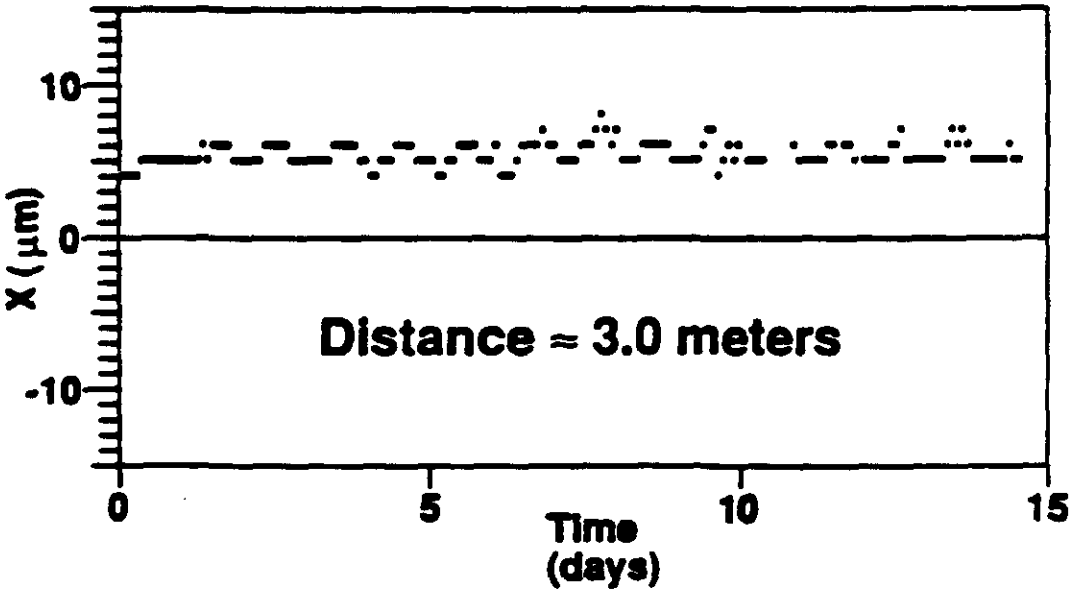

) IDENTICAL PLATES.
COND PLATE TO DISPLAY
GEND **IB** THIS LOCATION (*PBPDT-17)

THAT THE TWO PLATES ARE AS IDEN-
TICAL AS POSSIBLE IDENTICAL HOLE
PLACEMENT CRITICAL.

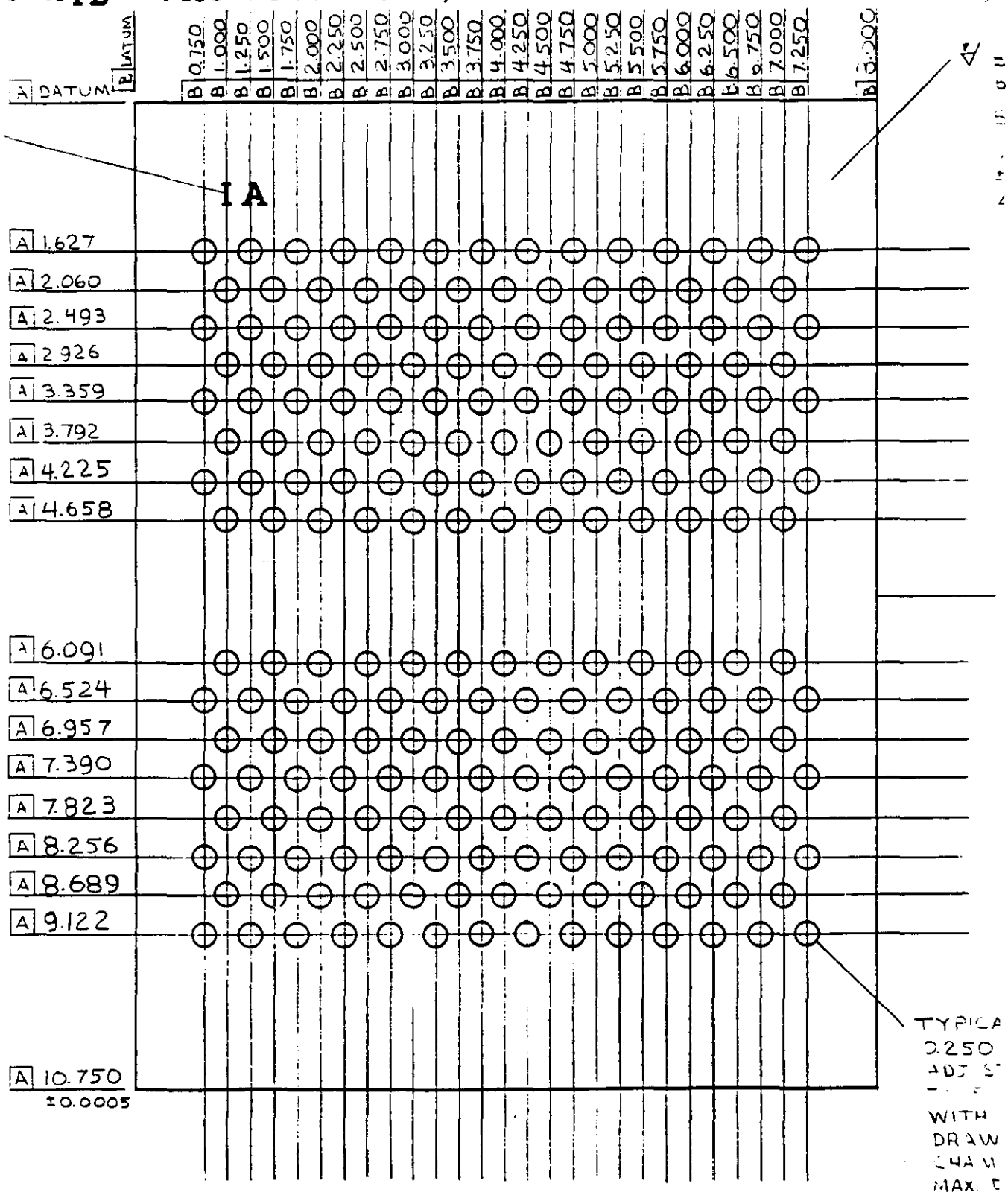

NOTE ADDED 12/15/86
OPENINGS OF THROUGH HOLES
MAY BE CHAMFERED SLIGHTLY
ON INSIDE SURFACE ONLY.
OUTSIDE SURFACE IS COUNTER BORED.
MAXIMUM CHAMFER 45° X 0.005"

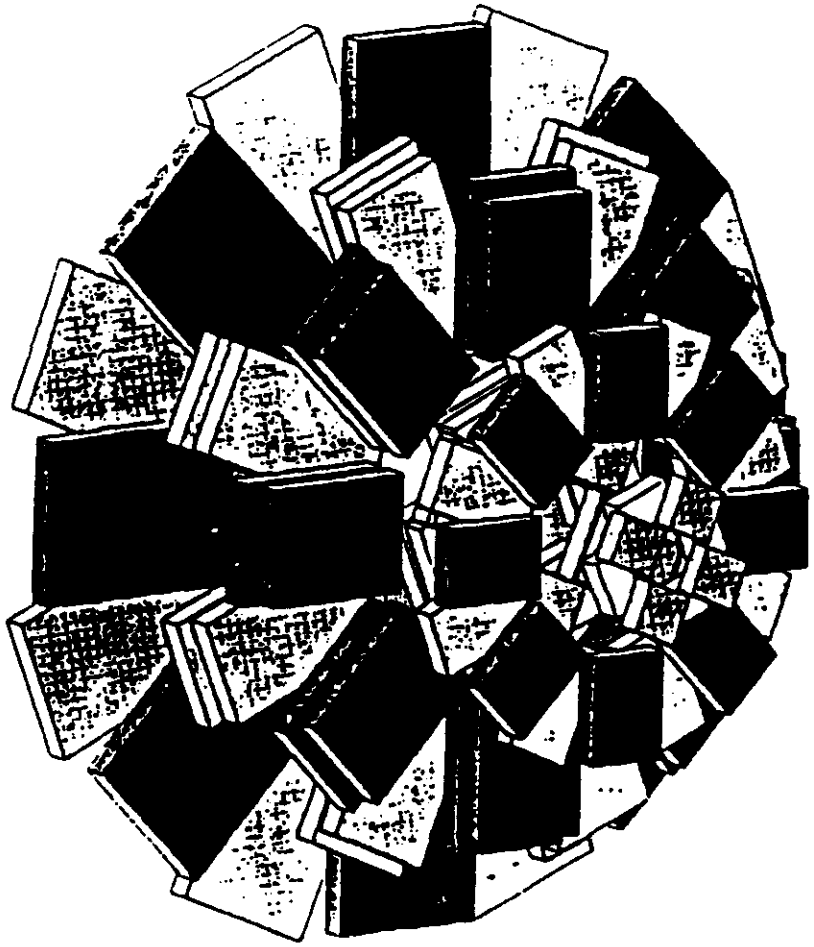

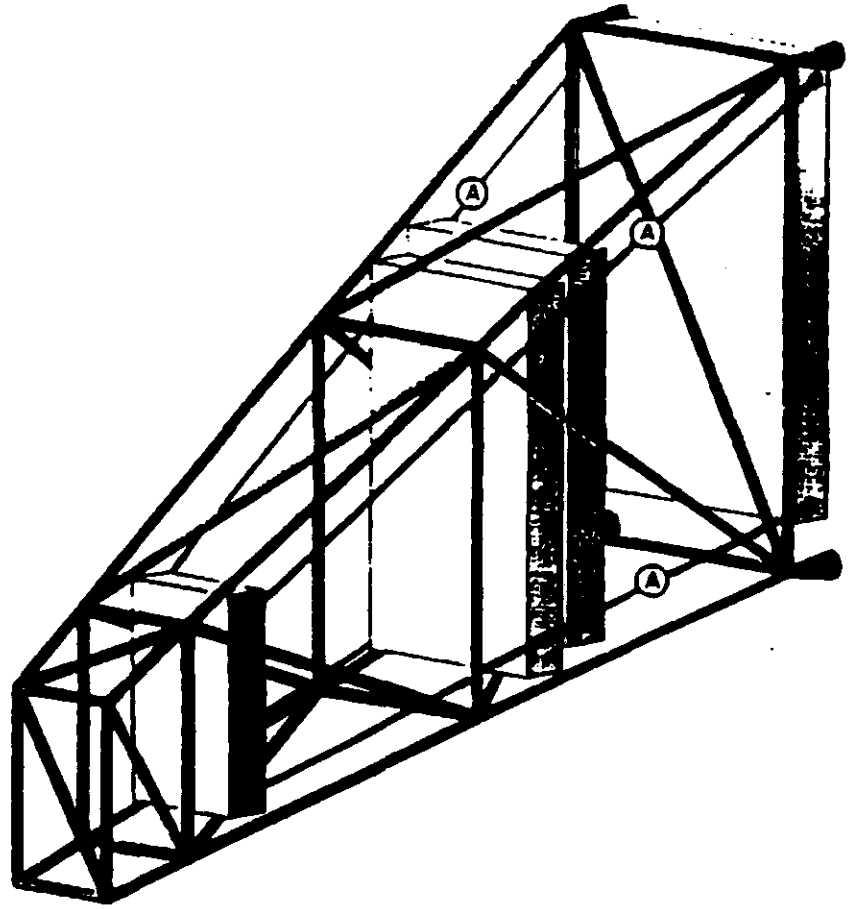

Figure IV.6: An Endcap Module. The lines denoted by Ⓐ are alignment paths.

Crucial R&D Issues

(1) Chamber Design

– wire position precision, stability, monitoring;
– Drift gas selection, max. drift time, σ/wire;
– Space-time function in non-uniform B-field;
– Pressurization, gas safety issues;
– End-cap chamber configuration design;
– Z-chamber technology & configuration;
– Mass production, quality control.

(2) Muon Trigger

– Read out link scheme;
– Fast trigger (RPC) / slow trigger (tube pattern);
– Ajustable p_T cut based on patterns;
– Resolve tracks from which beam cross (mean time method).

(3) Engineering

– Modular design;
– Alignment and monitoring;
– Structure support, stability;
– Assembly & installation procedures

PDT Subsystem R&D Plans

Necessary R&D before LoI :

– **HRS octant (2) test:** wire tension after 10 years; alignment scheme; sagitta systematic error.

– **Pressurized drift tube module prototype.**

– **RPC prototype, z-chamber selection.**

– **Drift gas studies with magnetic field:** drift velocities, Lorentz angles and space-time functions.

– **Intensive simulations:** end-cap chamber design; muon trigger issues; pattern studies in inner chamber.

– **Alignment scheme design.**

EMPACT Note 358
Dec. 3, 1990
Ammended,
Feb. 20, 1991

TUDIES OF DRIFT AND STRIP READOUTS FOR THE EMPACT/TEXAS MUON SYSTEM

(preliminary results)

Yu. Bonyushkin, N. Khovansky, A. Korytov, V. Malyshev, Yu. Sedykh, V. Tokmenin

Joint Institute for Nuclear Research

Dubna, U.S.S.R.

H. W. Kendall, L. S. Osborne, G. D. Ross, A. Sodickson, R. Verdier

Massachusetts Institute of Technology

Laboratory for Nuclear Science

Cambridge, Massachusetts

Abstract

We report on the most recent results measuring the behaviour of wire chambers which might be suitable for EMPACT muon detectors. This includes several measuring techniques, chambers, and gasses.

1. Introduction

This study was initiated to find a particle measuring technique with gas detectors that would be suitable for the EMPACT muon detector system. It would have to be :

1) fast, to tag events at their proper collision time;

2) accurate, $\sigma \simeq 200\mu m.$, but locatable to $50\mu m.$;

3) ammenable to mass production;

4) using non-flammable gas.

Gasses Conidered

A - Isobutane (IB)

A (few %), IB (10%), CO_2

A (few %), IB (10%), CO_2, CF_4

CO_2 - ohmic, slow, cool

CF_4 - flat, fast

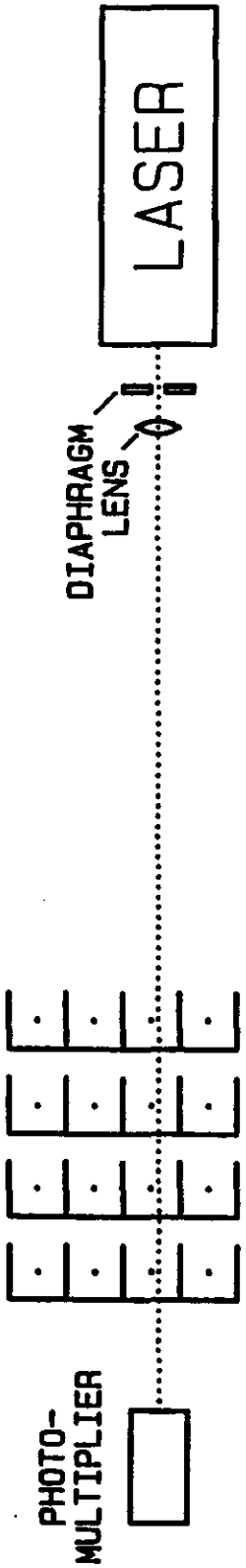

Fig. 2.1

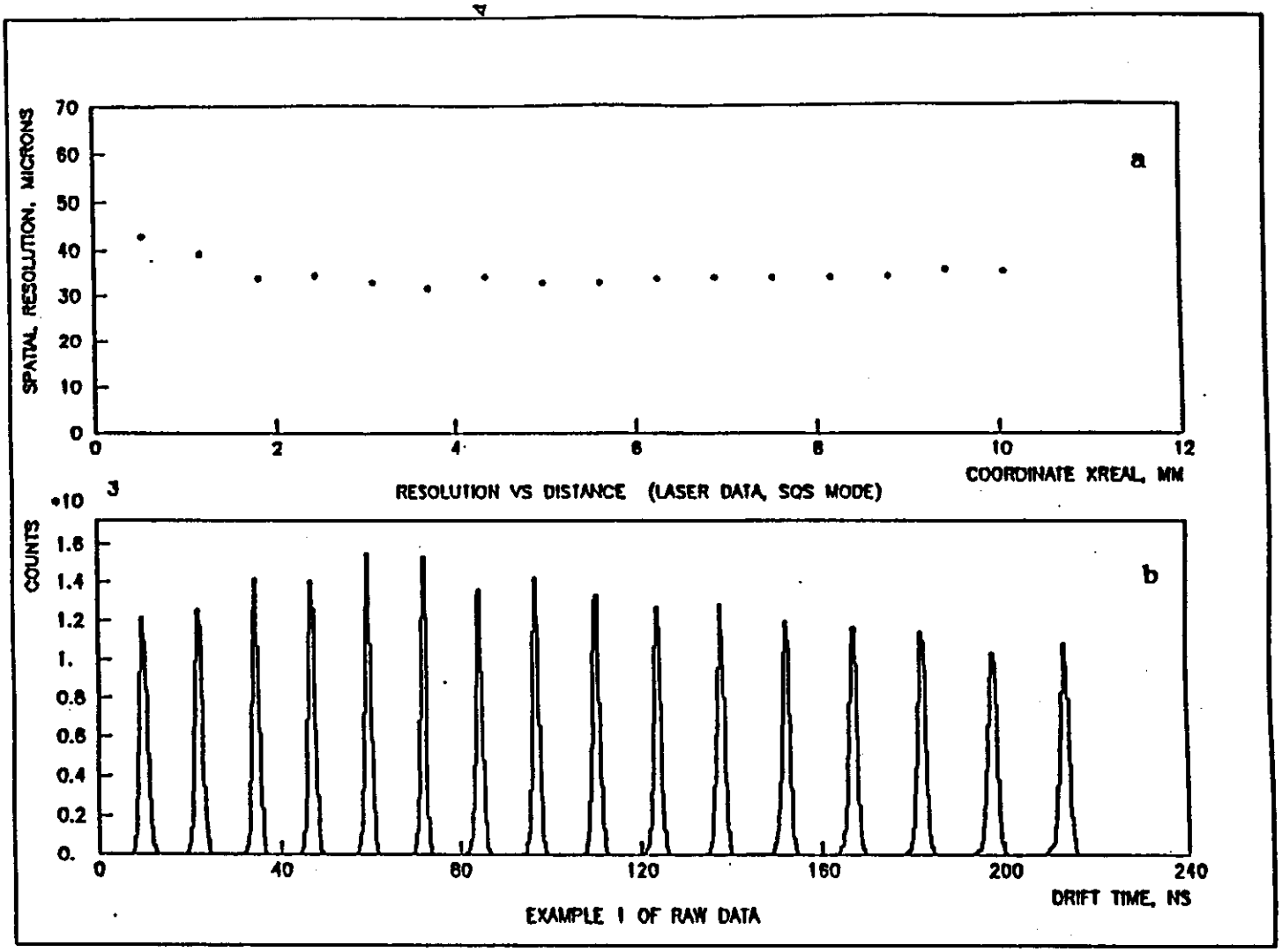
SPATIAL RESOLUTION, MICRONS
70
60
50
40
30
20
10
0
a
0
2
4
6
8
10
12
COORDINATE XREAL, MM
RESOLUTION VS DISTANCE (LASER DATA, SOS MODE)
COUNTS
*10 3
1.6
1.4
1.2
1.
0.8
0.6
0.4
0.2
0.
b
0
40
80
120
160
200
240
DRIFT TIME, NS
EXAMPLE 1 OF RAW DATA

Fig. 3.2

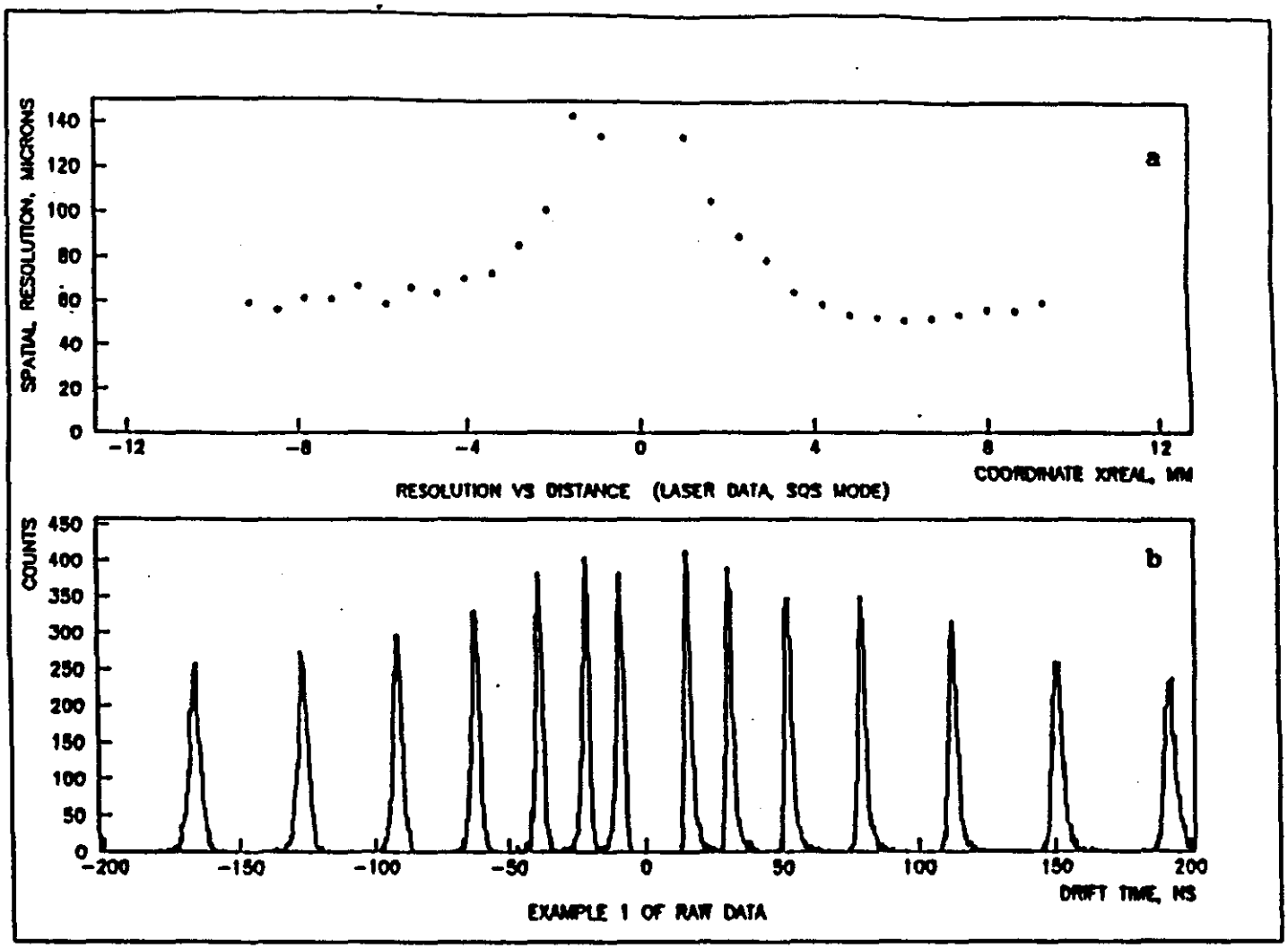
SPATIAL RESOLUTION, MICRONS
140
120
100
80
60
40
20
0
-12
-8
-4
0
4
8
12
a
COORDINATE XREAL, MM
RESOLUTION VS DISTANCE (LASER DATA, SQS MODE)
COUNTS
450
400
350
300
250
200
150
100
50
0
-200
-150
-100
-50
0
50
100
150
200
b
DRIFT TIME, NS
EXAMPLE 1 OF RAW DATA

Fig. 3.6

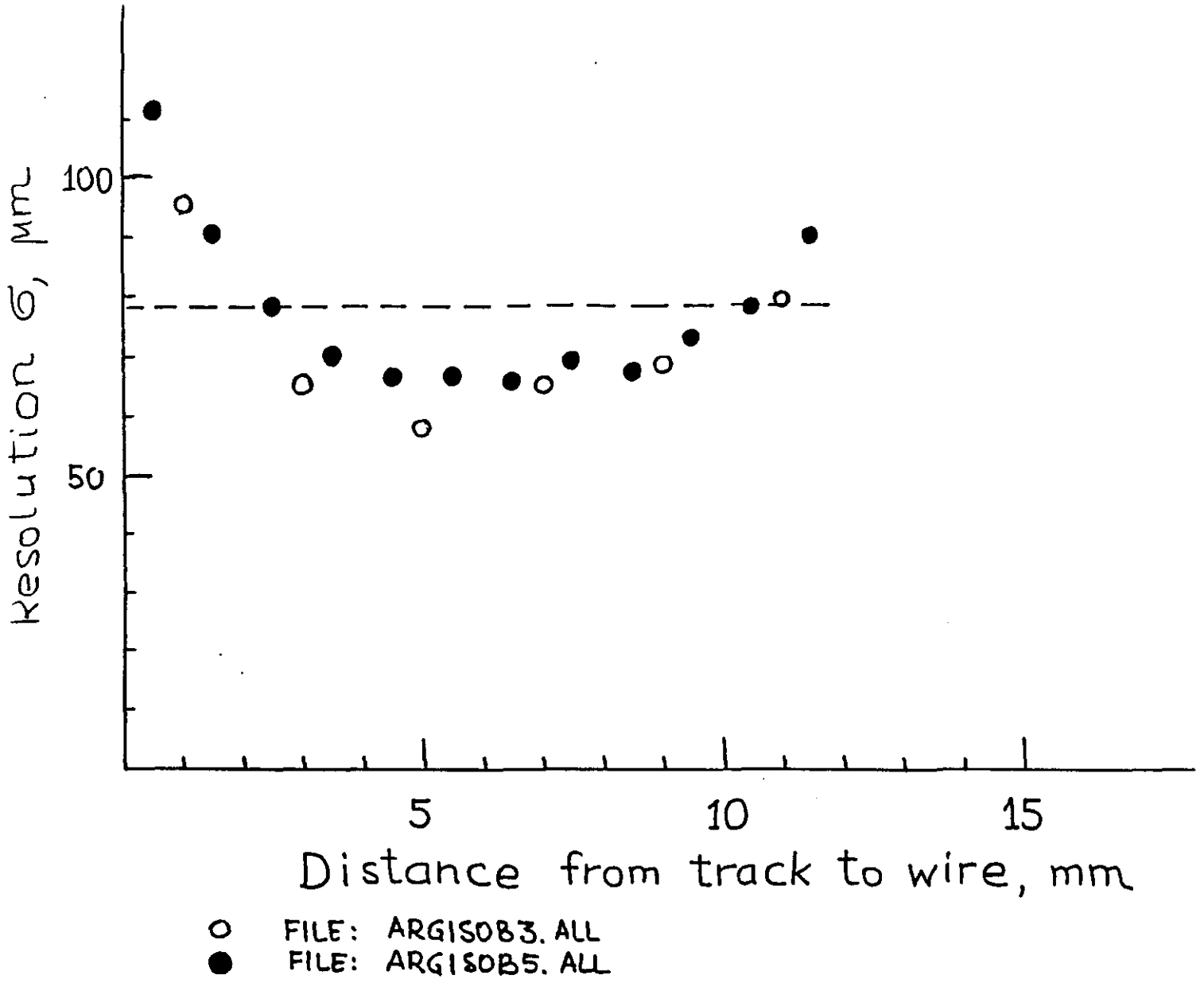
Resolution σ, μm
100
50
5
10
15
Distance from track to wire, mm
FILE: ARGISOB3.ALL
FILE: ARGISOB5.ALL

Fig. A.4

EMPACT MUON TELESCOPE EVALUATION AT FERMILAB

A. Korytov
Joint Institute for Nuclear Research
Dubna, U.S.S.R

K. Lau, B. Mayes, L. Pinsky, R. Weinstein
Institute for Beam Particle Dynamics
University of Houston
Houston, Texas 77204 – 5506

T. R. Marshall
Indiana University
Bloomington, Indiana 47405

J.I. Friedman, E. Hafen, P. Haridas, H.W. Kendall,
T. Lyons, L.S. Osborne, I. Pless, L. Rosenson, R. Verdier
Massachusetts Institute of Technology
Cambridge, Massachusetts 02139

CONTACT PERSON: L.S. Osborne

Bitnet	OSBORNE@MITLNS
Telephone	(617)253-2396
FAX	(617)253-1755

The muon measuring subsystem envisaged for the EMPACT detector at the SSC requires precision muon momentum measurements. Determining the ultimate accuracy of this subsystem requires measurements of high energy real muons, in the pair production region. We are currently building and testing at M.I.T. a telescope of aluminum extrusion streamer chambers. We propose bringing this telescope to Fermilab for evaluation in the E-665 Muon beam. We will study performance dependence on chamber gas, delta ray filters, gas pressure, etc. We will test their performance in drift mode, with pick-up strip detection, and in high pressure mode.

R & D Group

3 x [6m x 0.5m] chambers

Dubna - Design & Test

Houston - Wire placement technique

Le Croy - Timing electronics

Louisiana - Simulations - data analysis

MIT - Design, Construction, Tests

Schedule:

Design - Spring '91

Parts Ordered - June '91

Assembly - Fall '91

Tests - Winter '91 - '92

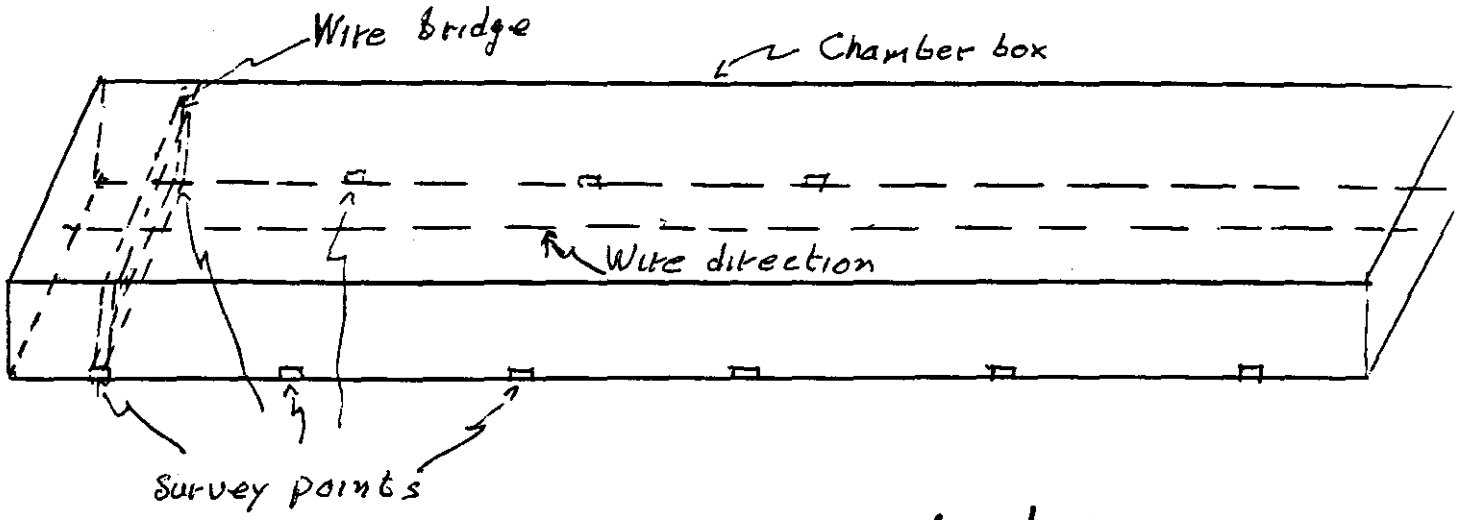

Suitable for mass production

1) Wires layed down mulbiply
2) Machining of boxes done on CNC
3) Cathodes extruded

Philosophy

Wires placed to ± 50 μm. with respect to survey points

1) independent of gravity
2) " " temperature
3) " " warp and sag in the chamber

Survey points known to ± 50 μm.

1) by surveying
2) by placement (unlikely)
3) by monitoring

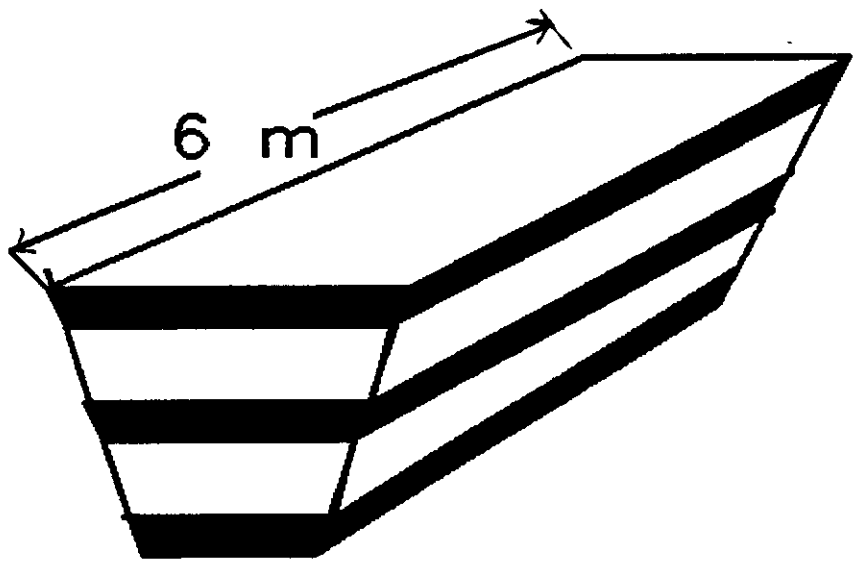

A prototype for R & D

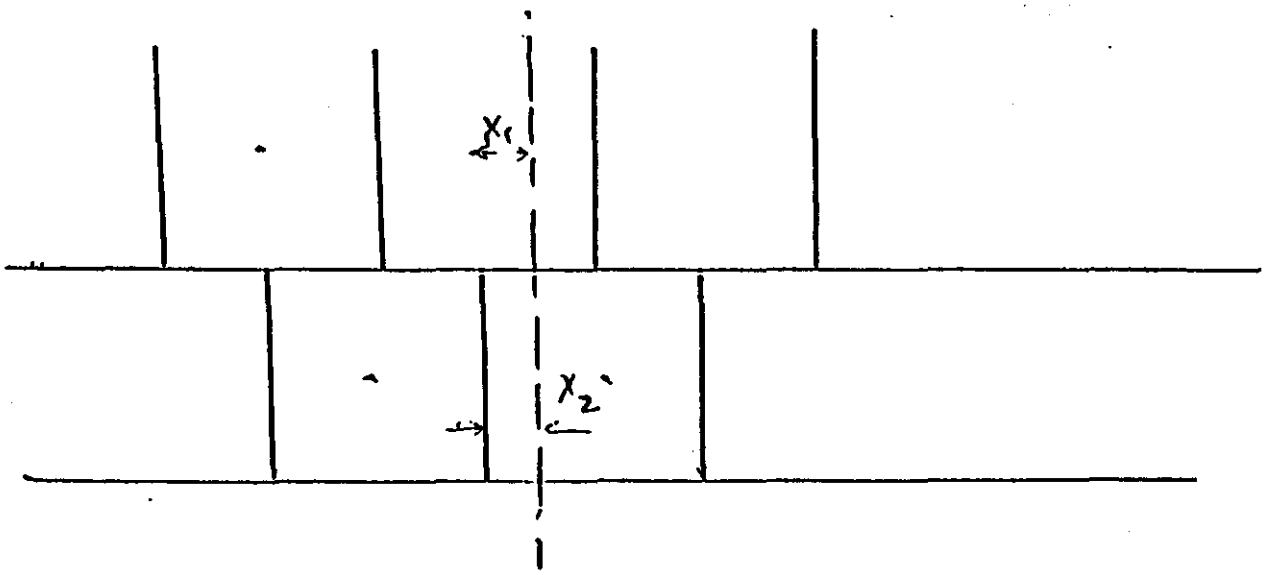

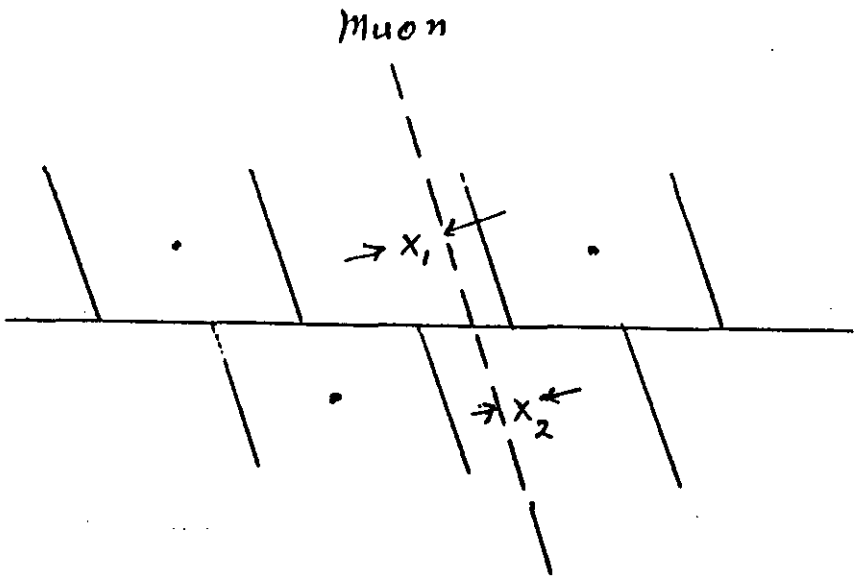

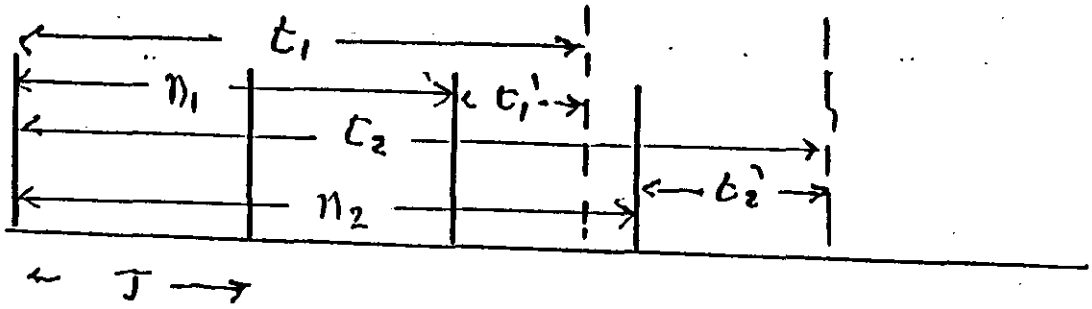

Trip to Le Croy

POLYCHRONAKOS

a) Precision Coordinate

DRIFT TIME MSRMNT

- * Drift Chambers
- Proportional Drif tubes (H.Press, Atm. Press)
- Limited Streamer tubes

etc

CATHODE STRIP CHARGE INTERPOLATION

Proportional Mode LSM

- Chevron Pads
- Honeycomb
- STRIPS

etc

* Basically same technique
* Similar underlying priciples
* Same fundamental limitation

Resolution
~ 0.01 strip pitch

b) Z- Coordinate

* Insensitivity to $\vec{E}, \vec{B}, \vec{v}_d$, P gas mixture
* Same device for Z-msrmnt

c) Trigger

* Same device for trigger

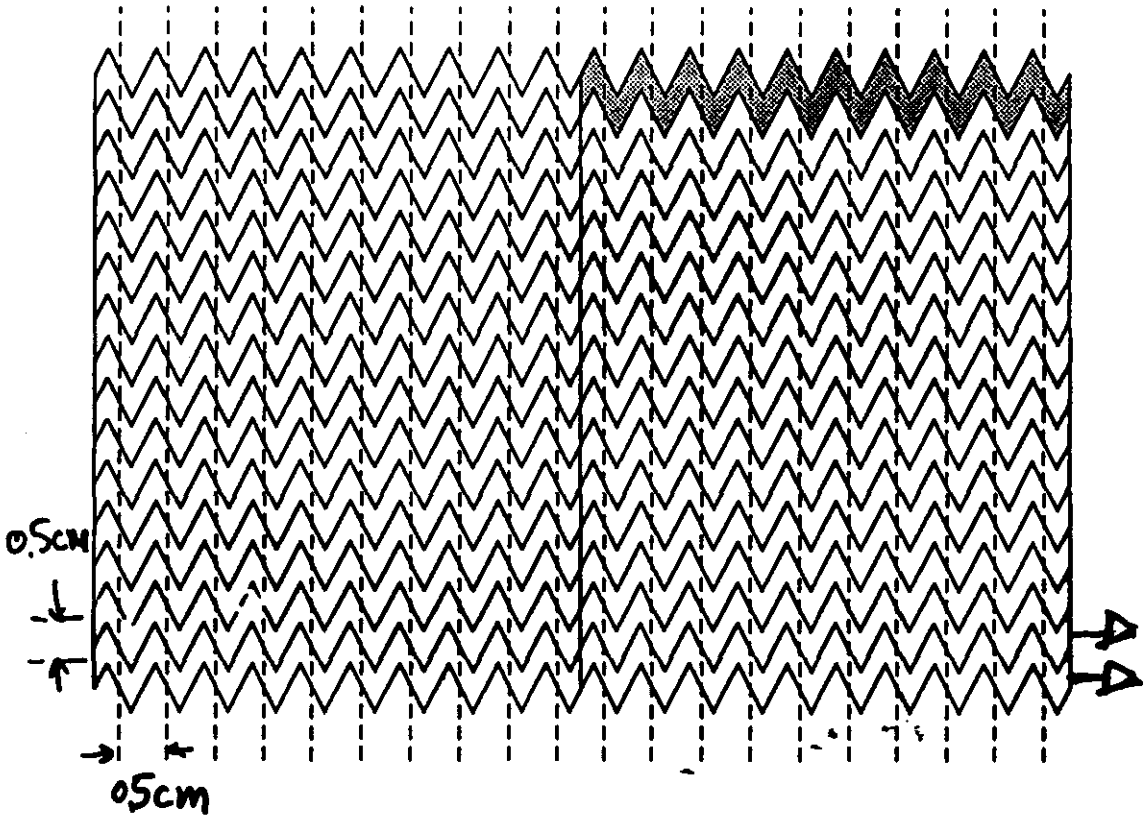
0.5cm
0.5cm

Resolution

Interpolation error $\approx 1\%$ of pad spacing, d
100μm achieved with $d = 1.2cm$

$$\sigma \propto \frac{\overline{ENC}}{Q}$$

$$\overline{ENC}^2 = 16\frac{2}{3}kTC_D(\frac{\tau_A}{\tau_m})$$

$$\tau_A = \frac{C_{GS}}{g_m}$$

Optimum when $C_D = C_{GS}$

$$\boxed{\overline{ENC}^2 = 16\frac{2}{3g_m}kTC_D^2(\frac{1}{\tau_m})}$$

Aim at $\overline{ENC} \simeq 1000$ e

Then gas gain $\approx 1 - 2 \times 10^4$

Position Resolution vs. Anode Charge
for a Single Chevron Cathode

(5.4 keV X-rays, 12mm readout spacing, 50% Ar + 50% C_2H_6 gas mixture)

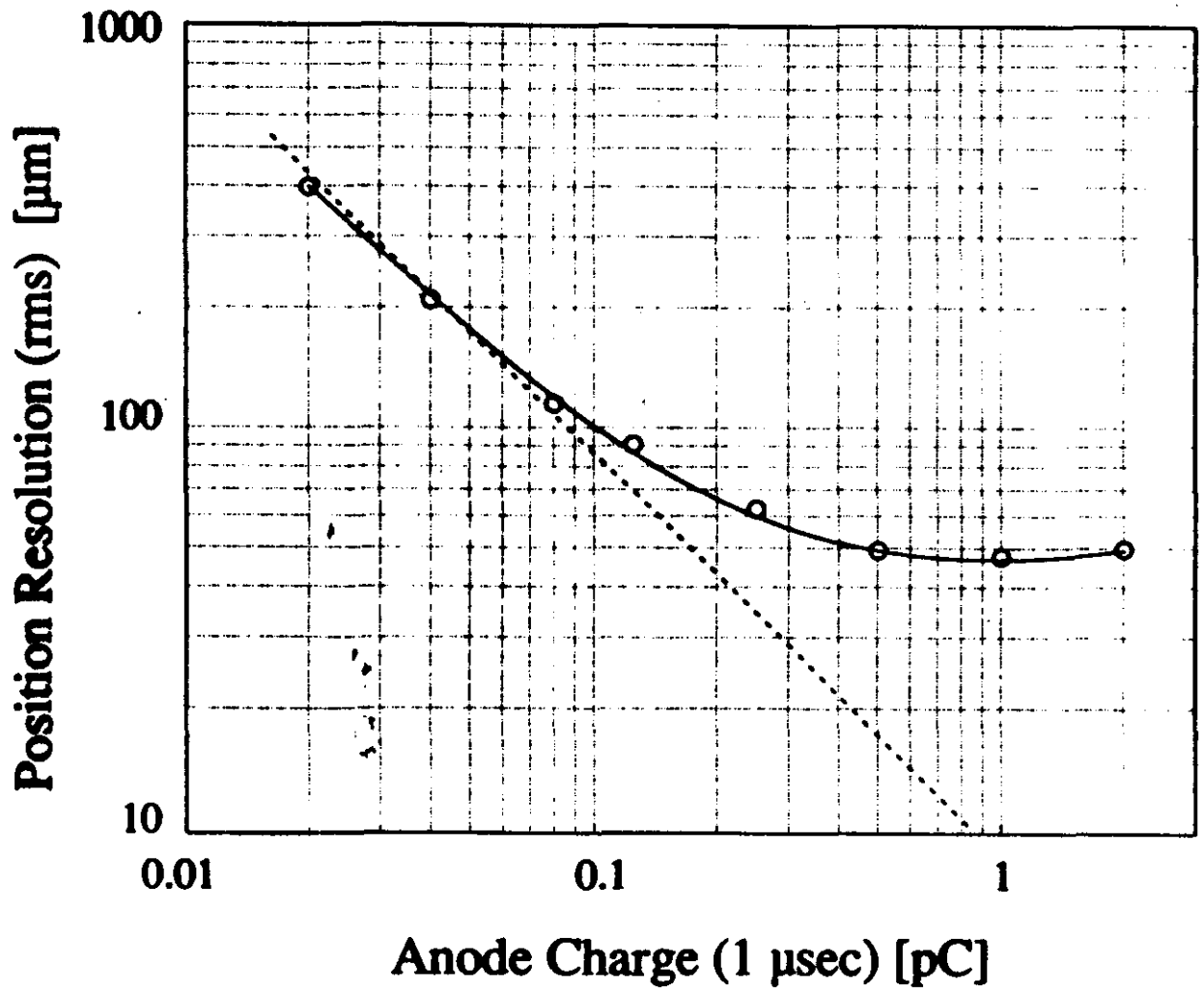

Pad Size

1. Interpolation direction
   - Required Interpolation Preecision ×100
2. Transverse to the interpolation direction
   - Occupancy
   - Channel count
   - Total pad capacitance (≈100 pf)
   - Shaping time (τ_m)

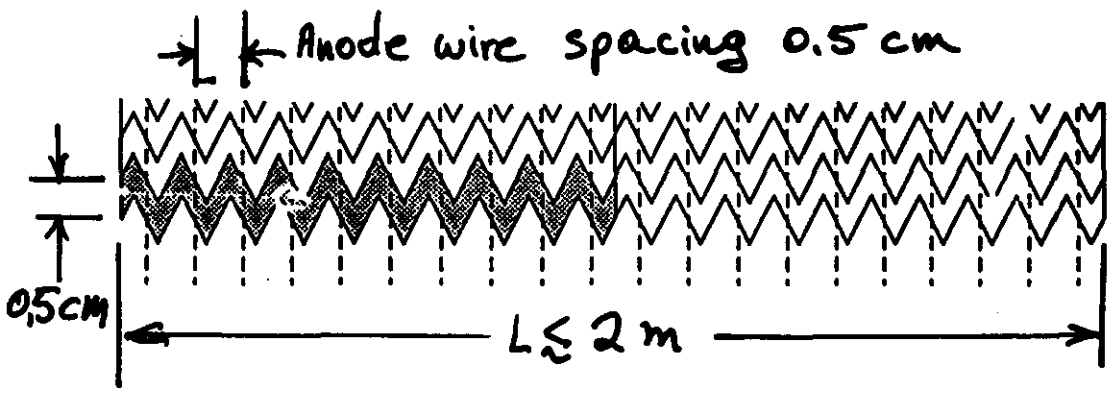

- Inter-chevron capacitance dominates
  $C = 0.2 - 0.3$ pf/cm

<u>Example:</u>
$\mathcal{L} = 10^{33}$, Max. rate/pad 5 Hz, $\tau_m = 1\,\mu s$

- $|\eta| = 2.5$ $L = 10$ cm Limited by occupancy
- $|\eta| < 1.5$ $L = 1.5 - 2$ m Limited by C_D

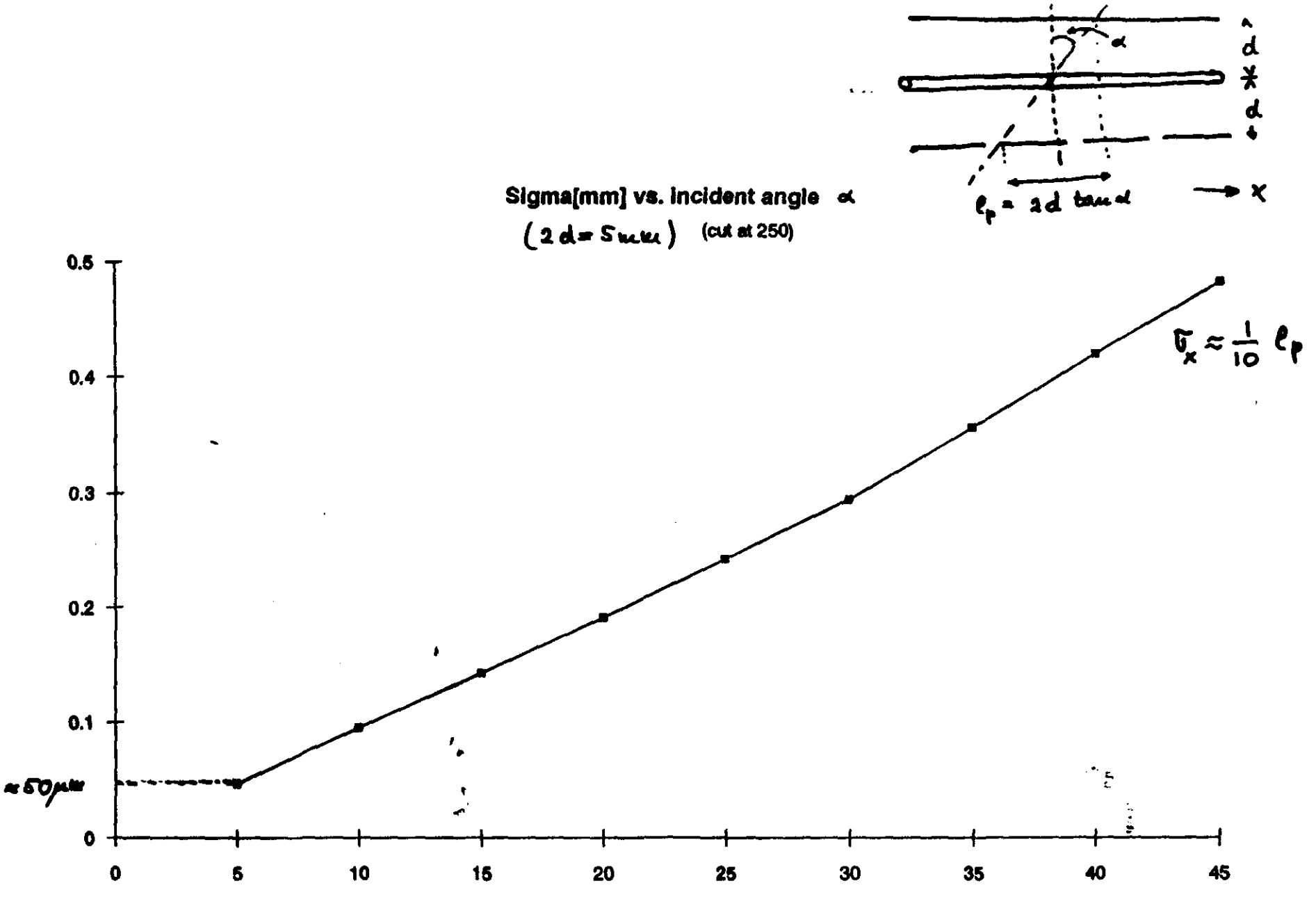
Sigma[mm] vs. Incident angle α
(2d = 5mm)
(cut at 250)
0.5
0.4
0.3
0.2
0.1
0
≈ 50μm
0
5
10
15
20
25
30
35
40
45
d
d
x
$\ell_p = 2d \tan\alpha$
$\sigma_x \approx \frac{1}{10}\ell_p$

Effect of the angle of incidence

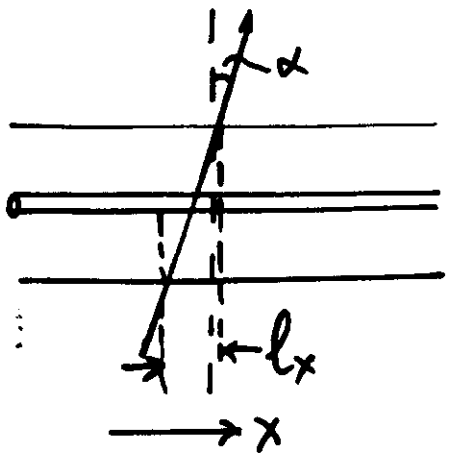

$\frac{\sigma_x}{l_x} \approx 0.10$

(V. Radeka, B. Yu, BNL)

(W. Blum, CERN Workshop)

$$\frac{\sigma_x}{l_x} = \frac{d \tan\alpha}{\sqrt{12}\,\sqrt{N_{eff}}}\, l_x^{-1} \qquad d = 0.5\,cm \quad N_{eff} = 3$$

$$= 0.08$$

Assuming $\sigma_z \approx 50\mu m$

$\theta_{max} \approx 4.5\,\text{deg} \Longrightarrow$ 40, 9deg segments (Tessaracondahedron)

$R = 4m \quad L_{R\phi} = 0.6m$

$R = 6.5m \quad L_{R\phi} = 1.0m$

$R = 9m \quad L_{R\phi} = 1.4m$

- **Largest chamber 2×1.5 m^2**
- **Chamber already exisiting in BNL E814, 0.5×2m^2**
- **Precision determined by lithography of cathode planes.**
- **No extraordinary precision in placement of anode wires required.**

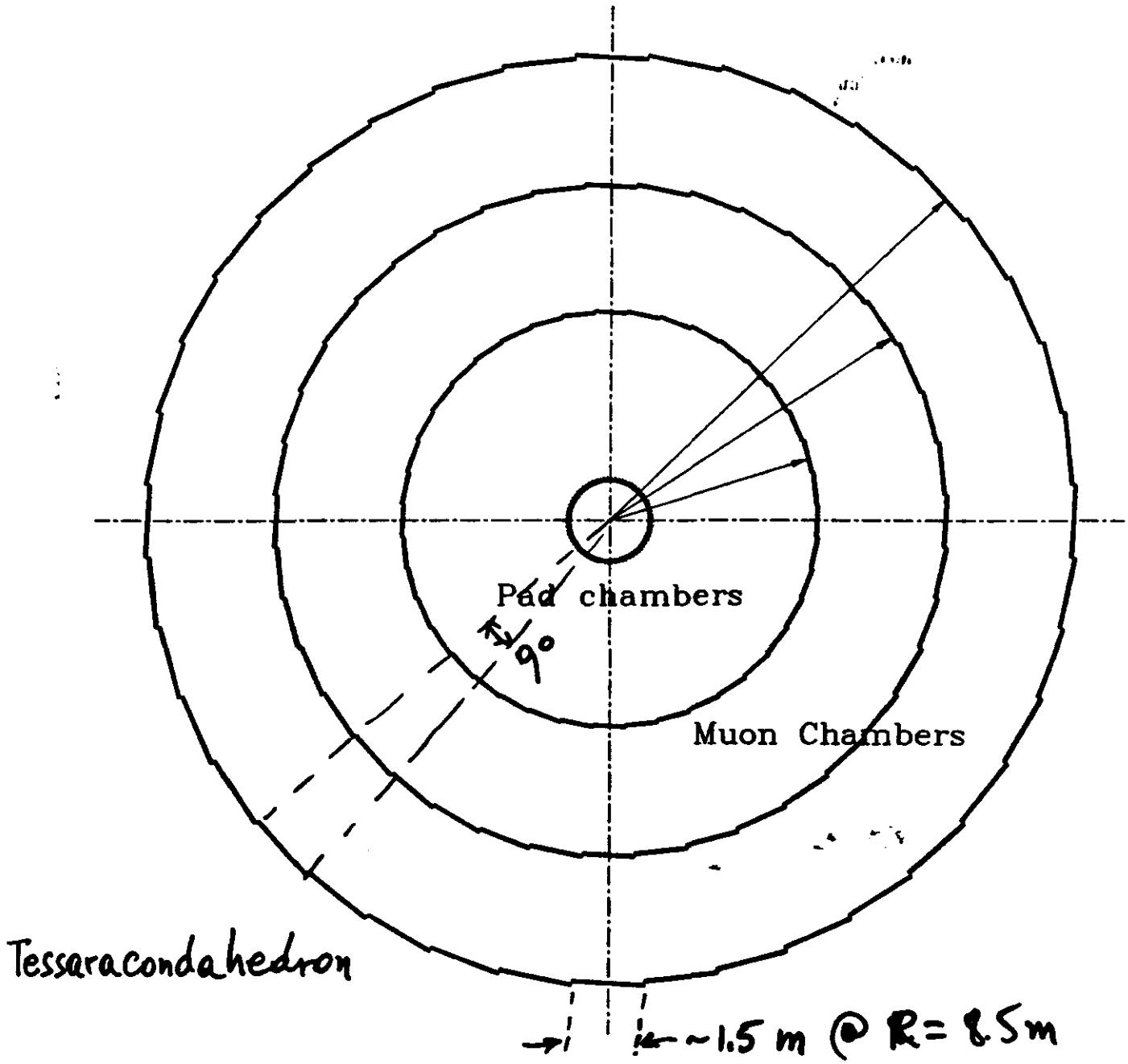
Pad chambers
9°
Muon Chambers
Tessaracondahedron
~1.5 m @ R= 8.5m

CAN BE ADJUSTED ...

$1.5 \lesssim \eta \lesssim 3$

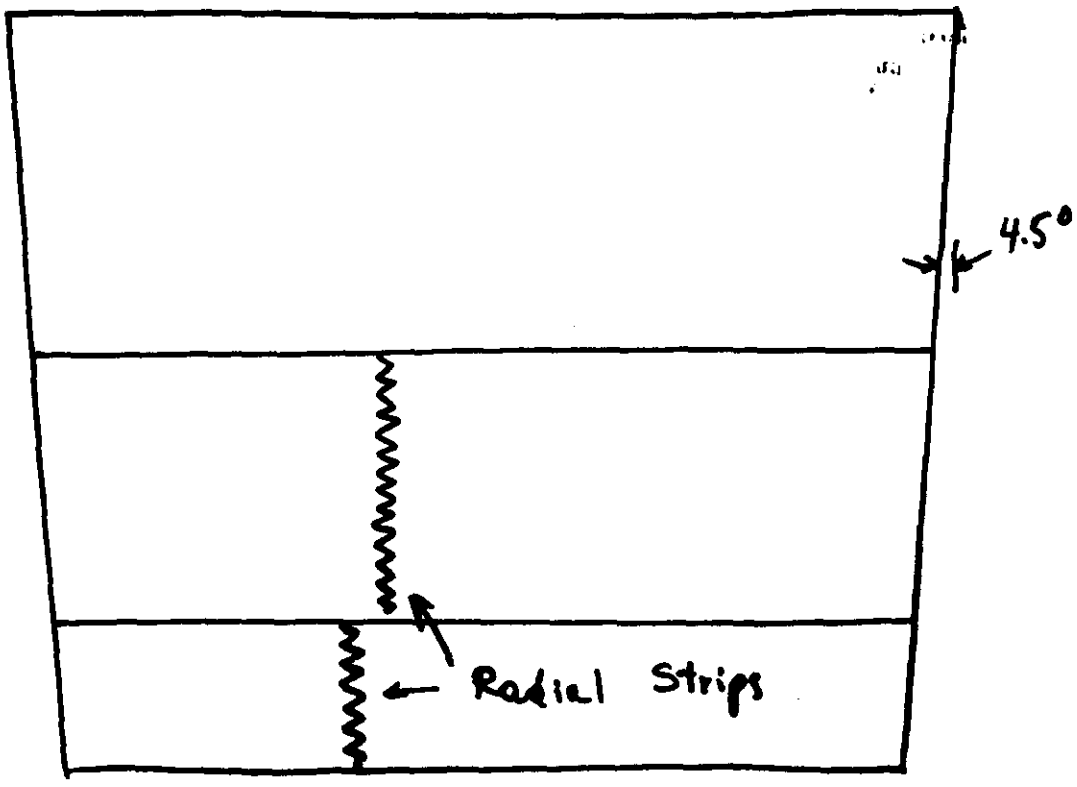

* Length can be adjusted to optimize occupancy
* Capacitance no longer a limitation
* Flexibility in integration time

READOUT

Long integration time (~1us)
⇒ built-in 1st level trigger delay
No analog pipe lines

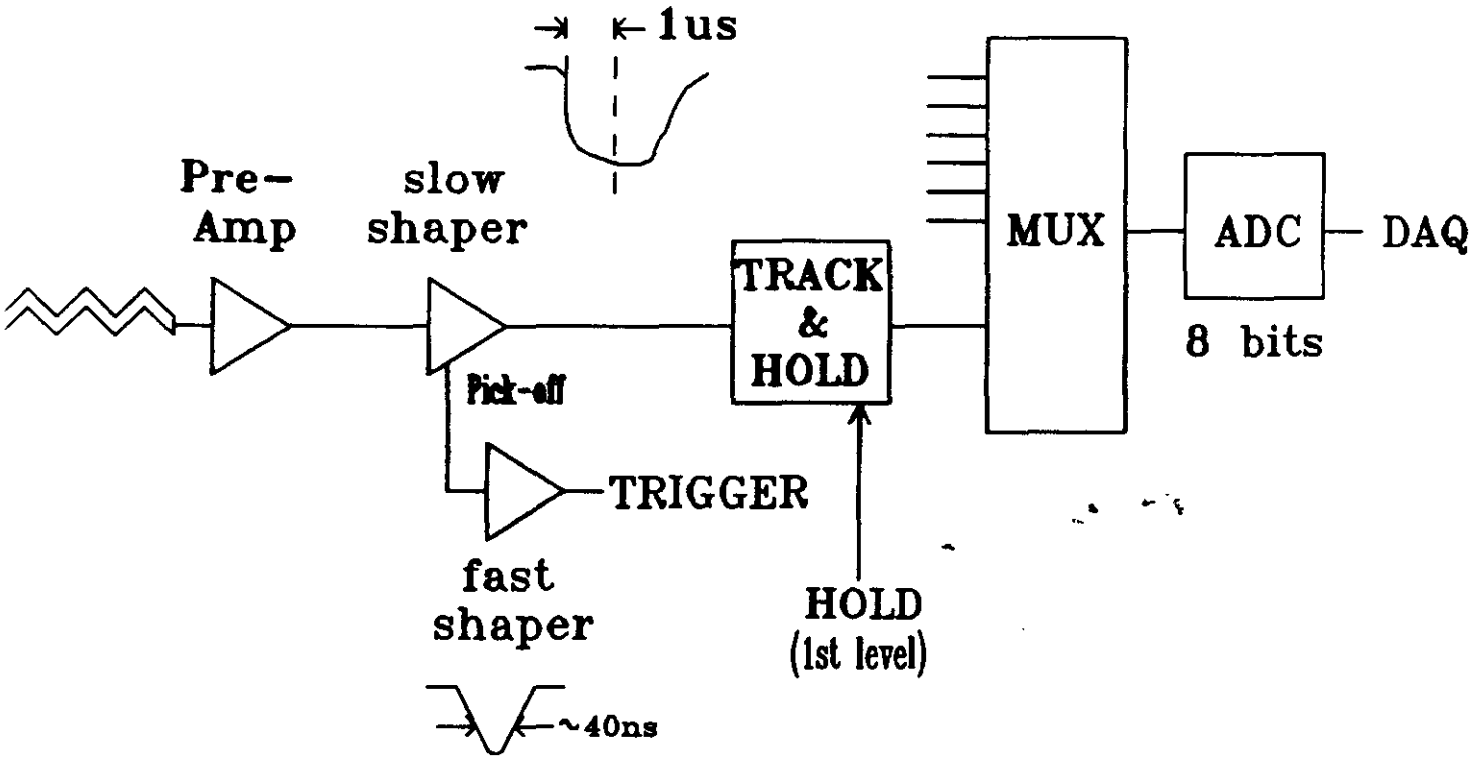

- Same detector for trigger
- Can be done with existing technology
- Path for precision charge measurement does not require 60 MHz clock

CONCLUSIONS

CHEVRON PAD CHAMBERS

* High Resolution (~ 50 μm achievable)
* Space-point measurements (if desired in high η regions)
* Compact Chambers, easy to mass produce
  Could be segmented for further robustness
* Suitable for high η regions
* Z-Readout with same chambers
* No additional chambers for triggering
* Readout with existing Technology
* Insensitivity of resolution on wire position
  $\vec{E}$, $\vec{B}$, $\vec{v}_d$, gas mixture variations

UH-SSC-001

July 16, 1991

Comments on Characteristics of SC/DC Chambers of Interest at SSC

K. Lau, B. Mayes, L. Pinsky, J. Pyrlik, and R. Weinstein
University of Houston

I. Spatial Resolution

A. Spatial resolution perpendicular to wire $\geq 50\ \mu$m (MIT). Dubna ($\sim$ 1980) found 150 μm resolution in a large primitive system.

B. Spatial resolution, along the wire, in principle, is 1 mm.

C. Time information on readout along wire by cross-strips, is useful for multi-hit resolution.

II. Dead Time

A. Dead time is now being studied experimentally in a muon beam at CERN.

B. Results indicate that the chambers operate very well up to a rate of at least 9 kHz/sec, except for expected dead time losses.

C. The expected value of dead time and dead length depends on gas, and the HV, and lies in the region

$$10\ \mu\text{s cm} < \tau_d l_d < 100\ \mu\text{s cm}$$

D. Fig 1 shows the singles rate at CERN. Our chambers extend from r=8 cm to r = 200 cm. We expect $\tau_d l_d$ about 50 μs cm, so dead time effects should be readily seen at smaller r.

E. Module Size. Fig 1 compares dead time inefficiency for $\tau_d l_d = 100\ \mu$s cm , for 1 cm modules and .4 cm modules. Probably modules of $\geq$ 3 cm are OK at angles above 10 degrees. Modules of 1 cm and even .4 cm may be desirable at smaller angles due to both dead time, and lifetime considerations to be discussed later.

F. Magnitude of dead time problem at SSC depends on the luminosity, angle, and background.

G. One problem with dead time noise it that it is correlated among many layers. It is not statistically independent.

III. Plateau Width

A. It is not yet clear what cathode material will be chosen.

B. We note the following about carbon-coated cathodes:

1. The average SCARF plateau on C-coated cathode is alomst 1000V. (See Fig 2)
2. The losses in producing such coating are only 2 % when materials are under SCARF control, and 10% when they are not.
3. The minimum acceptance for HV burn-in at SCARF is 5300 V, leading to a minimum plateau of about 600 V rather than 300 V which is typical elsewhere.
4. The ruggedness of the C-cathode coating was proven in the CERN test. After shipment by ordinary sea container with no special precautions, the loss on burn-in of about 800 chambers was 0.4 %. (This is to be compared to a coincidental test in which about 300 chambers were lost when 1000 chambers, produced at Frascati for LVD, were reburned-in.)

IV. Lifetime

A. Lifetime is generally expected to be of the order 1 Coulomb/cm of collected charge at the anode, or about 10^{10} pulses at 100 pC/pulse.

B. The lifetime is, however, very gas dependent and must be checked for any candidate gas.

C. At the EMPACT small angle rates (300/cm^2 /sec), lifetime for a 1 cm chamber would be about 1 year. This is from signal muons alone. The background will decrease this lifetime, which may argue for cell size less than 1 cm at small angles.

D. Double pulsing affects lifetime, dead time, and noise. In the non-flammable gas of CO_2 (88 %), Isobutane (10%), He (2%), as an example, considerable double pulsing occurs and the lifetime may be halved due to this. (Also note that this gas has a much shorter plateau. Fig

2 compares plateaus for this gas to the standard mix.)

V. Efficiency

A. Except for dead chamber areas due to bridges etc, the efficeincy is expected to be high.

B. In the CERN test, pairs of layers are used with about 1/2 cell displacement. Expected efficiency, not counting dead time, is expected to be near 100 %.

C. This measurement is in progress at CERN. To protect the chambers, HV is being gradually increased while efficency is measured. So far, at 50 V above the knee the double-plane efficency is $\geq$ 94 %. (This number includes software losses).

VI. Double Pulsing

As noted above double pulsing shortens lifetime, increases dead time and increases the noise rate. Double pulsing must be studied for a candidate gas.

VII. Poisons, Recirculation of Gas

A. Poison changes all pulse characteristics. In particular, air leakage is unavoidable. If recirculation is used to conserve operating funds this becomes serious.

B. Most recirculating systems remove oxygen, but allows nitrogen to accumulate. The effects of N_2 contamination on the plateau has been studied at SCARF. Fig 3 shows a summary of the results.

C. The design of both the chamber and gas system must be made as leak proof as possible. Blow off of gas may nevertheless be required due to nitrogen accumulation.

E. SC/DC chambers are sensitive to other poisons. For example for nominally 99 % pure isobutane in the US, about 10 % of the supply is contaminated with impurities which seriously affect SC operastion. Most of the poisons are lighter or heavier than isobutane. These are effectively gotten rid off by blow off the "top" of the gas, and discard the "bottom" of the gas. About 2-3 % of gas smaples are contaminated by

a gas of molecualr weight comparable to isobutane. Work to identify this gas is slowly proceeding at SCARF.

VII. Ohter Gas Studies

In addition to lifetime, dead time, and dead length, double pulsing, poison sensitivity, plateau length, all of which are gas dependent, gas drift velocity must be checked (with higher speed desired) and the gas mixture percentages must be varied and studied.

For this and other tests, a UH stack is being assembled. This is a 1 m x 1 m, 12 layer cosmic ray tracker, divided into 3 superlayers. It will have both SC and DC capability in variuos positions of its over 1100 tubes.

IX. Mass production

When the studies of gas, wire and cathode material are in progress mass production criteria must be repeatedly applied. Those SC assembly centers which failed, did so almost entirely on the problems of mass producion.

A thorough knowledge of what construction parameters can and cannot be allowed to slip is essential.

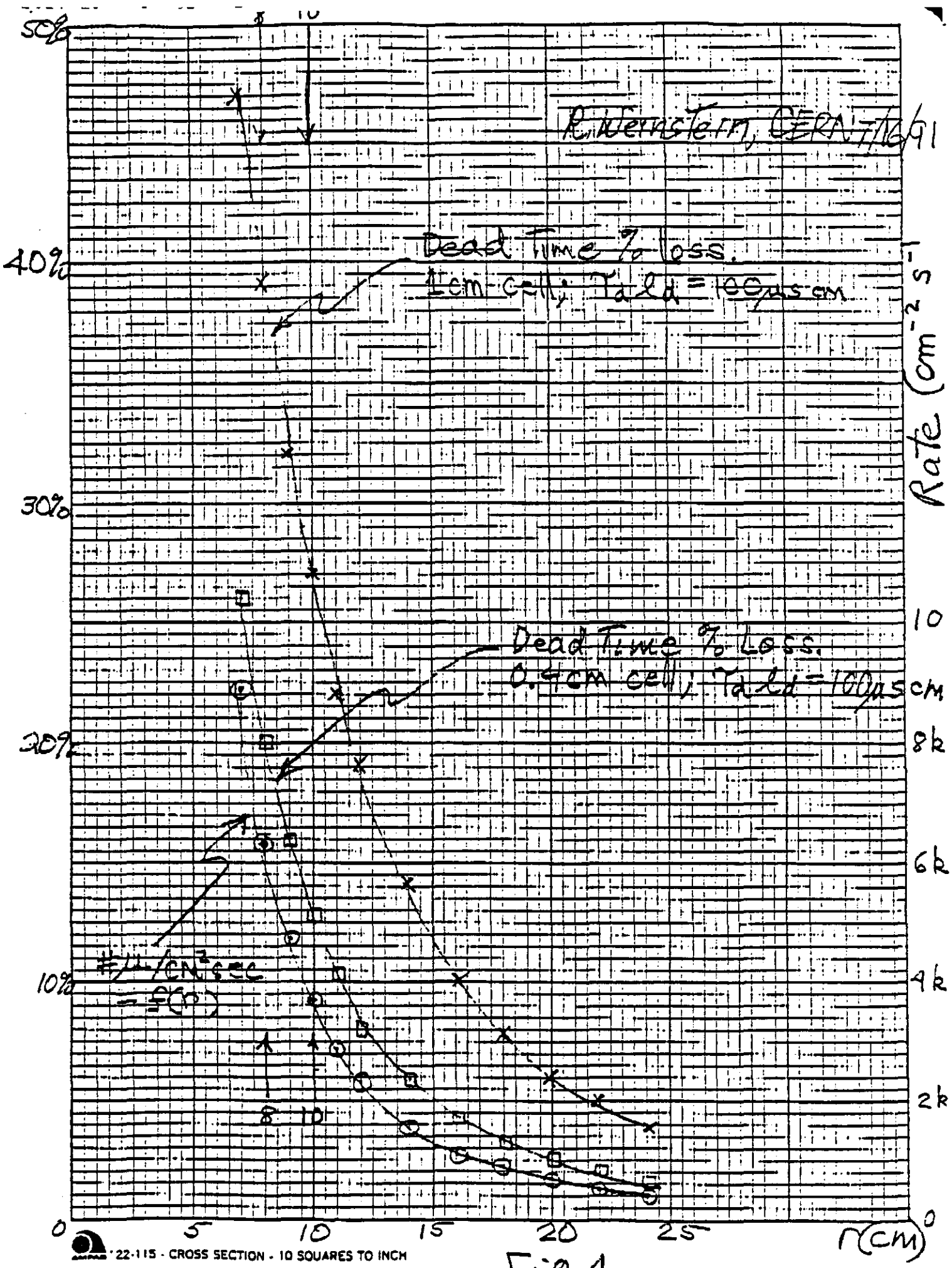
R. Wernstern, CERN 7/16/91
Dead Time % loss.
1cm cell, $\tau_d \ell_d$ = 100μs cm
Dead Time % Loss.
0.4cm cell, $\tau_d \ell_d$ = 100μs cm
#μ/cm²sec = f(r)
Rate (cm⁻² s⁻¹)
r(cm)
50%
40%
30%
20%
10%
0
5
10
15
20
25
10
8k
6k
4k
2k
0
8
10
22-115 - CROSS SECTION - 10 SQUARES TO INCH

Fig 1.

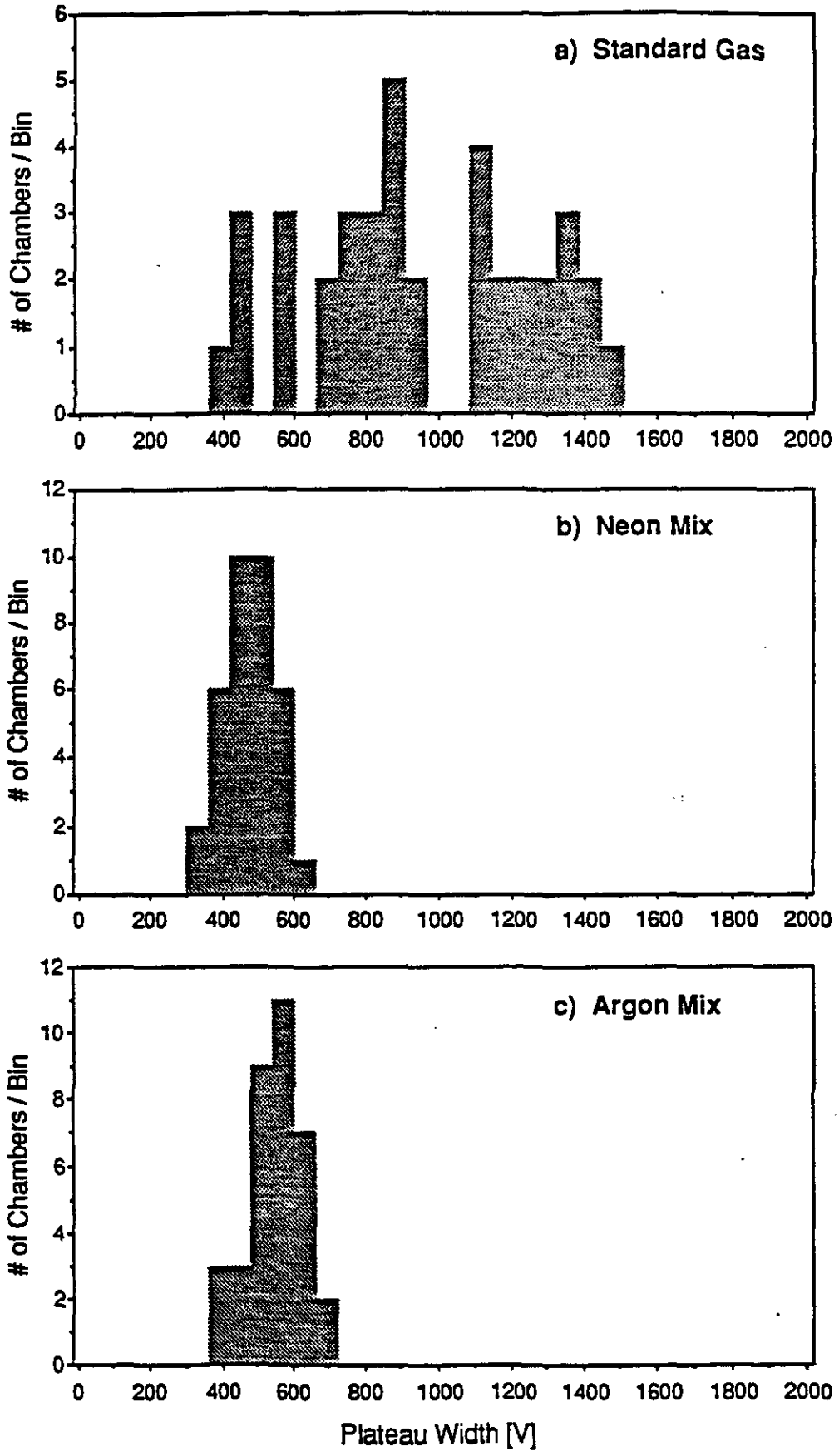

Fig 2 NIM A286 (1990) 155-159

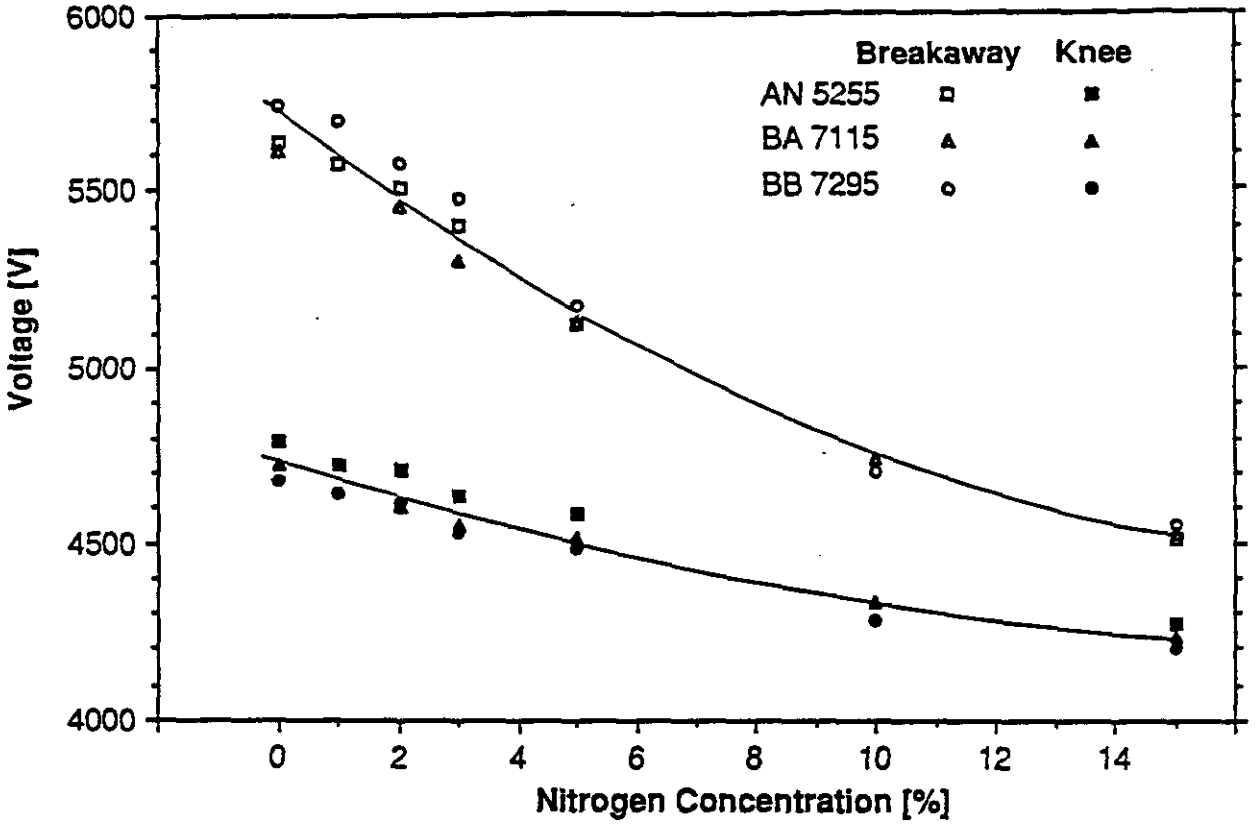

Fig. 3. NIM (in press)

P. HARIDAS
(MIT)
17 July 1991
SSC LAB.

RPC FOR MUON DETECTOR

FUNCTIONALITY

i) PROVIDE 3-FOLD COINCIDENCE MUON TRIGGER

ii) PROVIDE 2-COORDINATE MEASUREMENT USING STRIPS

ADVANTAGE

LOW COST

INTERESTED GROUPS:

E. HAFEN, P. HARIDAS · J. PLESS
MIT

D. ALYEA
INDIANA UNIVERSITY

M. WIDGOFF
BROWN UNIVERSITY

RPC CHARACTERISTICS

SIGNAL RISE TIME	~3ns
SIGNAL WIDTH	~10ns
SIGNAL CHARGE	~100pC

TIME RESOLUTION	~1nsec
SPATIAL RESOLOTION OF CHARGE CENTROID	< 1mm

PULSE AMPLITUDE 0.3 – 0.5 V

SIZE : (RPC layers) **6m x 0.5m.**
(Tested & also used in n-$\bar{n}$ oscillation Expt)

ABOVE INFORMATION FROM :

NIM A261 (1987) 447 R. Santonico et al
& R. Santonico – Talk at CERN MUON DETECTION WORK SHOP JULY, 91

TRIGGER SCHEME

3-FOLD COINCIDENCE.

CAN OBTAIN
FIRST LEVEL TRIGGER
IN < 400 ns.

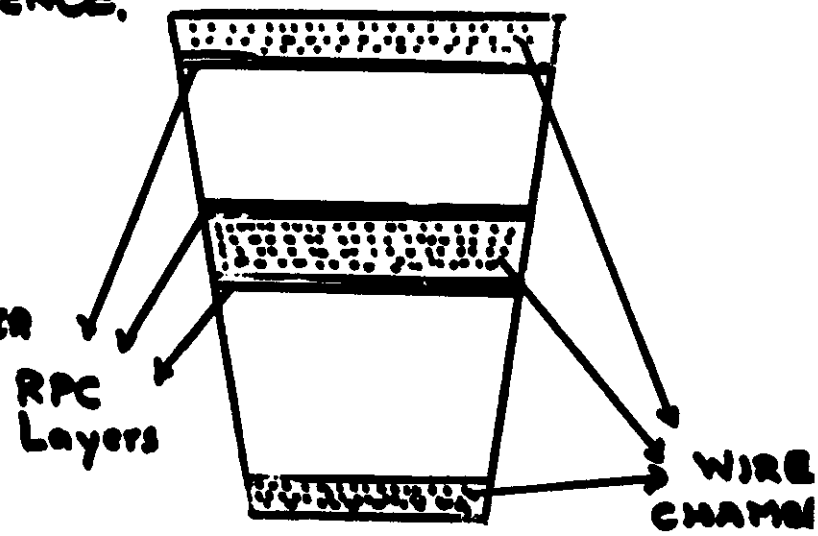

Z COORDINATE MEASUREMENT

U & V STRIPS

STRIPS SIZE :-
NEED TO OPTIMIZE
FOR BEST SPATIAL RES.

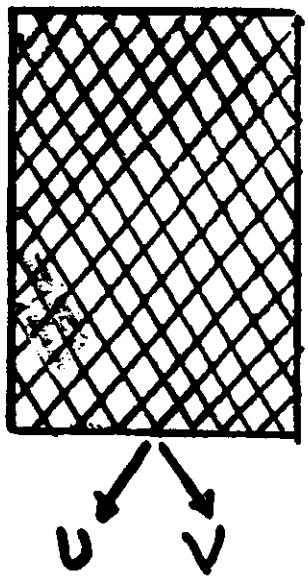

COSTS :-

RPC sheets : \$100 / m^2

READOUT :

DIGITAL (YES/NO)

\$10 /CHANNEL
(13 SP)

ADC READOUT

\$? /channel

R & D EFFORT

1. STUDY SPATIAL RESOLUTION
2. STUDY LARGE FLUX EFFECTS
3. READOUT ELECTRONICS
4. FAST TRIGGER LOGIC;

Introduction

Dallas, Texas

July 17, 1991

Charles Grinnell

- Formerly of C. S. Draper Lab in Cambridge, Mass.

- Currently at CERN for MIT since 09.85
  - 1985-1989; L3 Muon Group responsible for:
    - design and construction of chamber supports
    - assembly and alignment of detector modules
    - installation and alignment in experimental area
  - 1989-1991; L* Muon Group
    - Technical and Financial Coordinator

L* Detector Development

1. Concise description of what was done.

2. What exists?

3. What is applicable to other technology choices being discused?

4. What needs to be pushed now?

Insert 3D of L* - over the last 5 years and many tens of manyears of effort we developed this detector - how and why?

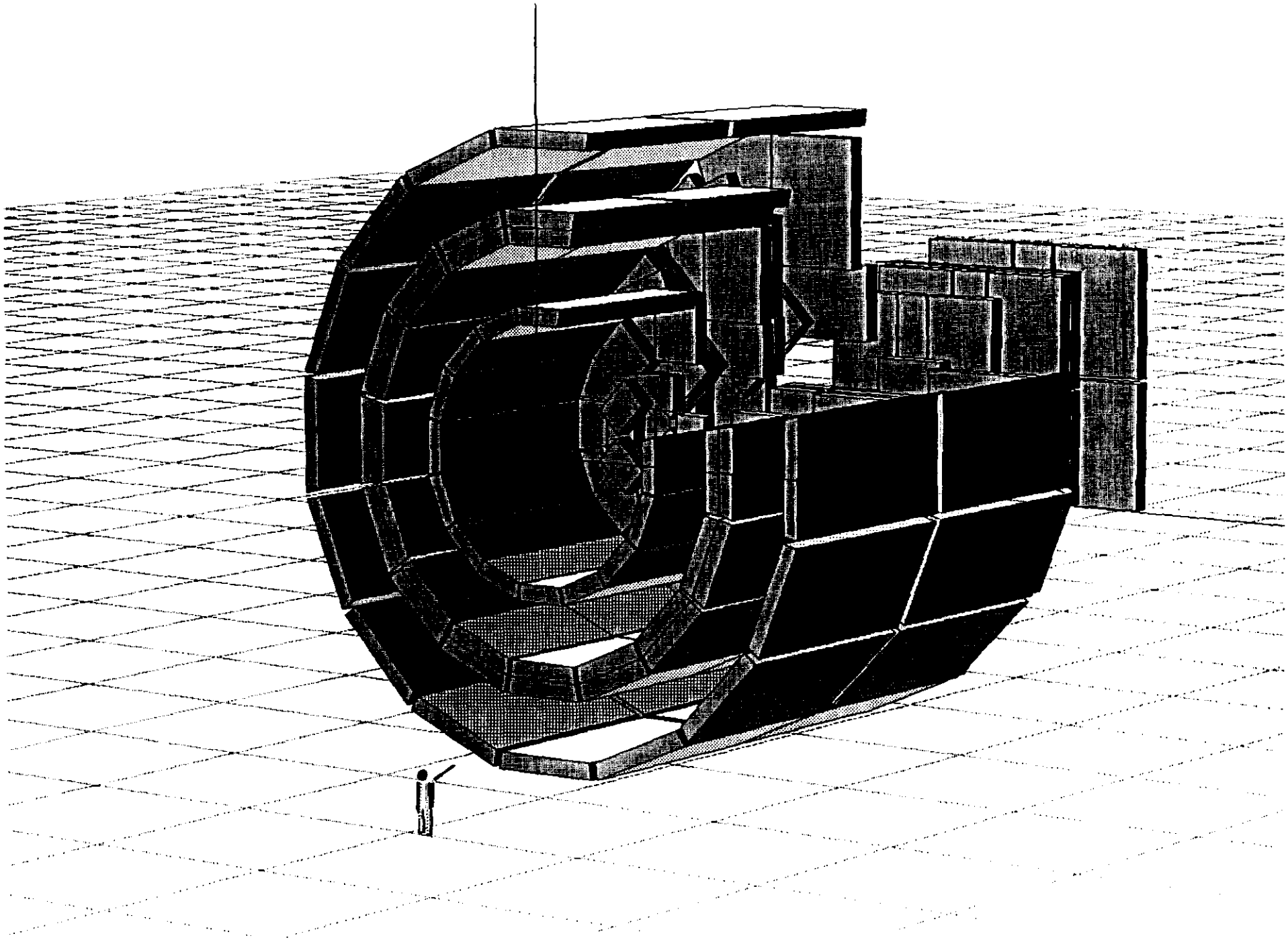

1. What was done?:
L* Layout History

Departure:

1. What had we done in L3 that we would do differently next time?

2. Keep close to L3 philosophies to limit development risks and costs.

Insert: start from origins and go through to L* LOI

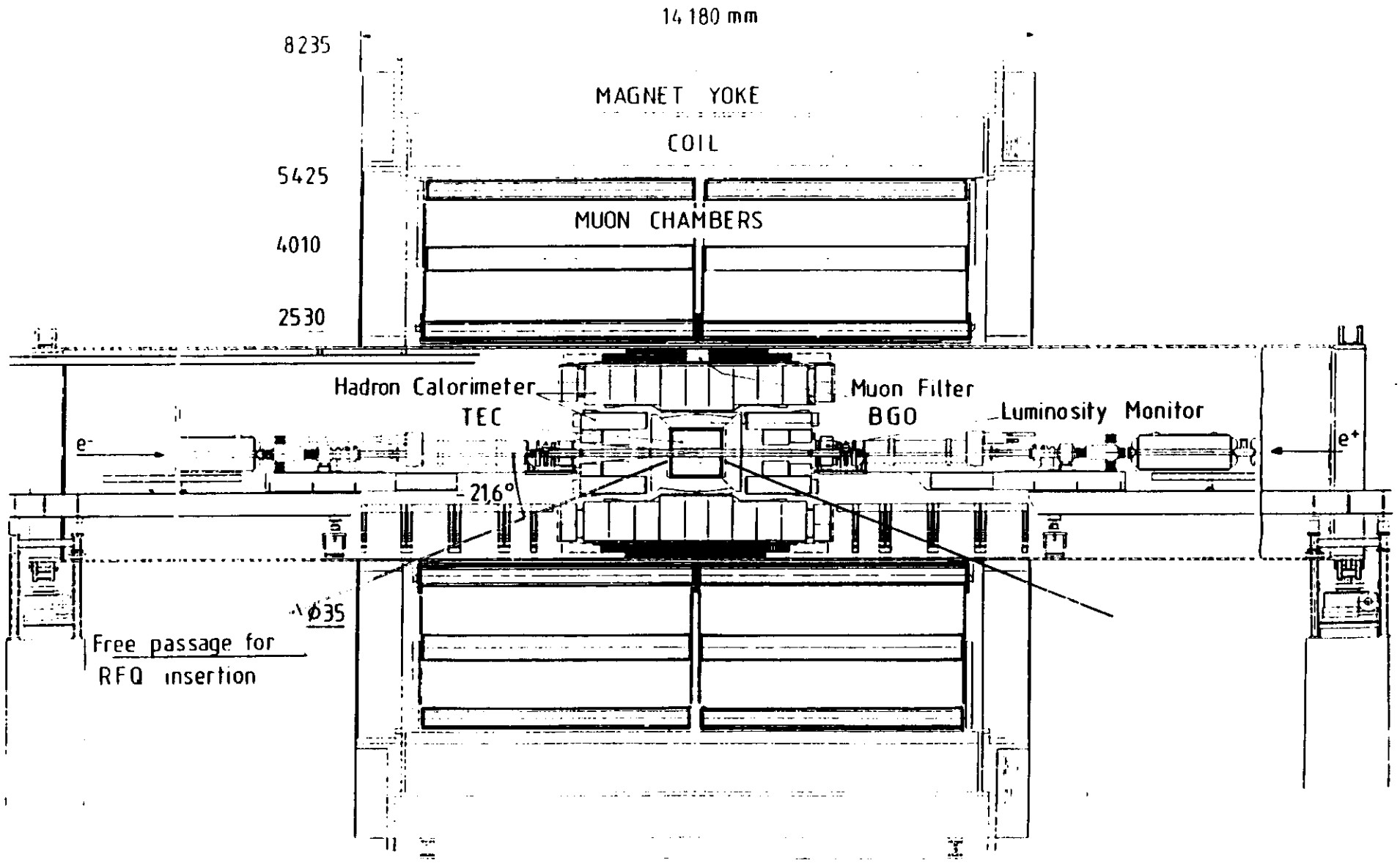

Experiment is on a slope of 1.39%

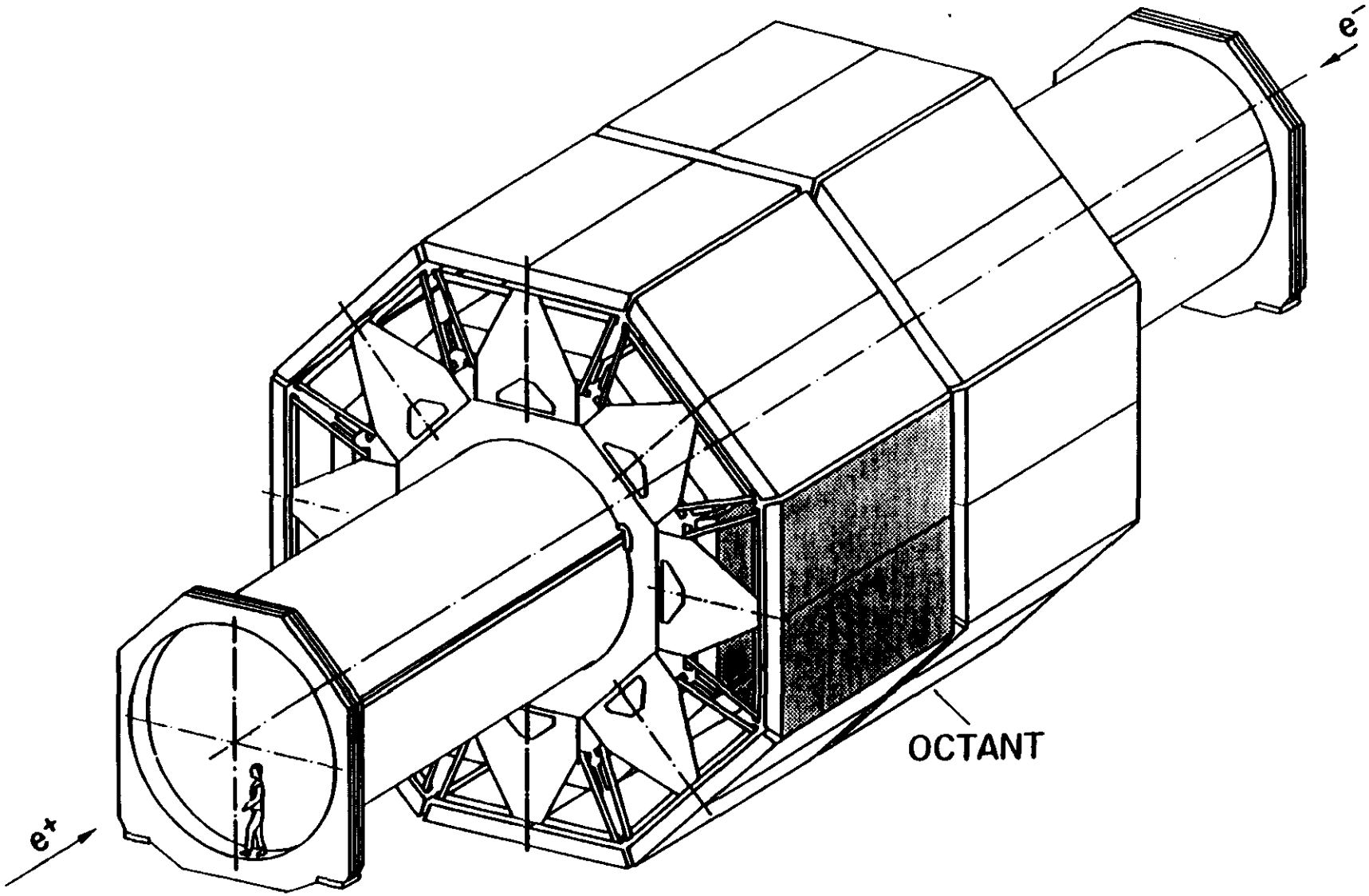
e⁻
OCTANT
e⁺

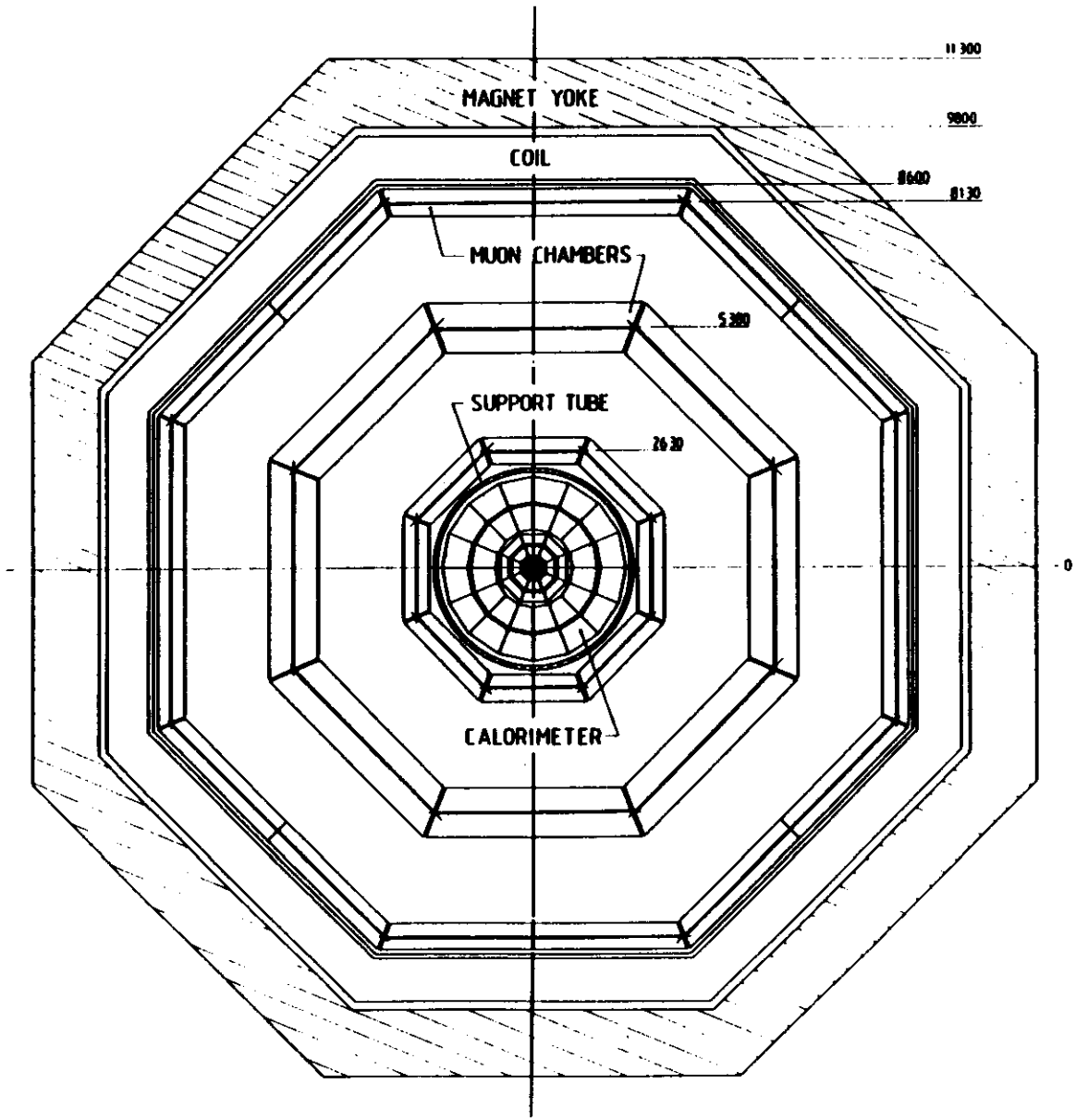

Scale 1 50
27 01 1986

L3+1
DETECTOR LAYOUT

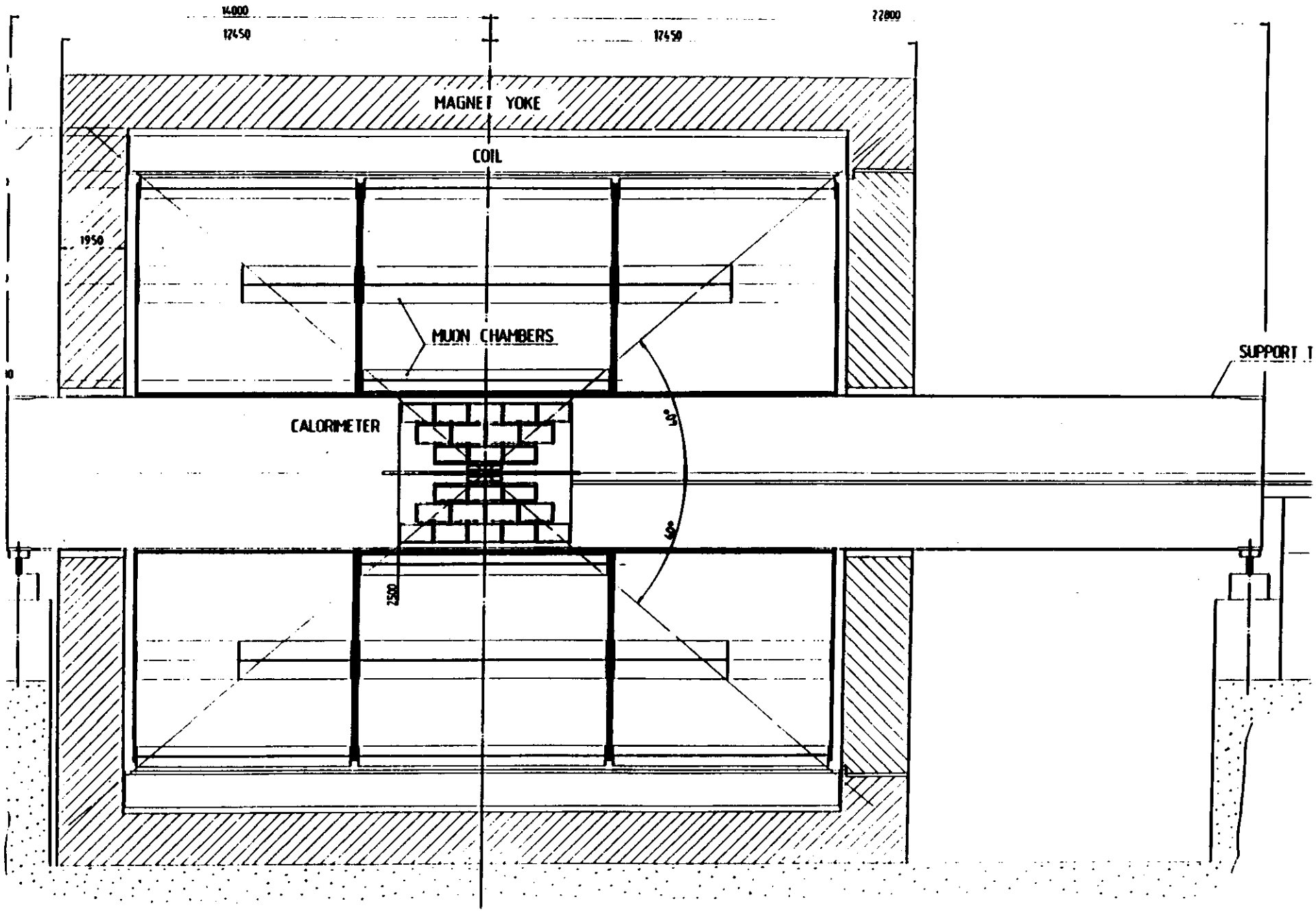
14000
17450
17450
22800
MAGNET YOKE
COIL
1950
MUON CHAMBERS
SUPPORT
CALORIMETER
2500

FIG. 1

13.1

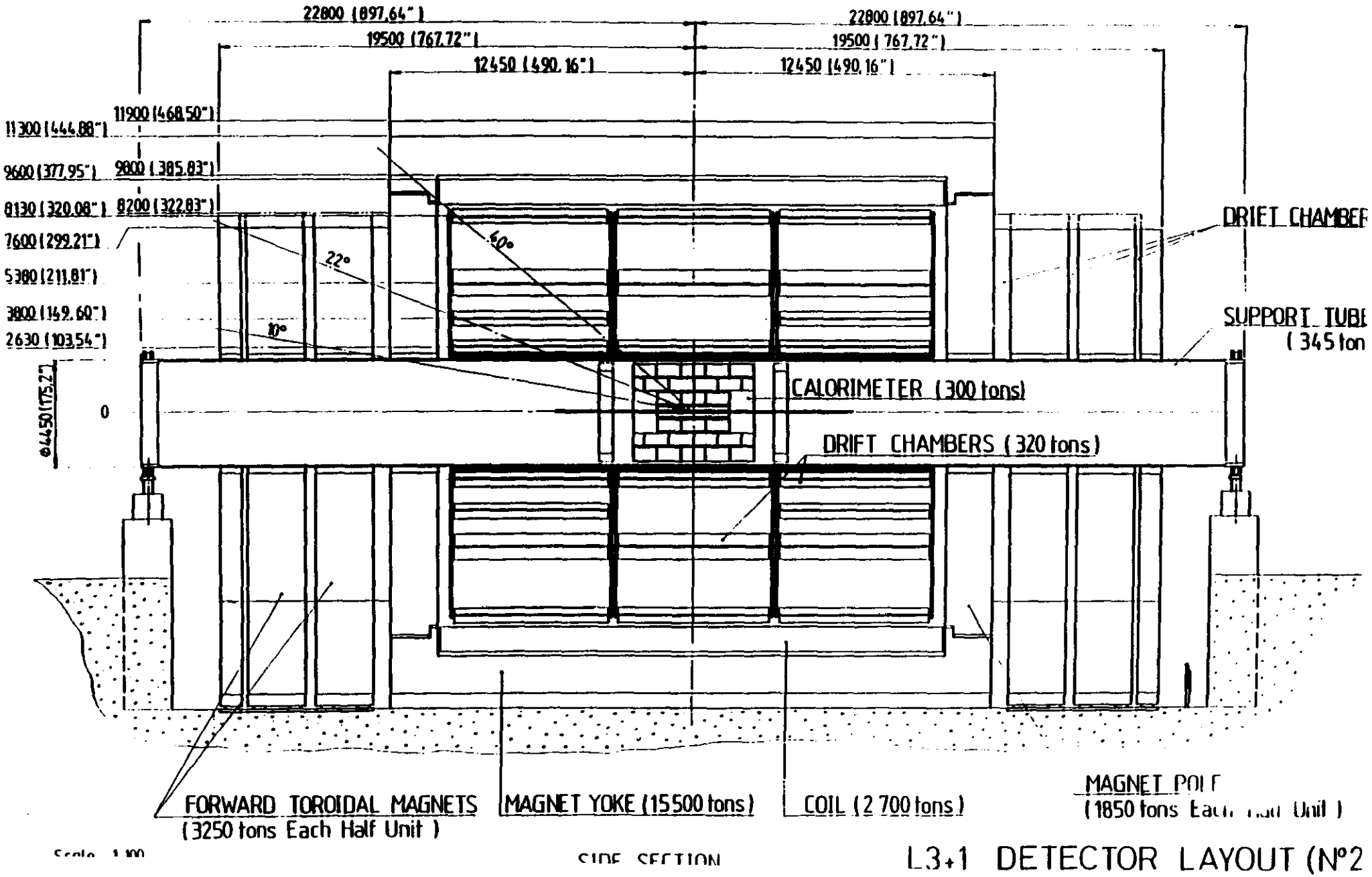
22800 (897,64")
19500 (767,72")
12450 (490,16")
22800 (897,64")
19500 (767,72")
12450 (490,16")
11900 (468,50")
11300 (444,88")
9800 (385,83")
9600 (377,95")
8200 (322,83")
8130 (320,08")
7600 (299,21")
5380 (211,81")
3800 (149,60")
2630 (103,54")
Φ4450 (175,2")
0
60°
22°
10°
DRIFT CHAMBER
SUPPORT TUBE
(345 ton
CALORIMETER (300 tons)
DRIFT CHAMBERS (320 tons)
FORWARD TOROIDAL MAGNETS
(3250 tons Each Half Unit)
MAGNET YOKE (15500 tons)
COIL (2 700 tons)
MAGNET POLE
(1850 tons Each Half Unit)
Scale 1:100
SIDE SECTION
L3+1 DETECTOR LAYOUT (N°2

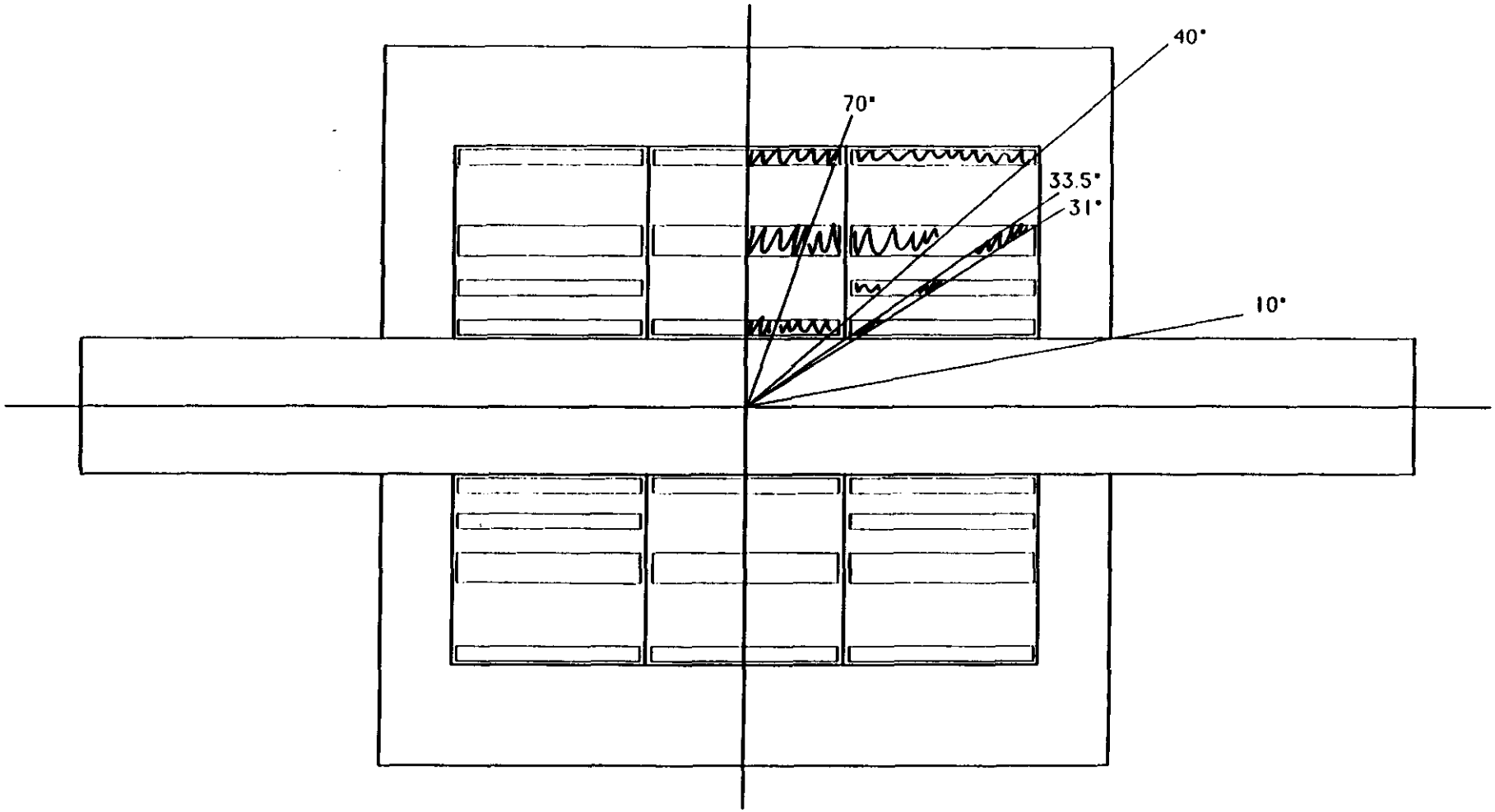
40°
70°
33.5°
31°
10°

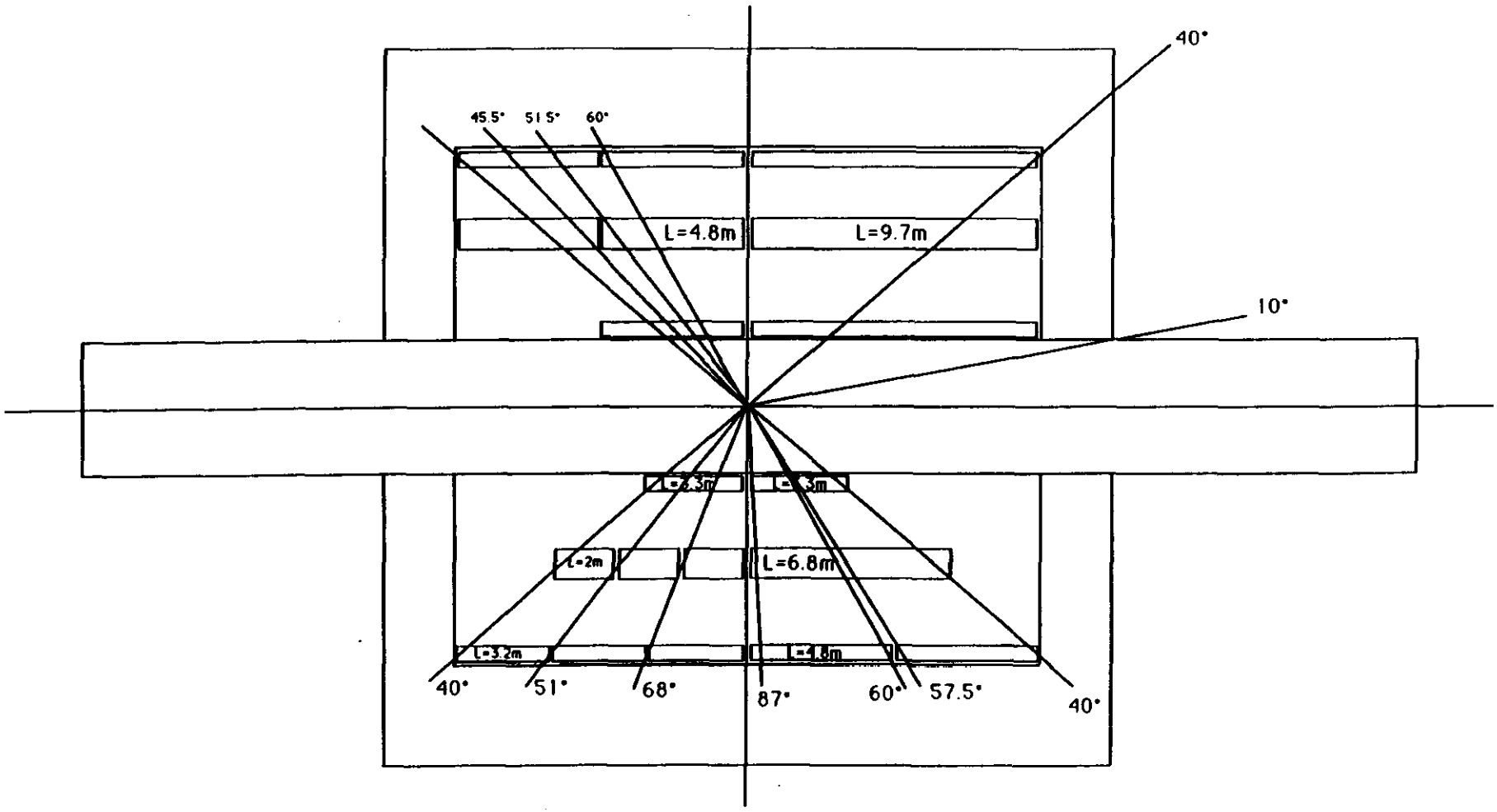
40°
45.5°
51.5°
60°
L=4.8m
L=9.7m
10°
L=2m
L=6.8m
L=3.2m
40°
51°
68°
87°
60°
57.5°
40°

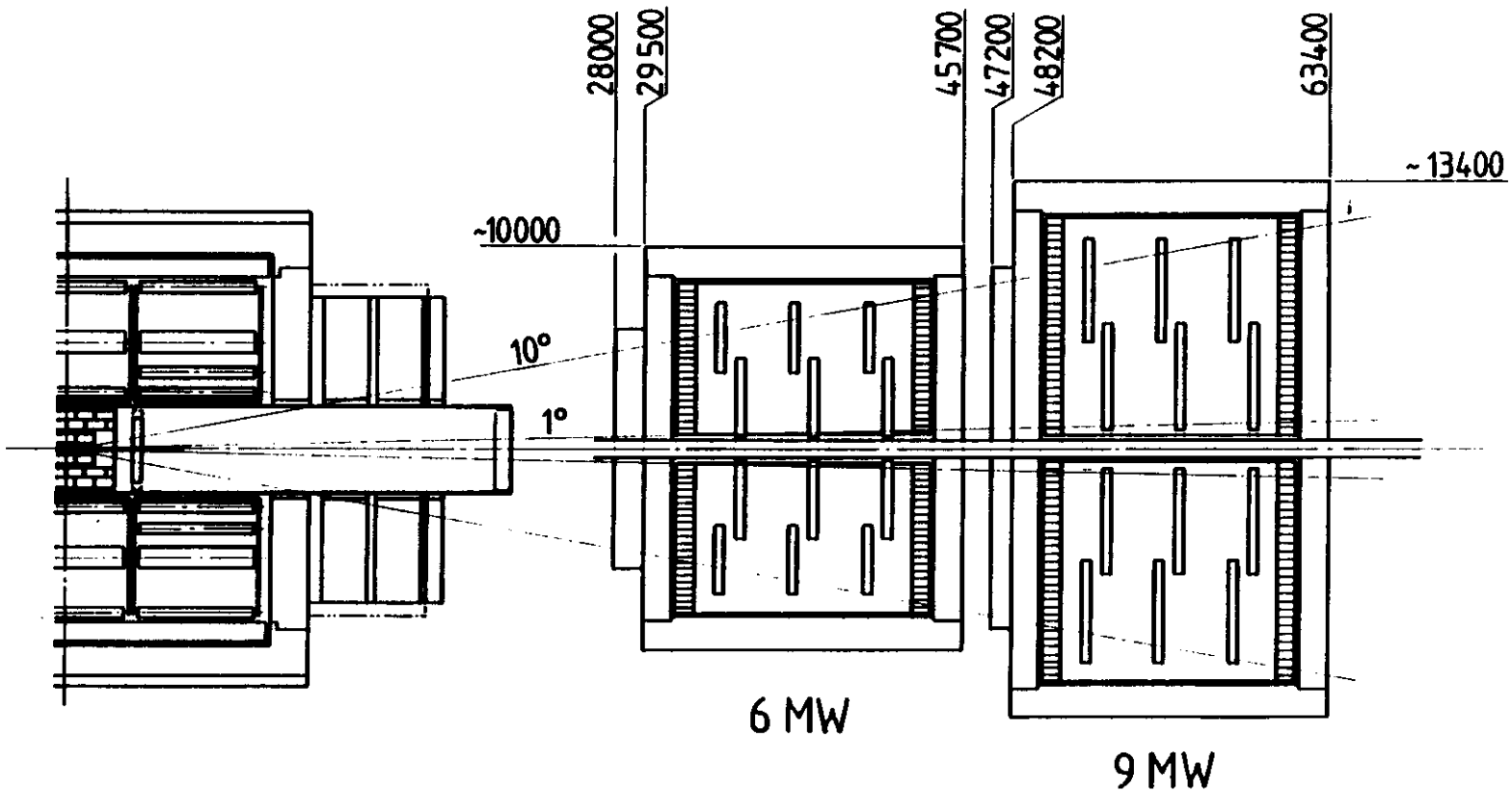

Scale 1:250
17.03.89
C.D

L3+1

CERN/LHC-012/3

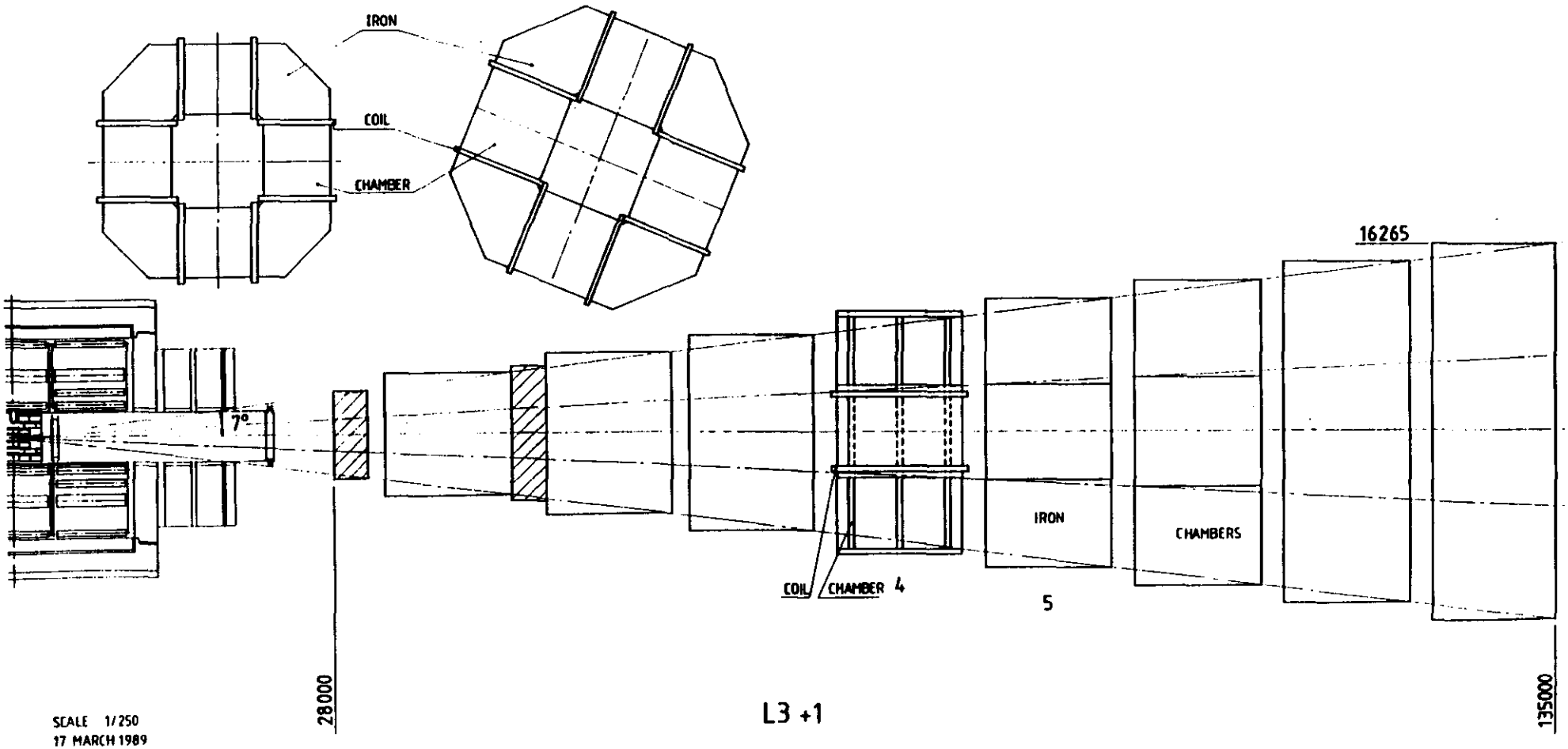
IRON
COIL
CHAMBER
16265
7°
IRON
CHAMBERS
COIL
CHAMBER
4
5
28000
135000
L3 +1
SCALE 1/250
17 MARCH 1989

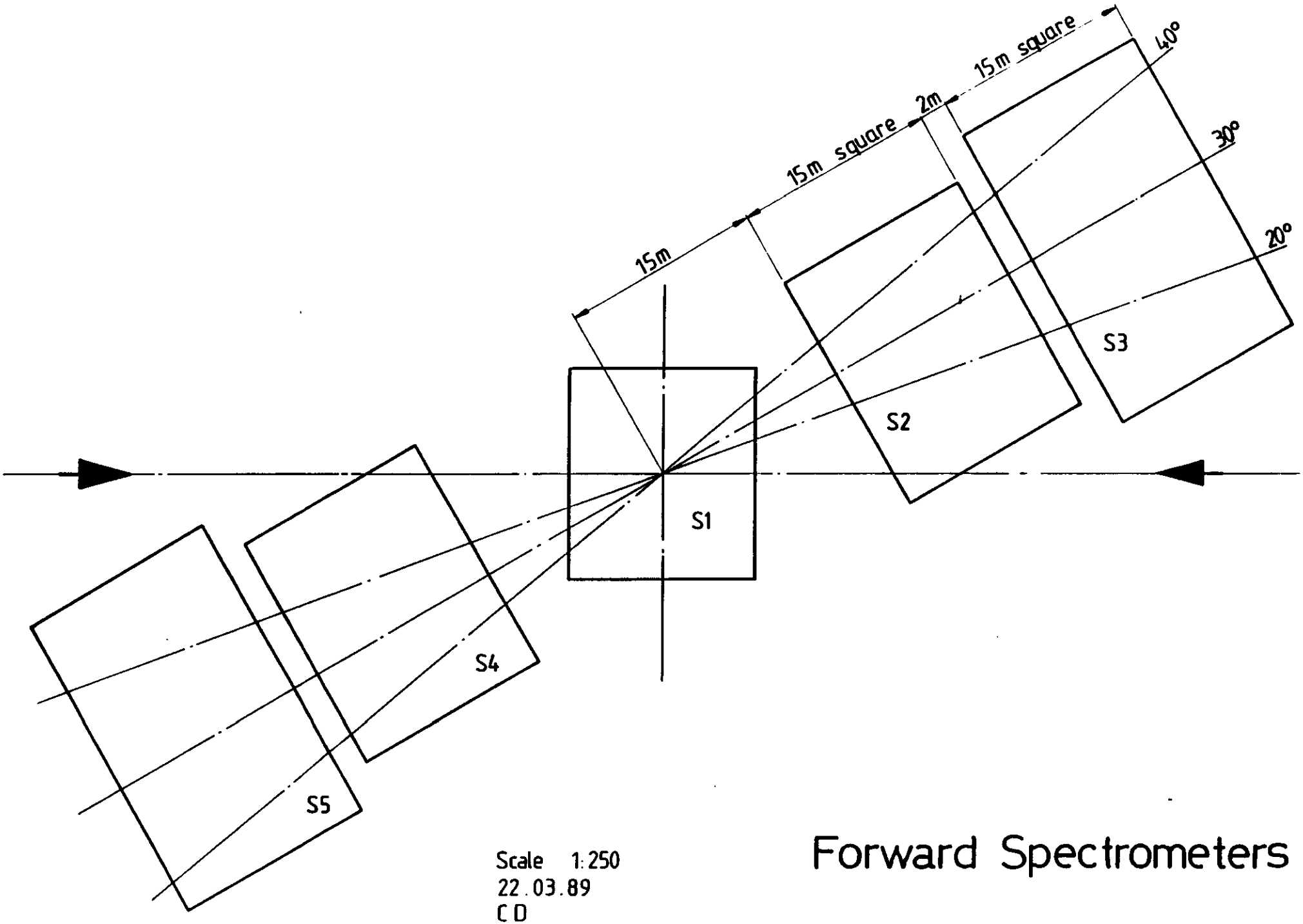

Forward Spectrometers

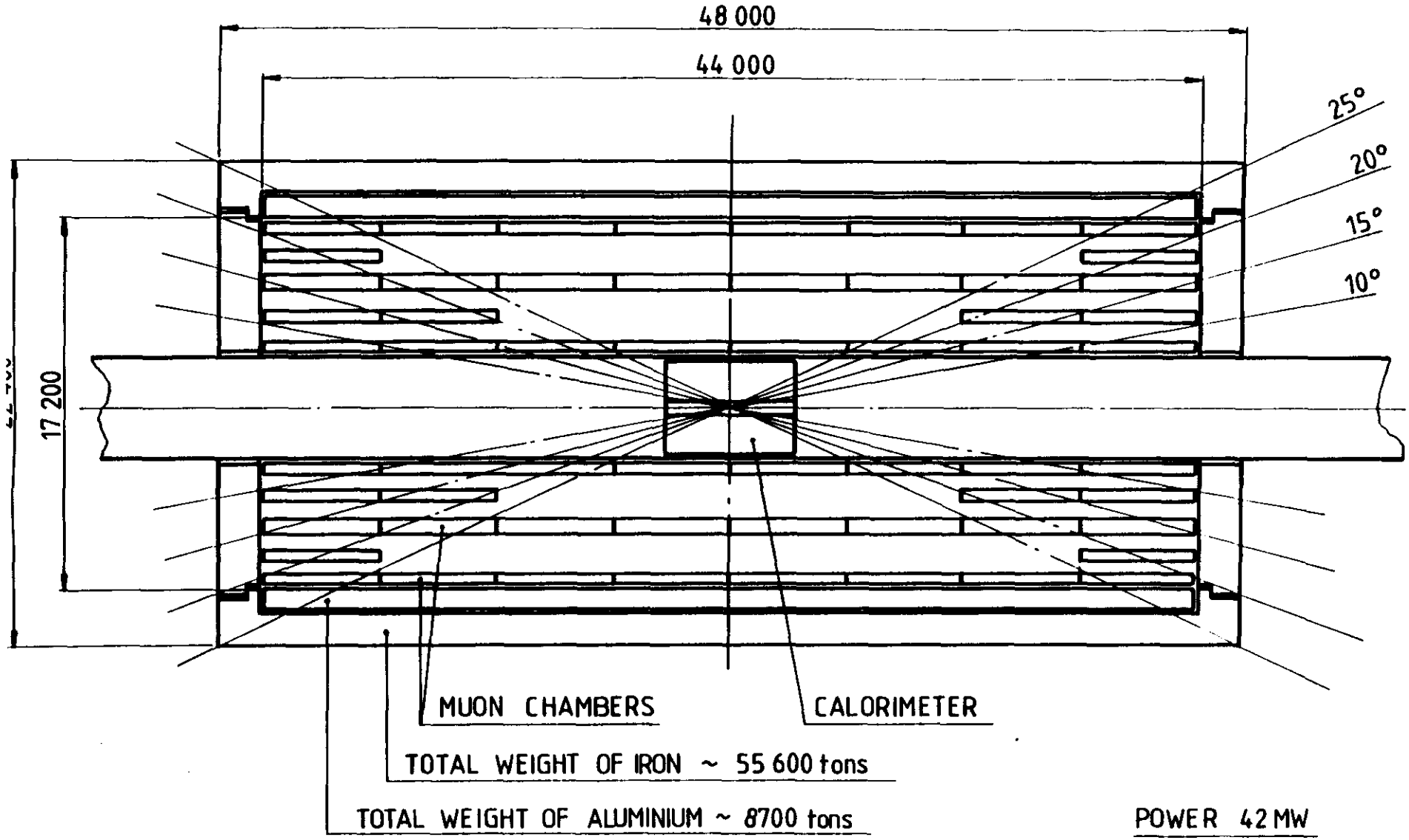

POWER 42 MW

02.05.89 C.D

1:250

DETECTOR LAYOUT

VERSION 1a

FFRN/LHC-030/4

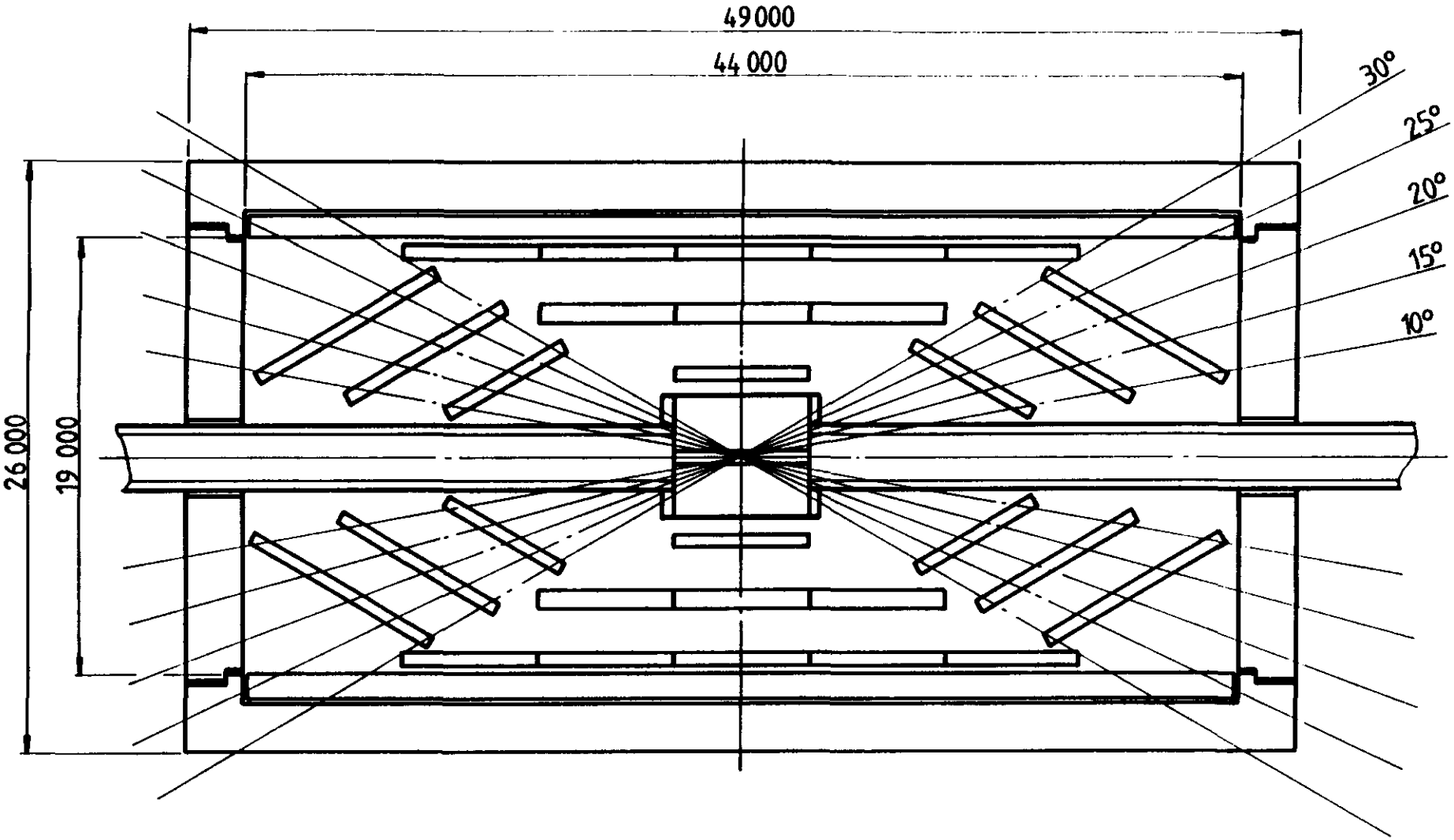

03.05.89 C.D
1:250

DETECTOR LAYOUT

CERN/LHC-033/4

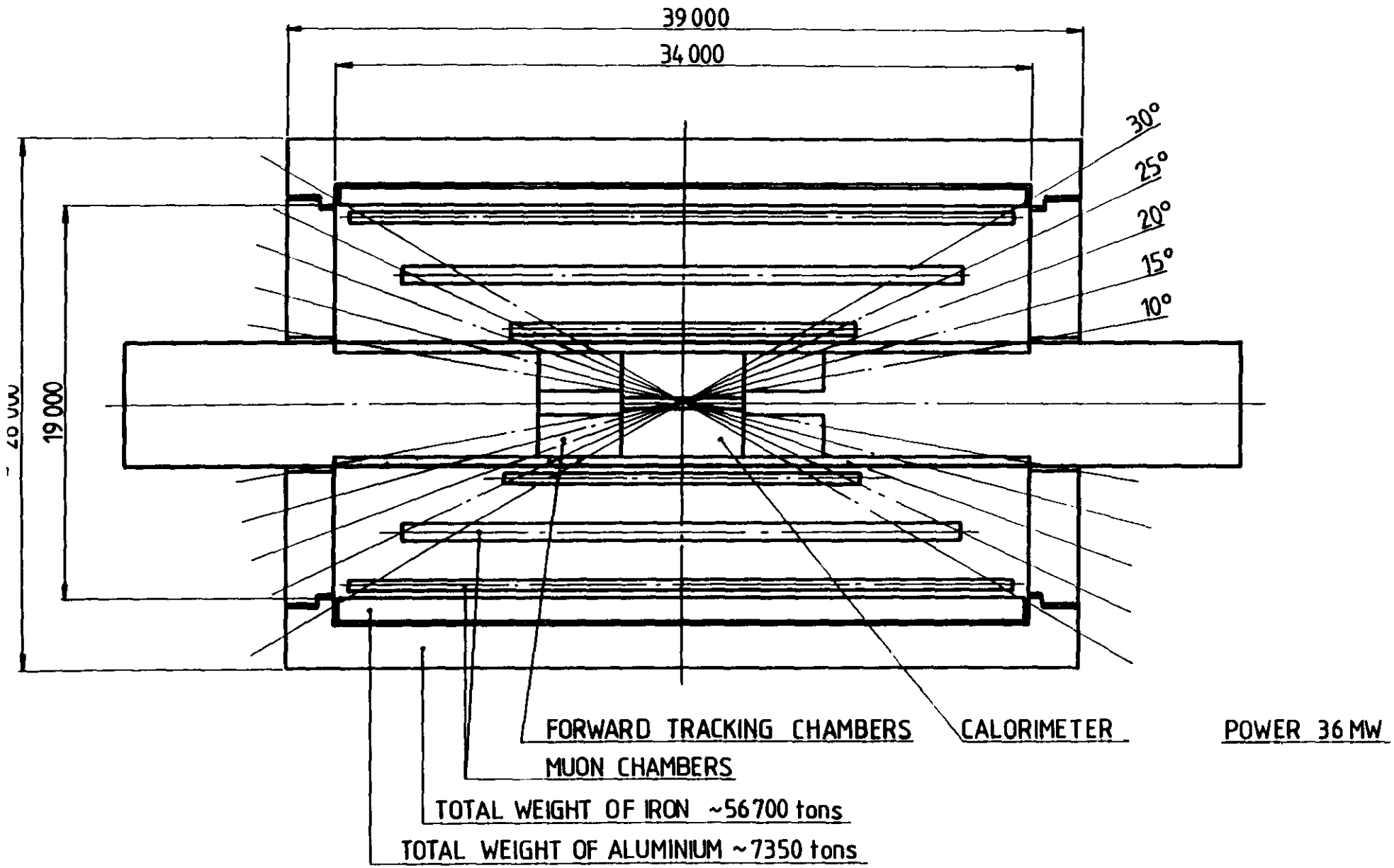

DETECTOR LAYOUT
VERSION 2a
CERN/LHC-031/4

02.05.89 C.D
1:250

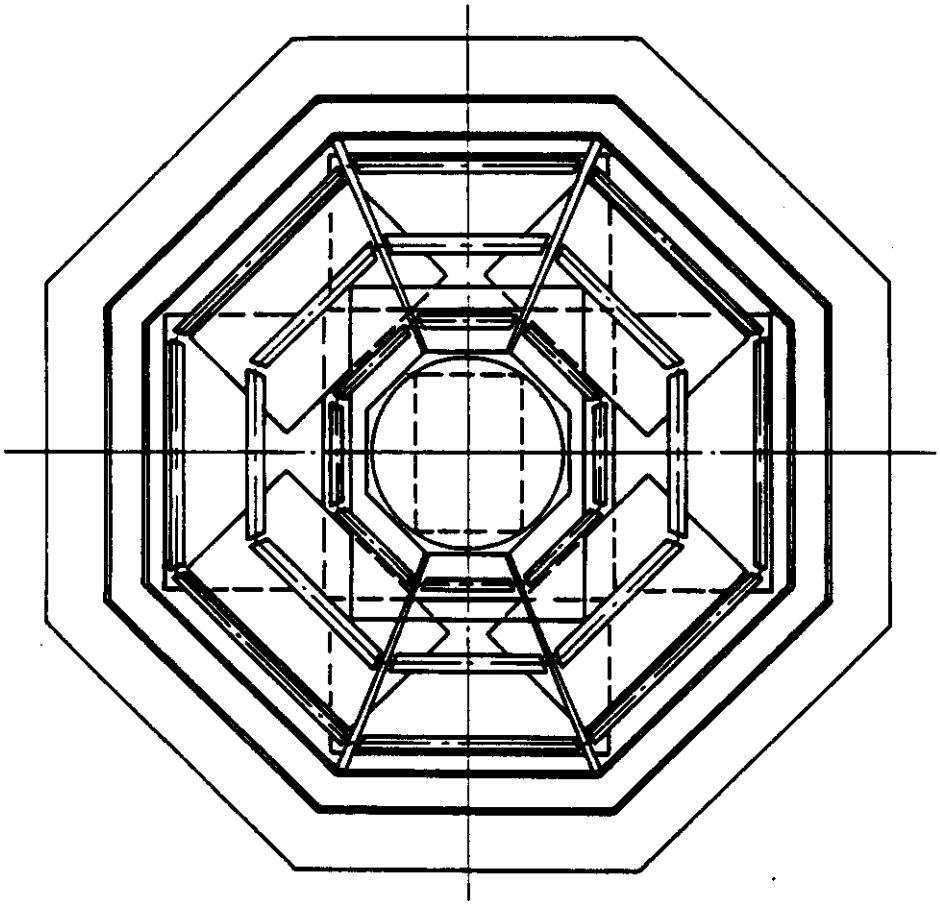

CROSS SECTION

09.05.89 C.D
1:250

DETECTOR LAYOUT
VERSION 3

CERN/LHC-035/4

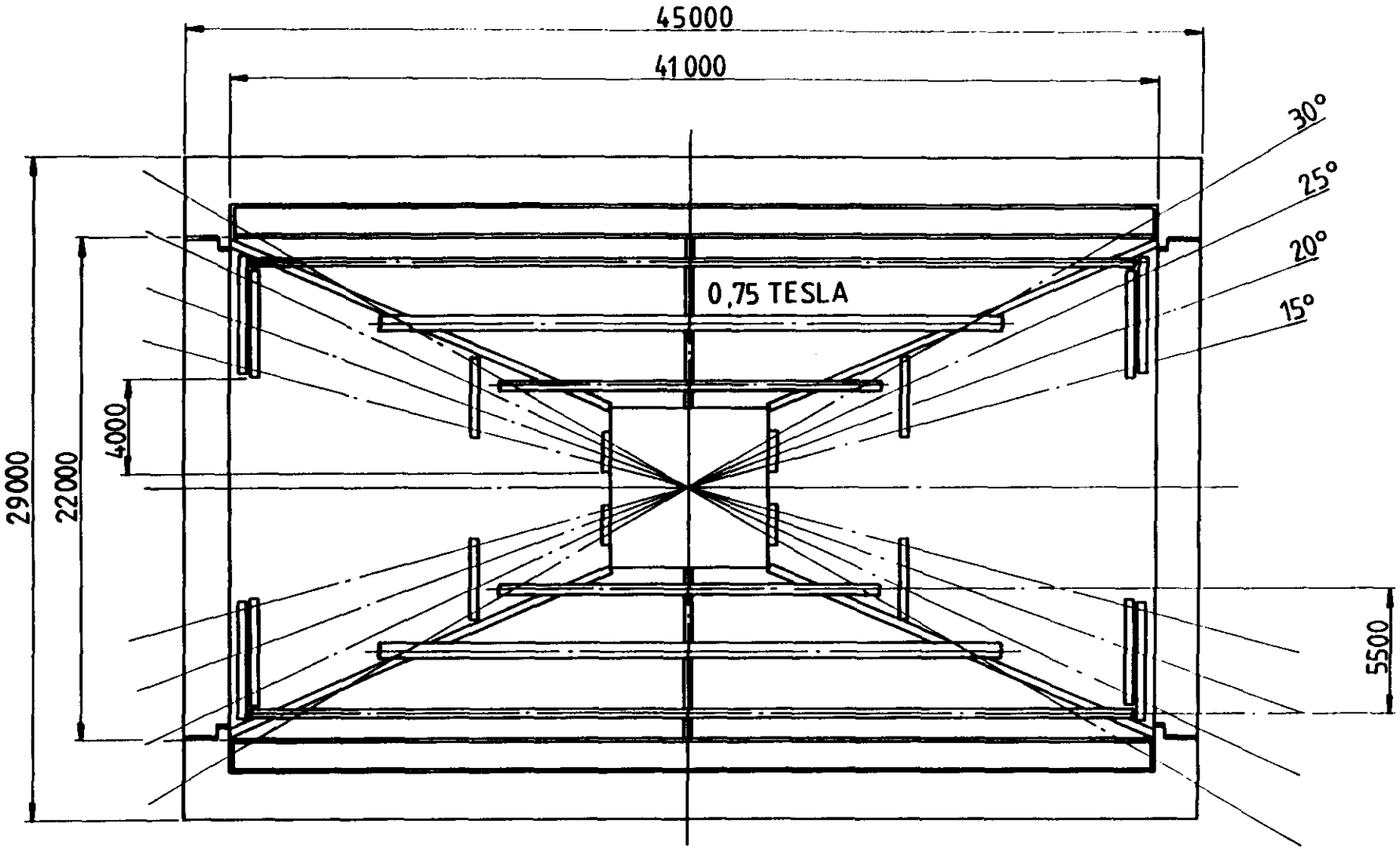

09.05.89 C.D
1:250

DETECTOR LAYOUT
VERSION 3
CERN/LHC-037/LA

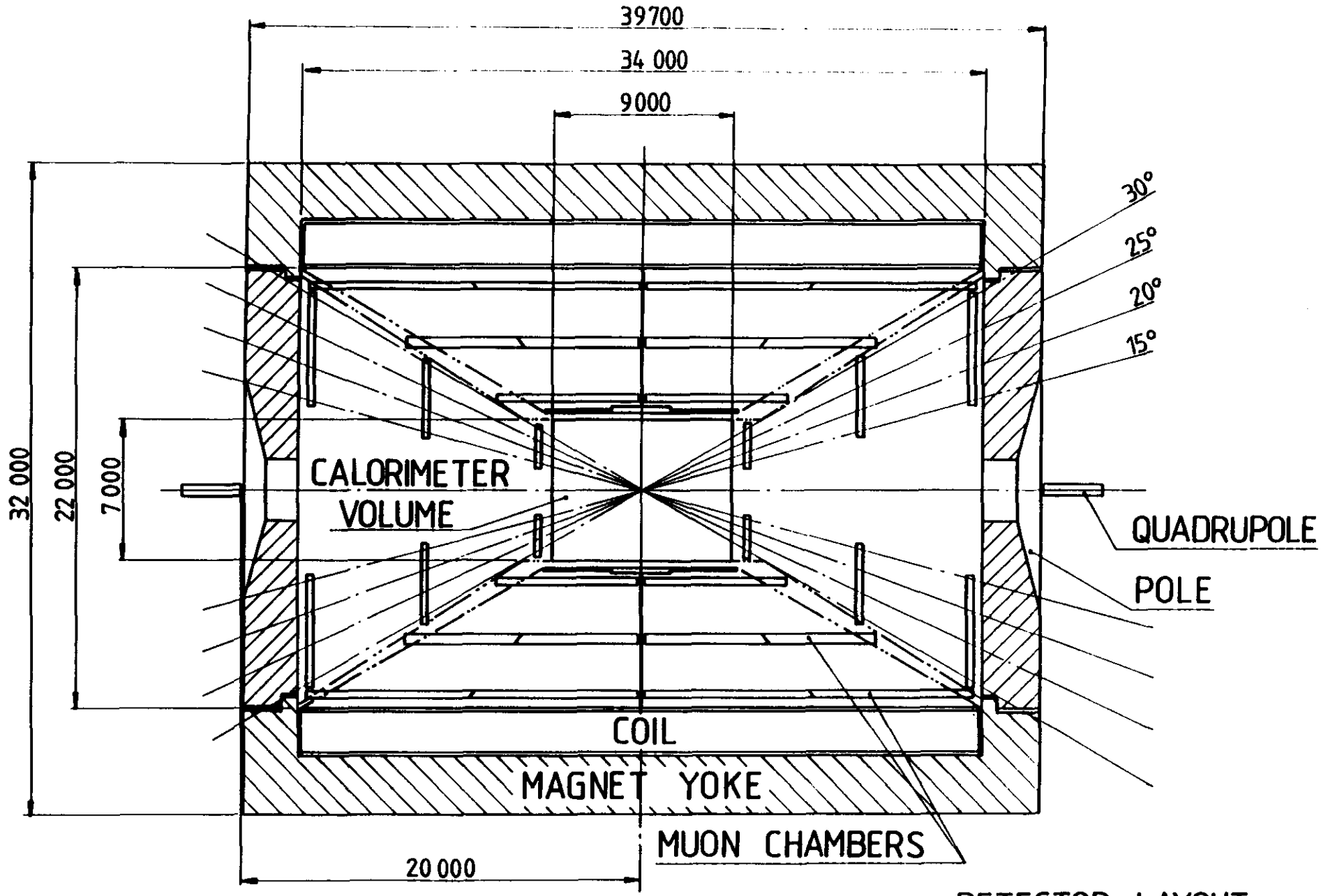

16.05.89 C.D
1:250

DETECTOR LAYOUT
VERSION 4

CERN/LHC-036/4A

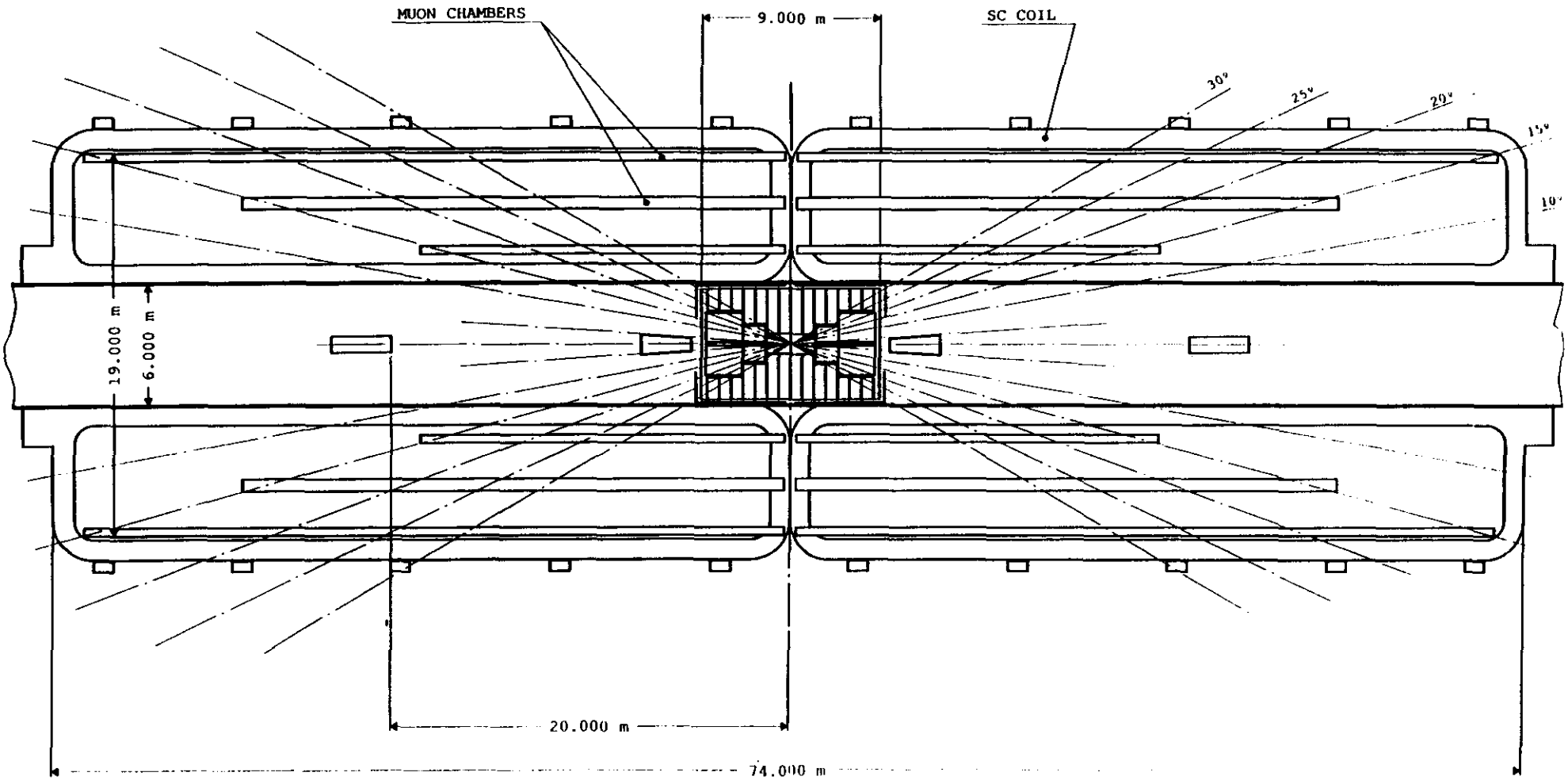

L3 Ref:CD/DO

CERN/LHC-054/M3

DOUBLE TOROIDAL MAGNET

Version 2

Scale 1:200
29 June 1989

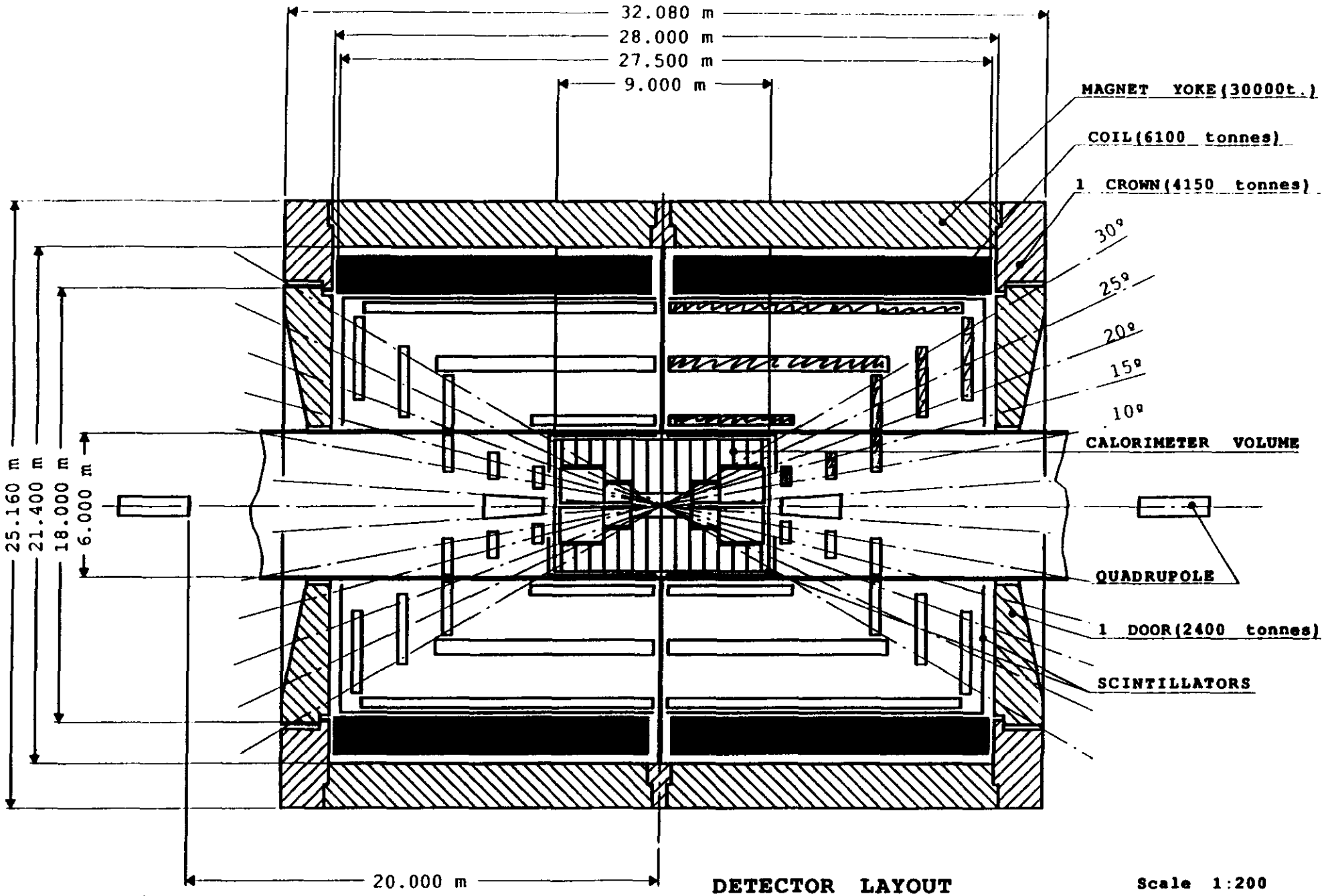

L3 Ref:CD/DO

CERN/LHC-046/M4

DETECTOR LAYOUT

20MW VERSION WITH SUPPORT TUBE

TOTAL WEIGHT OF IRON 43000 tonnes

Scale 1:200

09 June 1989

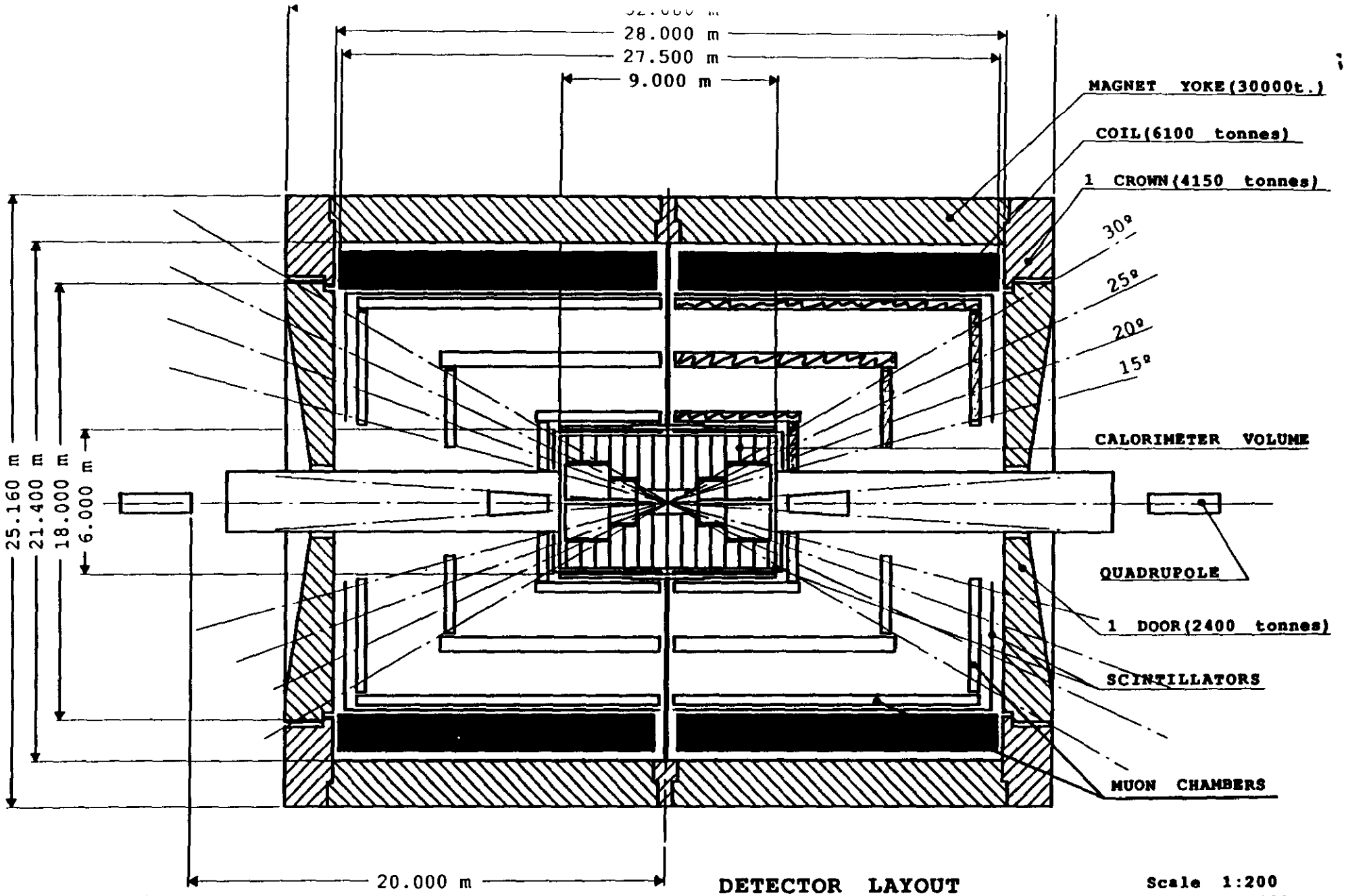

L3 Ref:CD/DO

CERN/LHC-043/M4A

DETECTOR LAYOUT

20MW VERSION

TOTAL WEIGHT OF IRON 43000 tonnes

Scale 1:200
08 June 1989
13 June 1989

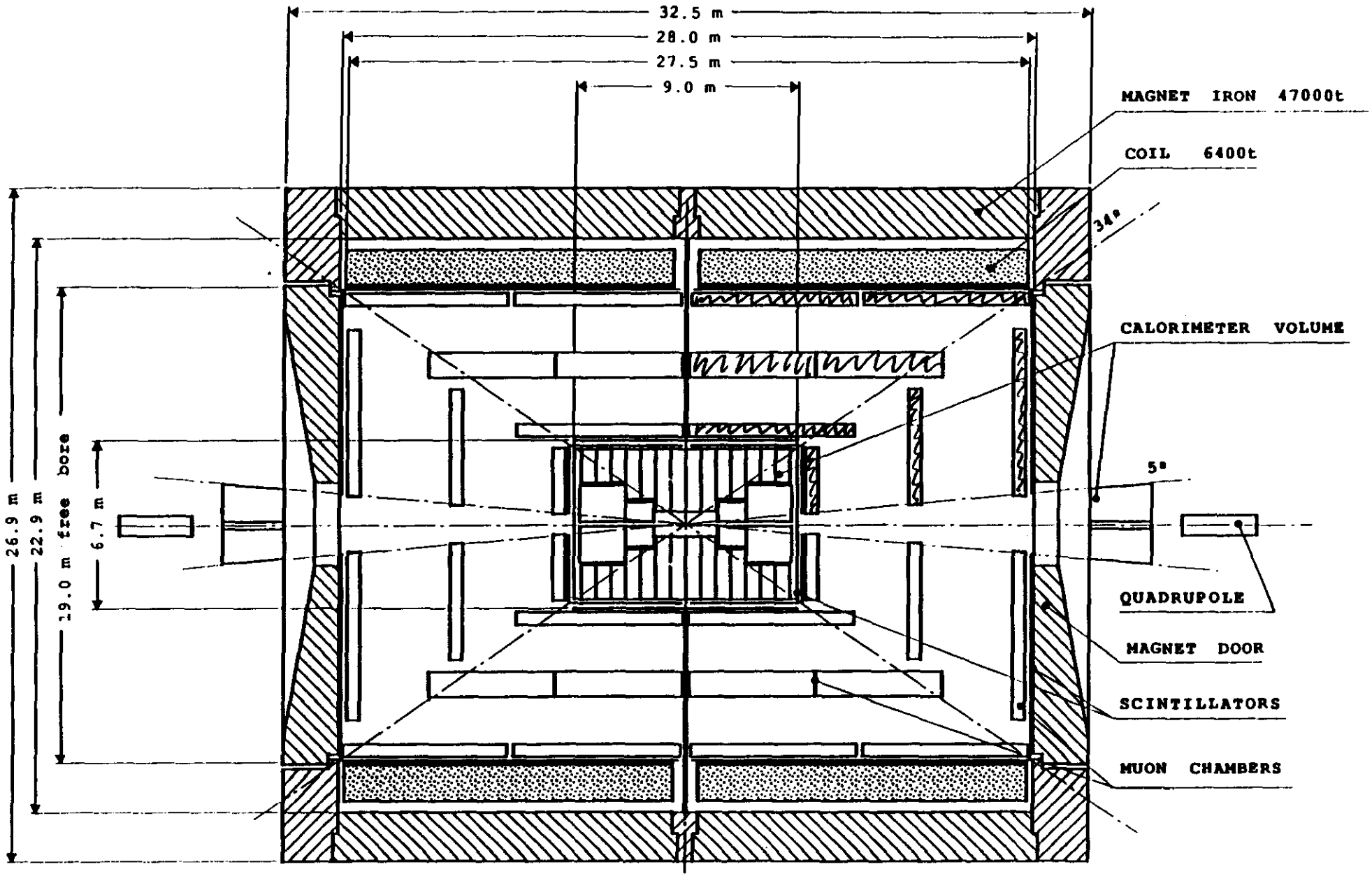

L* Ref:CD/DO
CERN/LHC-066/M4A

DETECTOR LAYOUT

20MW VERSION/4
0.75 Tesla

Scale 1:200
18 August 1989

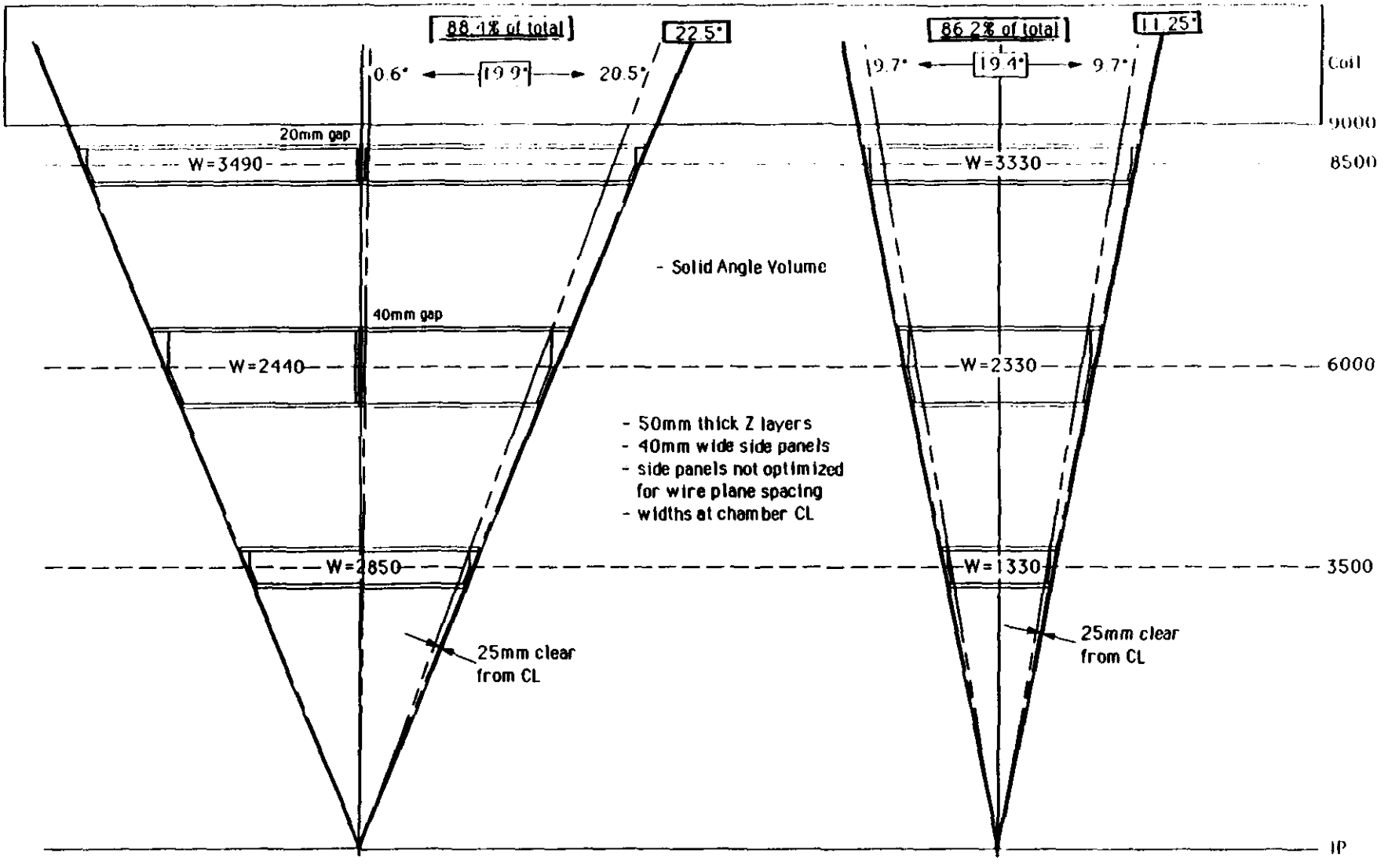

L3+1 Muon Spectrometer Volume

Central Region - Section

Chamber Geometry and Alignment

C Grannell
scale 1:50
version 1 11/07/89
from 2011W 13.06.89

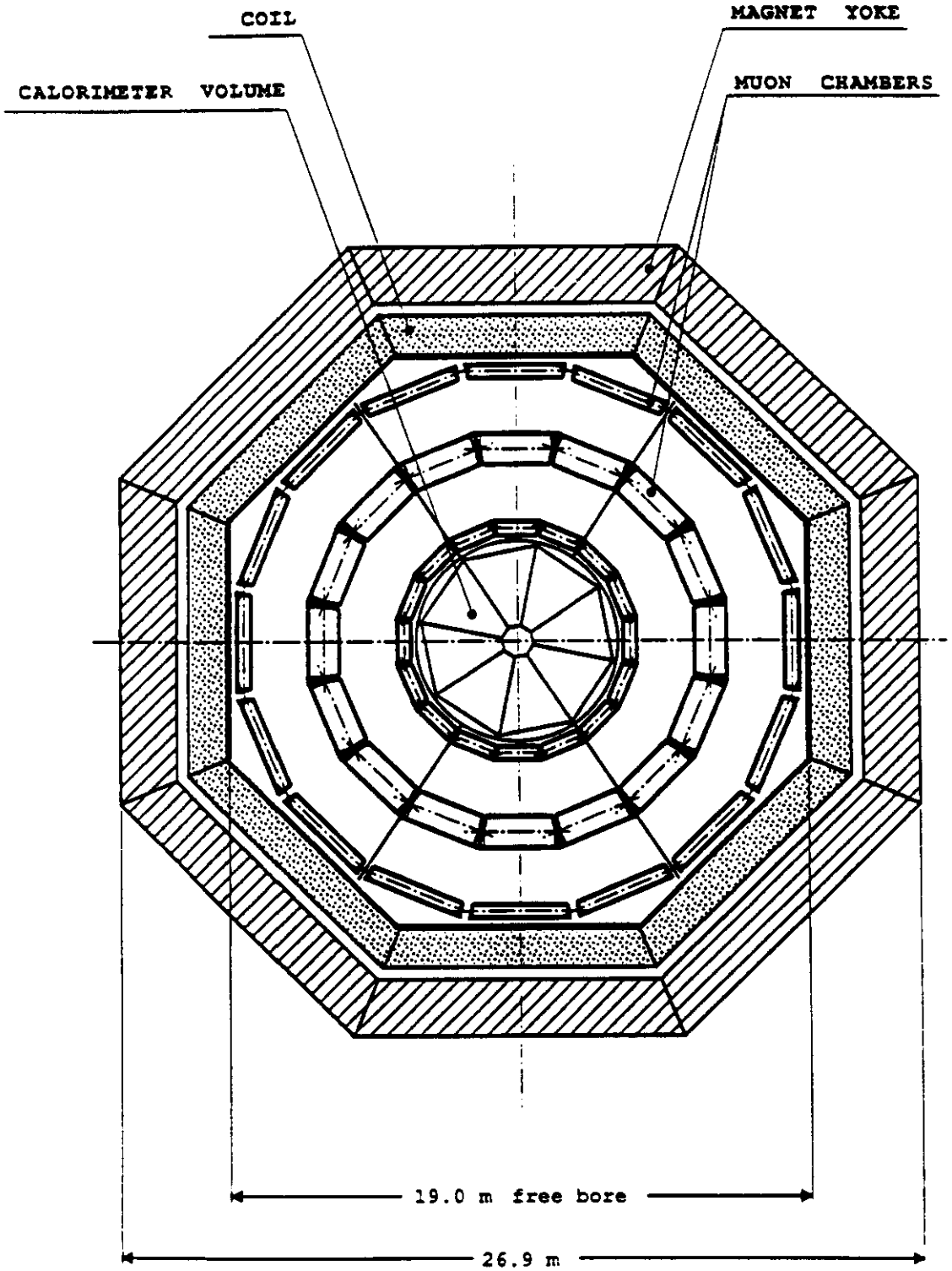

CROSS SECTION

DETECTOR LAYOUT

20MW VERSION/4

0.75 Tesla

Ref:CD/DO

ERN/LHC-067/M4A

Scale 1:200

18 August 1989

VARIANT IV

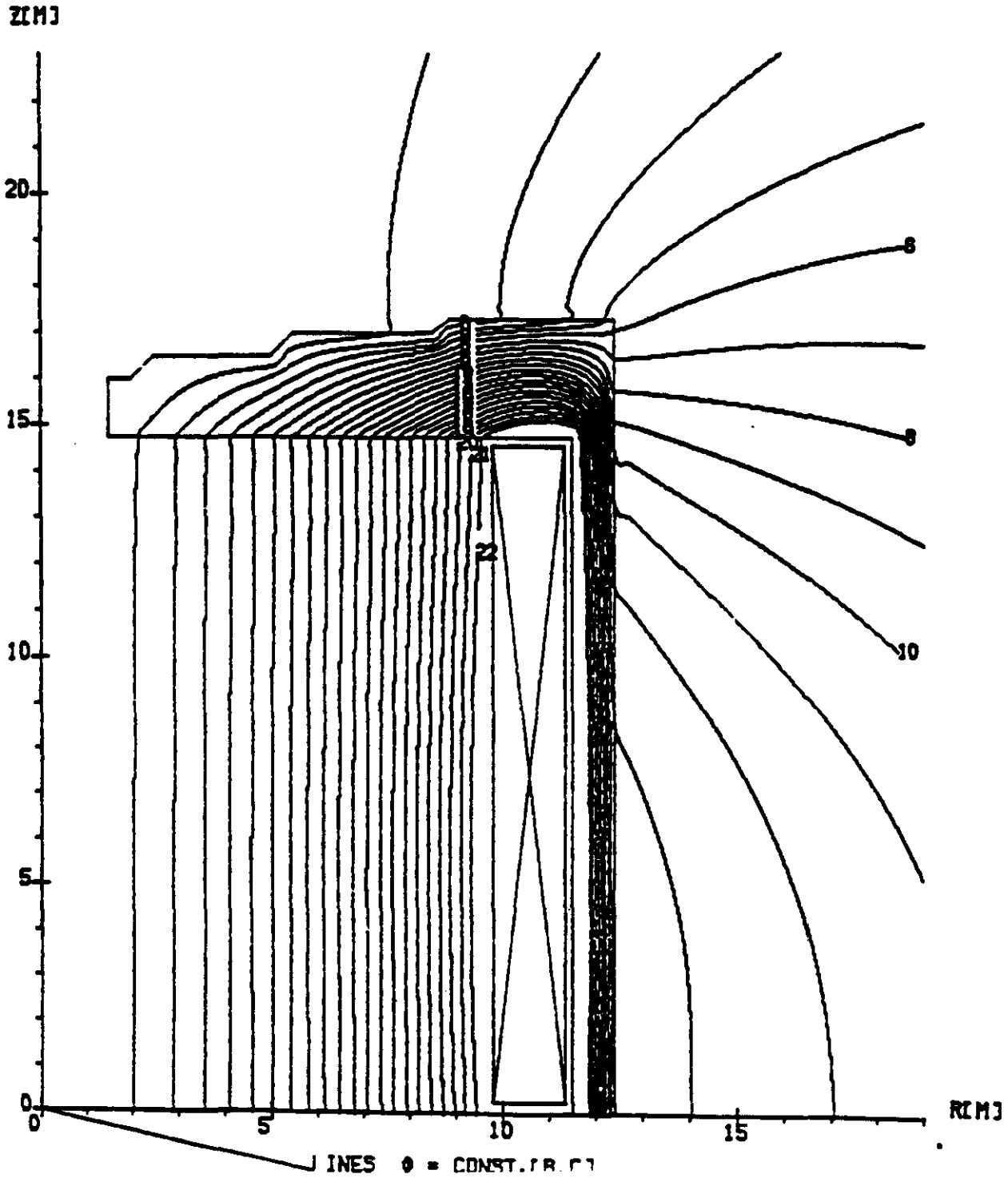

LSTAR26 - IRON-BOUND SYSTEM WITH END CAPS

MAP V1.0 4/ 4/90 15:46

Contour 1 = 0.000E+00 Delta = 6.881E-02

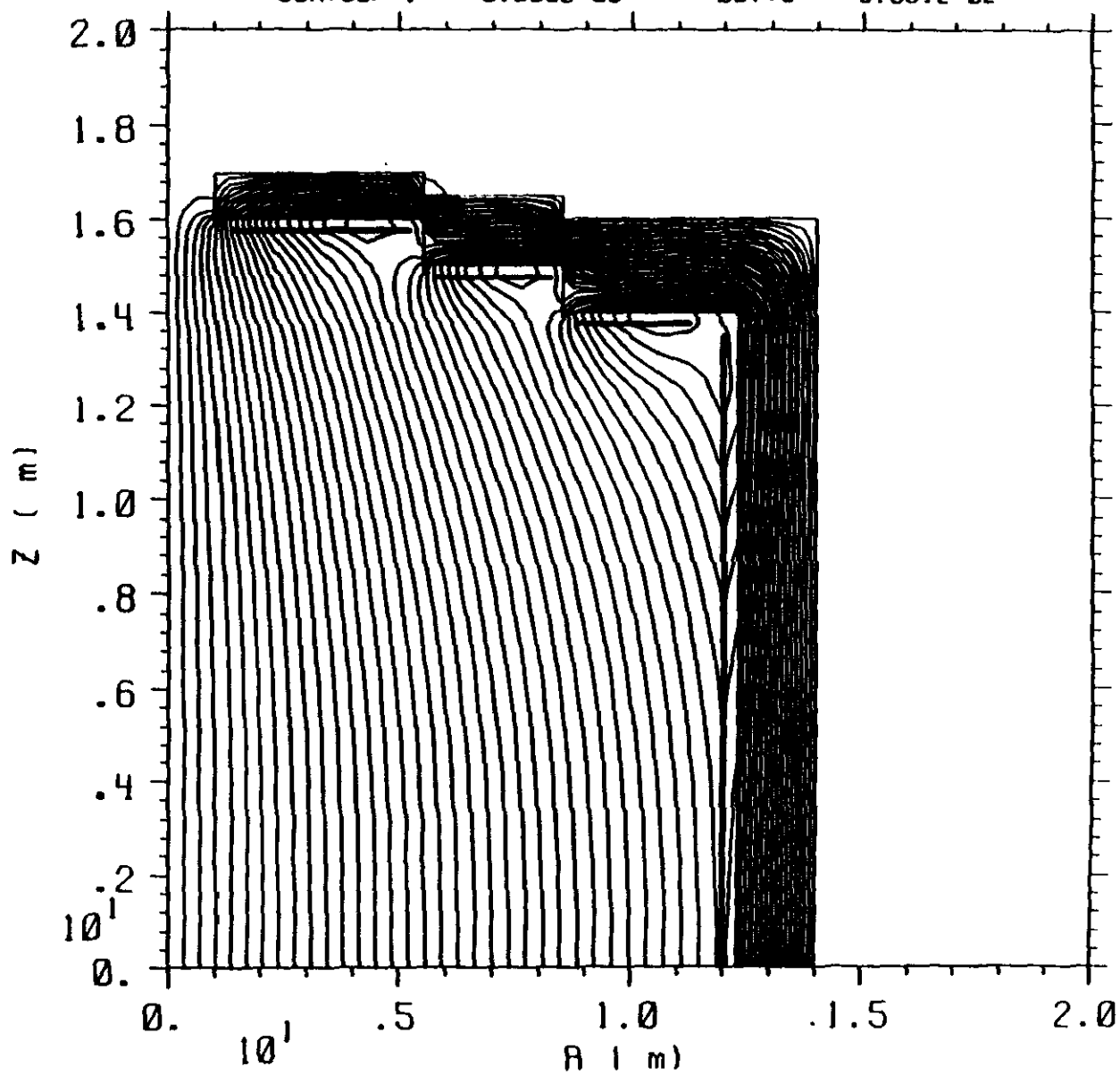

CONTOURS OF CONSTANT

VARIANT VIII

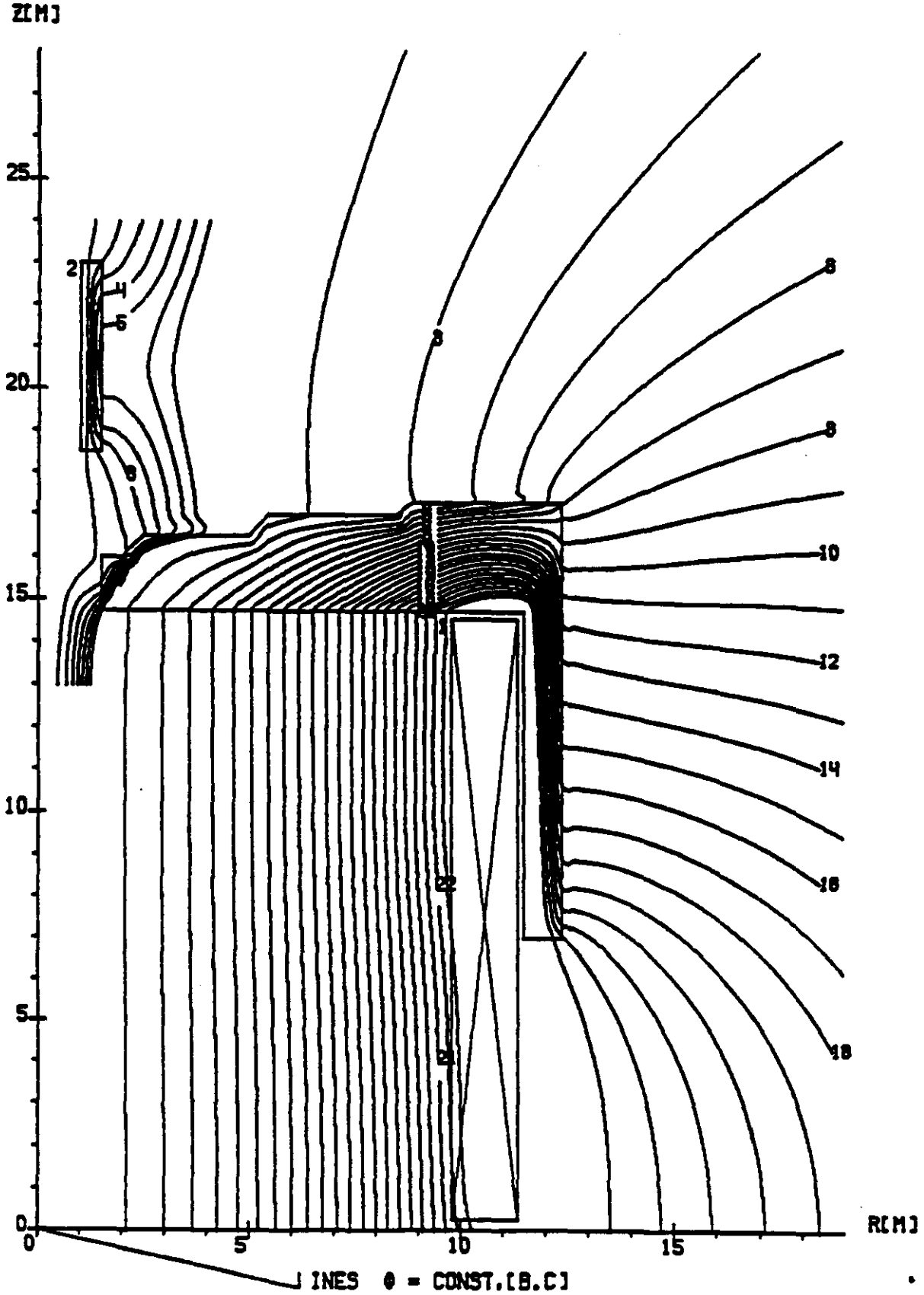

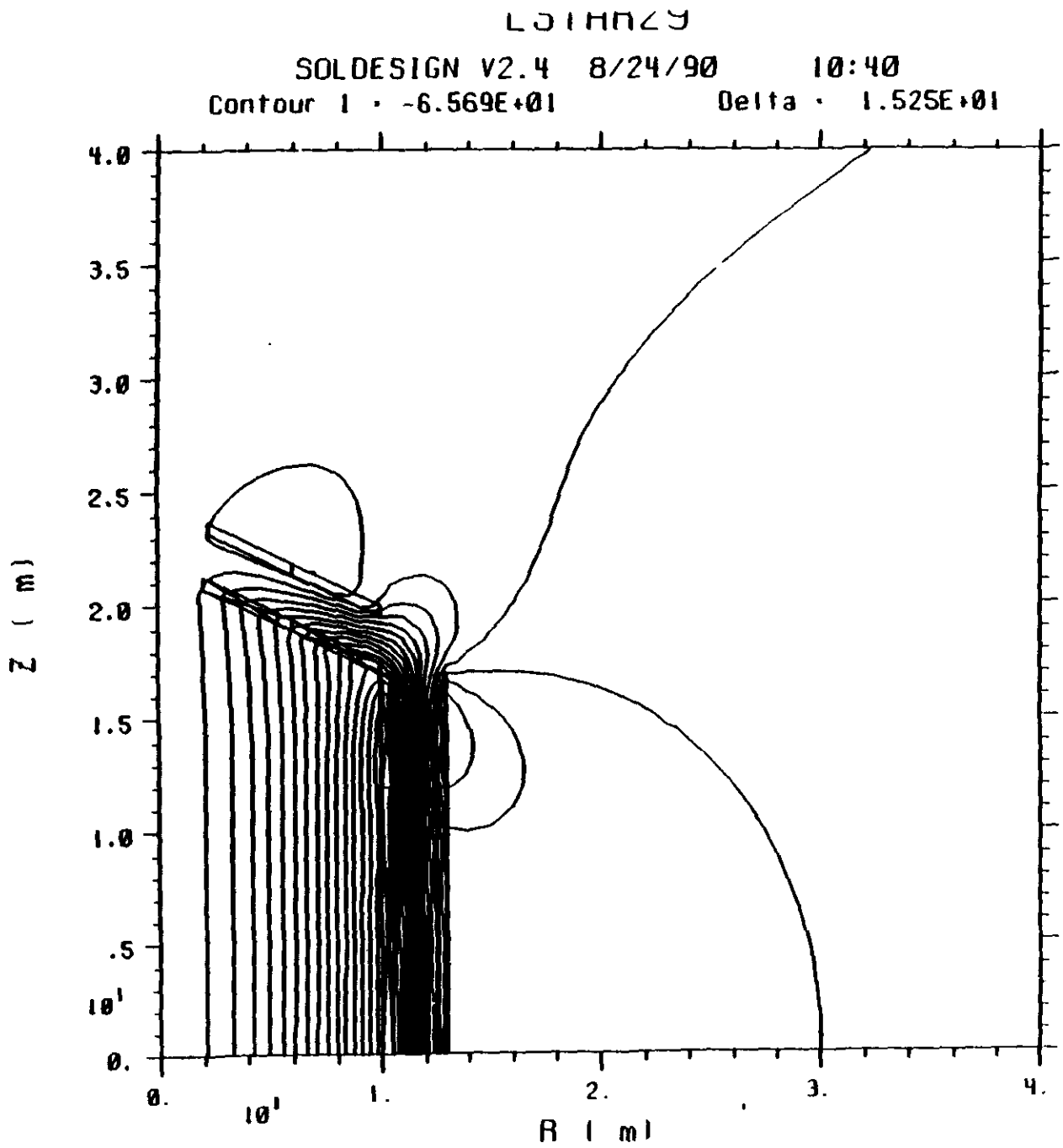
SOLDESIGN V2.4 8/24/90 10:40
Contour 1 · -6.569E+01
Delta · 1.525E+01
4.0
3.5
3.0
2.5
2.0
1.5
1.0
.5
10¹
0.
Z (m)
0.
10¹
1.
2.
3.
4.
R (m)

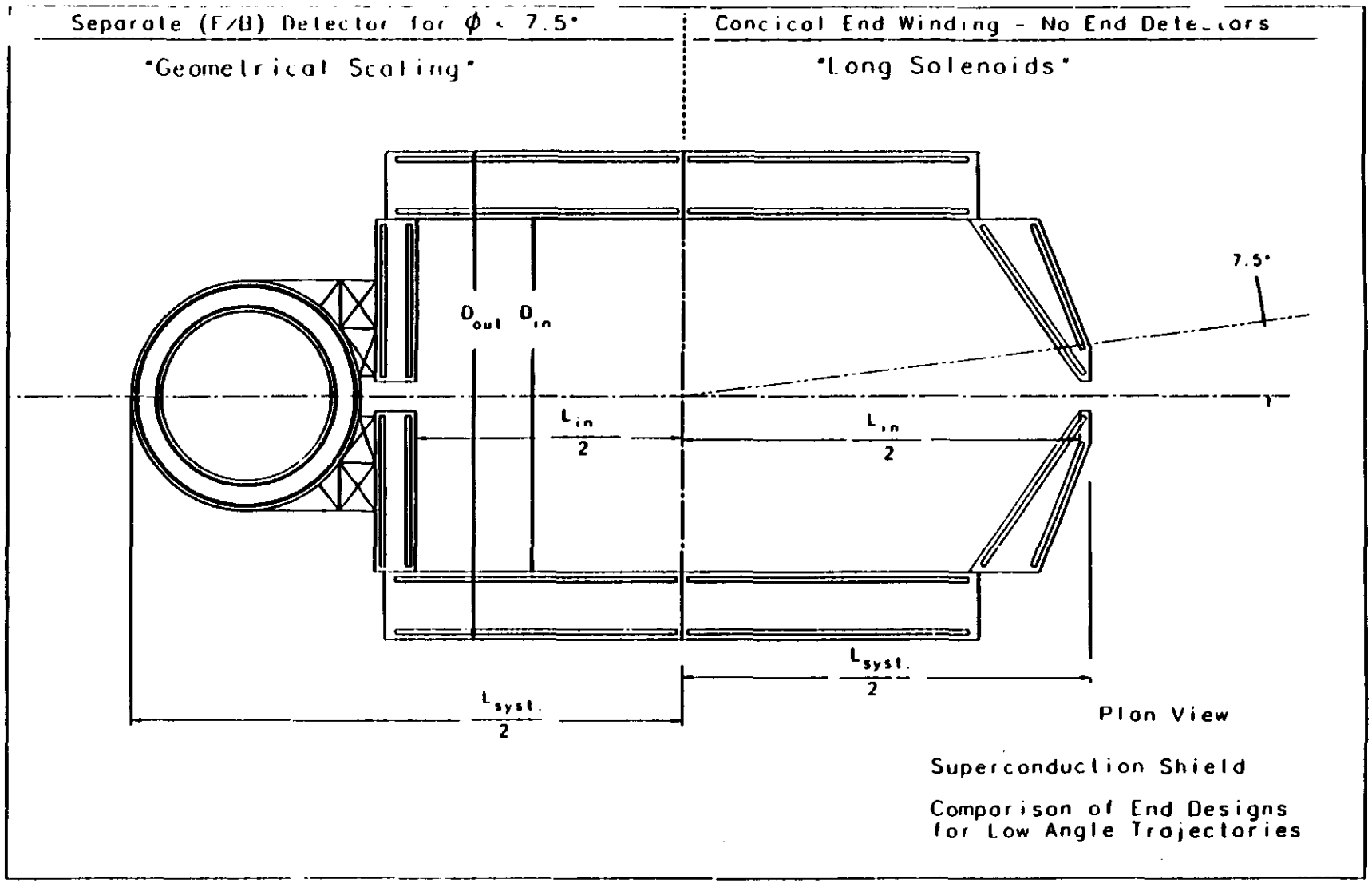
Separate (F/B) Detector for $\phi < 7.5°$
"Geometrical Scaling"
Concical End Winding - No End Detectors
"Long Solenoids"
7.5°
D_{out}
D_{in}
$\frac{L_{in}}{2}$
$\frac{L_{in}}{2}$
$\frac{L_{syst.}}{2}$
$\frac{L_{syst.}}{2}$
Plan View
Superconduction Shield
Comparison of End Designs
for Low Angle Trajectories

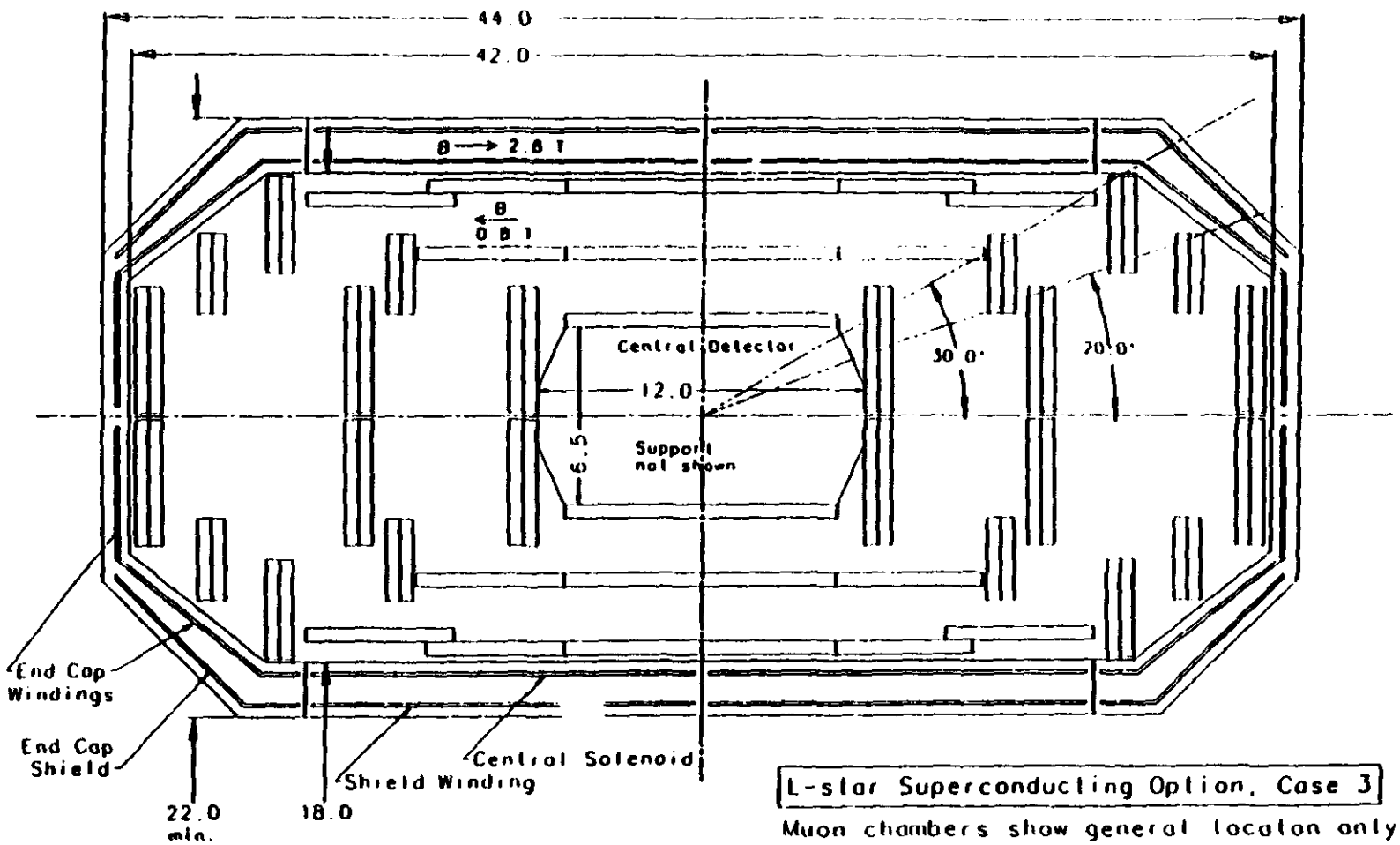

Trade study will evaluate cost vs. dia. to 26 m.

L-star Superconducting Option, Case 3

Muon chambers show general locaton only (assumed for estimate of bending power) Ref. attached notes

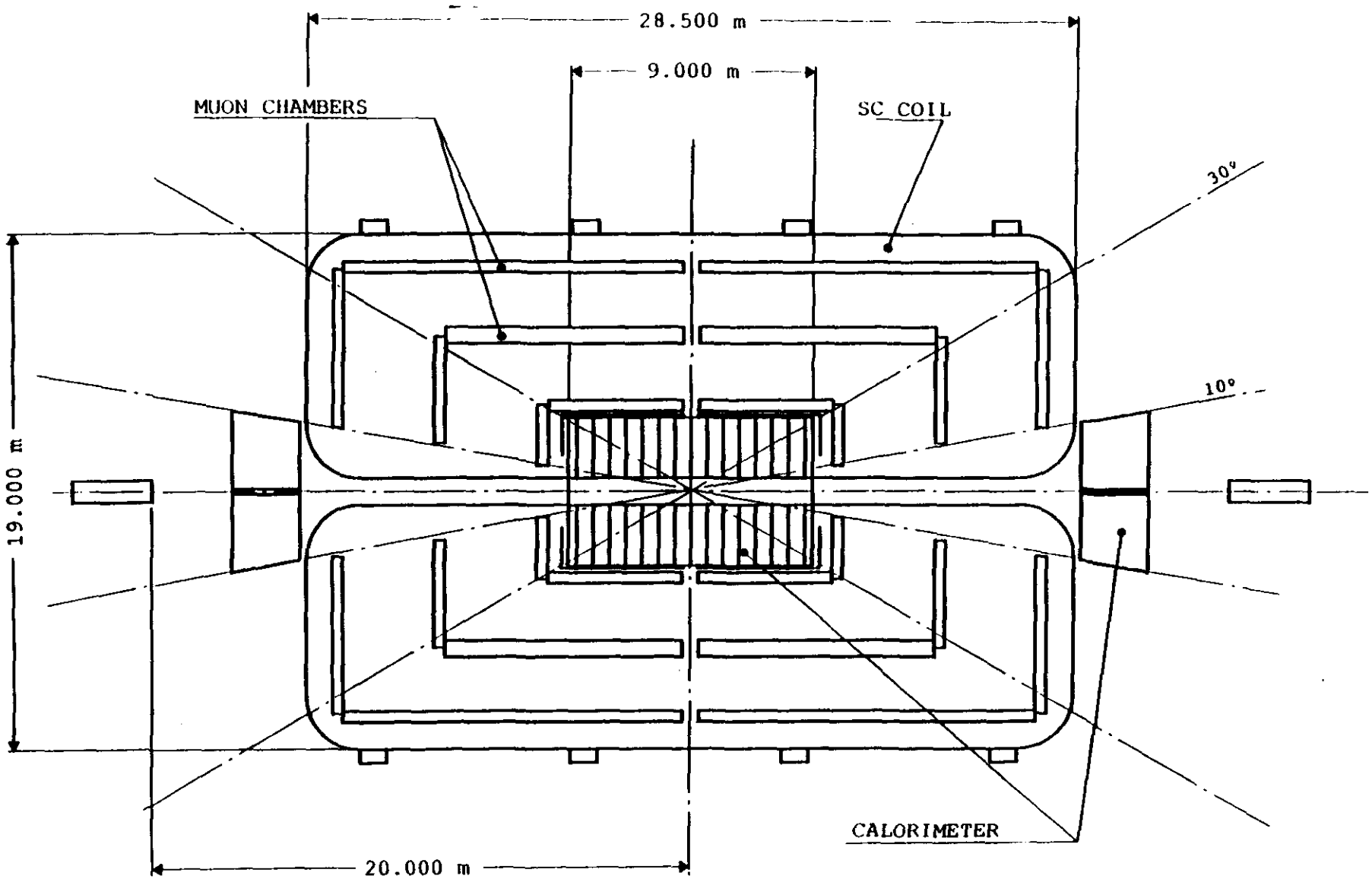

L3 Ref:CD/DO

CERN/LHC-056/M4

TOROIDAL MAGNET

Version 1

Scale 1:200
04 July 1989

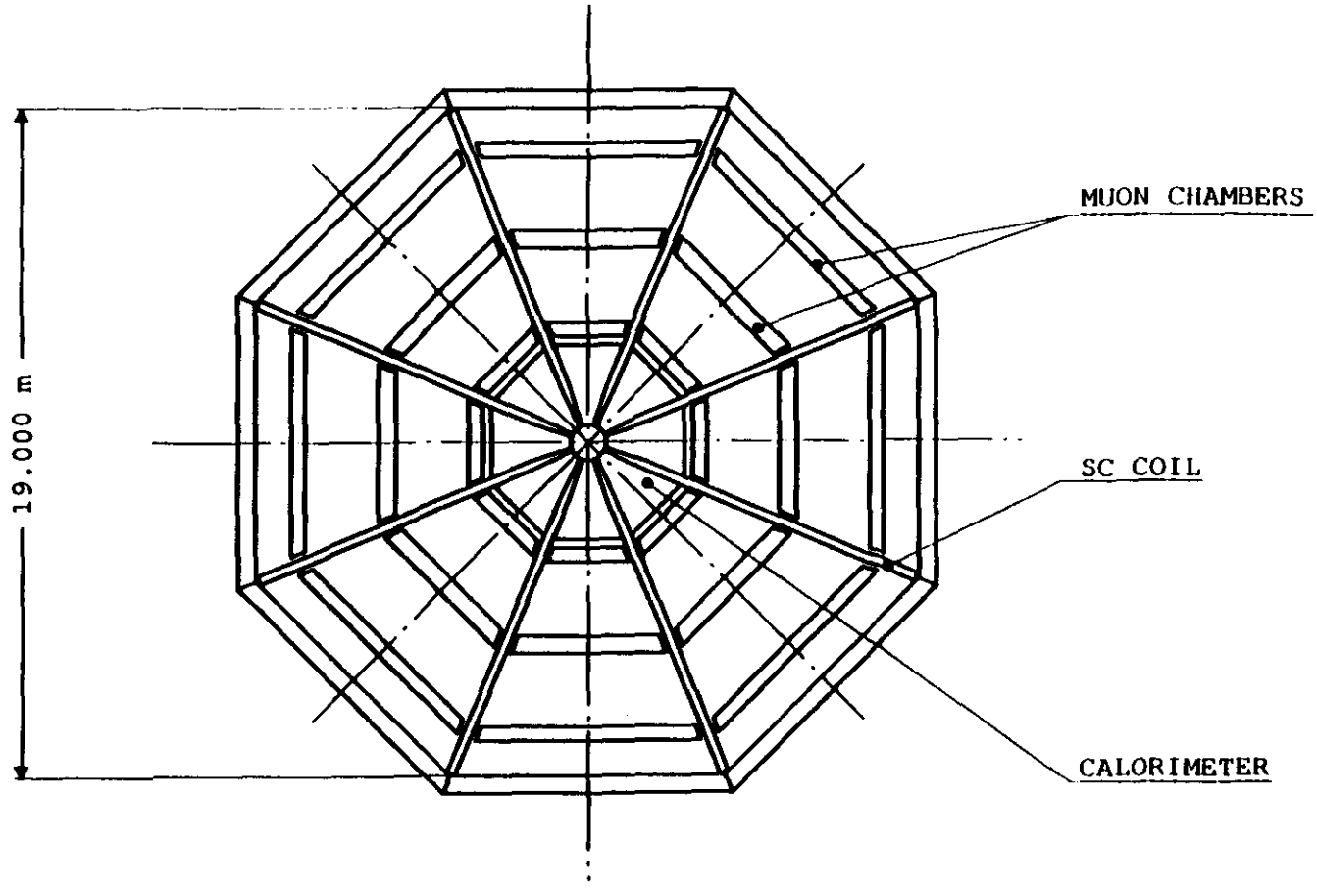

CROSS SECTION

L3 Ref:CD/DO

CERN/LHC-057/M4

TOROIDAL MAGNET

Version 1

Scale 1:200
04 July 1989

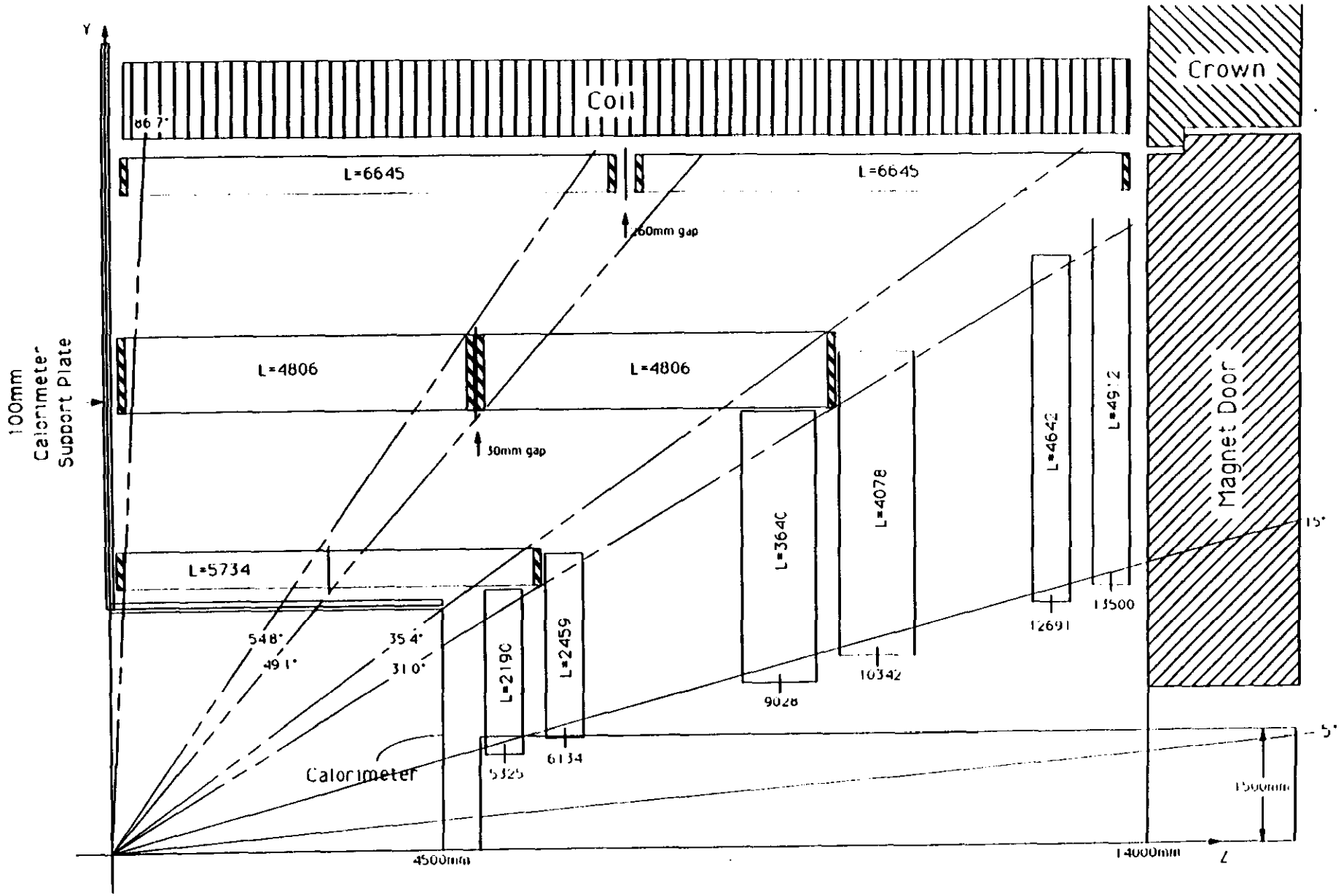

L* Muon Spectrometer Volume

Central Region Geometry

C. Grimett
Scale 1:50
version 4.1 10.01.90
from 20/12/89 13:10:07

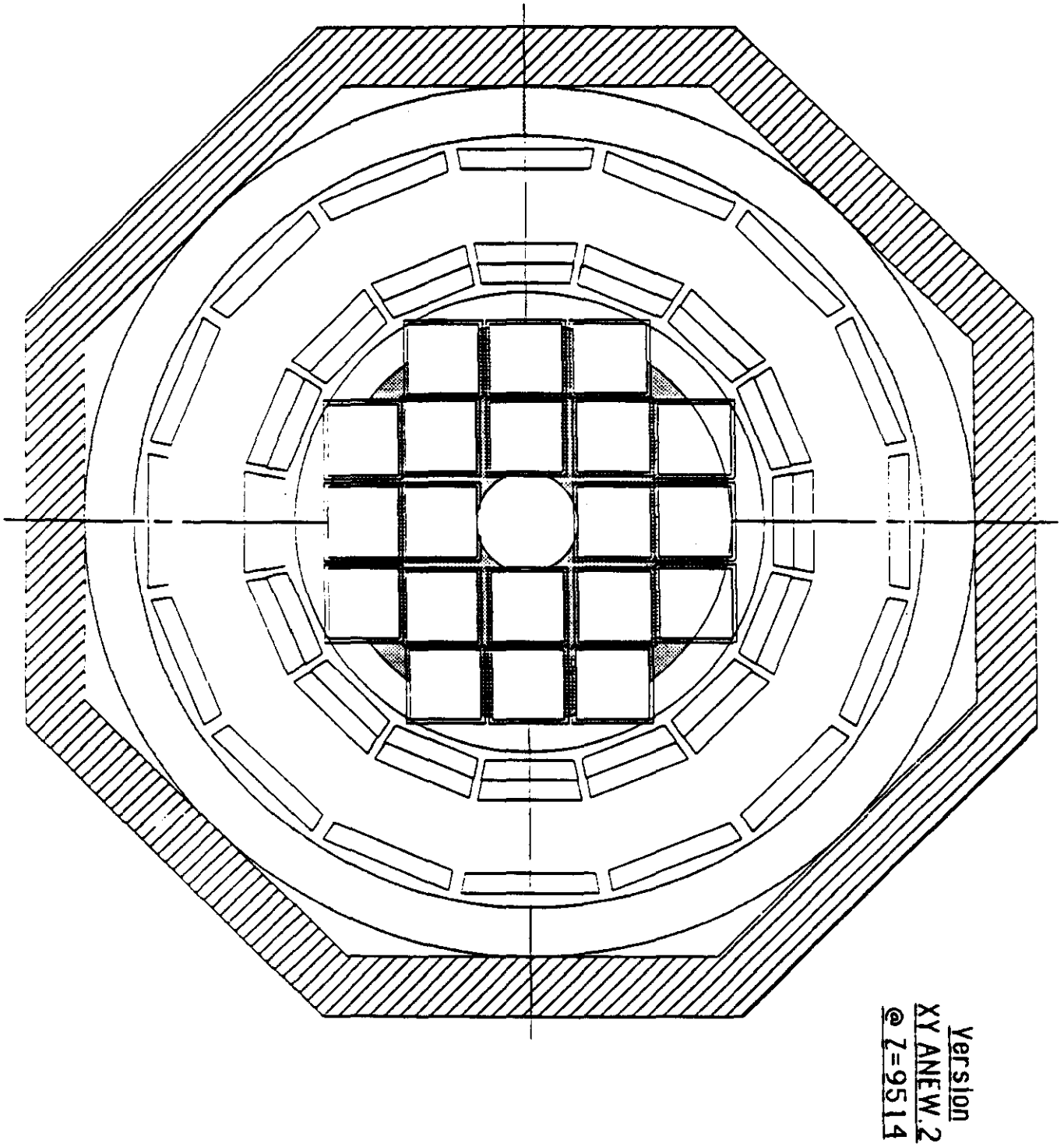

L* 20MW Magnet Version/4

Muon Spectrometer Volume

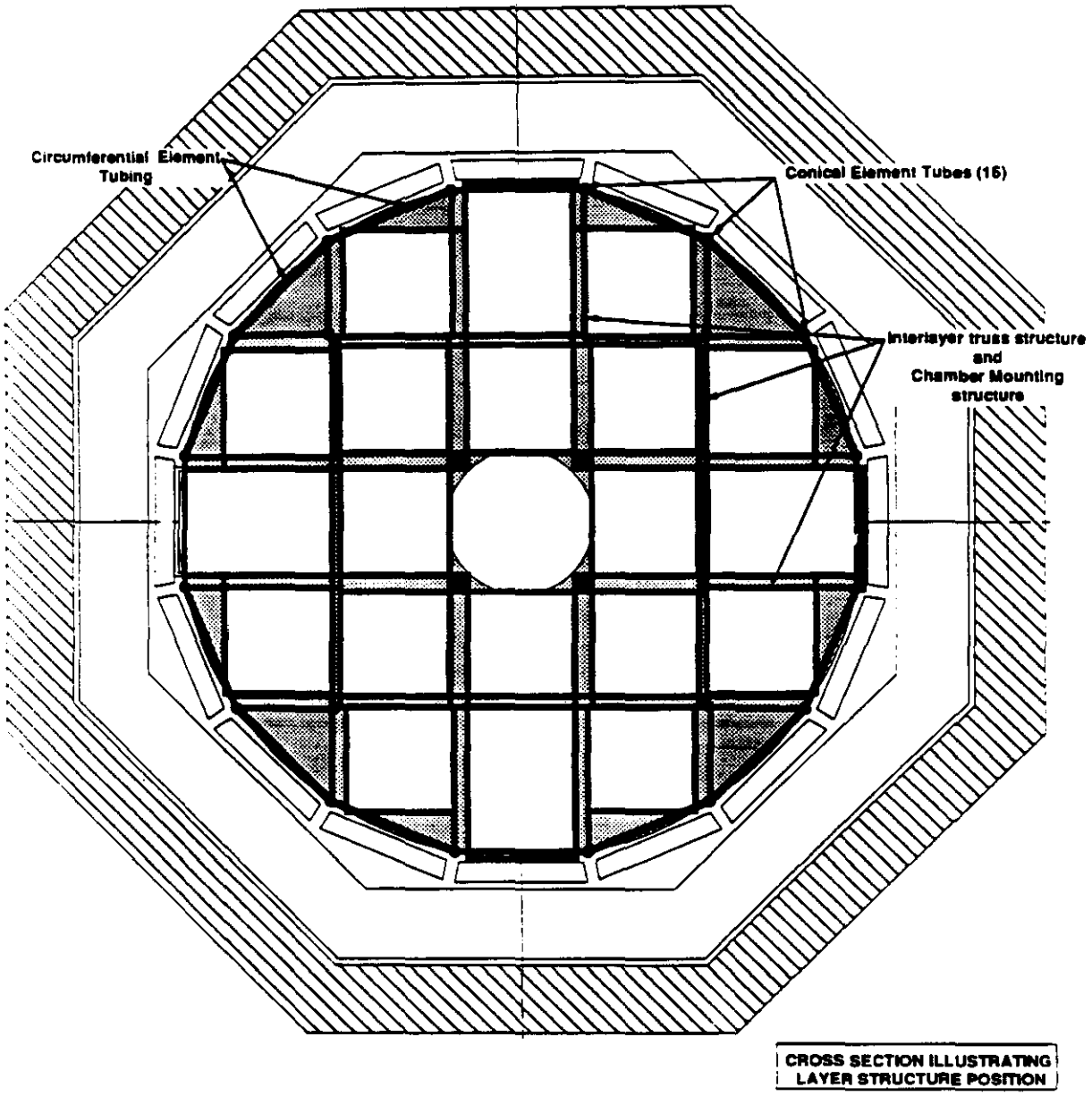

L* Muon Spectrometer Volume

Version XY ANEW.4 @ Z=14300

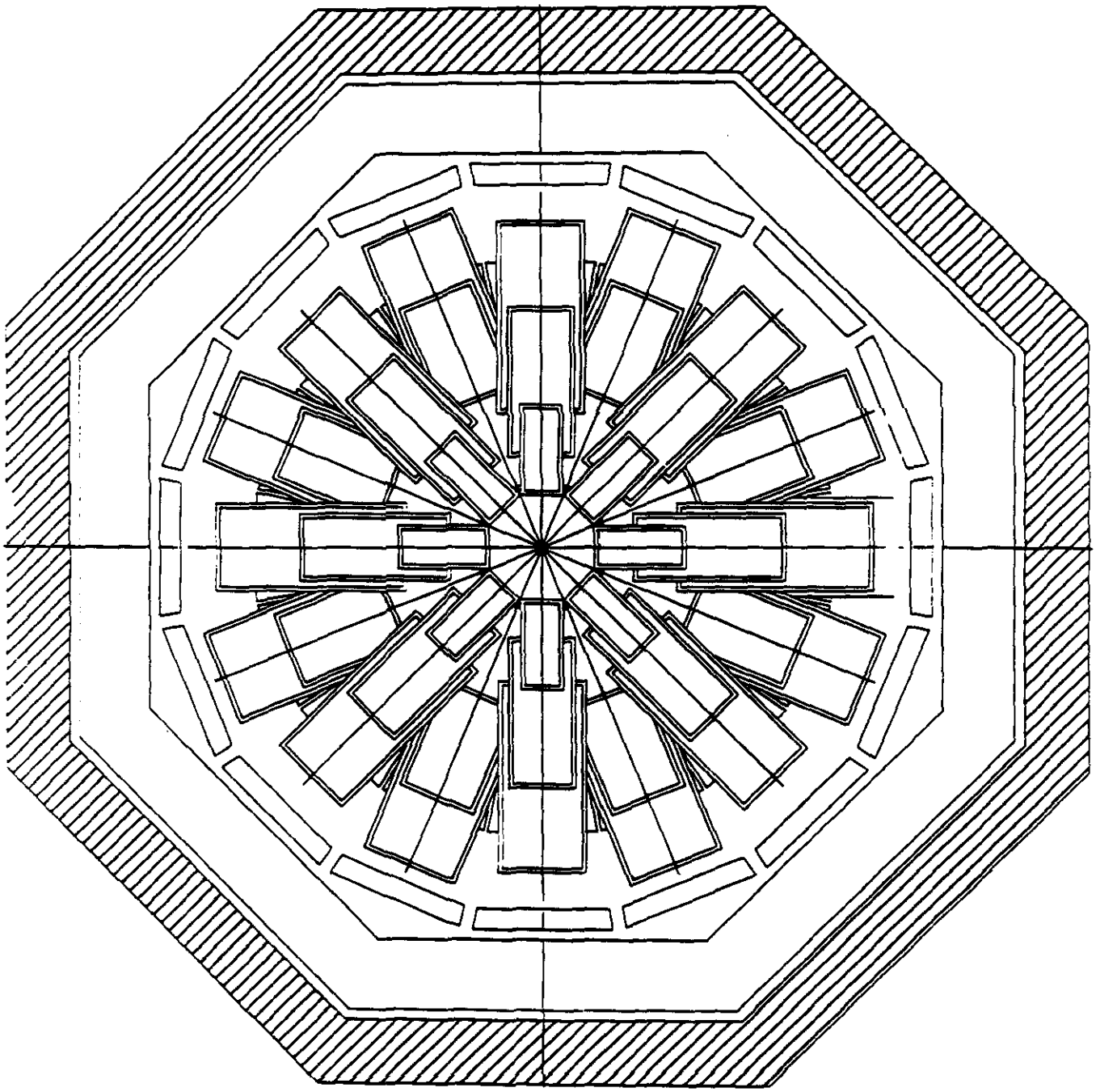

L* 20MW Magnet Version/4

Muon Spectrometer Volume

C Grinnell
scale 1:100
version 4:1 24 01 90
from 20MW/4 13 10 89

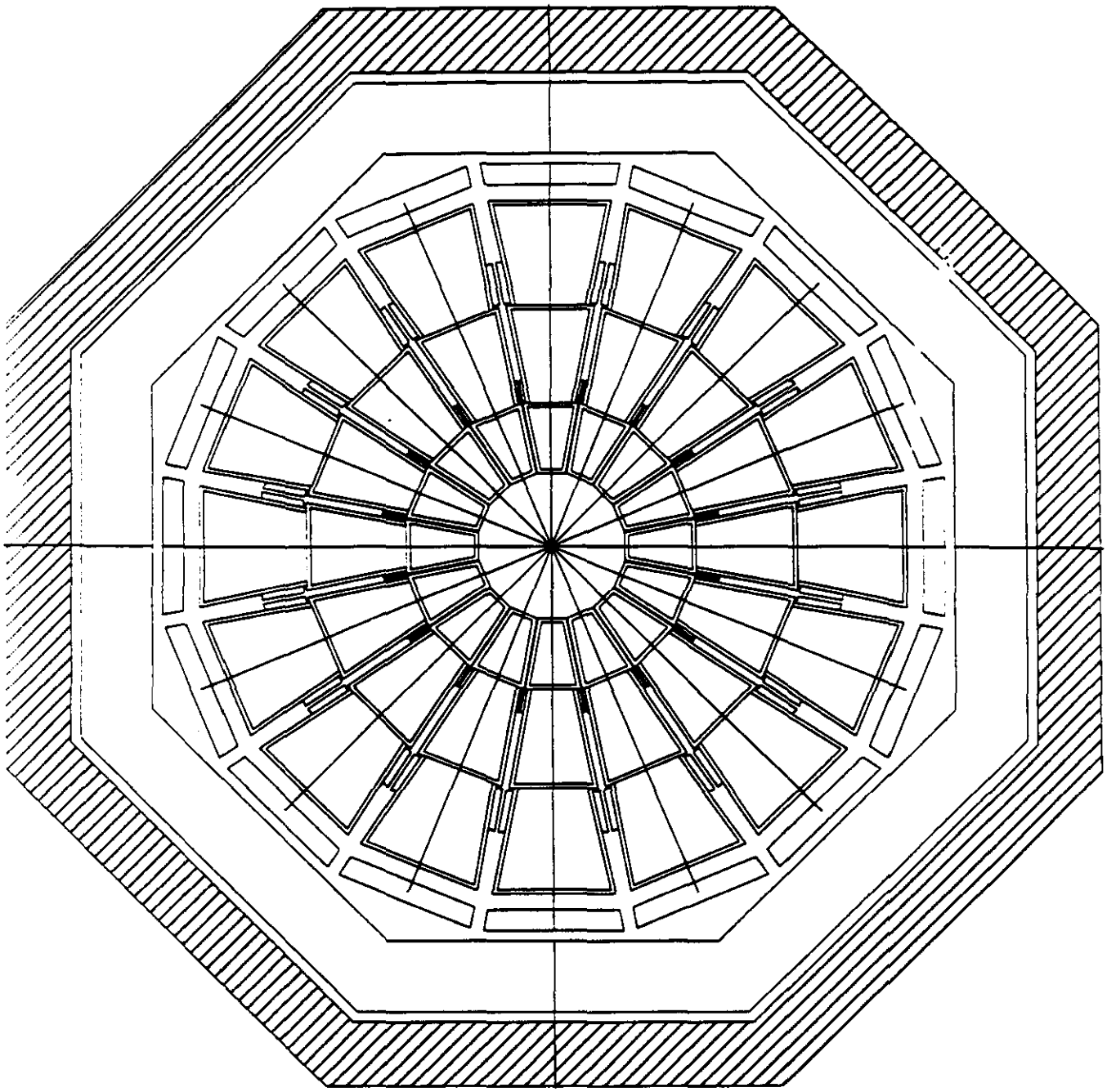

L* 20MW Magnet Version/4

Muon Spectrometer Volume

C Grinnell
scale 1 100
version 4 5 14 02 90
from 20MW/4 13 10 89

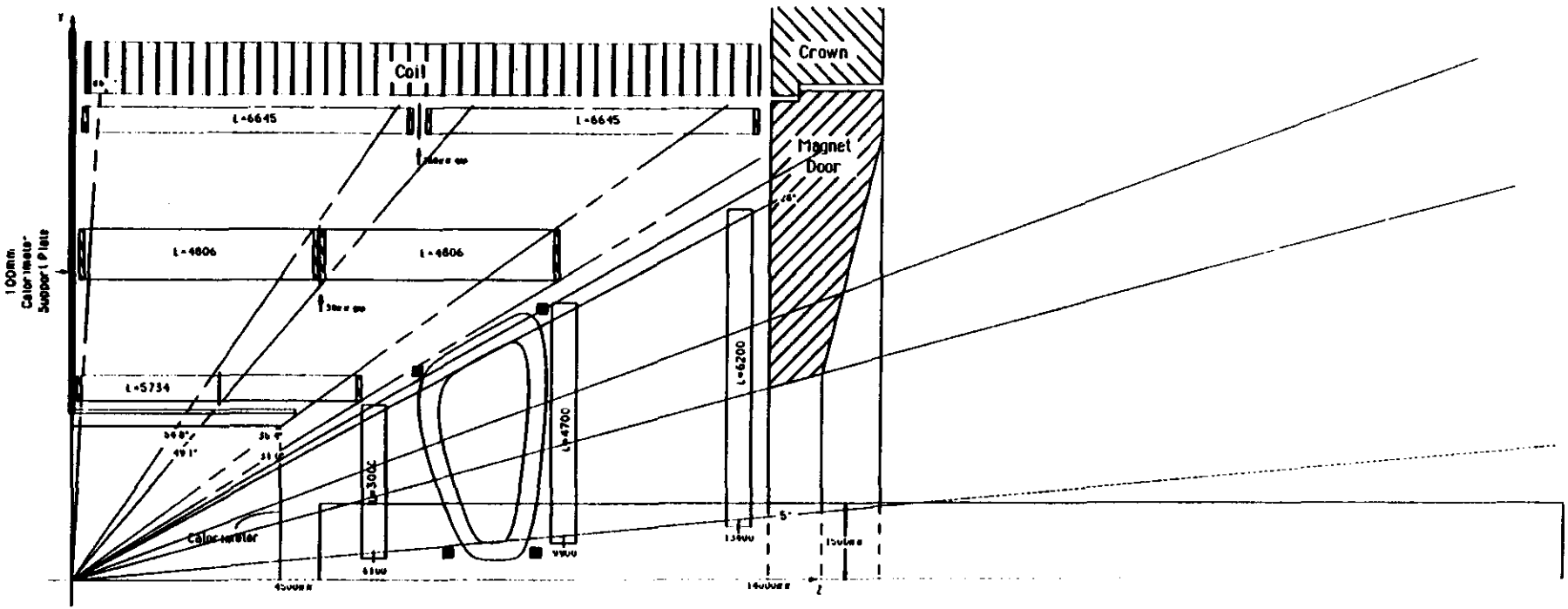

L* Muon Spectrometer Volume

Central Region Geometry

Version 4.3/15

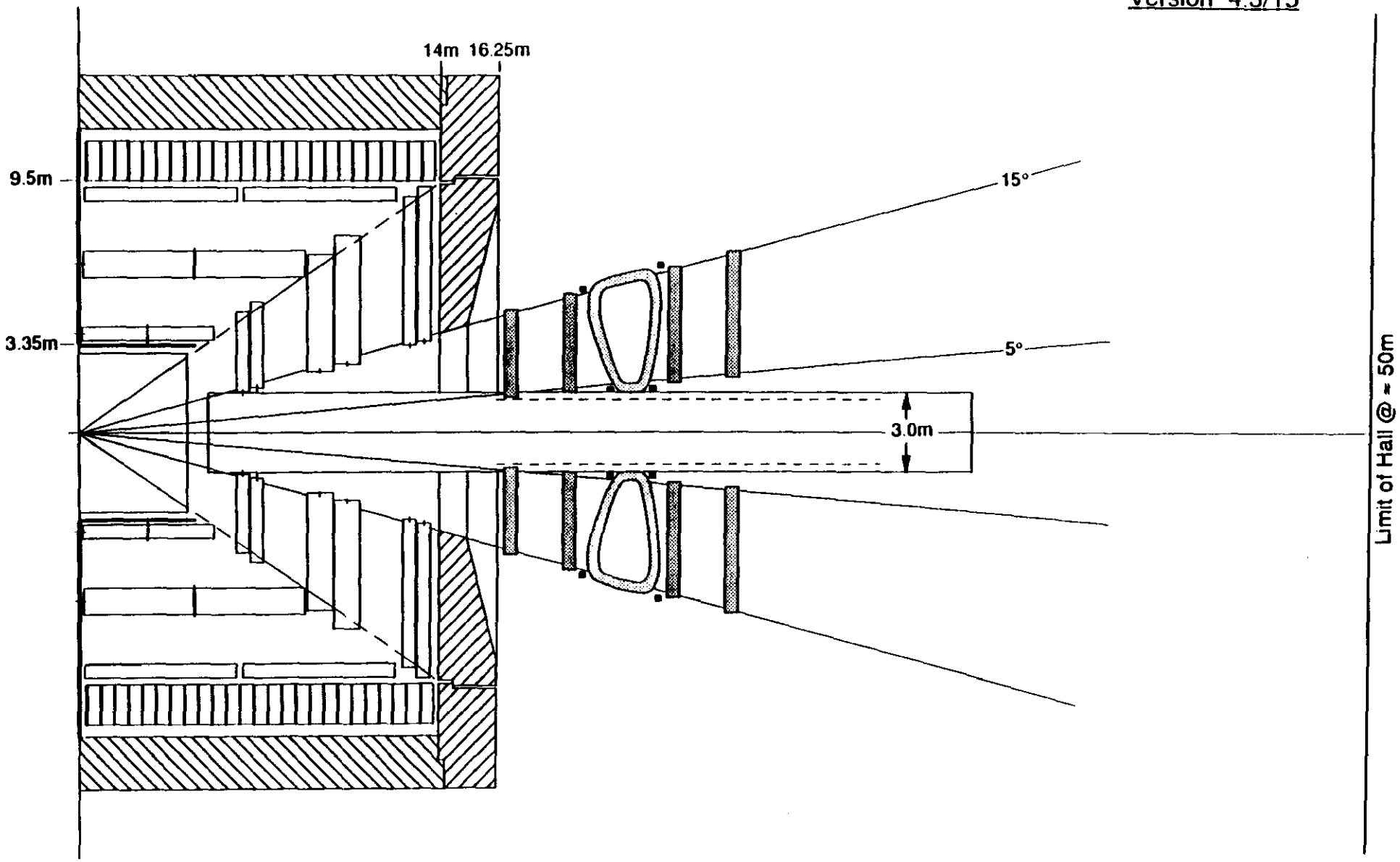

Version 4.4/15

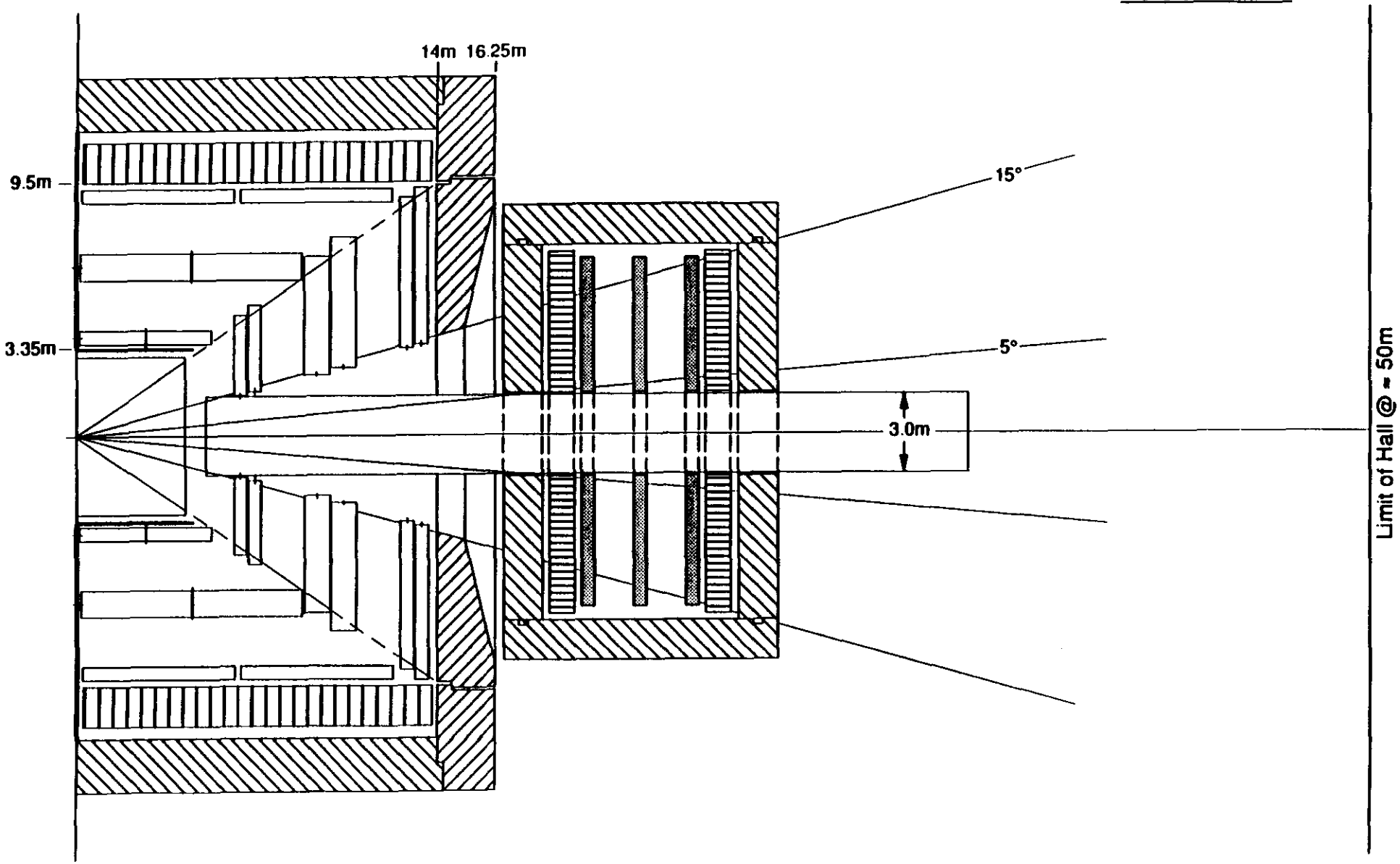

Version 4.4/15

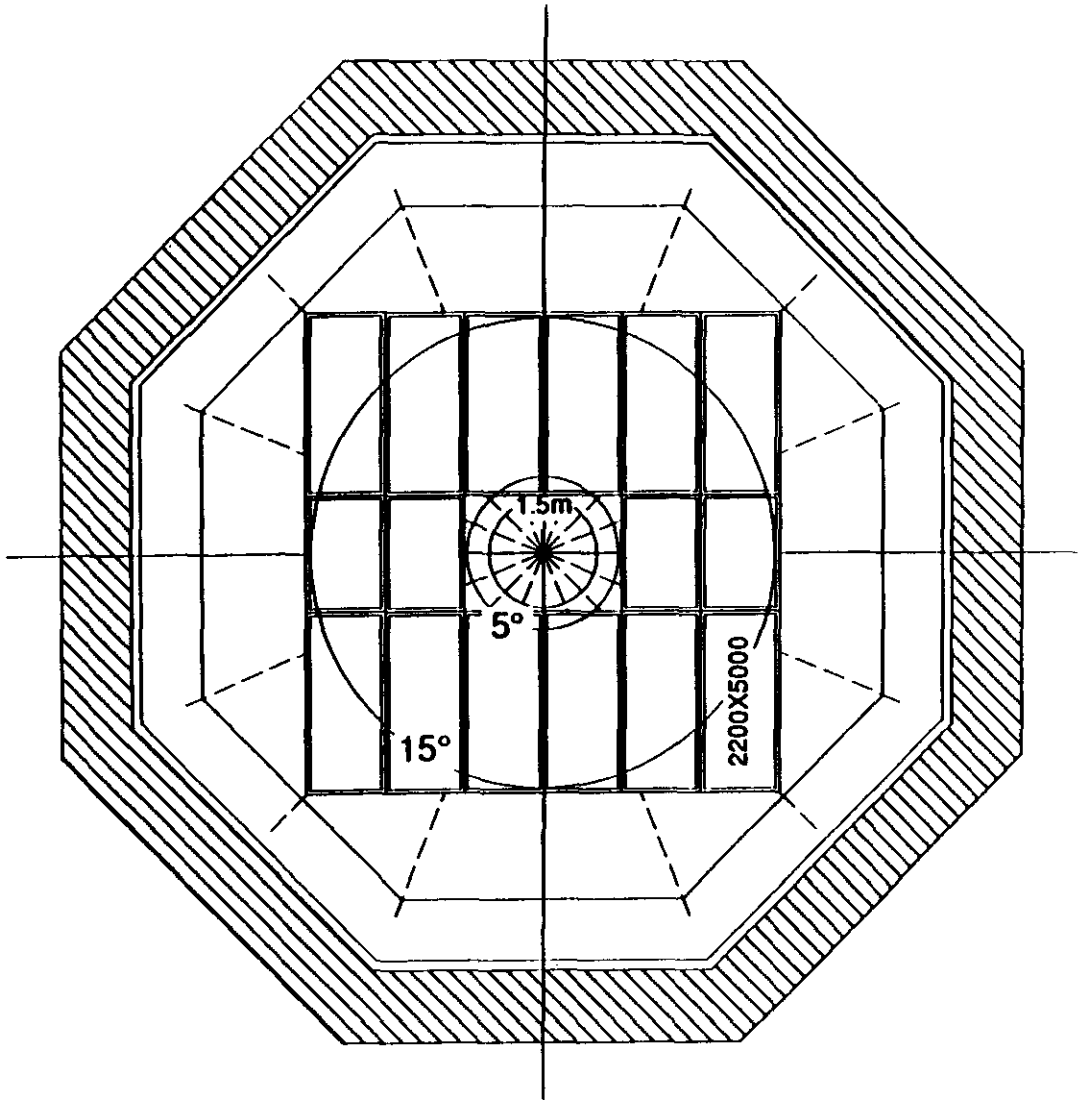

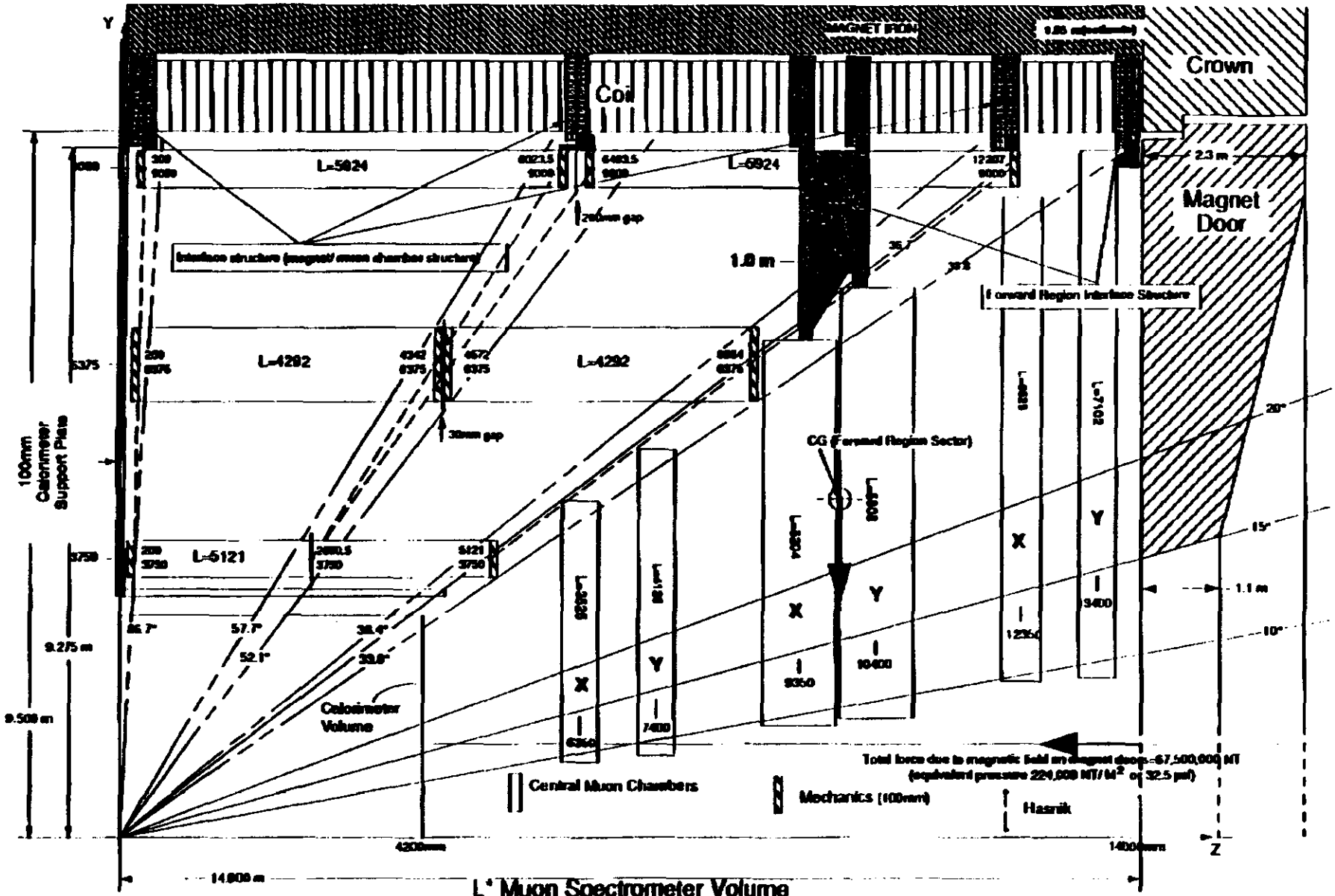

L* Muon Spectrometer Volume
Chamber Geometry and Alignment

INDICATED INTERFACE HARDWARE IS SHOWN ONLY TO STIMULATE ALTERNATIVE CONCEPTS AND THE FIELD REMAINS OPEN FOR ANY IDEAS WHICH ACCOMPLISH THE TASK AT HAND

F. Nichitiu
Similar to C. Gianelli's 4.2 17.01.90
With support structure indicated and forward region chambers lengthened to cover 10°

SHEET 2 OF 2

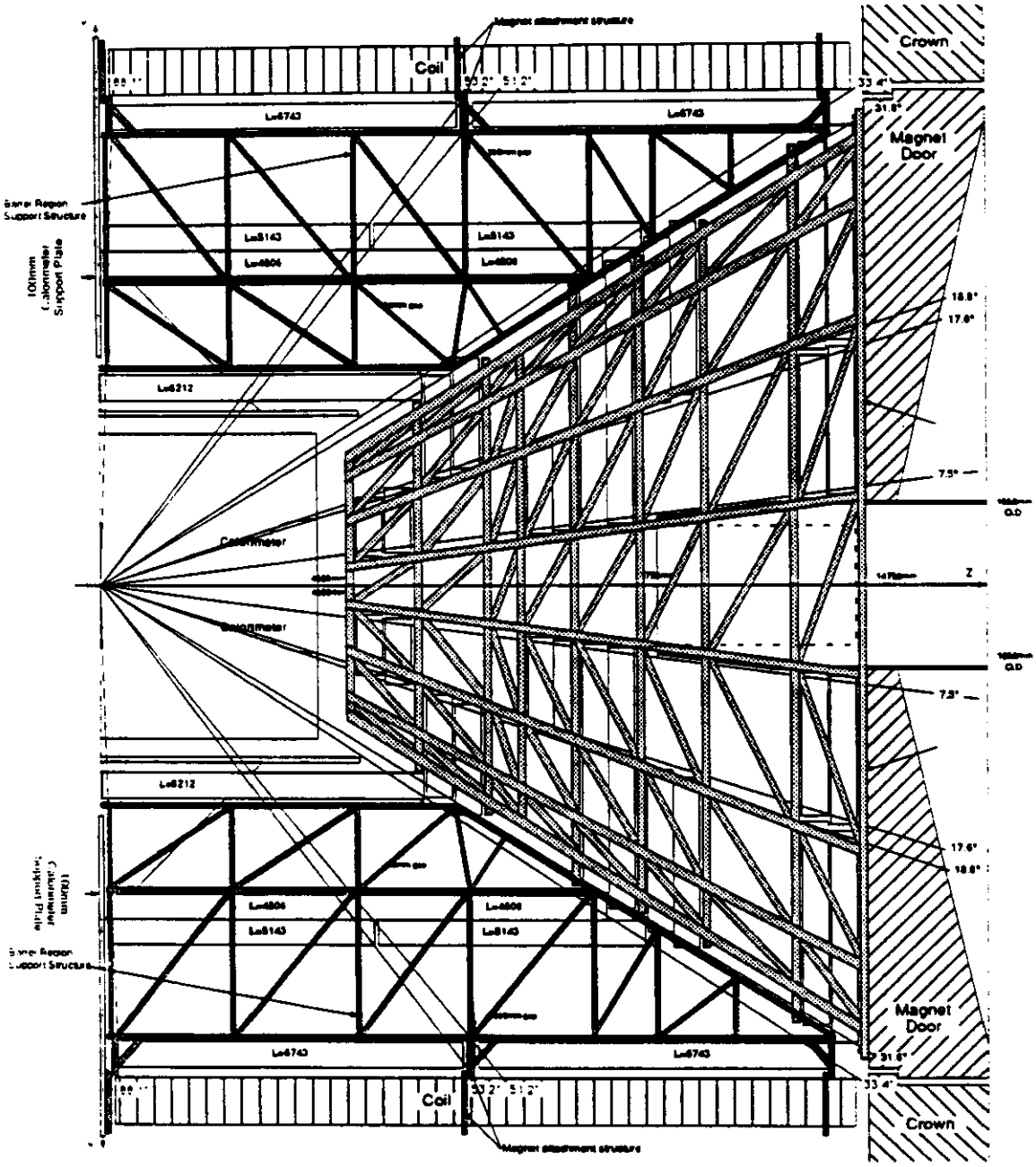
Coil
Crown
Magnet Door
Coil
Crown
Magnet Door

Who Wins?

Consider for:

1. Performance: Resolution, Acceptance
2. Cost
3. Local Alignment
4. Support Structure (analyzed)
5. Performance In Situ: Thermal effects, etc.
6. Global Support
7. Global Alignment
8. Services: Self and Others
9. Production: Fabrication and Assembly
10. Transport / Storage
11. Installation

Insert: same L* 3D

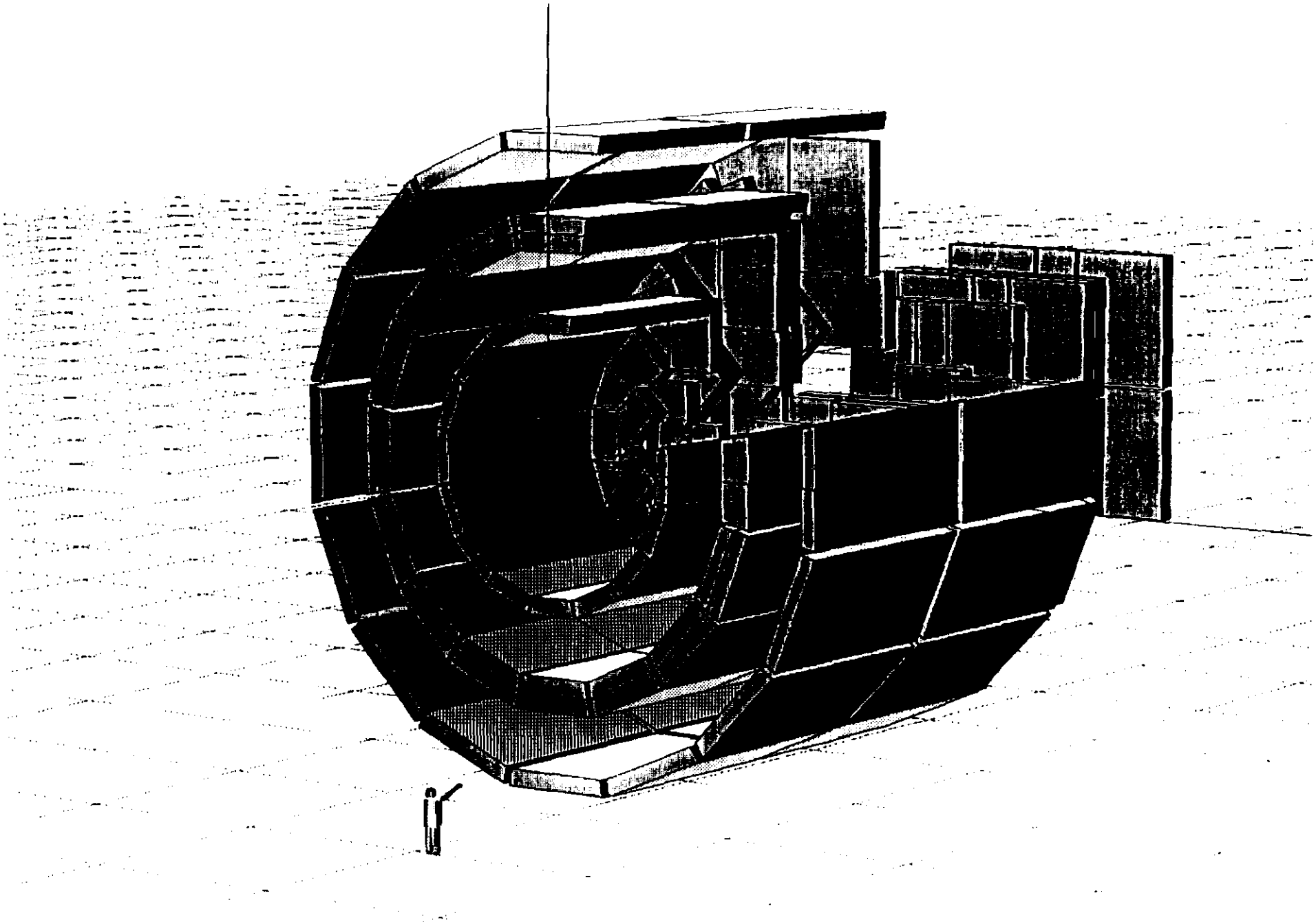

2. What Exists?:
L* Configuration Details

Defined Numerically:

- Database defines detector component active and physical envelopes constrained for alignment lines of sight, inner detectors, magnet parameters, etc.

- Linked to subroutines for multiple scattering calcs, services definition, resolution, acceptance, etc.

LOI Warm Coil Version Radial Endcap 13 (8)

MI Lim	5200											
MI R.O	6486					O = Outline	W = Width					
MM.i 2 R.O	9868					B = Bottom	M = Measure					
MM.o.2 R.O	10619		Side Mech.	50		T = Top						
Door	14750		End Mech.	100								
										Drawing Coordinates (Projection on outer plane)		
THETA MIN	9.0°		8 SIDED	8 SIDED	8 SIDED	8 SIDED	8 SIDED	8 SIDED	8 SIDED			
THETA MAX	17.0°											
Chamber	Z	B.O	B M	T M	T O	T.O-B.O	W.O	TCL-W O/2	BCL-W O/2	B M	T M	W M
MI.1.1	5750	811	911	1758	1858	1047	1439	50	91			
MM.I.1 1	9668	1431	1531	2956	3056	1624	2352	90	255			
MM O.1.1	10168	1510	1610	3109	3209	1698	2468	95	276			
MO.1.1	14300	2165	2265	4372	4472	2307	3430	137	450	2265	4372	3330
x/l	-0.01											
Common Z	9918											
THETA MIN	18 1°		16 SIDED	16 SIDED	16 SIDED	16 SIDED	16 SIDED	16 SIDED	16 SIDED			
THETA MAX	31.1°											
MI.1.2	6786	2115	2215	4094	4194	2079	1568	50	92			
MM.I.1.2	9668	3056	3156	5832	5932	2876	2192	84	170			
MM.O.1.2	10168	3219	3319	6133	6233	3015	2300	90	183			
MO.1.2	13750	4388	4488	8295	8395	4006	3075	132	280	4668	8626	3094
x/l	-0.05											
				6000	6500	8750						
THETA MIN	9.0°		8 SIDED	8 SIDED	8 SIDED	8 SIDED	8 SIDED	8 SIDED	8 SIDED			
THETA MAX	17.3°											
Chamber	Z	B.O	B M	T.M	T O	T.O-B.O	W.O	TCL-W O/2	BCL-W O/2			
MI 2.1	5200	724	824	1622	1722	998	1326	50	60			
MM.I.2.1	8618	1265	1365	2688	2788	1523	2132	88	199			
MM.O.2.1	9118	1344	1444	2844	2944	1599	2250	94	219			
MO.2.1	13750	2078	2178	4288	4388	2310	3343	146	406	2265	4460	3372
x/l	-0.07											
Common Z	9918											
THETA MIN	19.1°		16 SIDED	16 SIDED	16 SIDED	16 SIDED	16 SIDED	16 SIDED	16 SIDED			
THETA MAX	32.4°											
MI.2.2	7336	2433	2533	4656	4756	2323	1792	50	112			
MM.I.2.2	10919	3670	3770	6929	7029	3359	2618	89	211			
MM.O.2.2	11419	3843	3943	7247	7347	3504	2734	95	225			
MO.2.2	14300	4838	4938	9075	9175	4337	3398	126	305	4938	9075	3298
x/l	0.05											
					9250							

	MI	MMi	MMo	MO	Total
N° Chambers	48	48	48	48	192
Total Width (m)	69.2	107.6	113.1	155.1	444.9
N° P Cells	692	1076	1131	1551	4449
n° Sense Wires	22129	34418	36187	49631	142365
Total Length (m)	68.5	104.5	109.8	147.3	430.1
N° Z Cells	2741	-	-	5891	8632
Area (m^2)	104.3	240.7	265.3	474.5	1084.8

Insert:

- Central 3D bare
    - Side; alignment, chamber length limits, efficient use of space
    - Torque comments
    - End; alignment, chamber width limits, modularize

- Endcap 3D bare - the real challenge is to fill this conical volume
    - It fits together like this; 2 draper drawings
    - Side; alignment etc., people are fond of only showing this view
    - End layers projected on outer, rectangular geometry, alignment, cross calibration for global reference in overlaps, higher resolution in overlaps at low theta where needed(not in plots)
    - Installation; originally one of the 'unsurmountable problems'

- All side view

Central Region

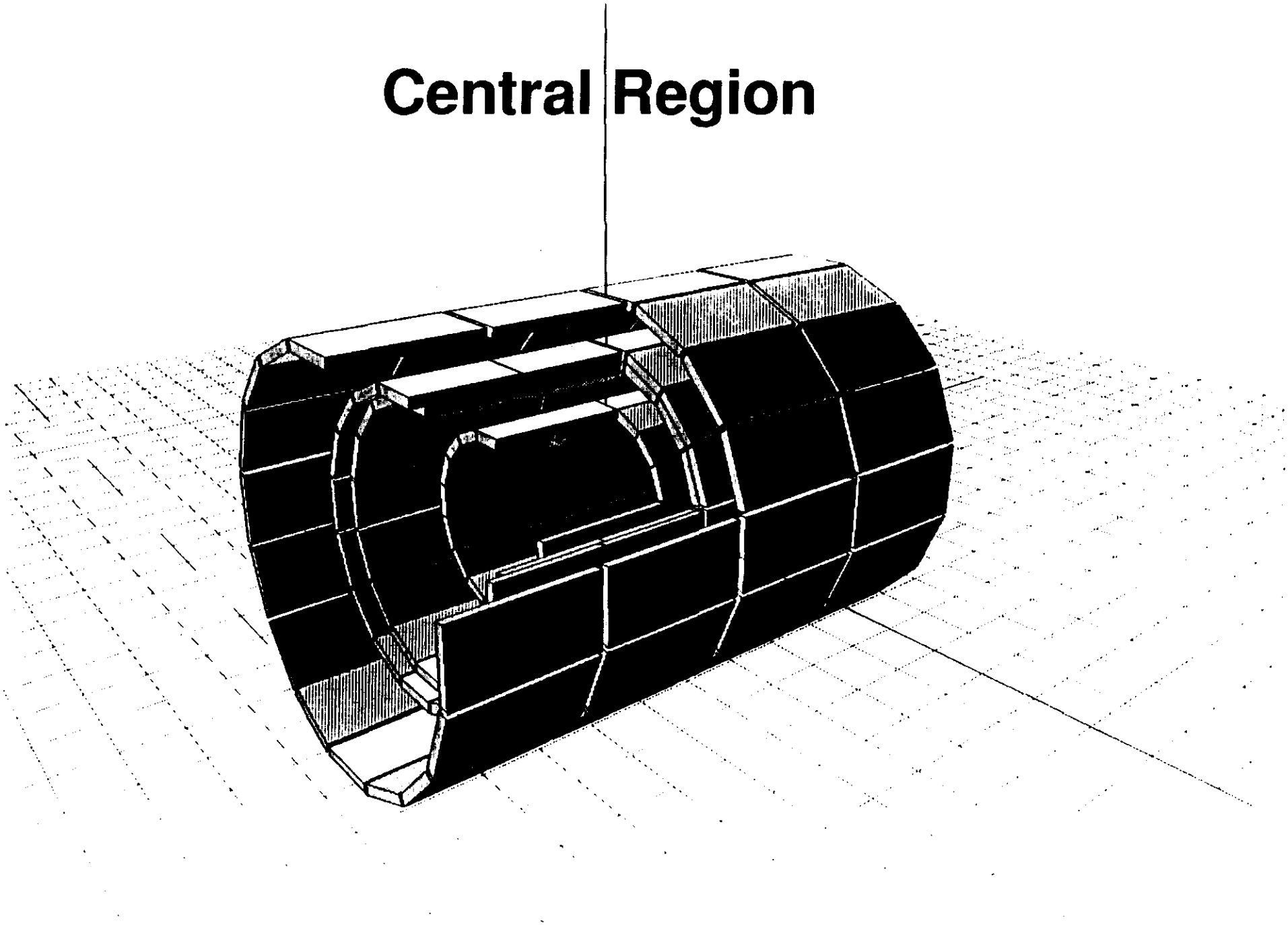

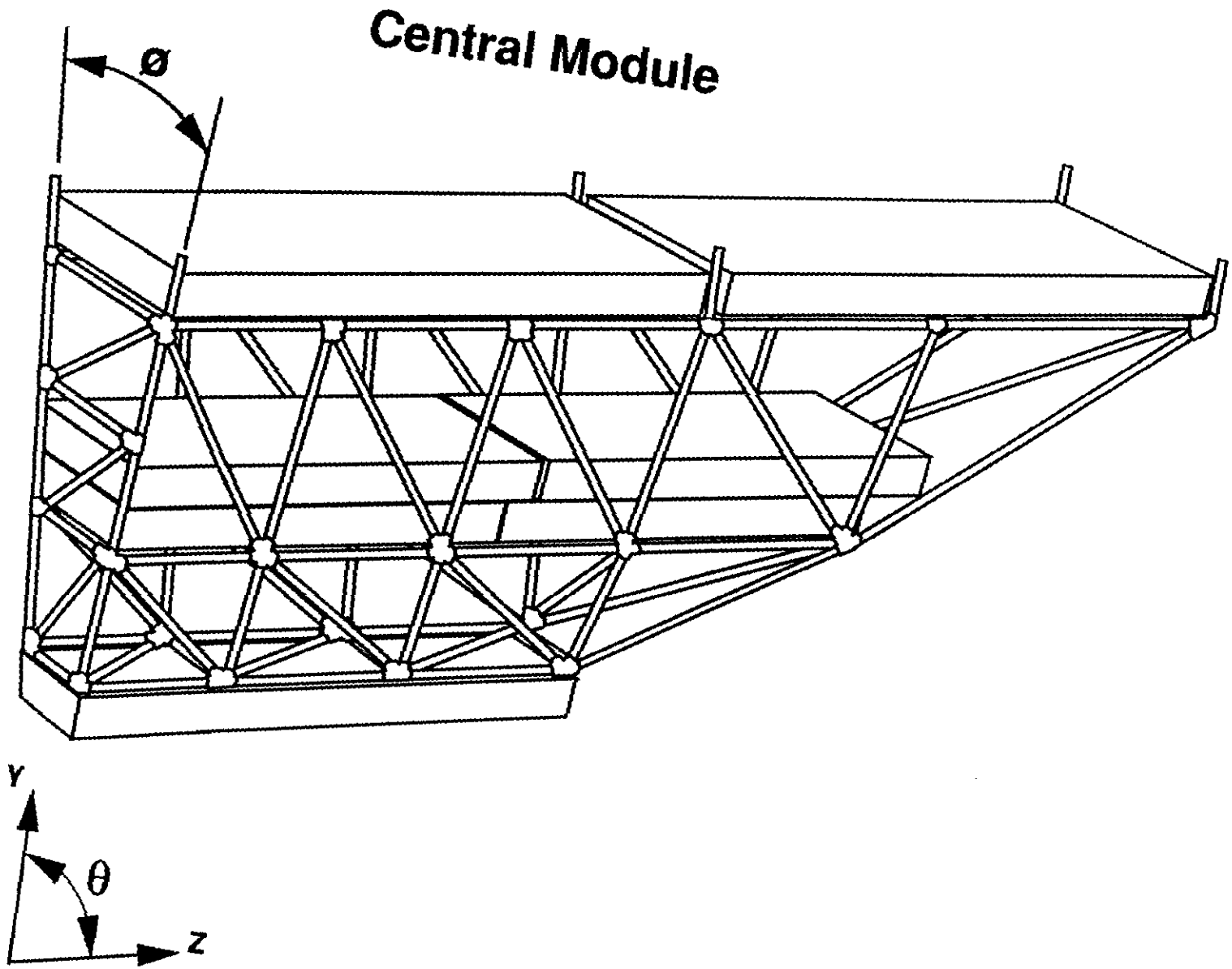
Central Module
ø
Y
θ
Z

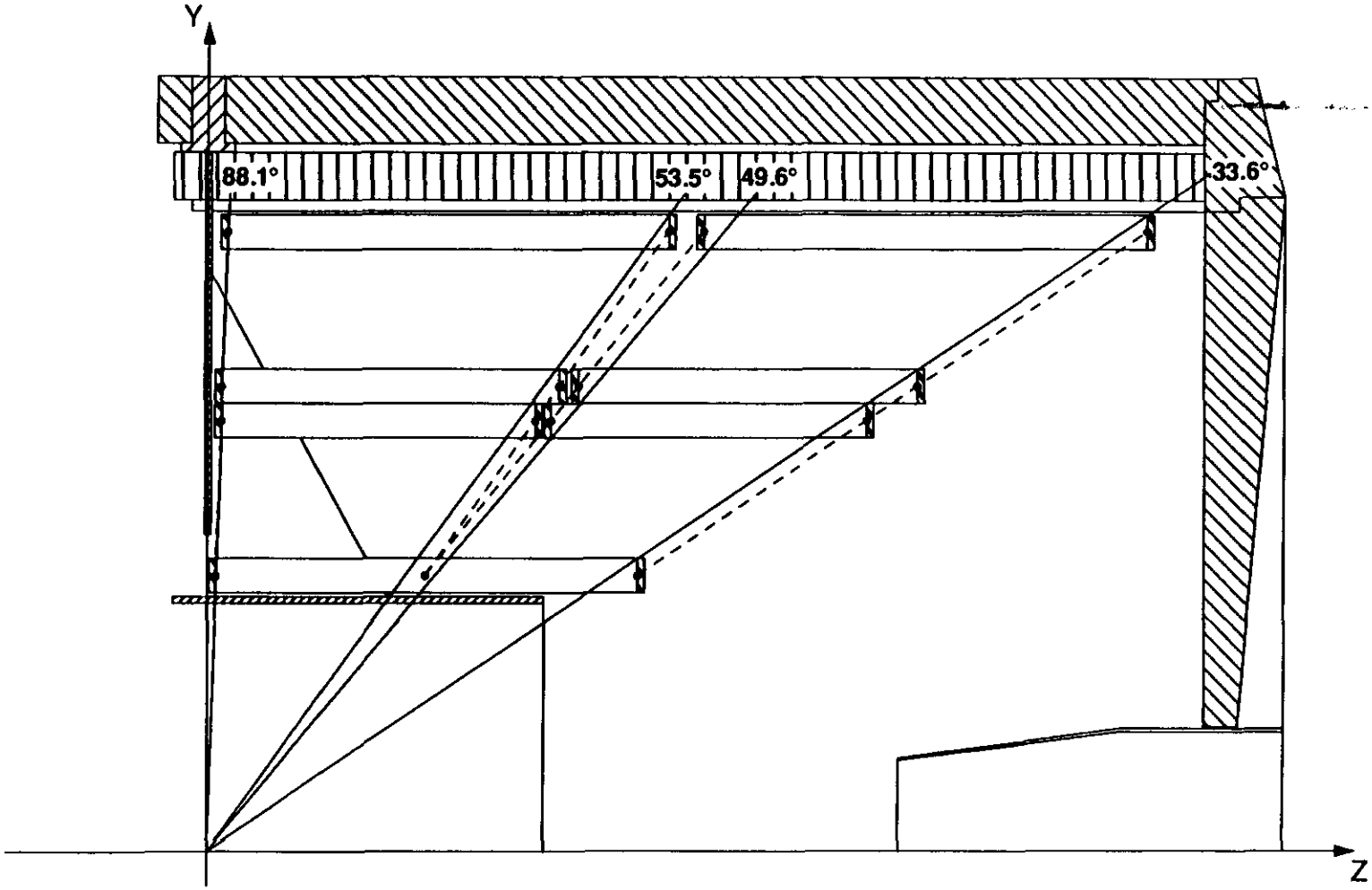

L* Central Magnet Parameters

Warm Coil Version

Version 13 12.10.90
Scale 1:100

Torque Effects on Sagitta Measurement

Lines of Sight pass through IP

L* Muon Spectrometer

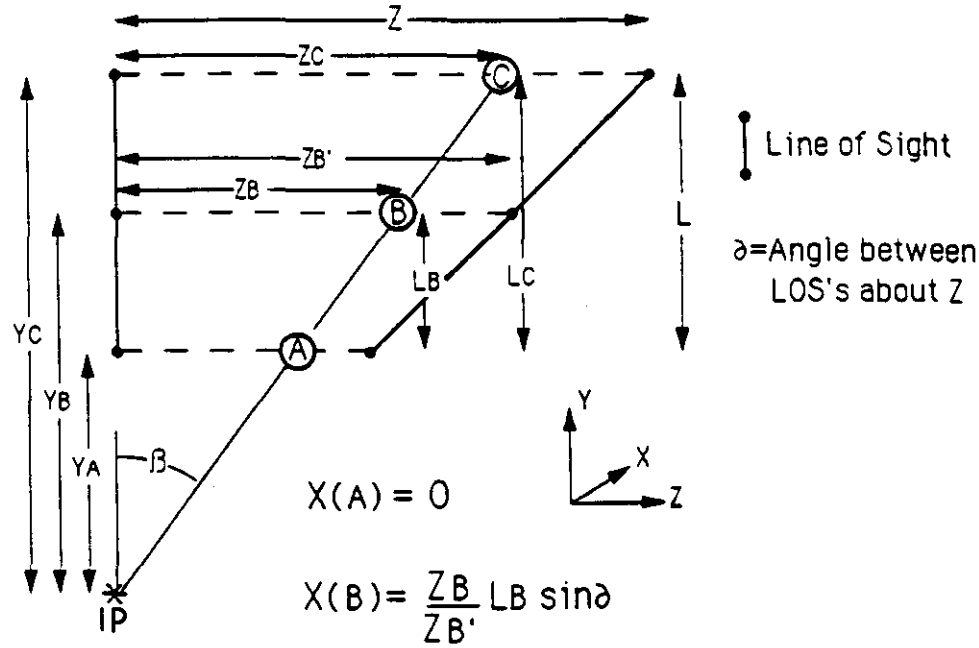

$$X(A) = 0$$

$$X(B) = \frac{ZB}{ZB'} LB \sin\partial$$

$$X(C) = \frac{ZC}{Z} LC \sin\partial$$

$$L(B) = (YB - YA) \qquad L(C) = (YC - YA)$$

$$Z(B) = YB \tan\beta \qquad Z(B') = Z\,\frac{YB}{YC} \qquad Z(C) = YC \tan\beta$$

$$X(B) = \frac{YB \tan\beta}{Z\,\frac{YB}{YC}} (YB - YA) \sin\partial \qquad X(C) = \frac{YC \tan\beta}{Z} (YC - YA) \sin\partial$$

$$S = XB - (XC - XA)\,\frac{LB}{LC}$$

$$S = \frac{YC \tan\beta}{Z} (YB - YA) \sin\partial - \frac{YC \tan\beta}{Z} (YC - YA) \sin\partial \, \frac{(YB - YA)}{(YC - YA)}$$

$$\boxed{S = 0\mu m}$$

<u>NOTE:</u> Torque measurement still required for acurate measurement of tracks not passing through IP (eg. cosmic ray calibration)

Torque Effects on Sagitta Measurement

L3 Muon Spectrometer Geometry

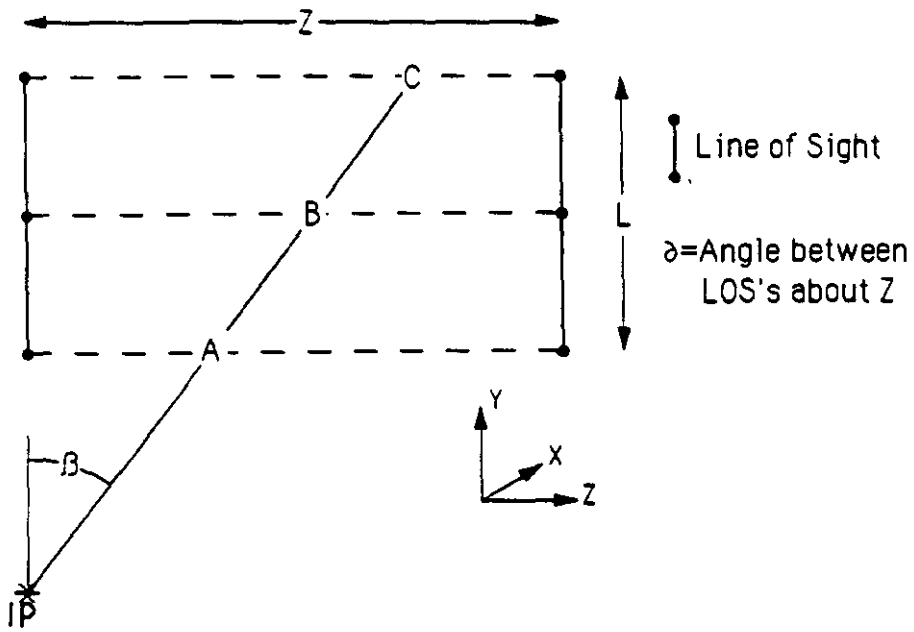

Sagitta Measurement with
LOS's set to Zero

$$S = \frac{L^2}{4Z} \tan\beta \sin\partial$$

L = 2900mm

Z = 5500mm

ßmax = 45°

∂max = 50μrads

Smax = 19μm

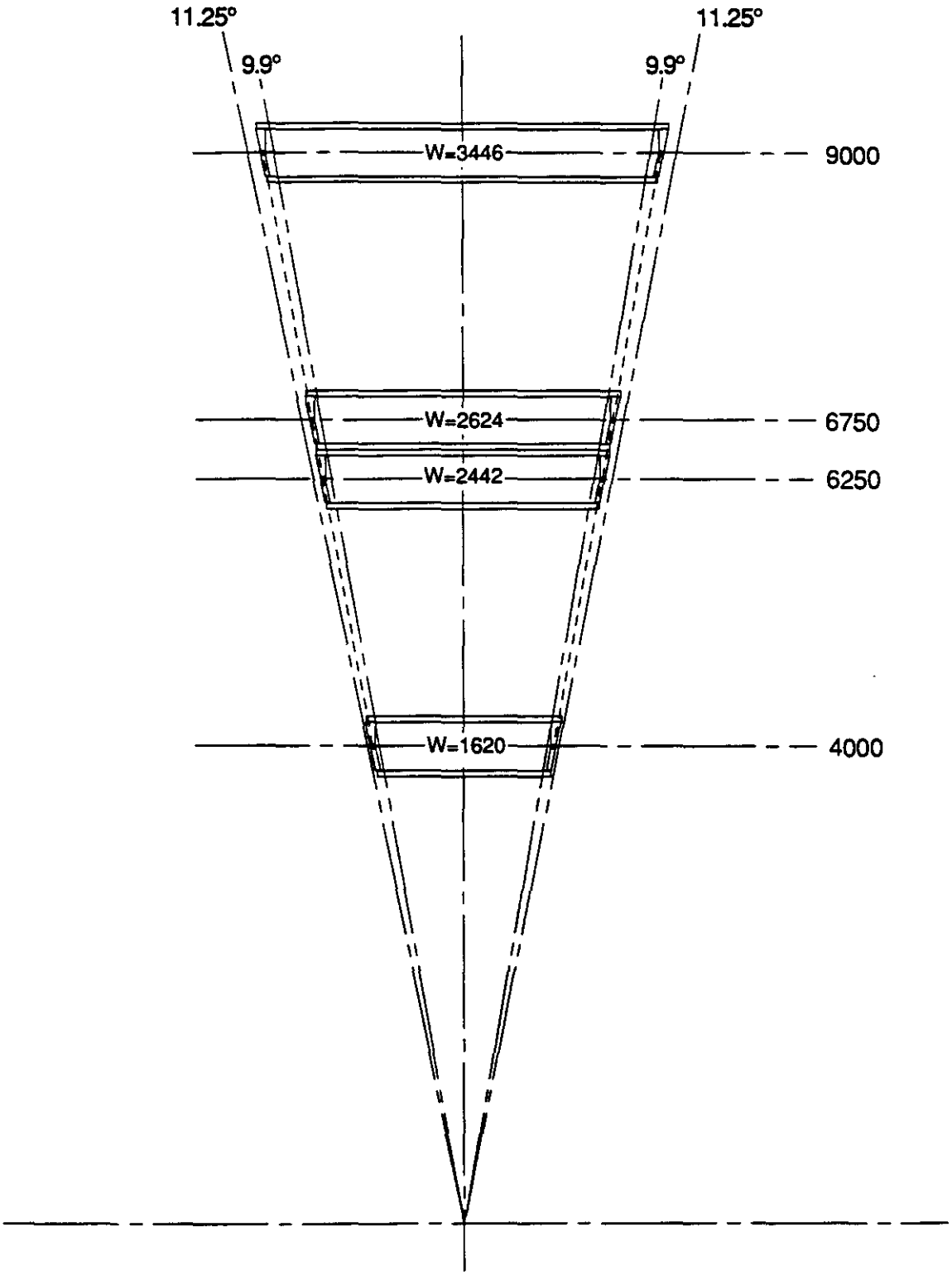

L* Muon Spectrometer Volume

Central Region Section

Version 7 12.12.1990
Scale 1:50

Endcap Region

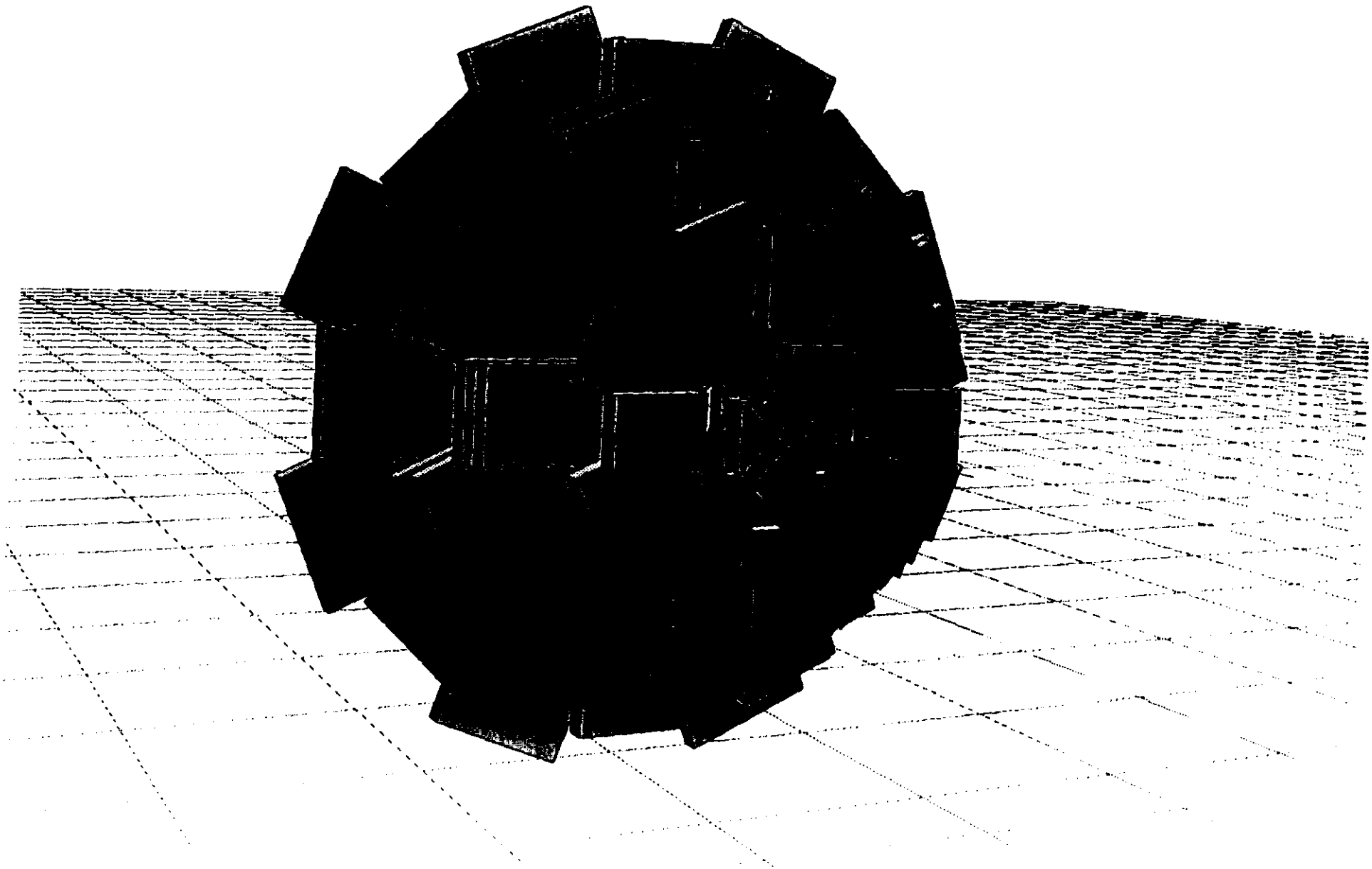

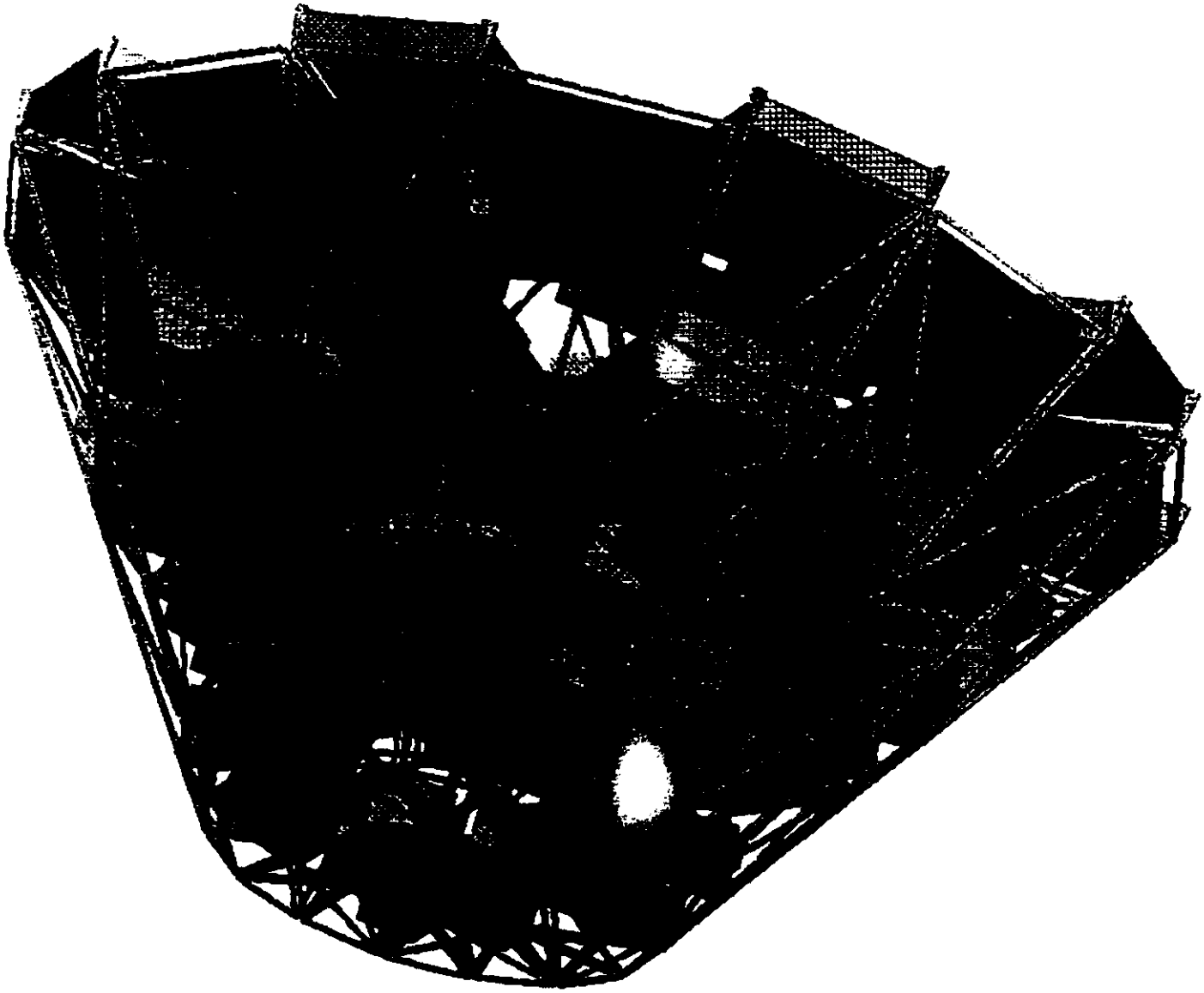

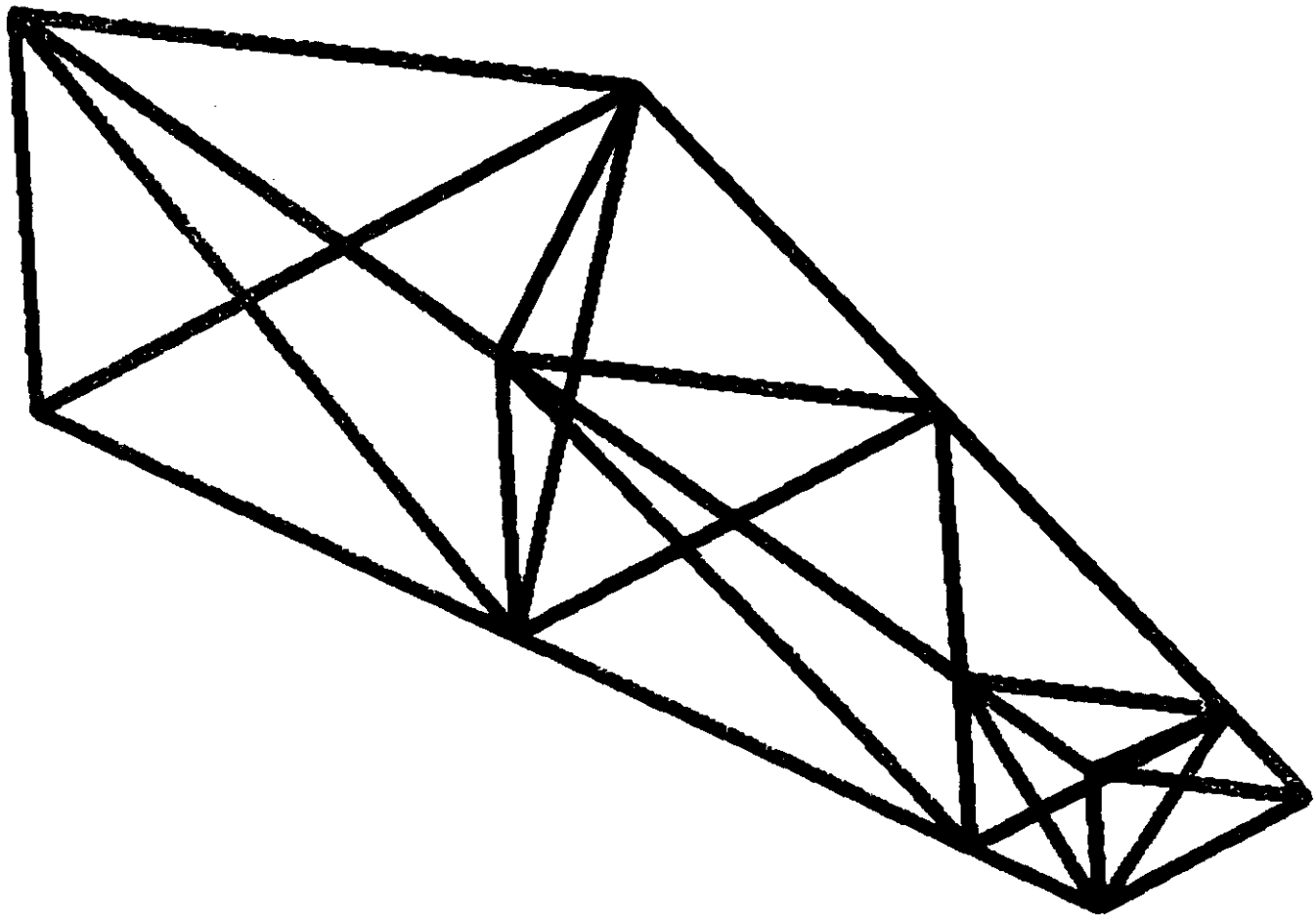

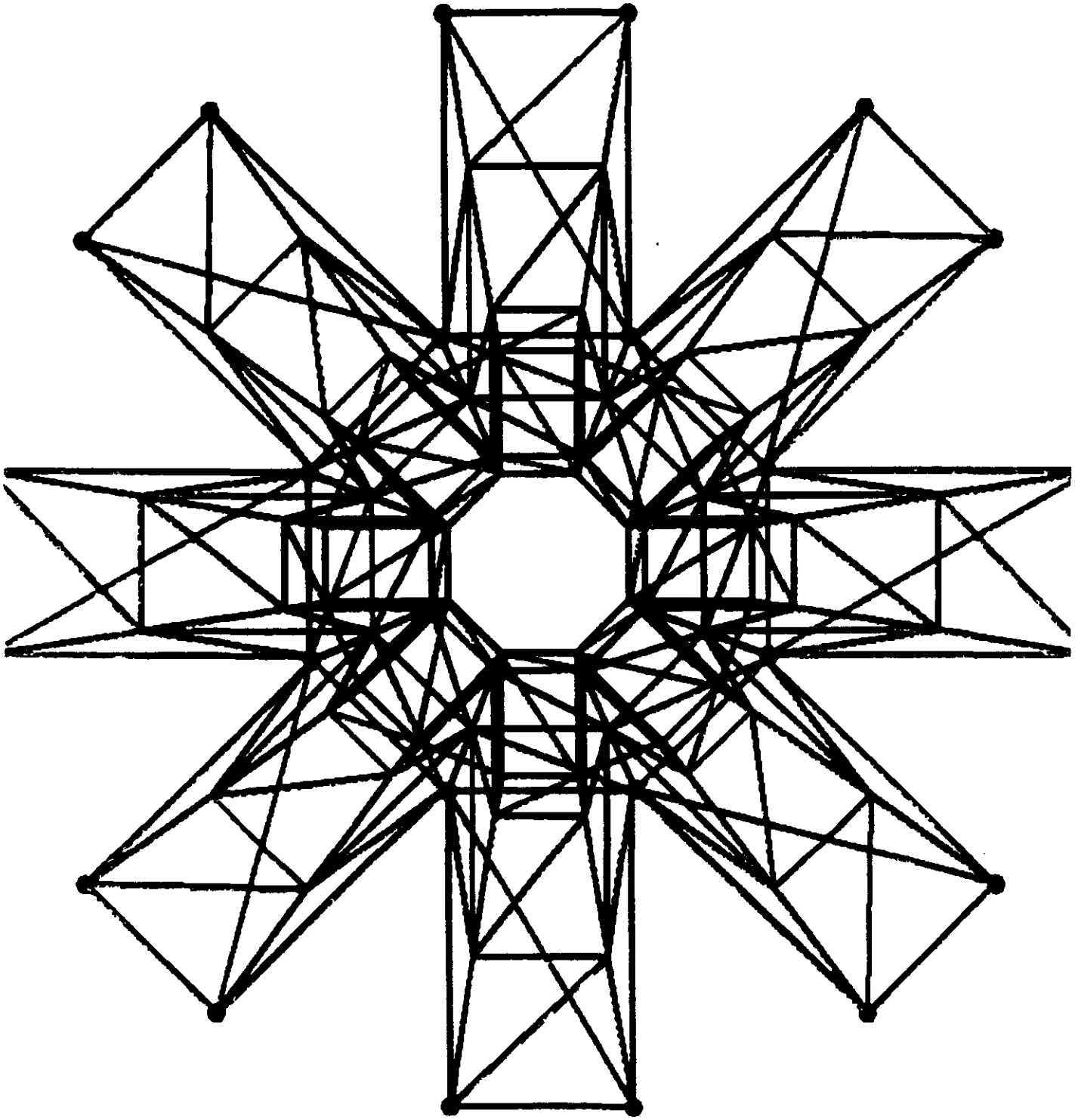

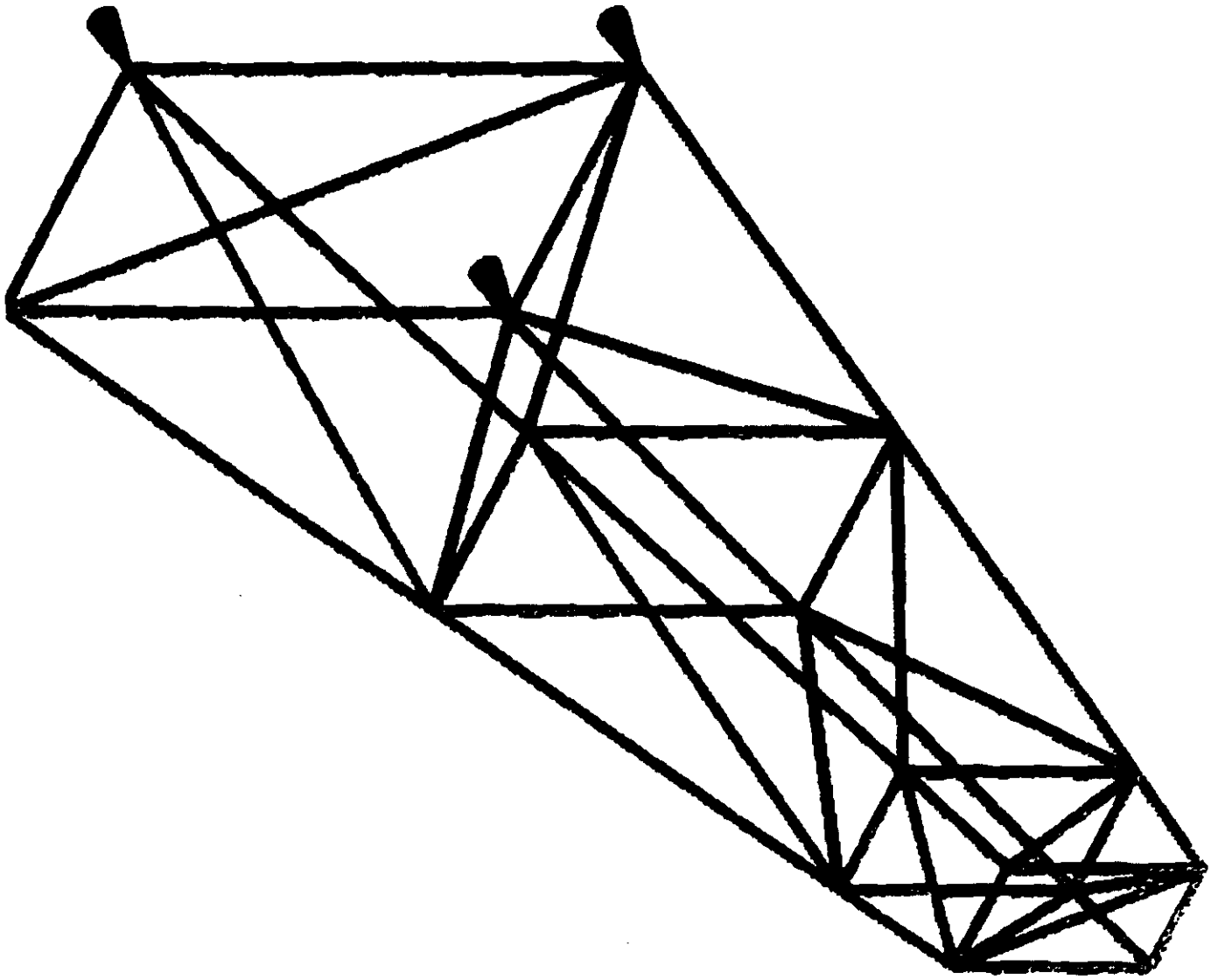

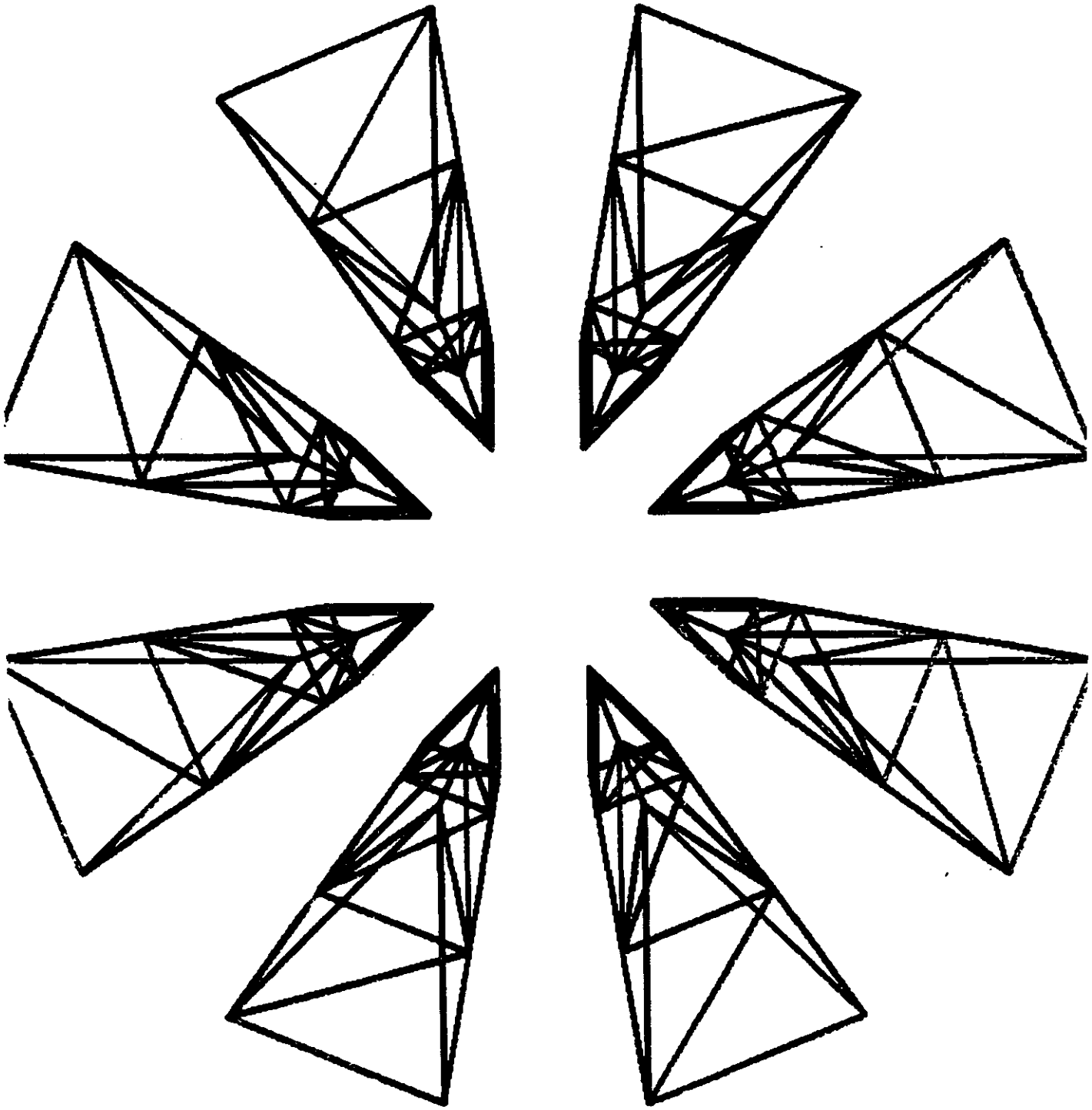

Endcap Module

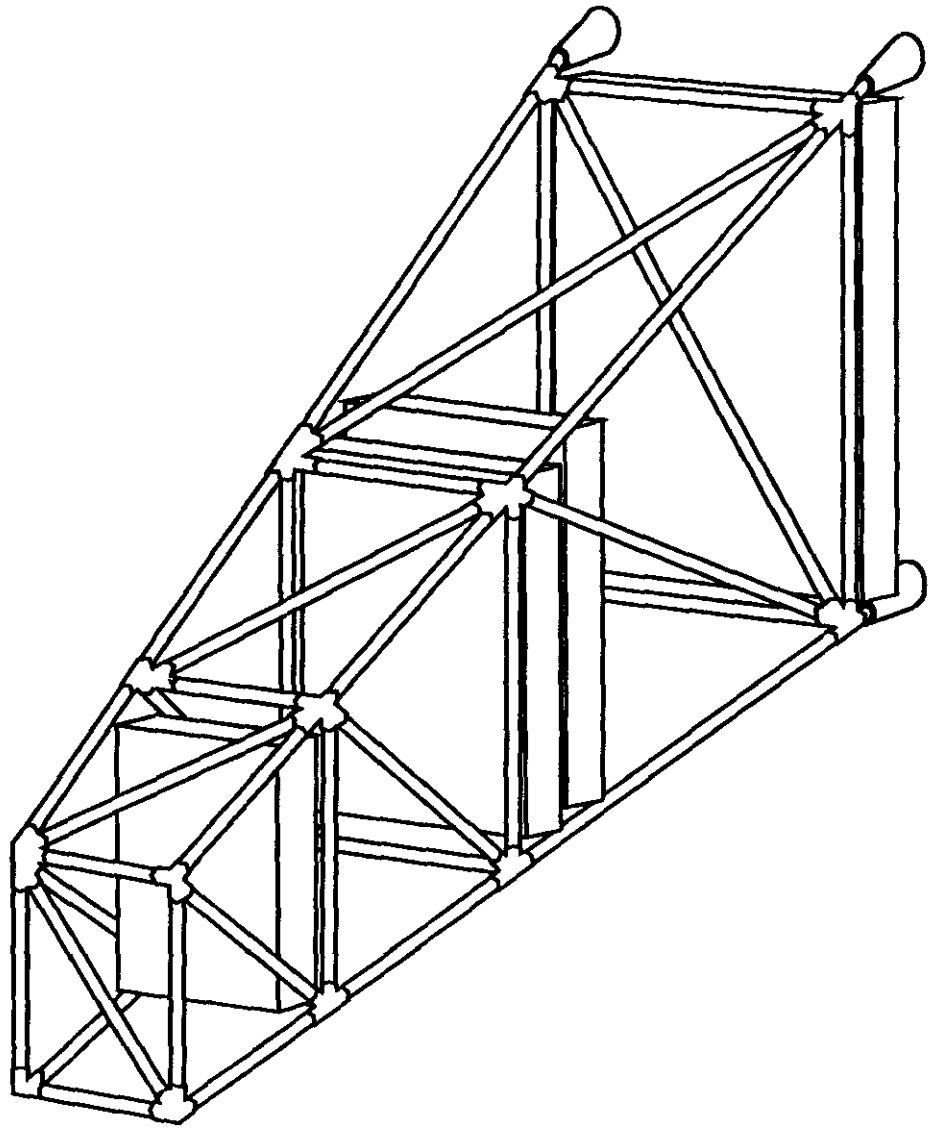

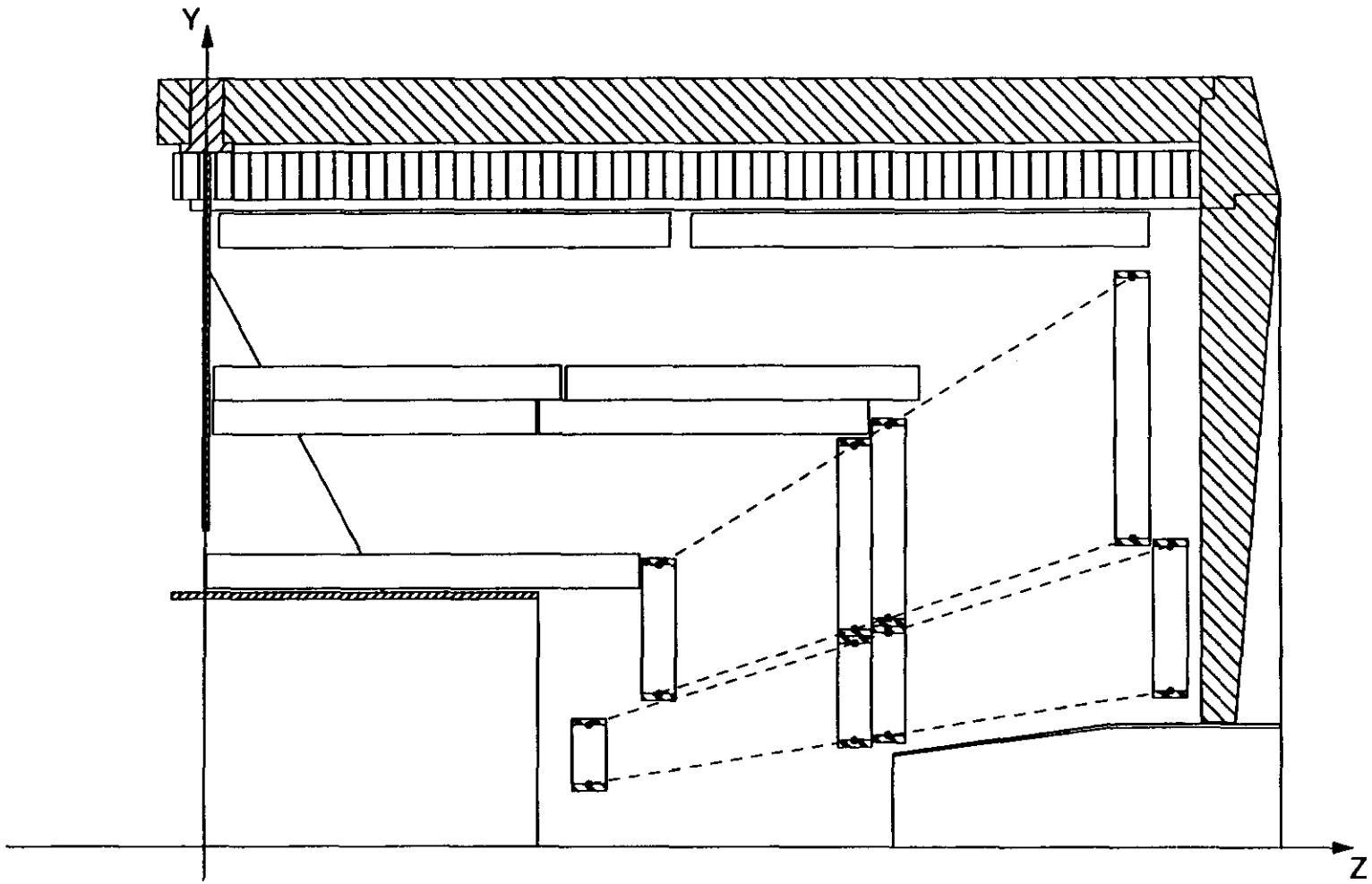

L* Central Magnet Parameters

Warm Coil Version

Version 13 12.10.90
Scale 1:100

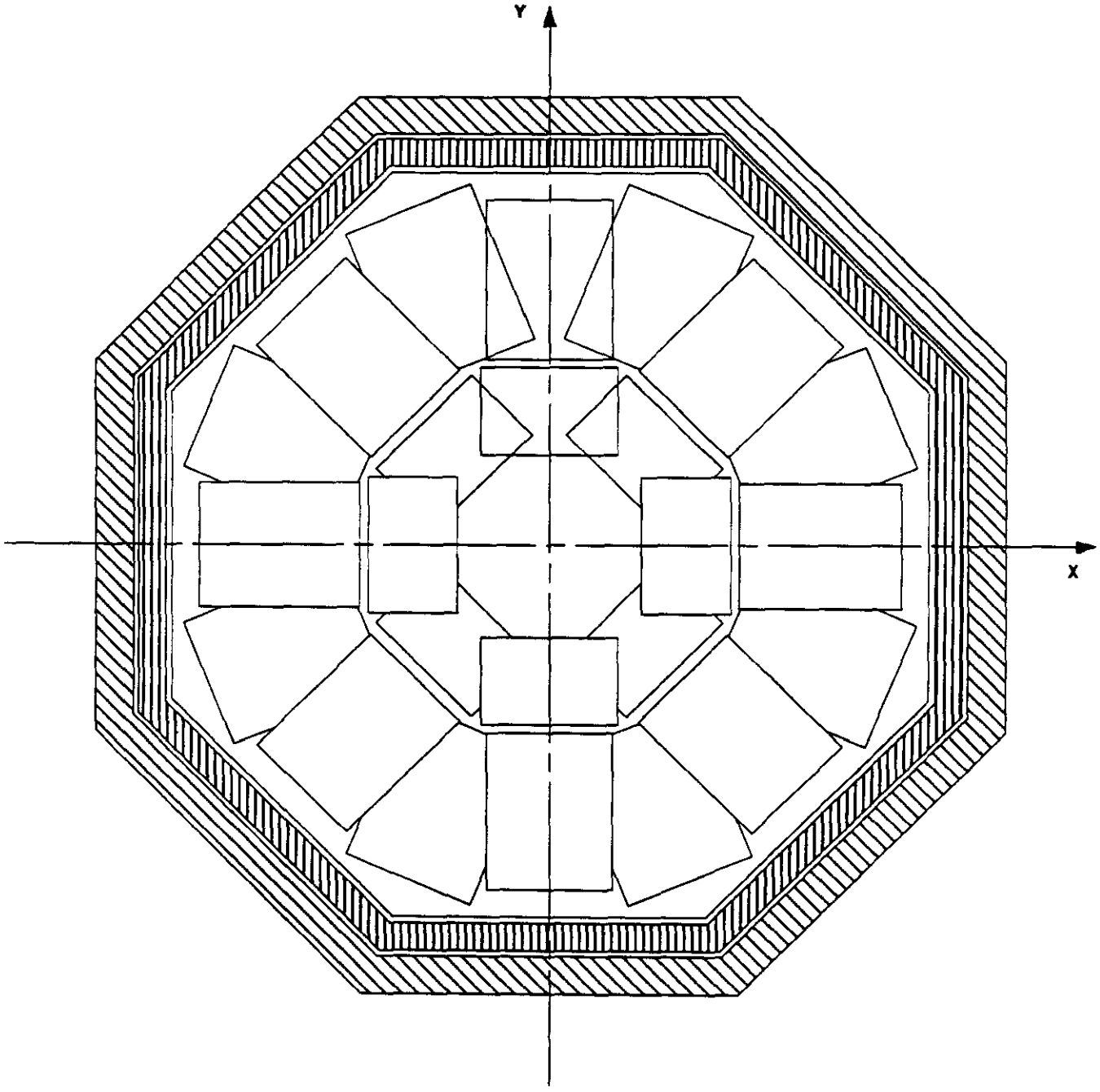

L* Muon Spectrometer Volume

Endcap Region

Projection on Z= 14300

Version 13 12.12.1990
Scale 1:100

Endcap Installation: Version A

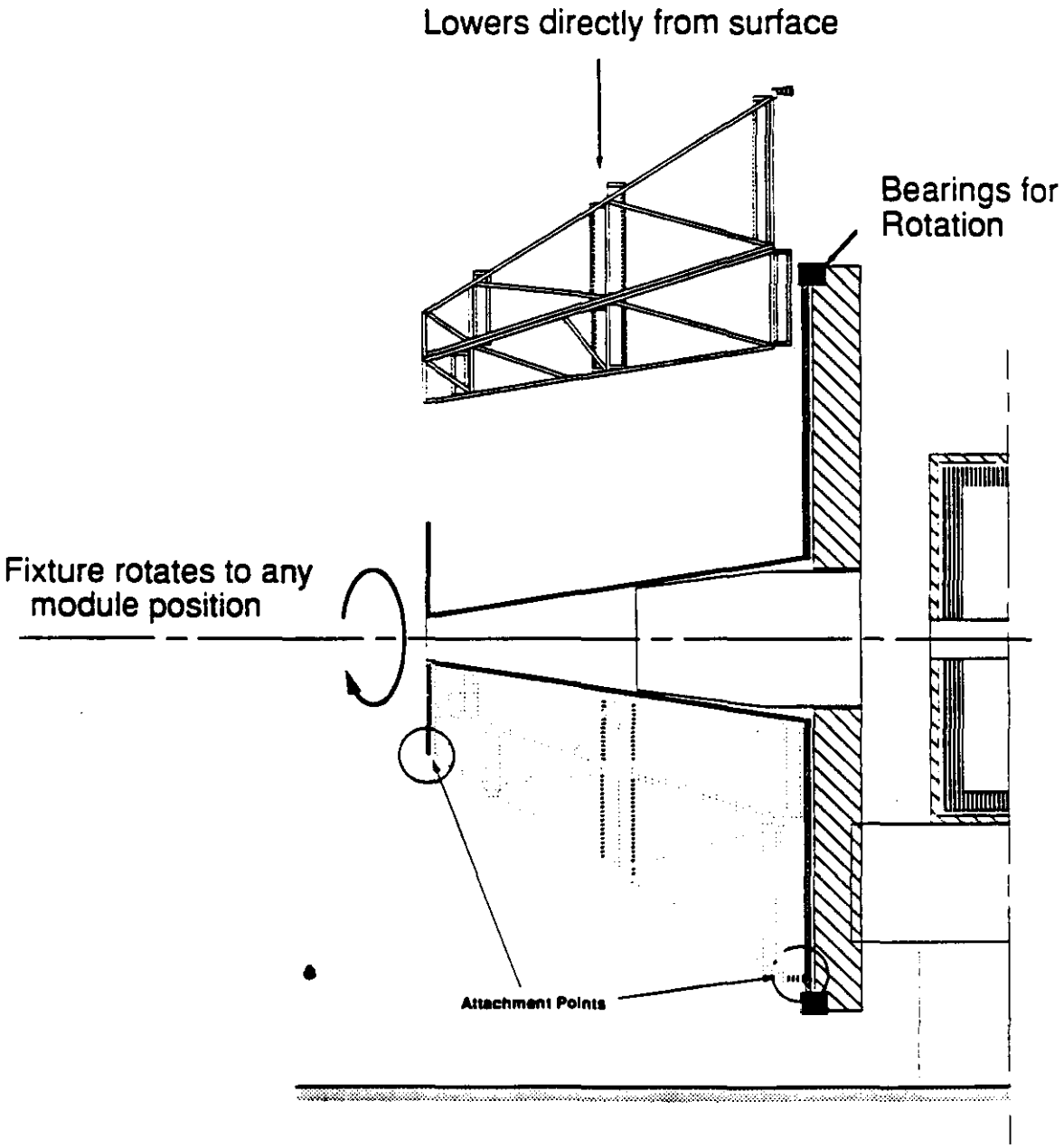

Alignment gauges (Ⓐ)
Point angle θ measurement
Ø mm angle measurement
Support structure
Honeycomb
Cover chamber
15000 mm
25000 mm
1400 mm
8250 mm
2500 mm
2400 mm
13800 mm
θ
Ø
x
y
z

2. What Exists?:
L* Configuration Details Summary

Extensive Knowledge of:

- Chamber function and mechanical designs
- Structural support; local and global
- Local alignment
- Assembly planning and fixturing
- Installation techniques
- Resource Requirements

Insert: Cover of most recent RRR

L★ DETECTOR

Resource Requirement Report

DRAFT No. 5

December 1, 1990

2. What Exists?:
2nd Detector

Principle changes from L*:

- No forward system
- Less half the wires/electronics and no double layer at middle plane
- Much smaller

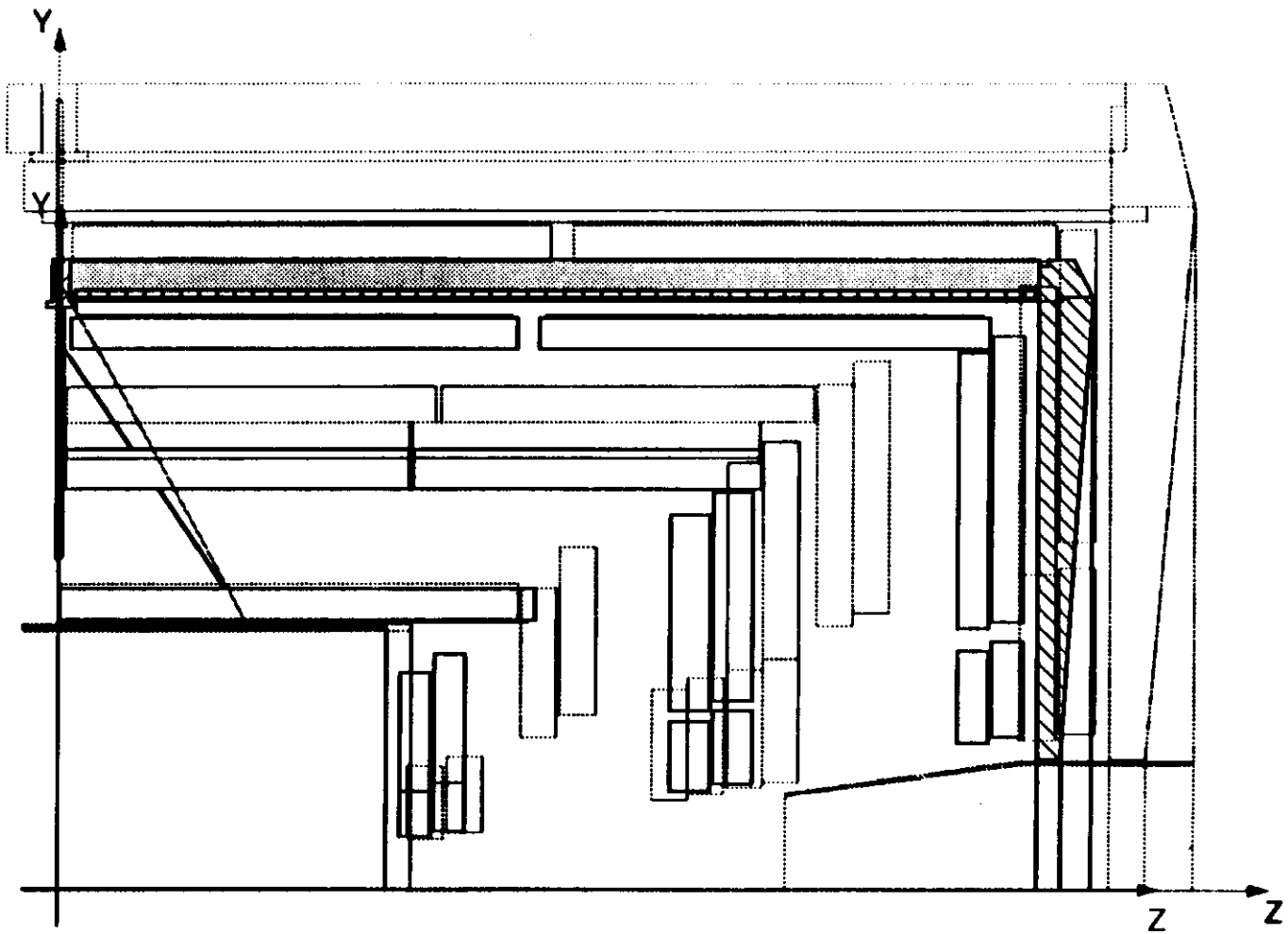

Dimensional Comparison

L* LOI to 2nd Detector

	L* LOI	2°	L* LOI→2°
Magnetic Field	0.4T	0.83T	2.1X
Resolution @90°	4.9%	5.0%	≈
Worst Resolution	12.0%	7.3%	+4.7%
Minimum Theta (C+EC)	9.0	9.4	≈
Chamber Area	4227m2	2612m2	62%
Central Region 'L'	5.3m	3.8m	-1.5m
Magnet Free Length	29.5m	26.5m	-3m
Magnet Free Bore (R)	18.6m	16.3m	-2.3m
Sense Wires/Electronics	321809	108838	34%
Complexity Factor	1.0	0.6	0.6

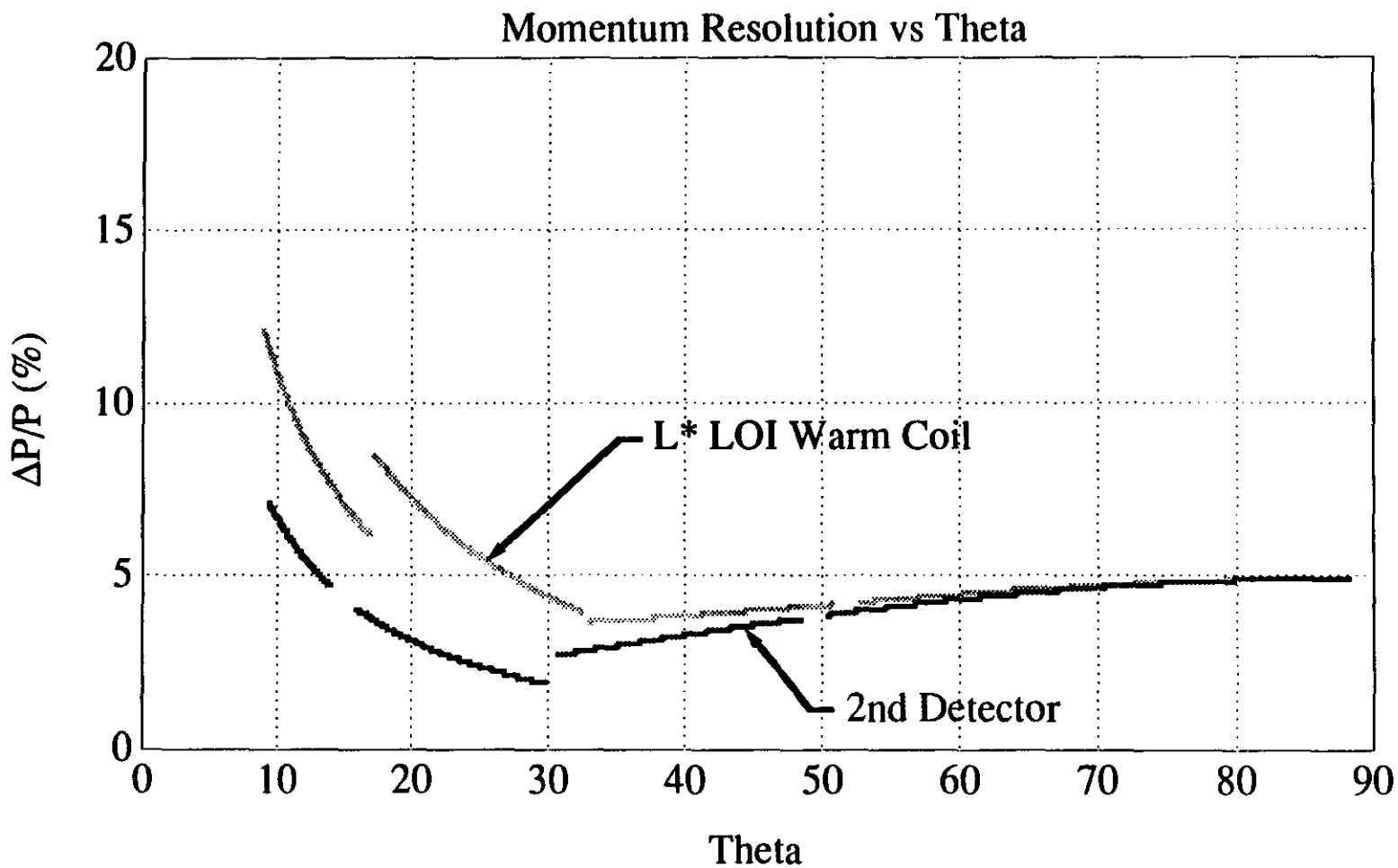
Momentum Resolution vs Theta
ΔP/P (%)
20
15
10
5
0
0
10
20
30
40
50
60
70
80
90
Theta
L* LOI Warm Coil
2nd Detector

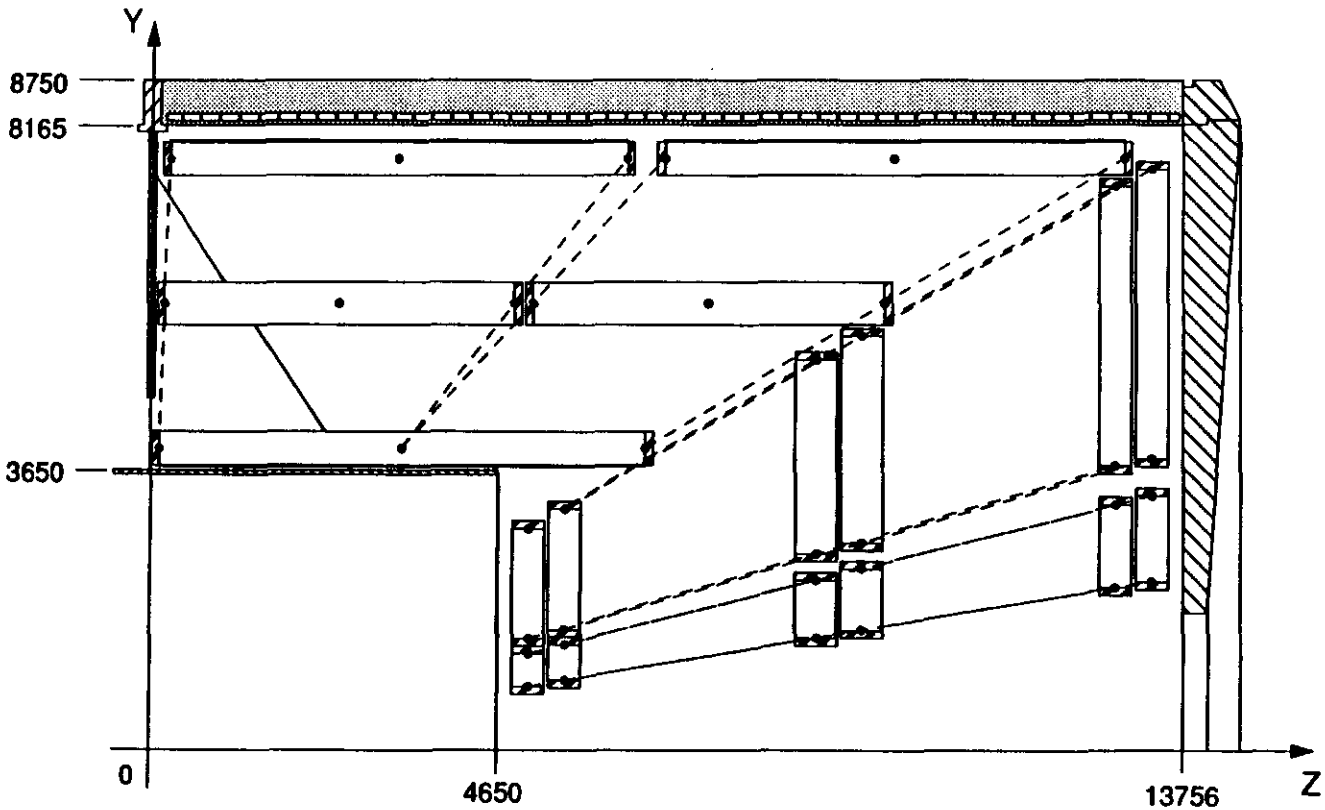

2nd Detector Central Magnet Parameters

LOI HC Version

Magnet Parameters

Version LOI/HC 09.07.91
Scale 1:100

3. What is applicable to other technology choices being discussed?

1st: Regardless of technology

Choose a simple solenoid for:

- Relatively simple design and development
- Simple field
- Relatively easy to upgrade with coils in forward, a forward system, etc.

2nd: Regardless of technology

Choose a rectangular geometry for detector elements:

- Relatively simple design and development
- Maximize precision
- Minimize cost

Detector layout concept is applicable to <u>ALL</u> choices being discussed, not simply muon chamber technology choices.

3rd: Regardless of technology

Choose a modular layout concept to facilitate:

- Local alignment
- Global alignment
- Fabrication
- Assembly
- Installation
- Transport
- Financing
- etc.....

4. What needs to be pushed NOW?:

Acceptance of this detector layout such that work may continue on:

- Magnet Design - Magnet Group, SSCL
- Structural Support Systems - CSDL, Other
- Local Alignment Systems and Applications
- Global Alignment Systems and Applications
- Hall Definition and Civil Engineering - SSCL, PB/MK
- Services and Surface Facilities - Muon Group, SSCL, PB/MK

Comment:

The objective has been to show some who may not have been aware before of the considerable amount of thought that has gone into the development of the detector layout. A choice to depart from this means repeating that effort to some extent and a choice to adopt means a substantially advanced position in the development as well as the immediate continuation of the peripheral activities mentioned.

MAGNET ENGINEERING AND R&D SCHEDULE

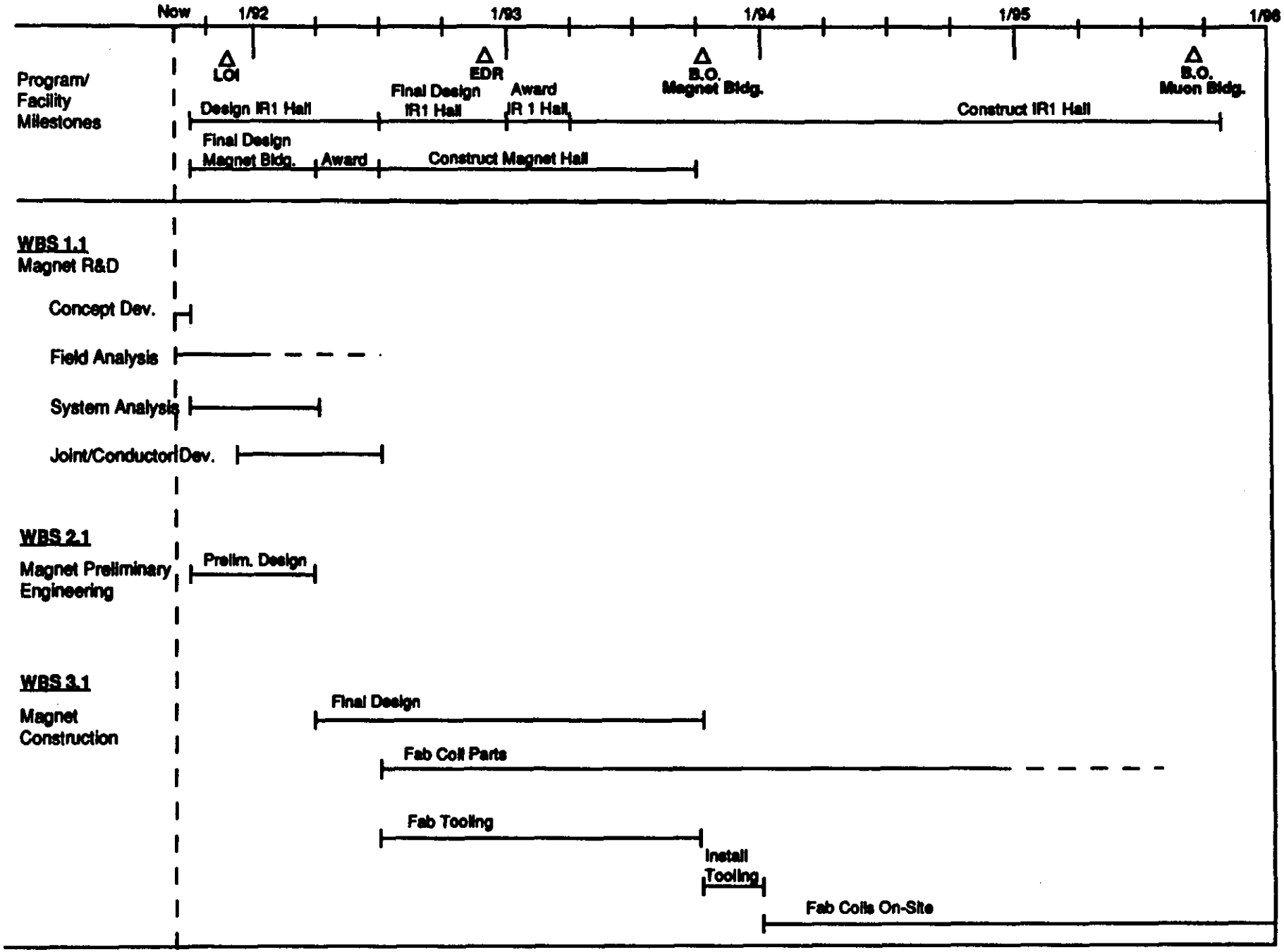

MUON ENGINEERING AND R&D SCHEDULE

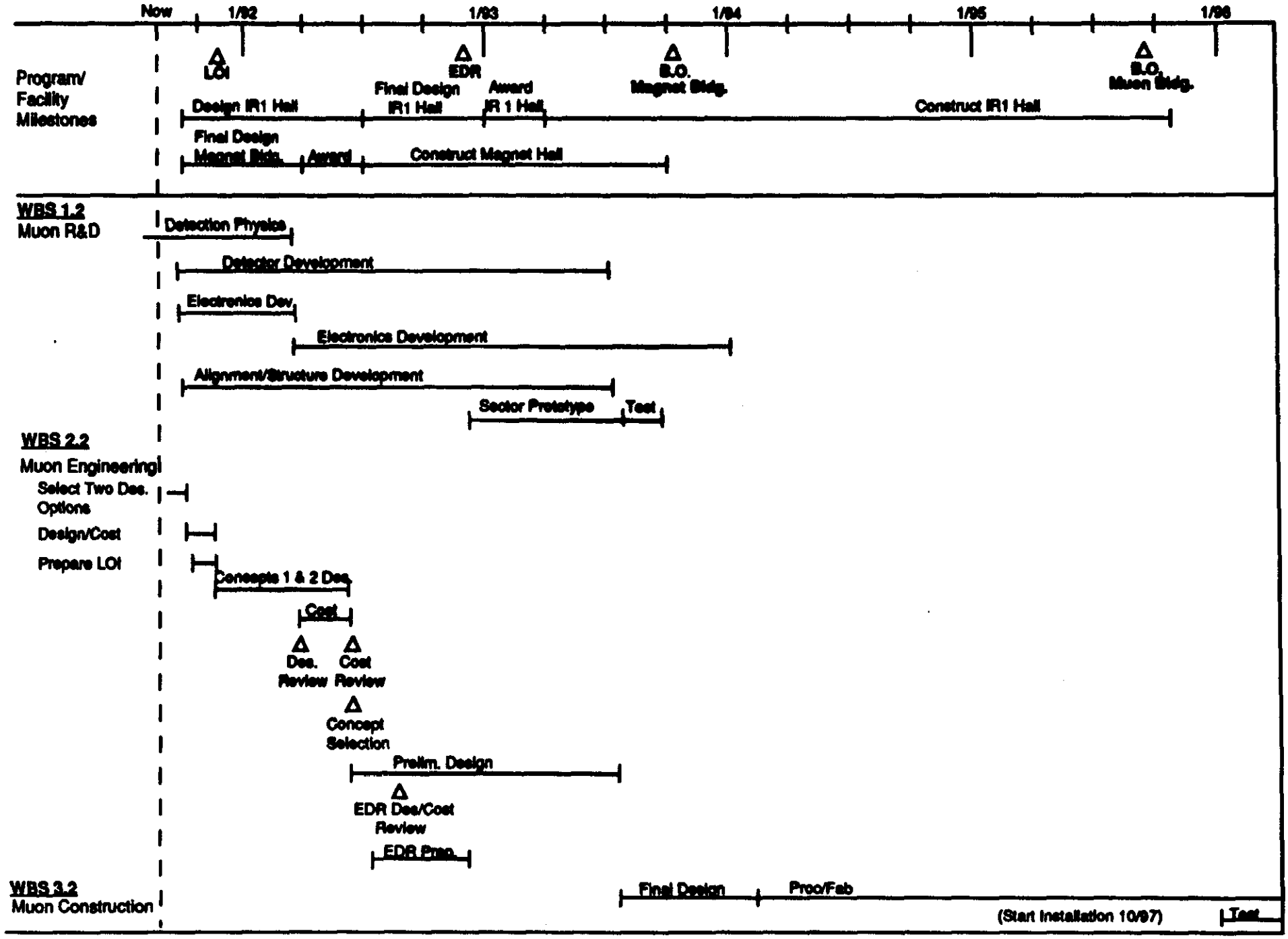

L★

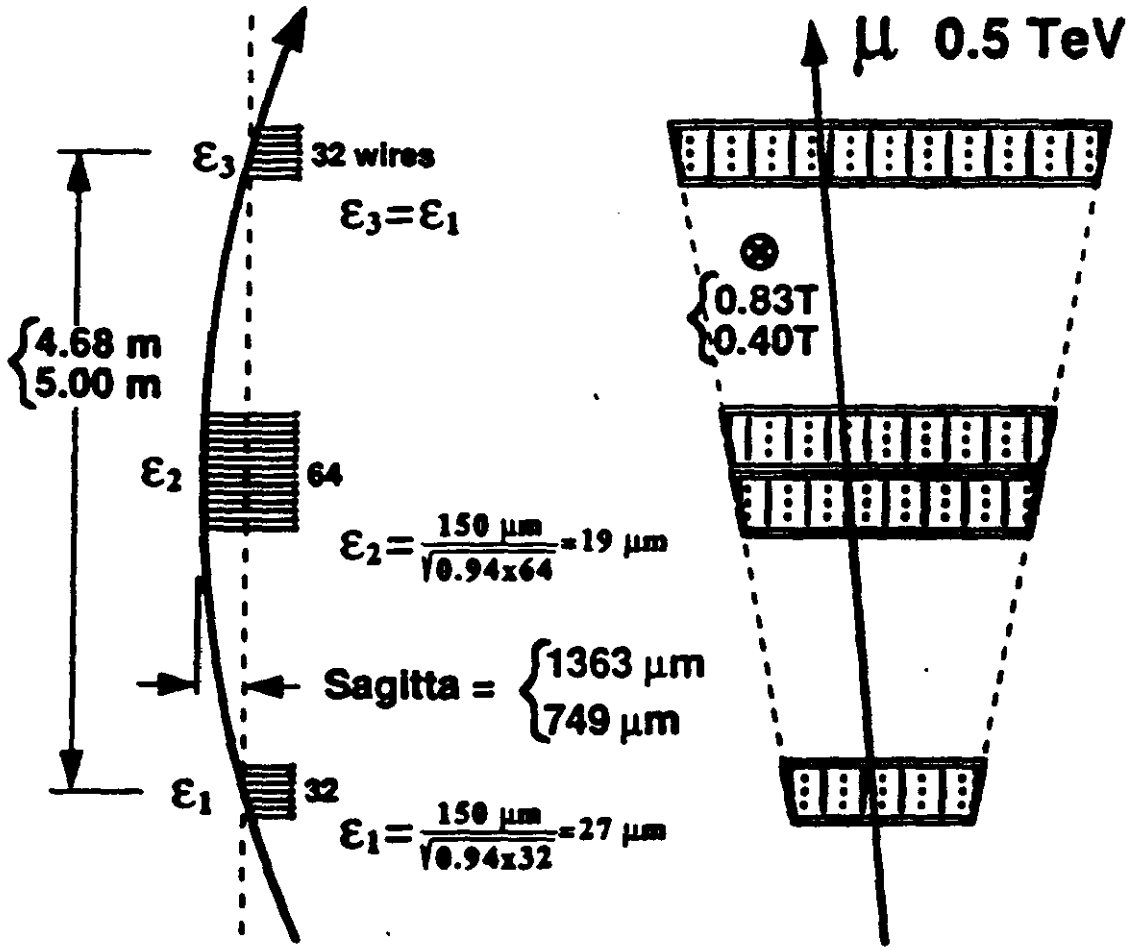

$$\Delta S=\sqrt{\frac{1}{2}\times\varepsilon_1^2+\varepsilon_2^2+\Delta S_{sys}{}^2+\Delta S_{ms}{}^2}$$

$$=\sqrt{\frac{1}{2}\times 27\mu m^2+19\mu m^2+20\mu m^2+15\mu m^2}$$

$$=37\mu m$$

$$\frac{\Delta S}{S}=\begin{cases}2.8\% & \text{Superconducting}\\ 4.9\% & \text{Normal}\end{cases}$$

L3 is a Half Size Prototype of the L* Muon Chambers

L3 Tests:

- Alignment Techniques
- Long and Short Term Stability

Lessons learned from L3 give confidence in the L* design because of the small extrapolation in necessary alignment accuracy

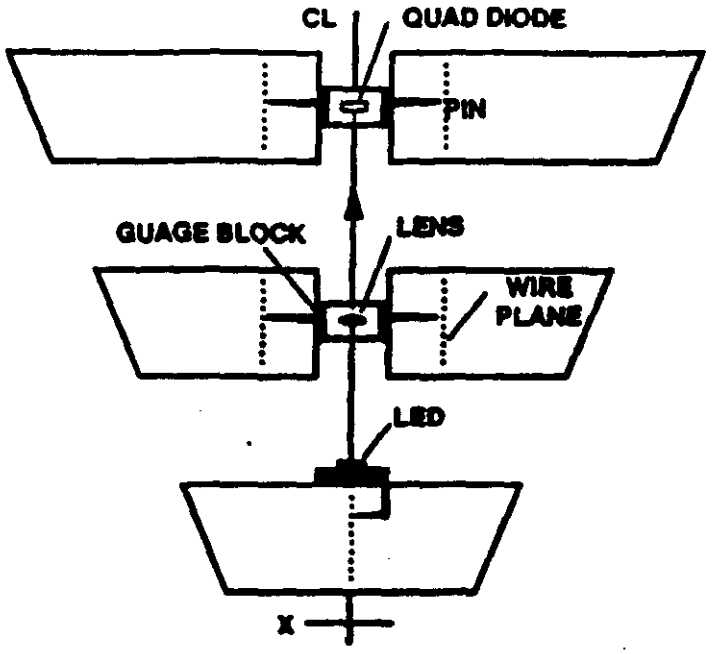

Stability of L3 Alignment for 3 Layers of Chambers

4μm

Reproduces after 1 Year

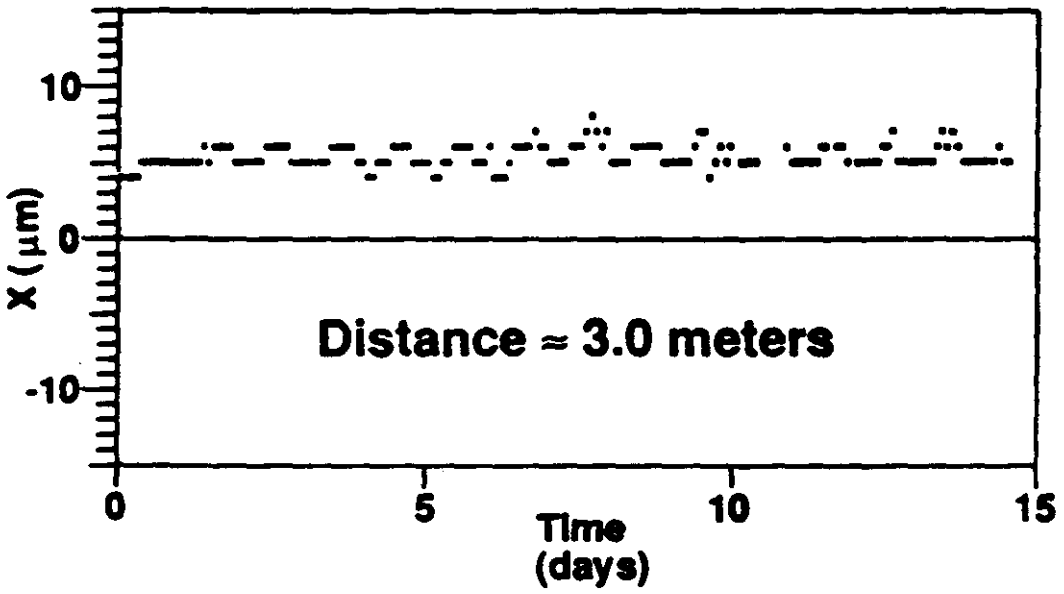

L3 AND L★
WIRE POSITIONING ACCURACY

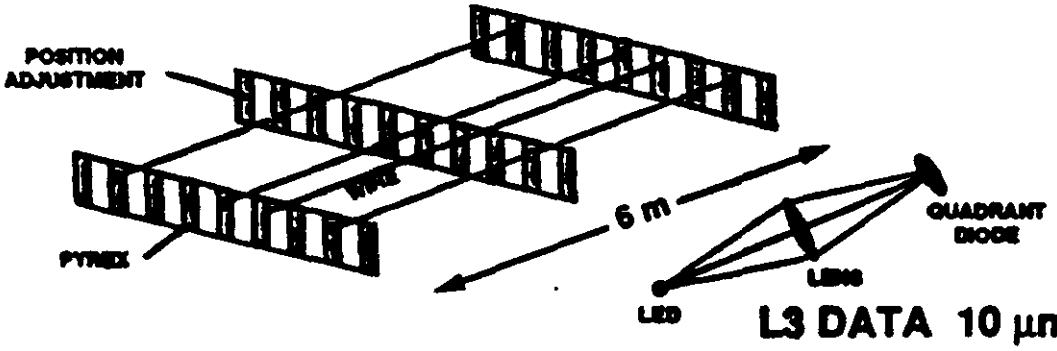

L3 DATA 10 μm
L★ 8 μm

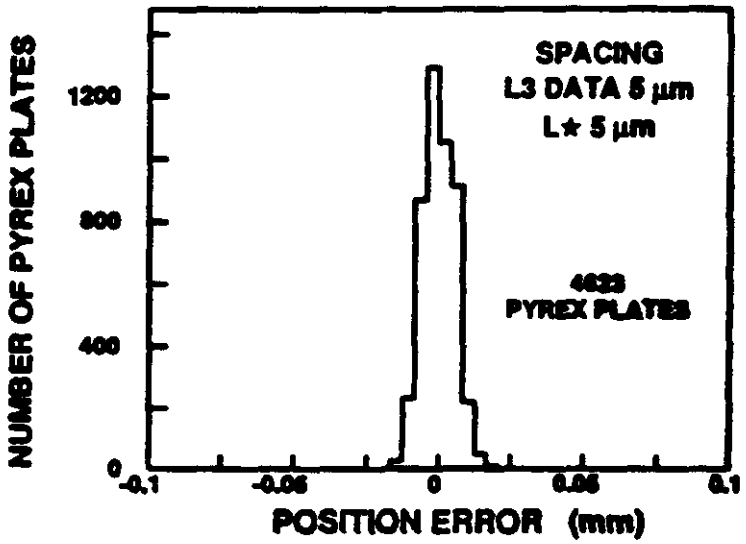

X STRAIGHTNESS MONITOR

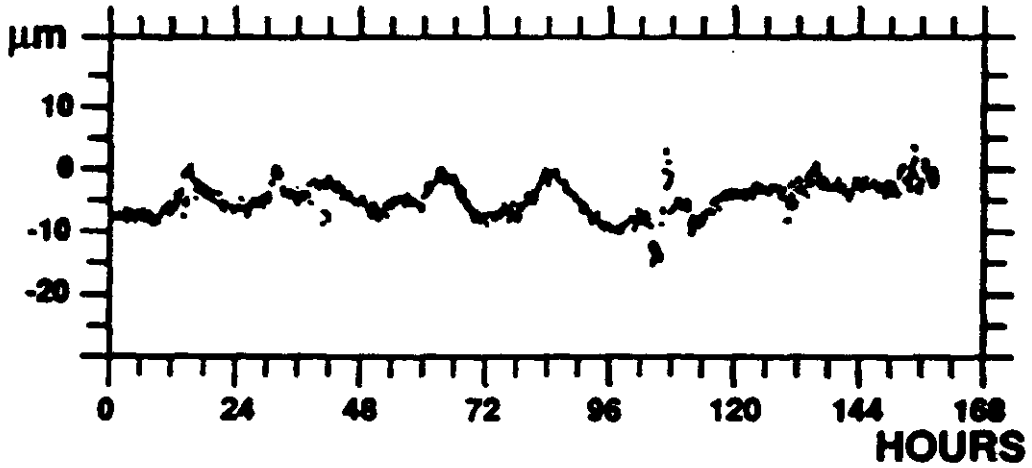

L* Alignment

	L*	L3 - Achieved
P- Measurement 3 Layers - Absolute Monitored - Relative	8 μm 1 μm	10 μm 0.2 μm
Global All tracks point to intersection	0.7 mm	1.0 mm

Work Breakdown Structure
Detector 2
-DRAFT-

1.0 Detector 2 Research and Development

- 1.1 Magnet R&D
  - 1.1.1 Magnet Concept Development
    - 1.1.1.1 Magnetic Field Analysis
    - 1.1.1.2 Study External Detector Options
      - 1.1.1.2.1 Aluminum-stabilized magnet options
      - 1.1.1.2.2 Support/allignment issues
  - 1.1.2 Coil Development/Cu Stabilized (baseline)
    - 1.1.2.1 Model Conductor Testing
    - 1.1.2.2 Joint Development
    - 1.1.2.3 Bobbin Material Characterization
  - 1.1.3 Analysis
    - 1.1.3.1 Thermal/Structural
    - 1.1.3.2 Magnet System Analysis
  - 1.1.4 Coil Development/Al stabilized (option)
    - 1.1.4.1 Model Conductor Testing
    - 1.1.4.2 Joint Development
    - 1.1.4.3 Bobbin Material Characterization
- 1.2 Muon R&D - GENERIC
  - 1.2.1 Detection Physics Studies
    - 1.2.1.1 Safe Gas Studies
    - 1.2.1.2 Resolution Measurement

    Possibly Continuing with Becker at MIT
  - 1.2.2 Detector Development
    - 1.2.2.1 Wire Attachment Development
    - 1.2.2.2 Fabrication/Producibiltiy Studies
    - 1.2.2.3 Small Prototype Test and Development

    Wire Pulling + Attachment + Characterization
  - 1.2.3 Electronics Development
    - 1.2.3.1 New Device Demonstration
    - 1.2.3.2 Fabrication/Cost Studies

    Electrooptics,
  - 1.2.4 Alignment Development
    - 1.2.4.1 Develop alignment approaches
    - 1.2.4.2 Bench-scale demonstration
  - 1.2.5 Structure Development
    - 1.2.5.1 Truss joint characterization
    - 1.2.5.2 Small Structural prototype

    Integrated with Magnet
  - 1.2.6 Sector Prototype Testing
  - 1.2.7 Beam Testing

Triggering — RPC's, Scintillators ?

2. Detector 2 Conceptual/Preliminary Engineering and Design (WBS by activity)

- 2.1 Magnet subsystem
  - 2.1.1 Pre-LOI Engineering/Design
    - 2.1.1.1 Study design options, select 1
    - 2.1.1.2 Conceptual design
    - 2.1.1.3 Conceptual costing
    - 2.1.1.4 Installation/facilities planning
    - 2.1.1.5 Prepare LOI
  - 2.1.2 LOI to Engineering Design Report (EDR)
    - 2.1.2.1 Preliminary Design
      - 2.1.2.1.1 Preliminary Design
      - 2.1.2.1.2 Installation/facilities planning
      - 2.1.2.1.3 Preliminary costing
      - 2.1.2.1.4 Preliminary scheduling
      - 2.1.2.1.5 Safety/reliability analysis

- 2.2 Muon subsystem
  - 2.2.1 Pre-LOI Engineering/Design
    - 2.2.1.1 Study design options, select 2
    - 2.2.1.2 Pre-conceptual design, 2 concepts
    - 2.2.1.3 Pre-conceptual costing, 2 concepts
    - 2.2.1.4 Prepare LOI
  - 2.2.2 LOI to Engineering Design Report (EDR)
    - 2.2.2.1 Conceptual design (concept 1)
      - 2.2.2.1.1 Conceptual design
      - 2.2.2.1.2 Installation and facilities planning
      - 2.2.2.1.3 Conceptual-level costing
    - 2.2.2.2 Conceptual design (concept 2)
      - 2.2.2.2.1 Conceptual design
      - 2.2.2.2.2 Installation and facilities planning
      - 2.2.2.2.3 Conceptual-level costing
    - 2.2.2.3 Concept review/selection
      - 2.2.2.3.1 Select baseline concept
      - 2.2.2.3.2 Prepare final facilities input
    - 2.2.2.4 Preliminary Design
      - 2.2.2.4.1 Preliminary Design
      - 2.2.2.4.2 Installation/facilities planning
      - 2.2.2.4.3 Preliminary costing
      - 2.2.2.4.4 Preliminary scheduling
      - 2.2.2.4.5 Safety/reliability analysis

- 2.3 Hadron Calorimeter Subsystem

- 2.4 Electromagnetic Calorimeter Subsystem

- 2.5 Central Tracker Subsystem

Electro-optics Data Acquisition Development

- LLNL has built Mach Zehnder interferometric modulators with the following characteristics of possible use to L★:
  - 20 GHz bandwidths (1-2 GHz desired for the inner tracker)
  - Charge sensitivities of less than 1 femtocoulomb (can be directly attached to a muon chamber sense wire with no intervening electronics)
  - Dynamic ranges >10,000 for possible use in the Hadron calorimeter
- Exploring techniques for:
  - Fabrication cost reduction
  - High integration density
  - Fabrication automation

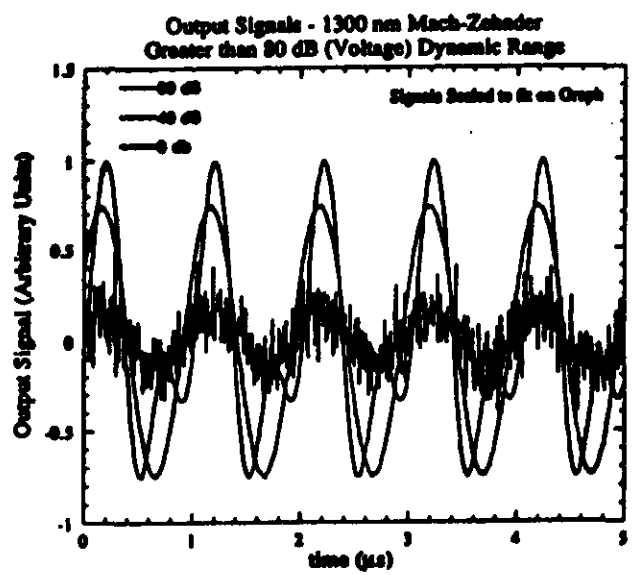

Electro-Optical Readout of Muon Chambers

- Advantages:

  Provides an optical replication of sense wire signal

  Passive–no active electronics within the magnet

  Noise Immunity: No ground loops, etc.

  All signals carried in a few cable bundles a couple of inches in diameter

- Disadvantages:

  Cost: R&D necessary to reduce cost to a few tens of dollars per channel

EXPER'MT HALLS 1, 4, 5, 8 TIER II SCHEDULE

THE PB/MK TEAM

DRAFT

ACTIVITY	DESCRIPTION	START	FINISH
	IR1 EXPERIMENTAL HALL - UNDERGROUND FACIL		
100005	DESIGN SUMMARY FOR I/R 1	01OCT91	28DEC92
200015	BID AND AWARD I/R HALL #1	29DEC92	29MAR93
100005	NOTICE TO PROCEED IR1 HALL	30MAR93	29MAR93
100010	IR1 HALL CONSTRUCTION SUMMARY	30MAR93	02SEP95
	IR1 EXPERIMENTAL HALL - SURFACE FACILIT		
200122	IR1 DESIGN MAGNET COIL ASSY BUILDING	16OCT91	16APR92
200122	BID & AWARD MAGNET COIL ASSY. BLDG.	17APR92	16JUL92
200005	CONST. MAGNET COIL ASSY. BLDG.	17JUL92	30SEP93
200050	FACILITY COMPLETE MAG. COIL ASSY. BLDG.	01OCT93	30SEP93
200123	IR1 DESIGN INDUSTRIAL ASSY. BLDG. (MUON)	23OCT93	22APR94
200123	BID & AWARD IND. ASSY. BLD. (MUON CHAMB)	23APR94	22JUL94
200010	CONST IND ASSY BLDG - (MUON CHAMB)	23JUL94	30JUN95
200051	FACILITY COMPLETE IND. ASSY BLDG (MUON)	01JUL95	30JUN95
200124	IR1 DESIGN CATEGORY II SHOP BUILDING	30OCT93	29APR94
200124	BID & AWARD CAT. II SHOP BLDG.	30APR94	29JUL94
200015	CONST. CAT. II SHOP BLDG.	30JUL94	30JUN95
200052	FACILITY COMPLETE CATEGORY II SHOP BLDG	01JUL95	30JUN95
200125	IR1 DESIGN IR1 HEADHOUSE	03OCT94	01APR95
200125	BID & AWARD IR1 HEADHOUSE	03APR95	01JUL95
200020	CONSTR IR1 HEADHOUSE	03JUL95	30MAR96
200053	FACILITY COMPLETE IR1 HEADHOUSE	01APR96	30MAR96
200126	IR1 DESIGN INDUST. ASSY. BLDG. (CALORIM)	24OCT94	22APR95
200126	BID & AWARD IND. ASSY. BLD. (CALORIMETER)	24APR95	22JUL95
200025	CONST IND ASSY BLDG (CALORIM.)	24JUL95	29JUN96
200054	FACILITY COMPLETE IND. ASSY. BLDG (CALOR	01JUL96	29JUN96
200127	IR1 DESIGN UTILITY/PERSON BLDG.	07JUN95	05DEC95
200127	BID & AWARD UTILITIES BLDG.	06DEC95	05MAR96
200030	CONST. UTIL/PERSONL.BLDG	06MAR96	31DEC96
200055	FACILITY COMPLETE UTIL/PERSONELL BLDG	01JAN97	31DEC96
200128	IR1 DESIGN OPERATIONS BLDG.	07JUN95	05DEC95
200128	BID & AWARD OPERATIONS BLDG.	06DEC95	05MAR96
200035	CONSTR. OPS. CENTER	06MAR96	31DEC96
200056	FACILITY COMPLETE - OPERATIONS BLDG.	01JAN97	31DEC96
200129	IR1 DESIGN GAS MIXING HOUSE	27MAY96	23NOV96
200129	BID & AWARD GAS MIXING HOUSE	25NOV96	22FEB97
200040	CONSTRUCT. GAS MIXING HOUSE	24FEB97	30JUN97
200057	FACILITY COMPLETE - GAS MIXING BLDG.	01SEP97	30JUN97

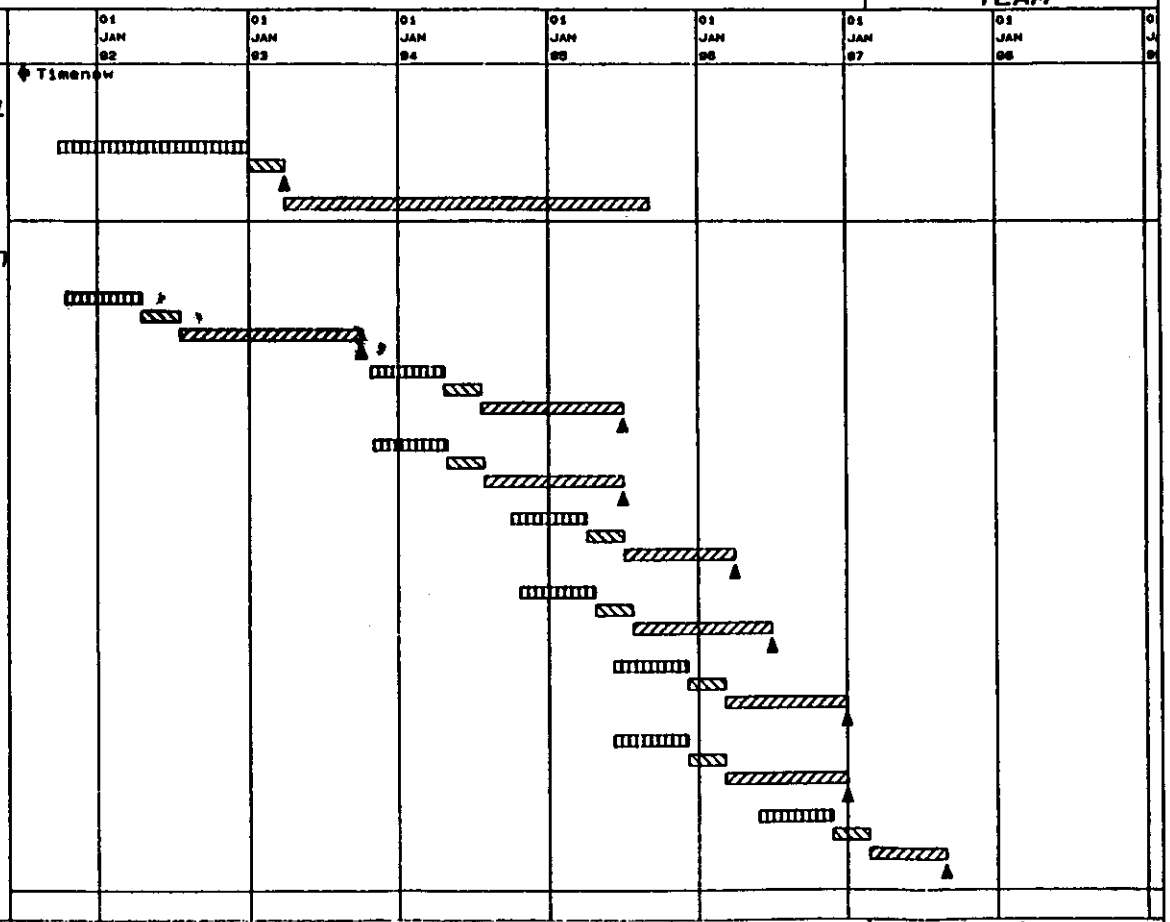

Legend
- DESIGN
- BID & AWARD
- CONSTRUCTION

Signatures
Prep: _____
Aprv: _____

Coleman
Johnson

SSC DETECTOR 2 MAGNET FABRICATION FACILITY

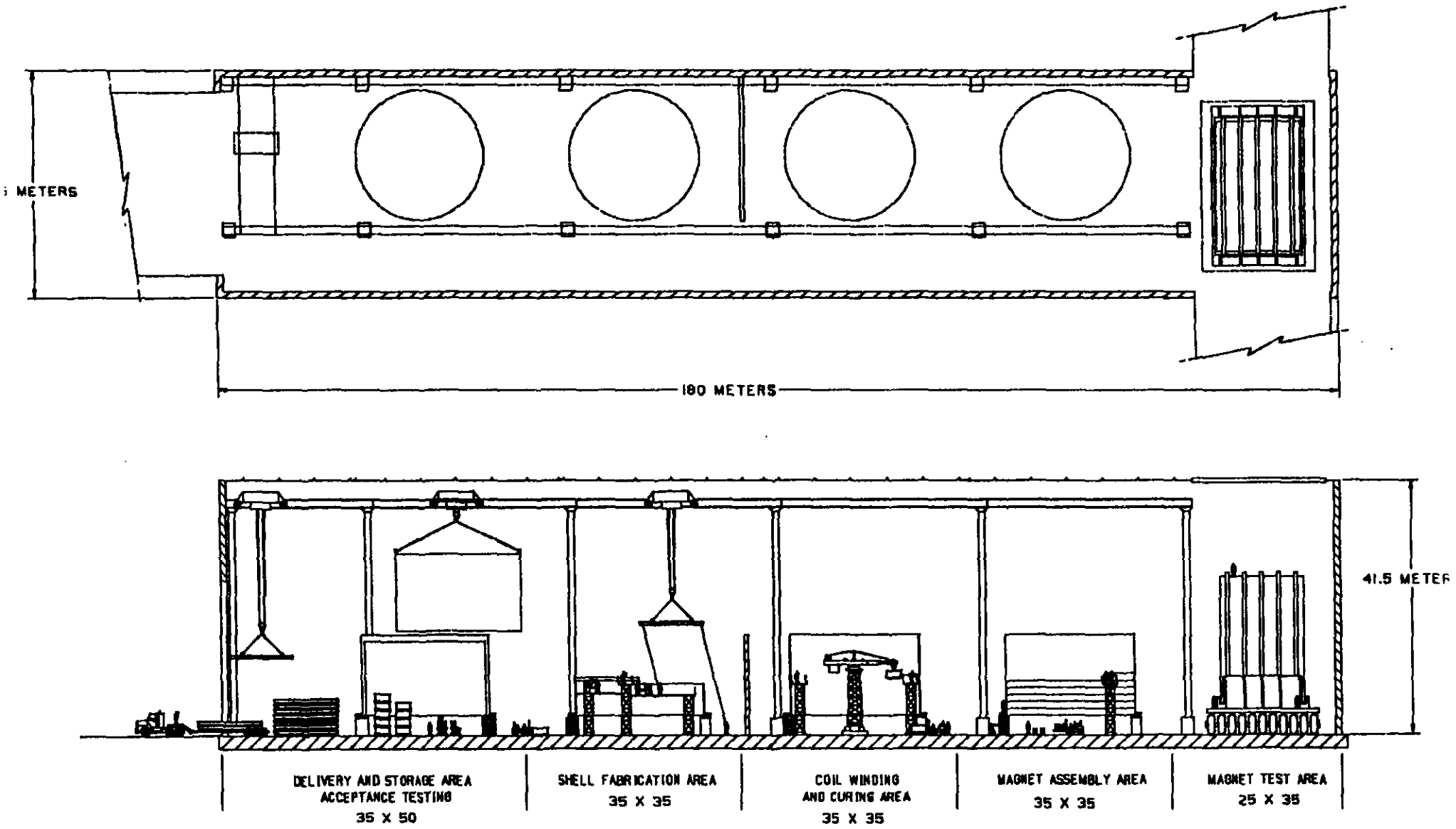

SSC DETECTOR 2 MAGNET FABRICATION FACILITY

AREA #1 - DELIVERY AND STORAGE AREA/ACCEPTANCE TESTING

- CONDUCTOR DELIVERY AND TESTING
- BOBBIN SECTIONS,VACUUM SHELL SECTIONS,RADIATION SHIELD SECTIONS.....INSPECTION AND STORAGE
- COMPLETED SHELL STORAGE (NESTED)

AREA #2 - SHELL FABRICATION AREA

- WELDING
- GRINDING
- GRIT BLASTING
- STRAIGHTENING

AREA #3 - COIL WINDING AND CURING AREA

- SEGREGATED FROM FABRICATION PROCESSES AREAS FOR CLEANLINESS

AREA #4 - MAGNET ASSEMBLY AREA

- SUPERINSULATION INSTALLATION
- LEAK CHECKING

AREA #5 - MAGNET TEST AREA

- ROLL MAGNET
- WELD ON SUPPORTS
- COOL DOWN
- FURTHER TESTS

OVERALL FACILITY DIMENSIONS-

- LENGTH-180 METERS
- WIDTH-35 METERS
- HEIGHTH-41.5 METERS

AREA 1

DELIVERY AND STORAGE AREA/ACCEPTANCE TESTING

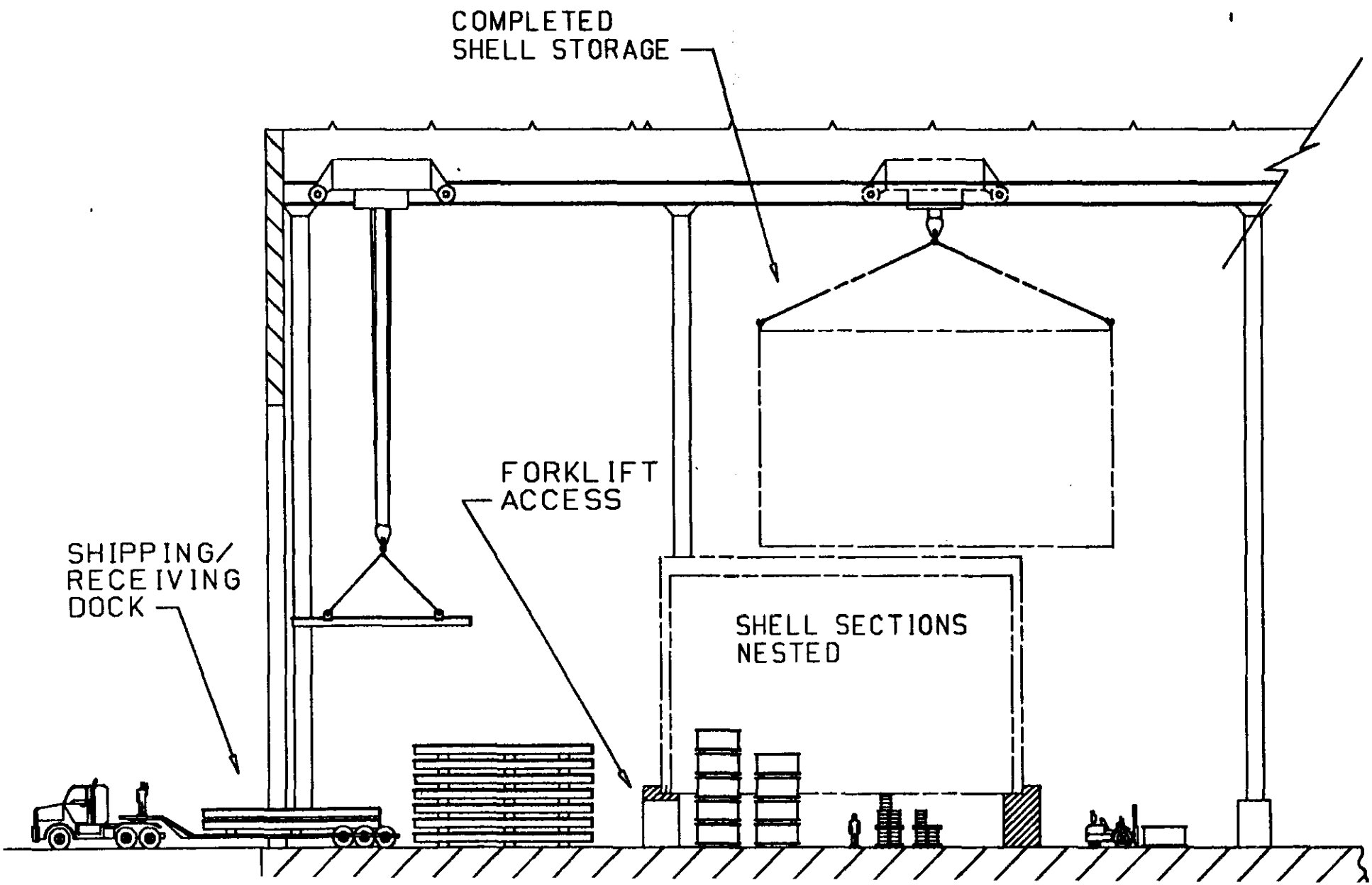

AREA 2

SHELL FABRICATION AREA

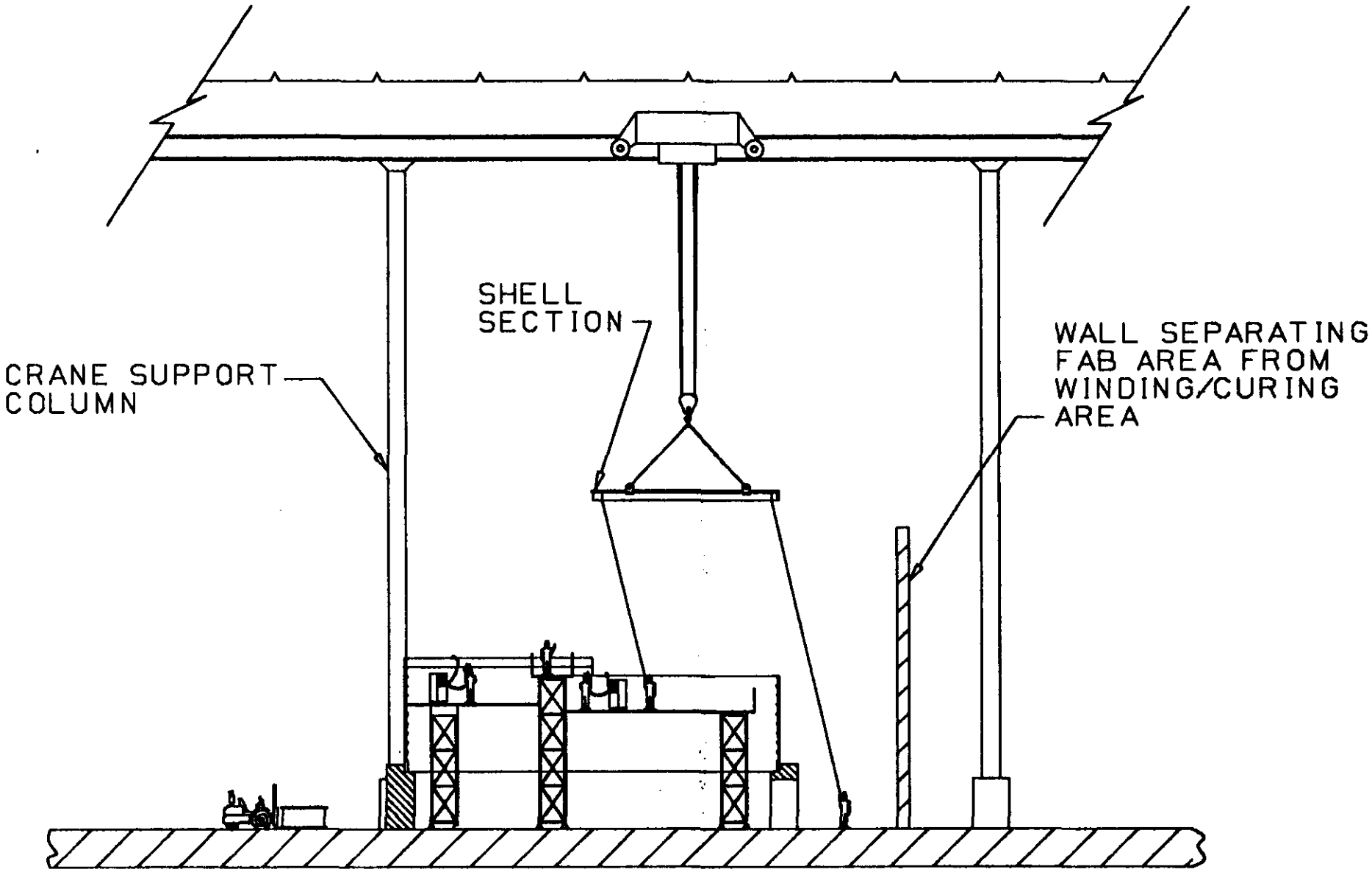

AREA 3

COIL WINDING AND CURING AREA

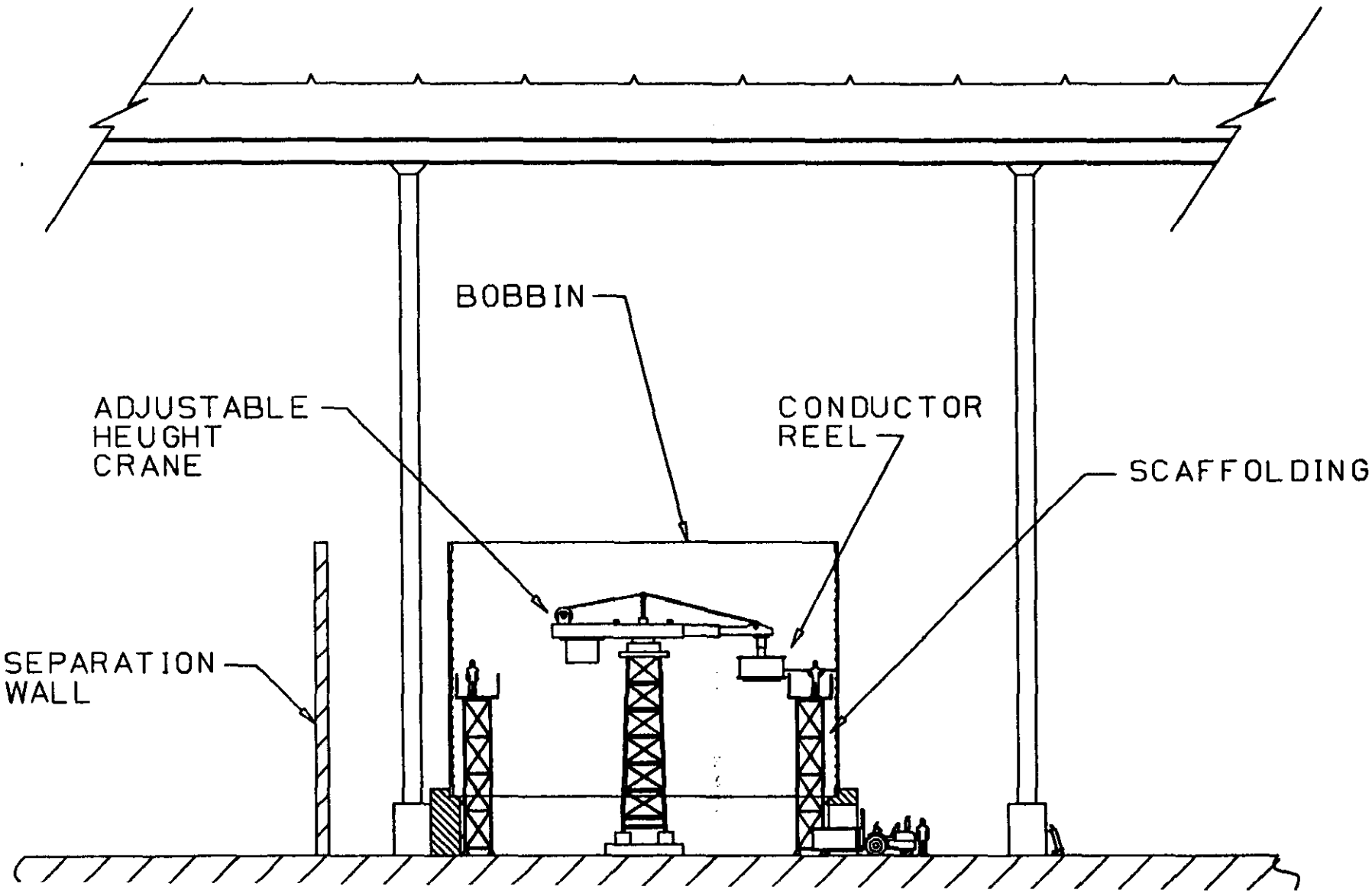

AREA 4

MAGNET ASSEMBLY AREA

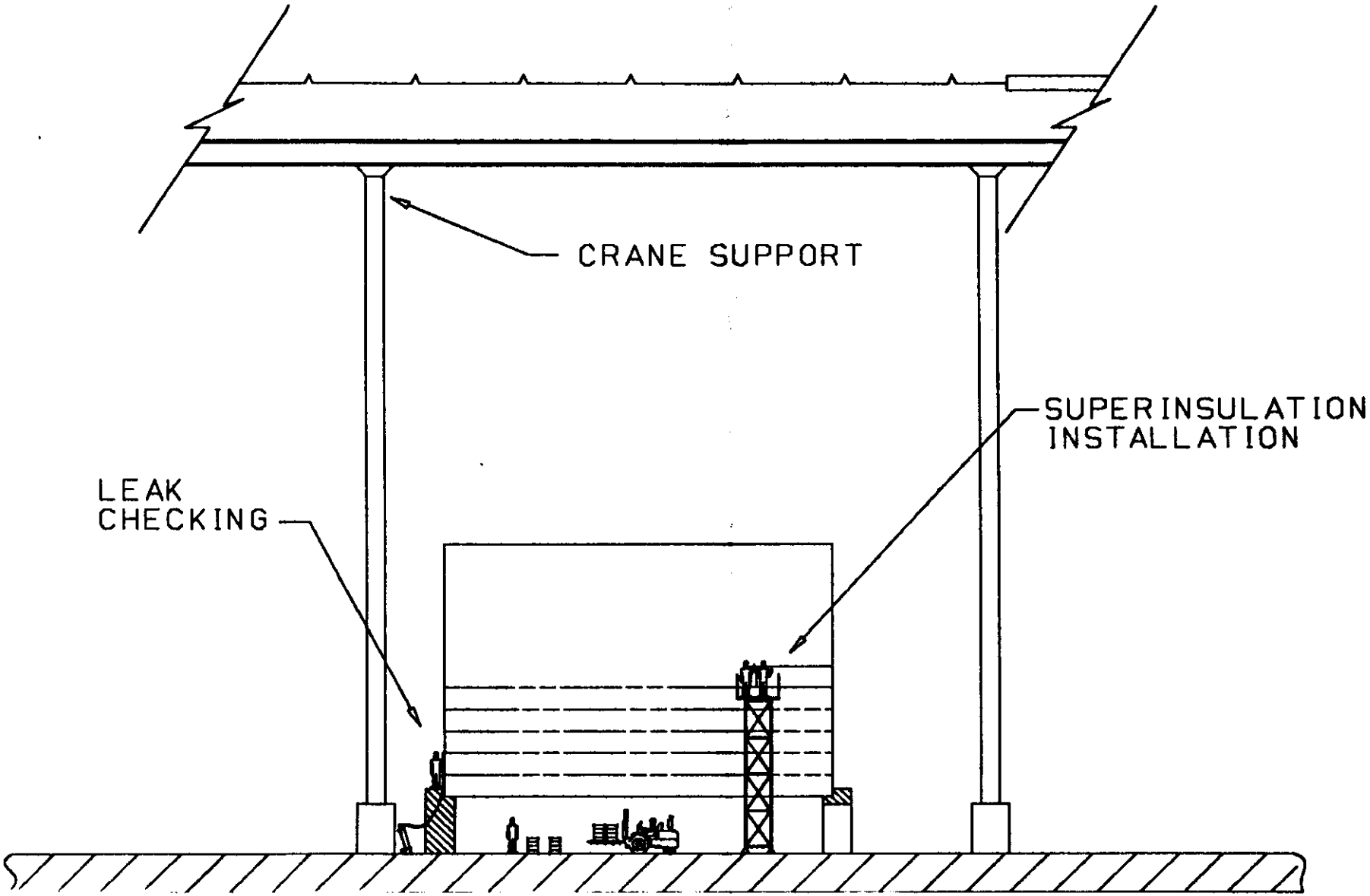

AREA 5

MAGNET TEST AREA/ROLLOVER TRANSPORT PREP

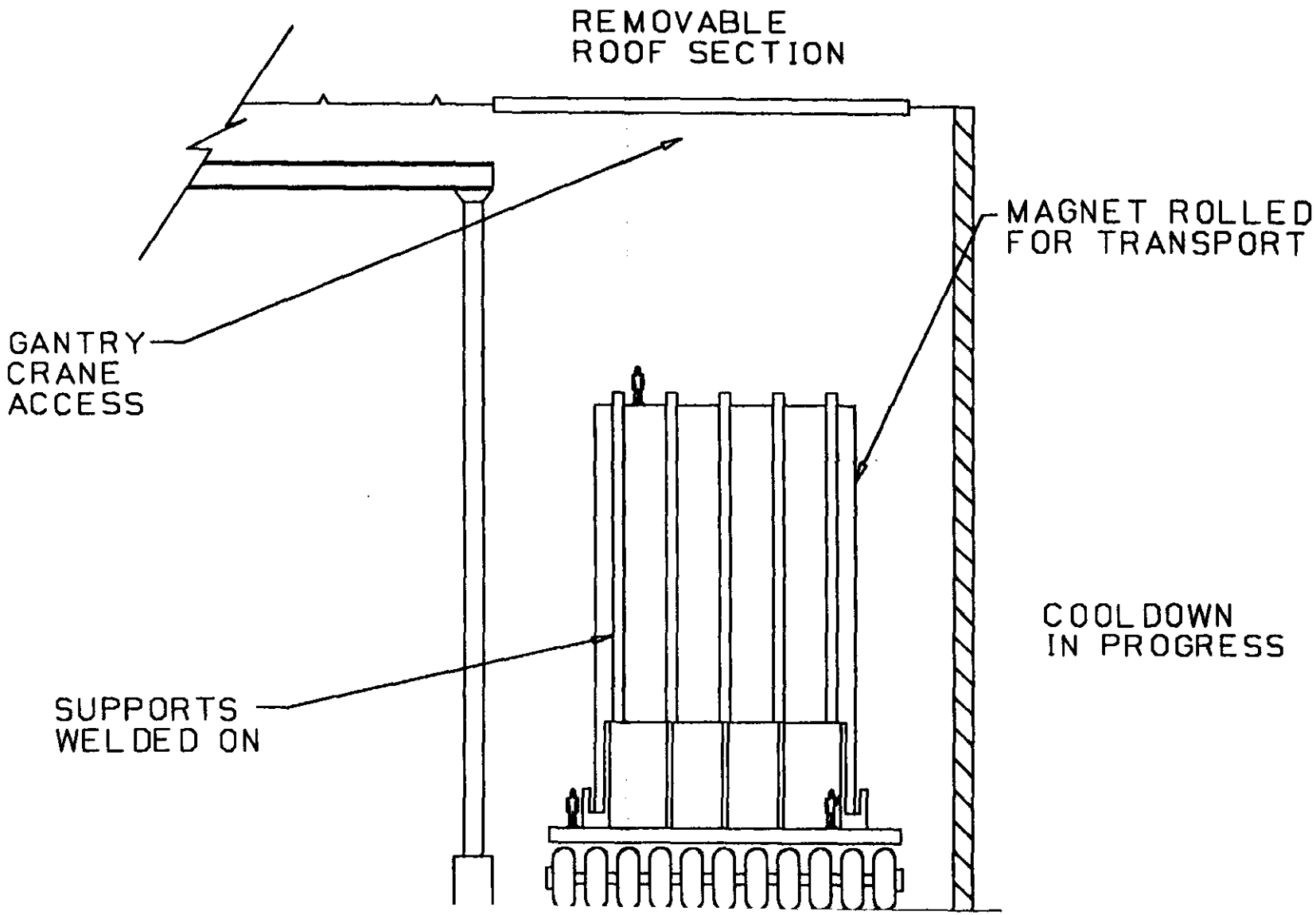

SSC DETECTOR 2 MAGNET FABRICATION FACILITY

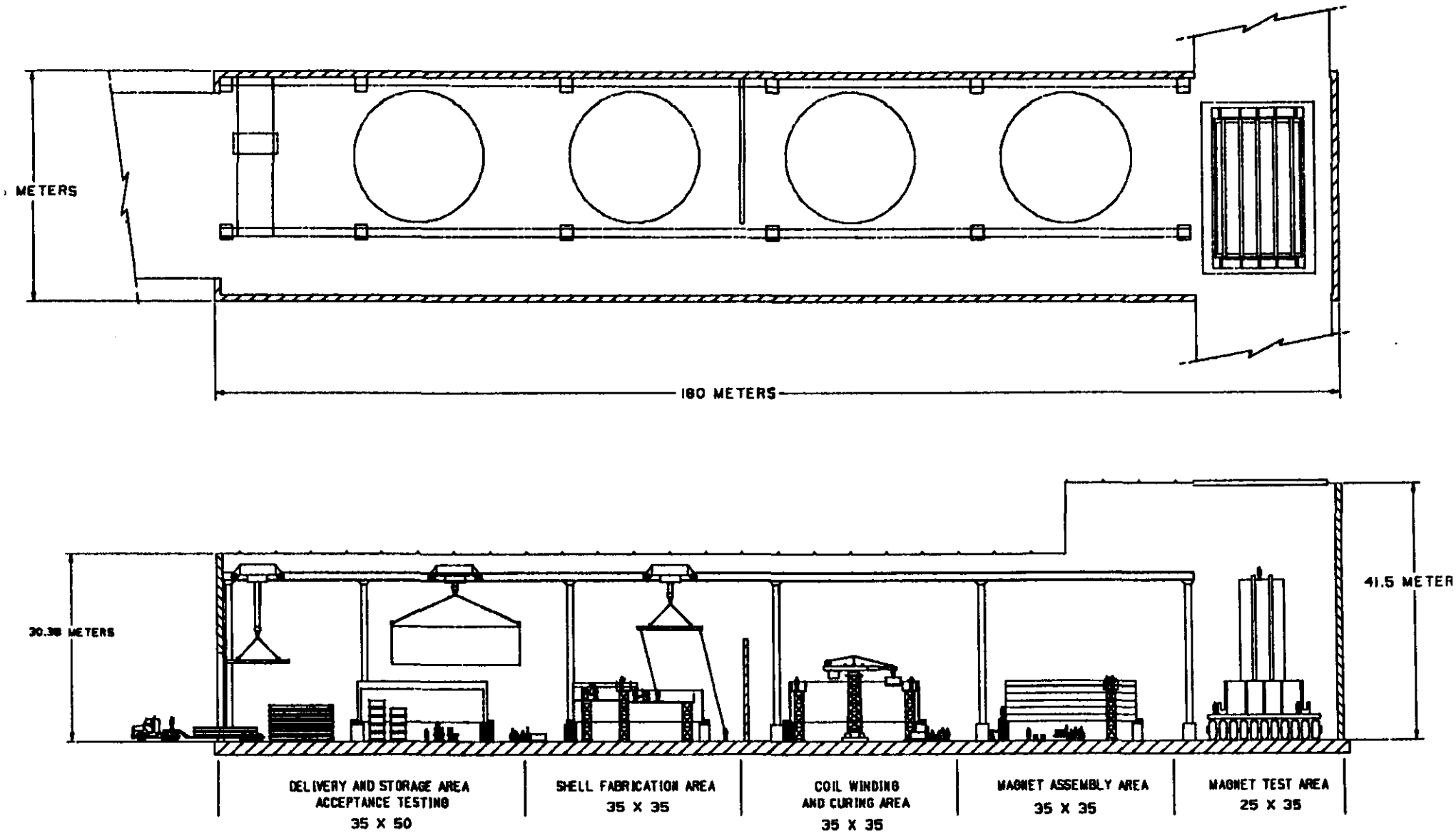

MUON BEAM TESTS
have just been started

INTENTION

1. DETECTOR PROTOTYPE PERFORMANCE
   1a. LST with DRIFT READOUT
   1b. LST with STRIP READOUT

2. SOME INVESTIGATIONS of e^+e^--pair production by high energy muons

WHAT WE WANT TO GET
by the end of the run

1. DRIFT READOUT:
   * resolution for different gas mixtures
     (H.V. and threshold optimization is assumed)

2. USEFULNESS of TIME MEASUREMENTS from STRIPS (correlations and etc.)

3. STRIP READOUT:
   * resolution for different gas mixtures, proportional and SQS modes, vs angle
     (optimization of HV and gate is assumed)

4. ANALYSIS of E.M. DEBRIS produced by high energy muons passind thru (different) materials.

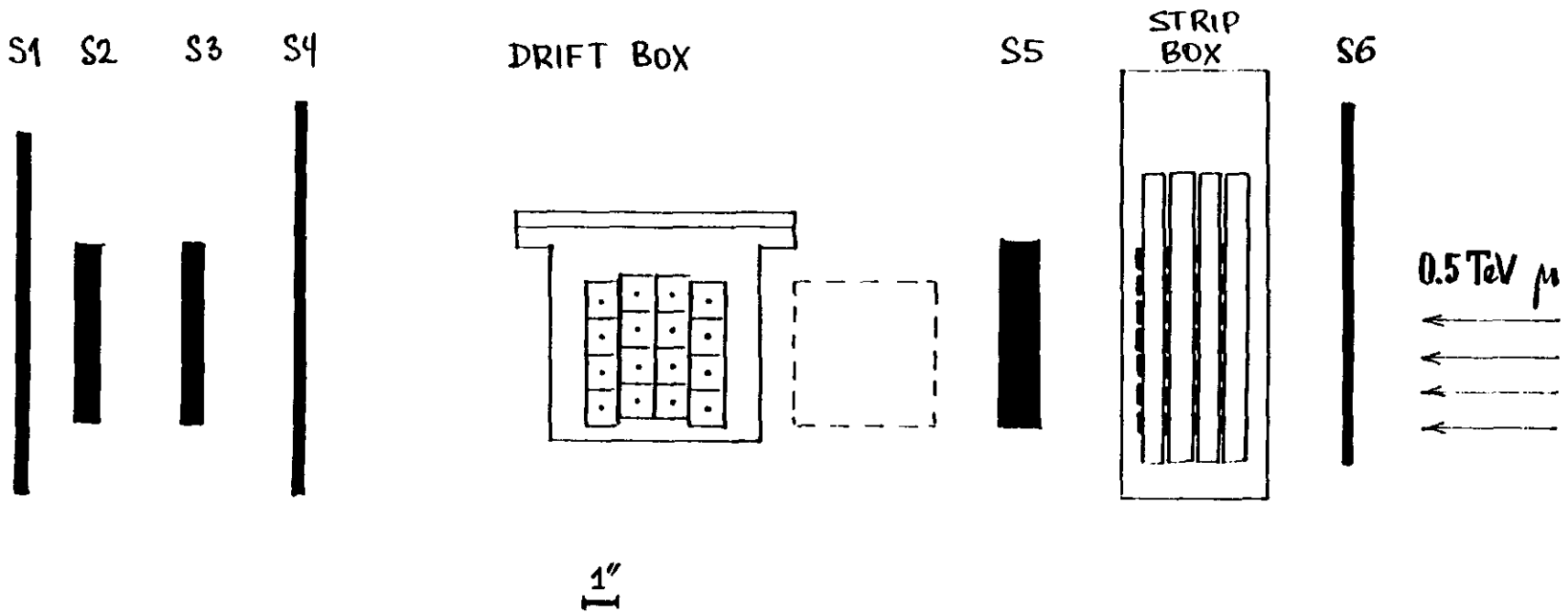
S1
S2
S3
S4
DRIFT BOX
S5
STRIP BOX
S6
0.5 TeV μ
1"

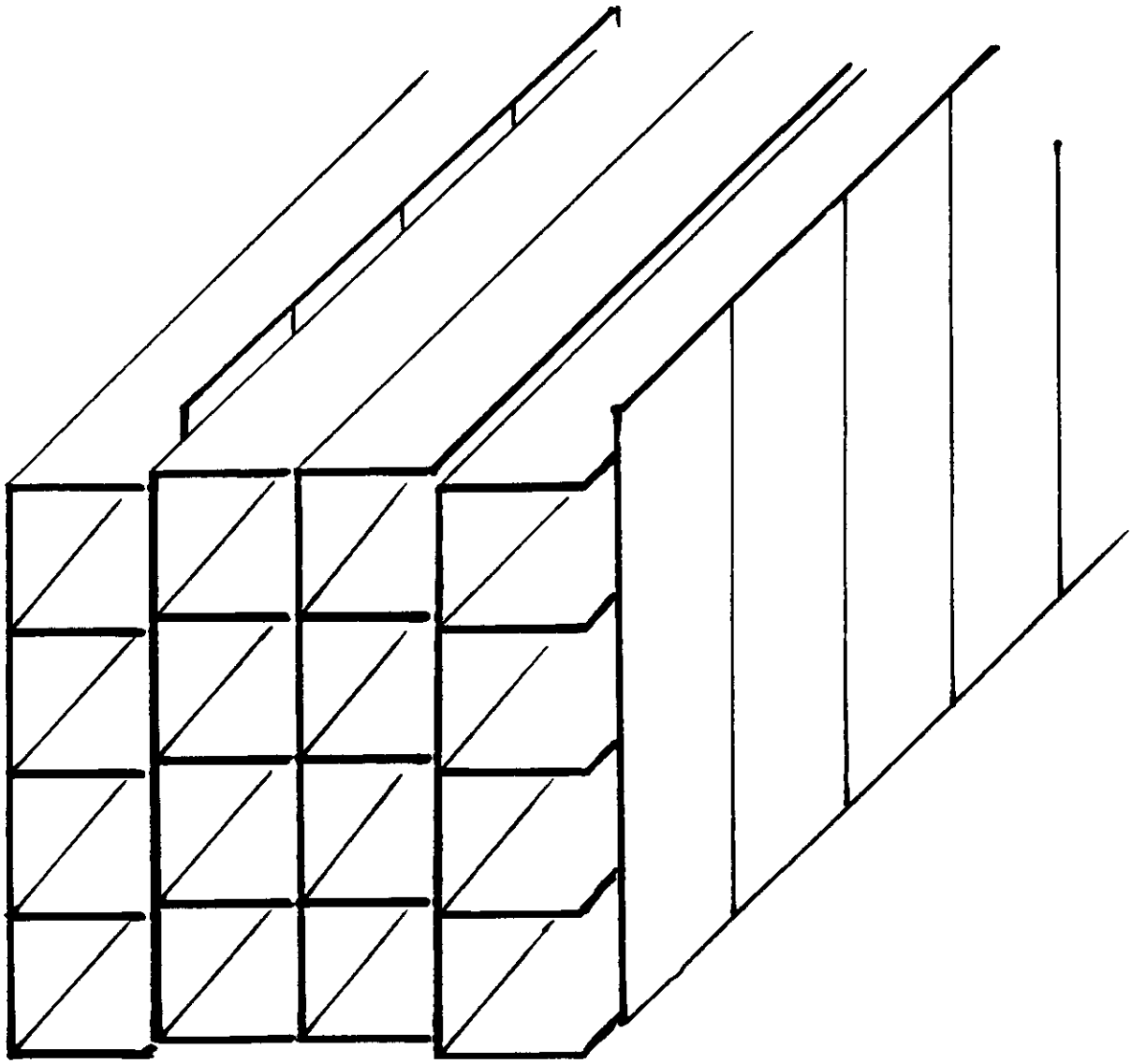

1″

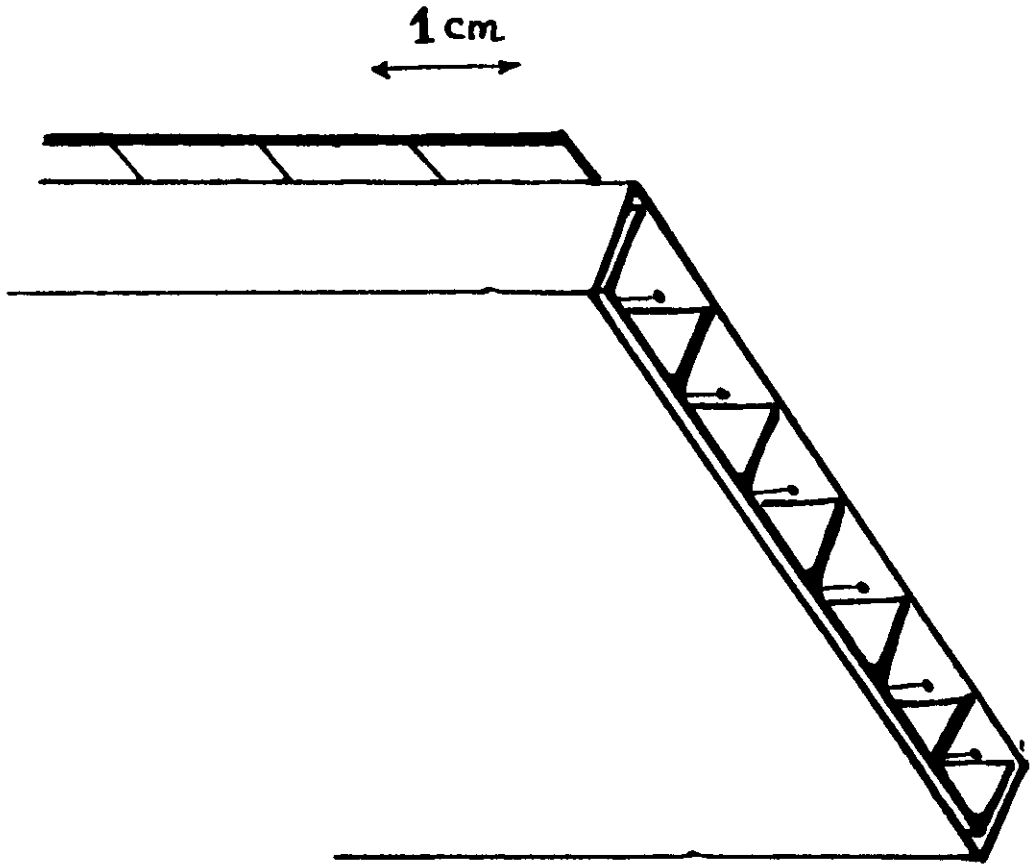
1 cm

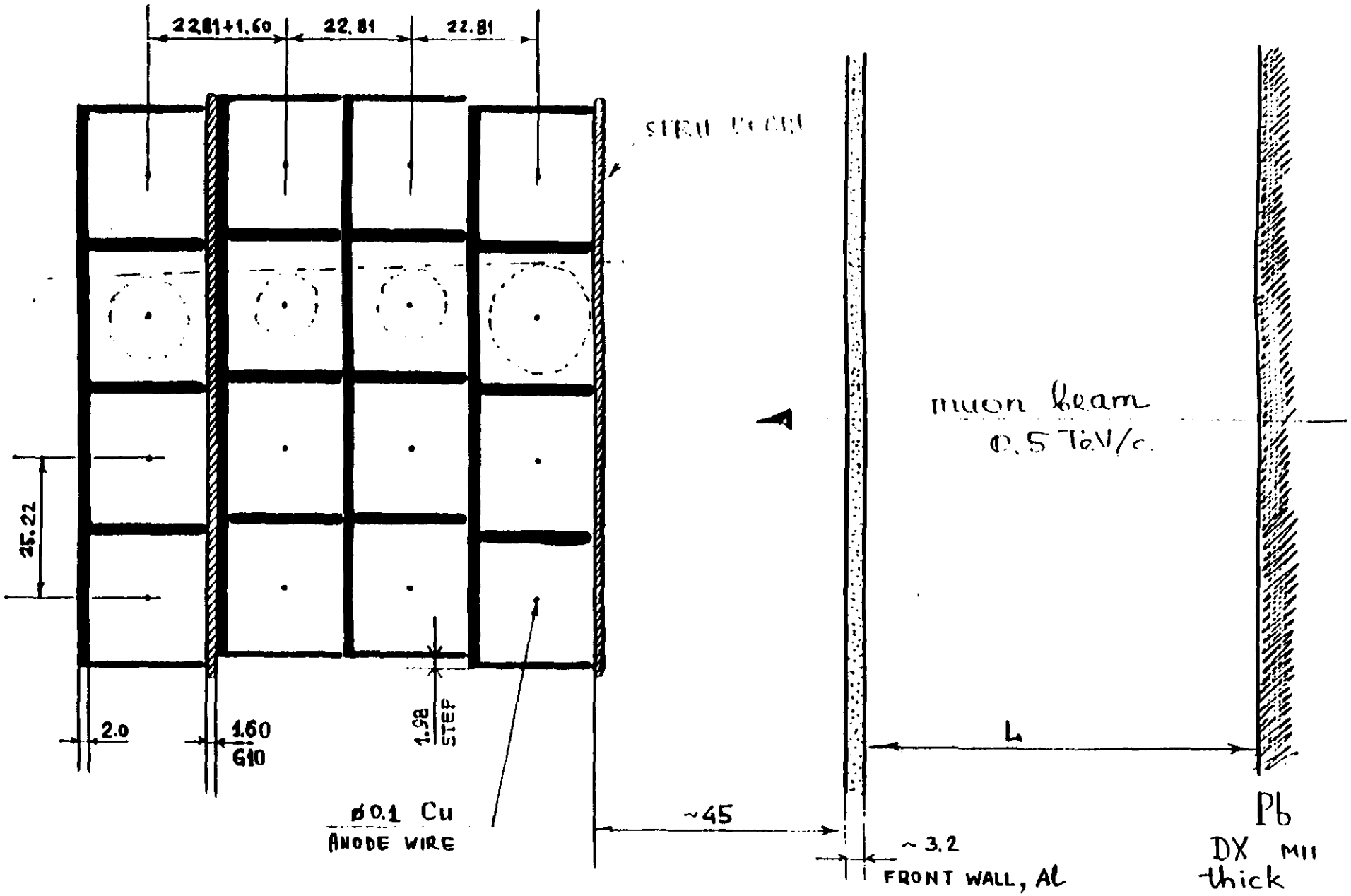
22.81+1.60
22.81
22.81
STEEL FOCUS
25.22
2.0
1.60
G10
1.98
STEP
ø0.1 Cu
ANODE WIRE
~45
~3.2
FRONT WALL, Al
muon beam
0.5 TeV/c
L
Pb
DX MII
thick

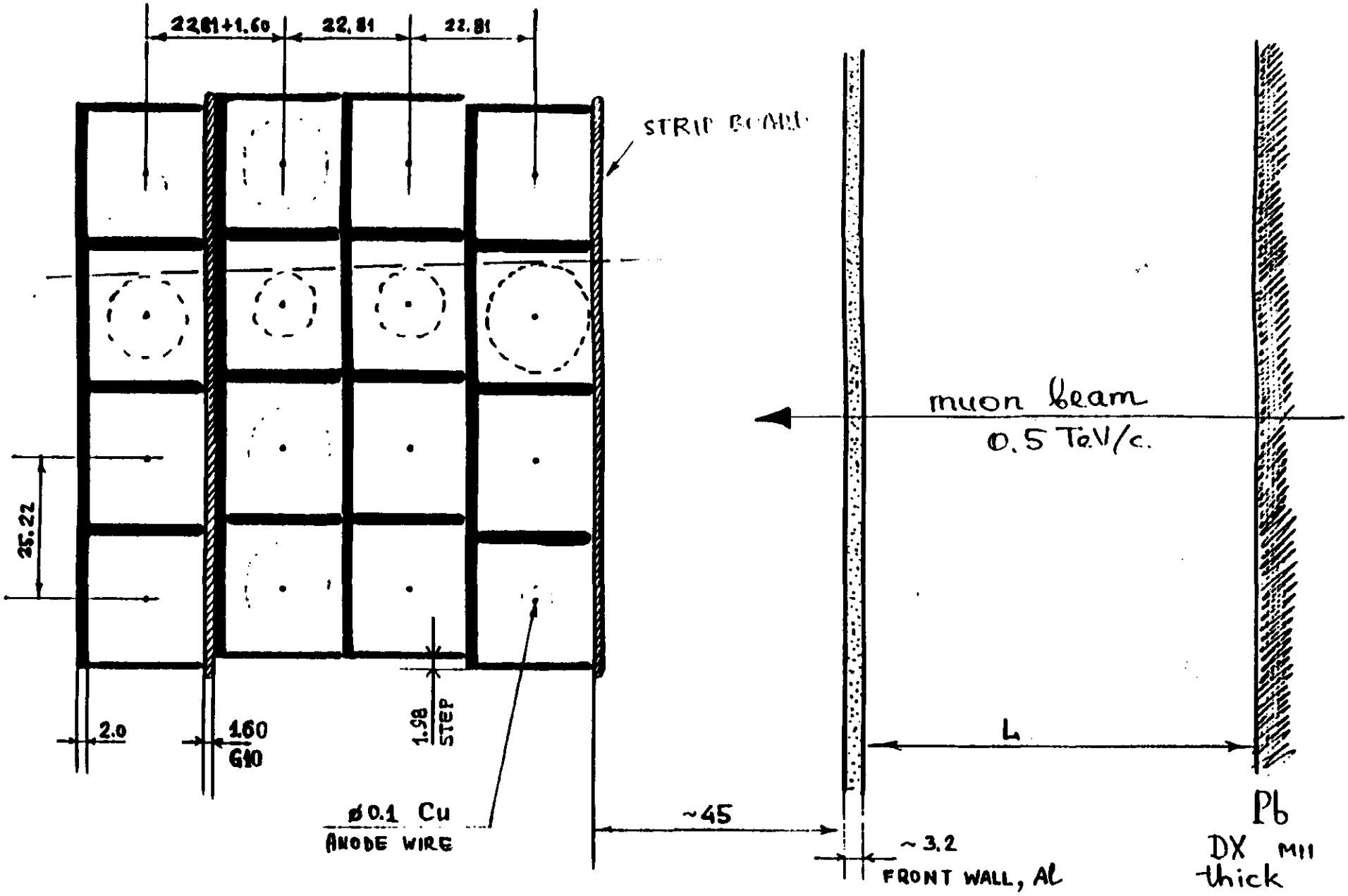
22.81+1.60
22.81
22.81
STRIP BOARD
25.22
2.0
1.60
G10
1.98
STEP
ø0.1 Cu
ANODE WIRE
~45
~3.2
FRONT WALL, Al
muon beam
0.5 TeV/c.
L
Pb
DX MII
thick

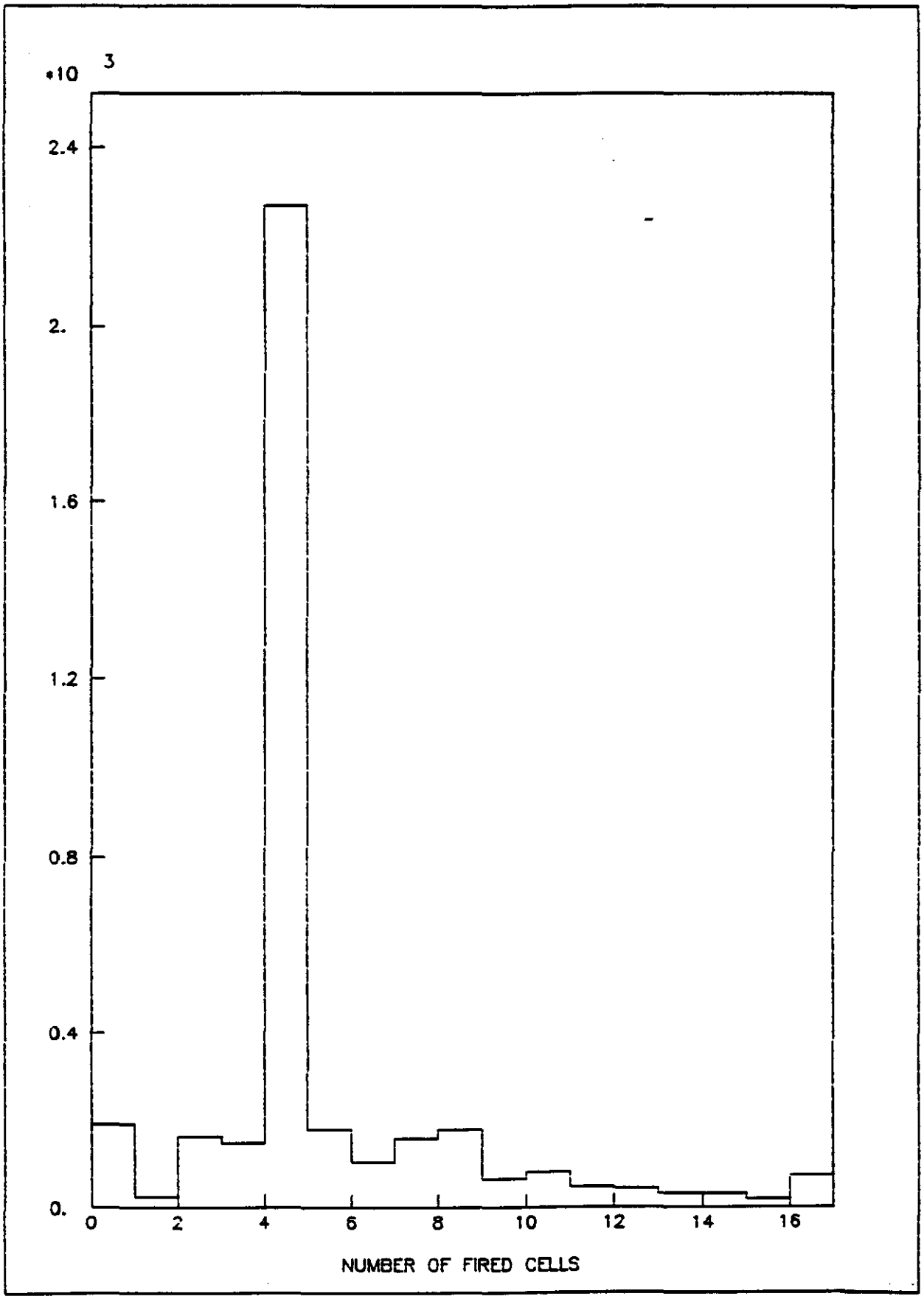
*10 3
2.4
2.
1.6
1.2
0.8
0.4
0.
0
2
4
6
8
10
12
14
16
NUMBER OF FIRED CELLS

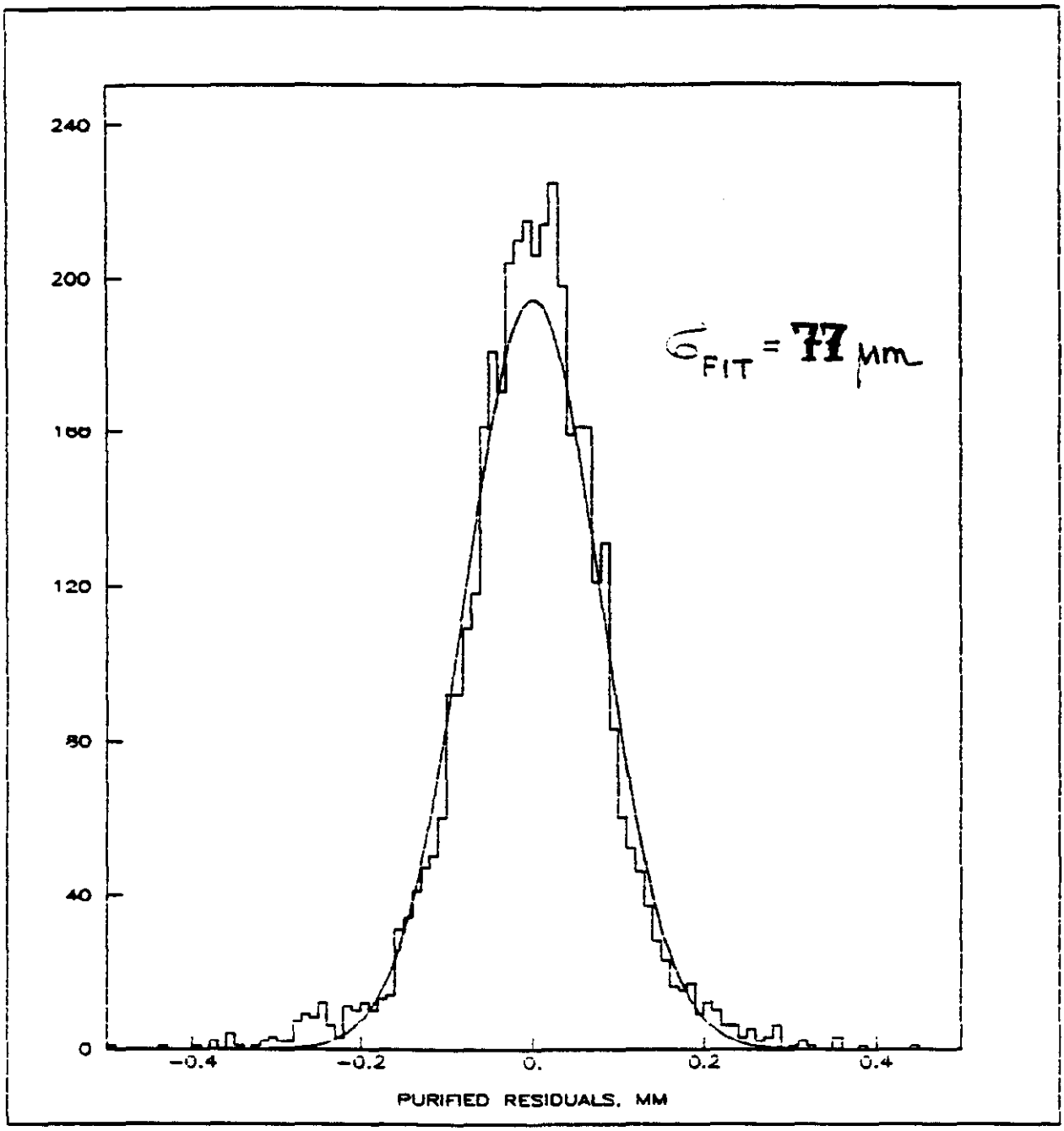

Detector efficiency = 98.5%

Ar+CH$_4$ = 1+3 SGS mode.

only clean (1-cell) events

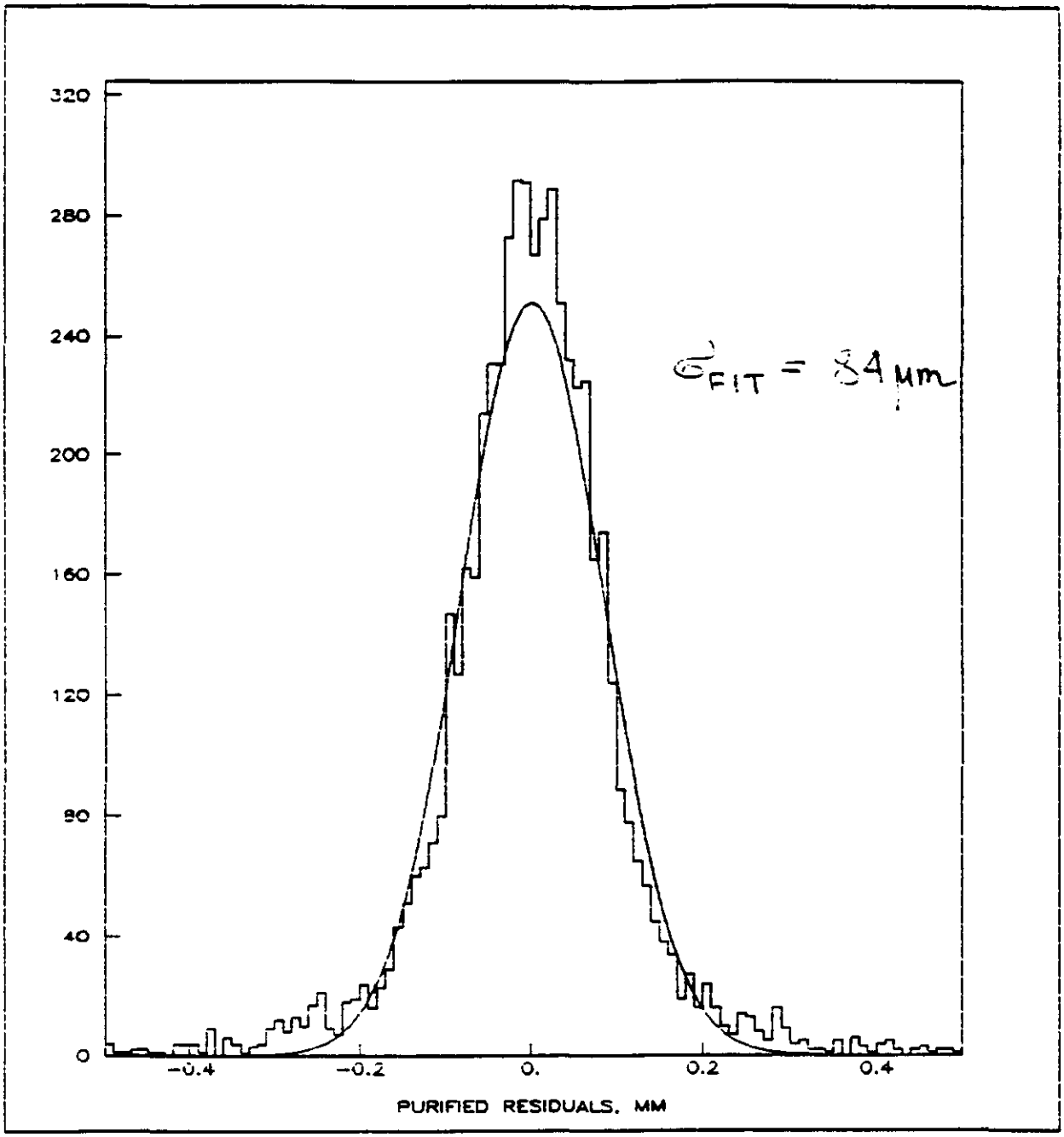

all the same,
but all events (unambiguous)

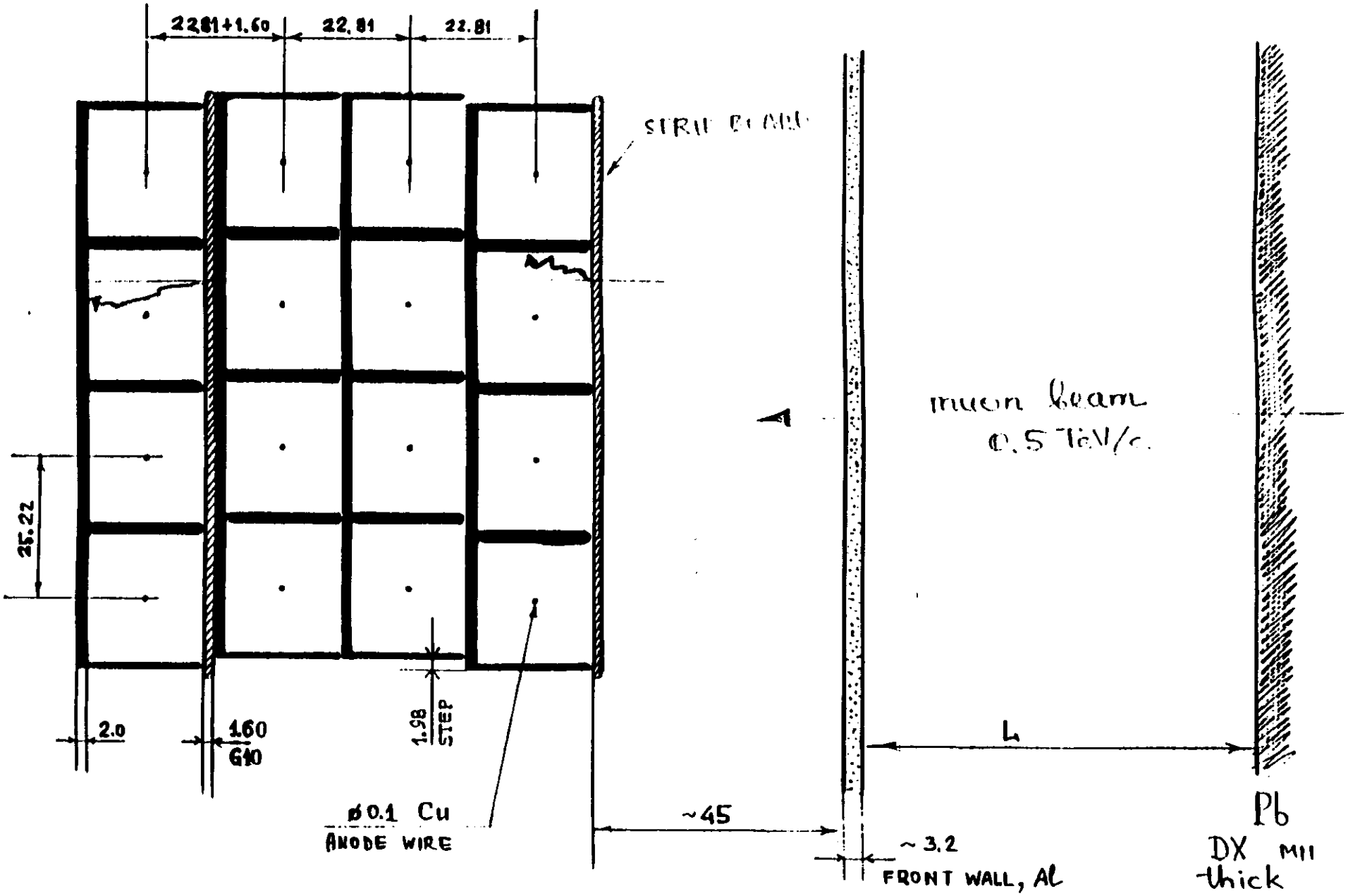
22.81+1.60
22.81
22.81
STRIP PLANE
25.22
2.0
1.60
G10
1.98
STEP
ø0.1 Cu
ANODE WIRE
~45
~3.2
FRONT WALL, Al
muon beam
0.5 TeV/c
L
Pb
DX M11
thick

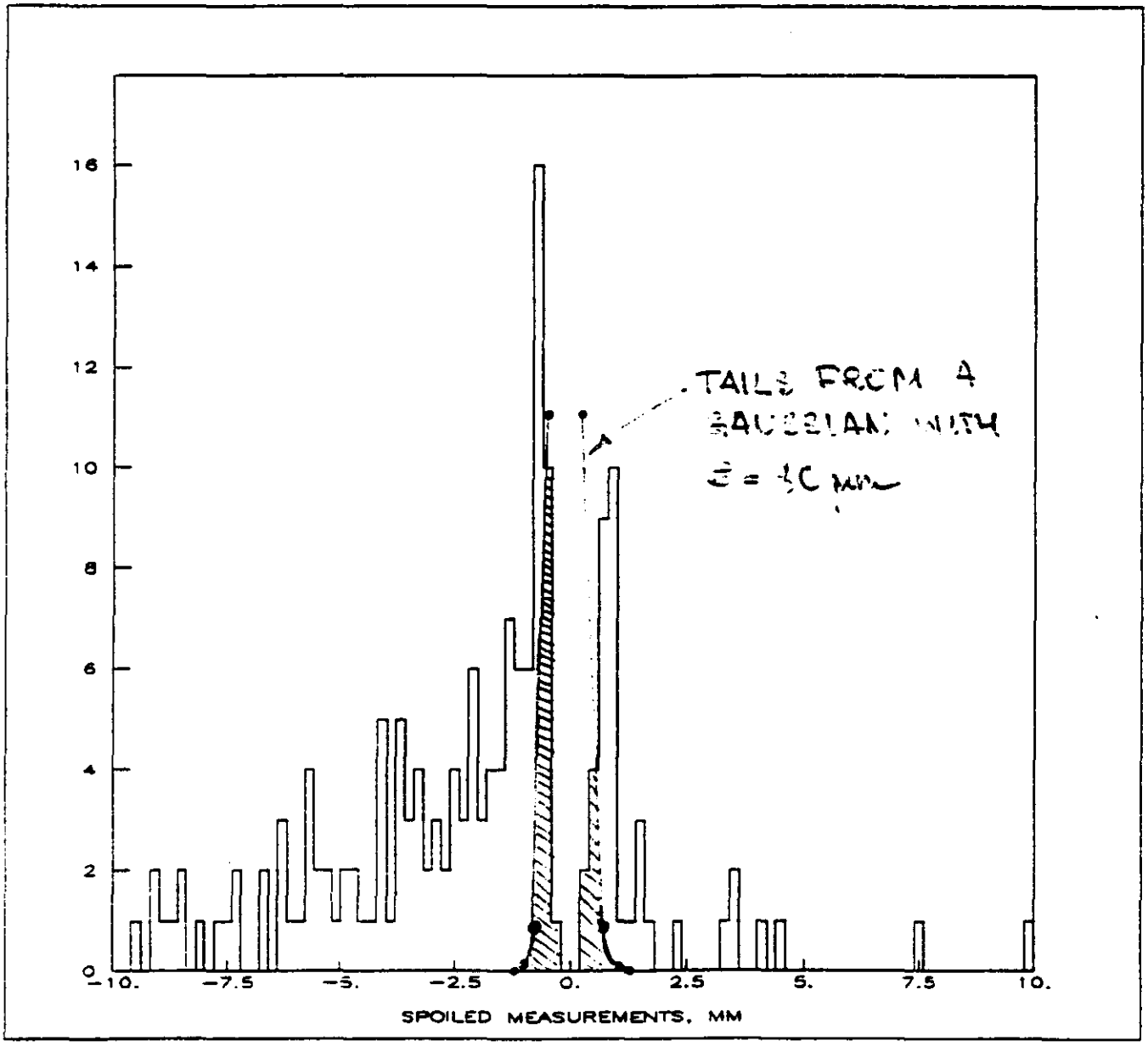

residuals $\geq 1 \times \sigma = 1 \times 30\,\mu m$

probability to get 1 spoiled measurement (dev $> 1 \cdot \sigma$) per track (i.e. 4 measurements)

$= 16\%$

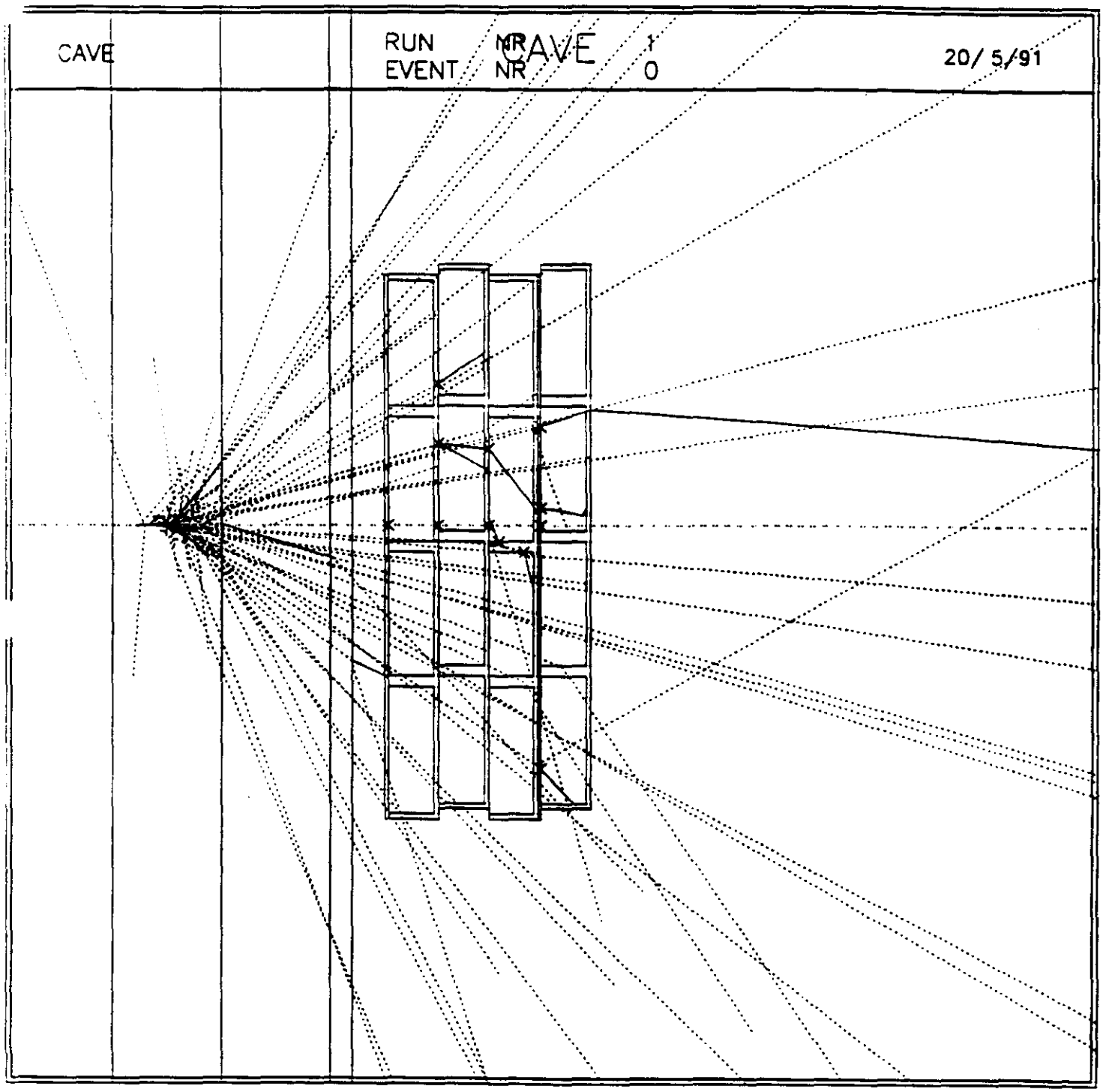
CAVE
RUN NR 1
EVENT NR 0
CRAVE
20/ 5/91

[illegible] simulation

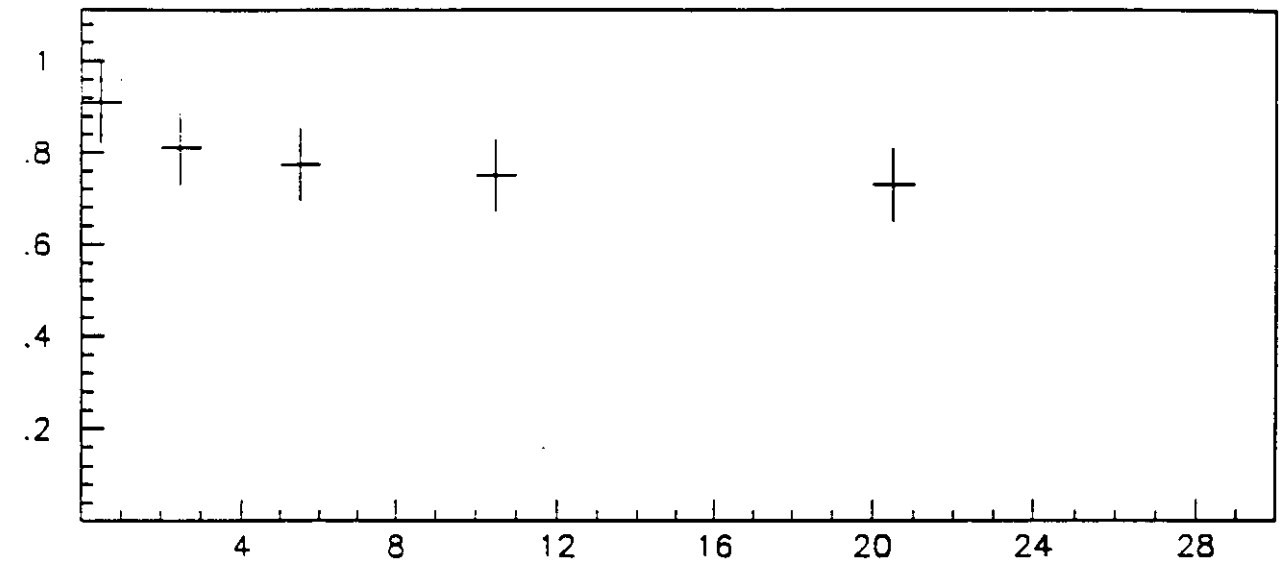

Muon track is closer to a wire than electron in all cells

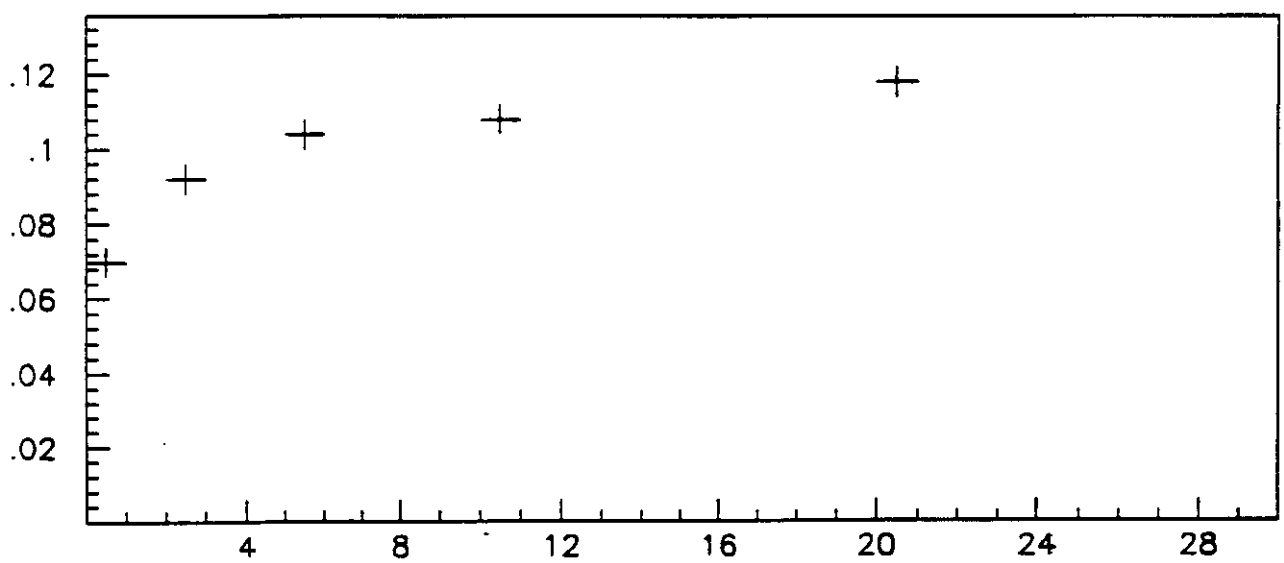

Muon track is closer to a wire than electron in 3 cells

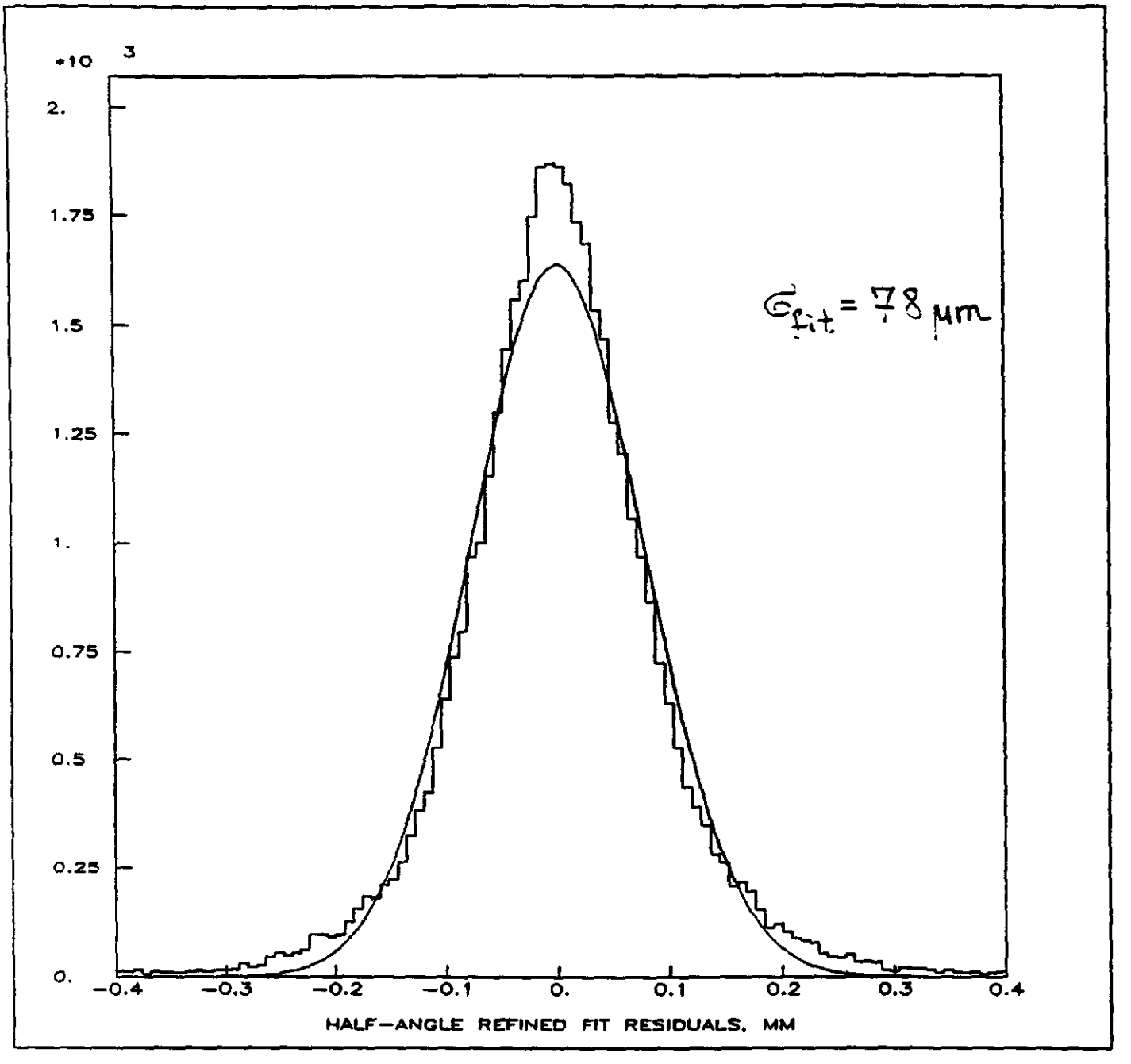

Ar + C_4H_{10} = 1 + 3, SGS mode

cosmic rays data

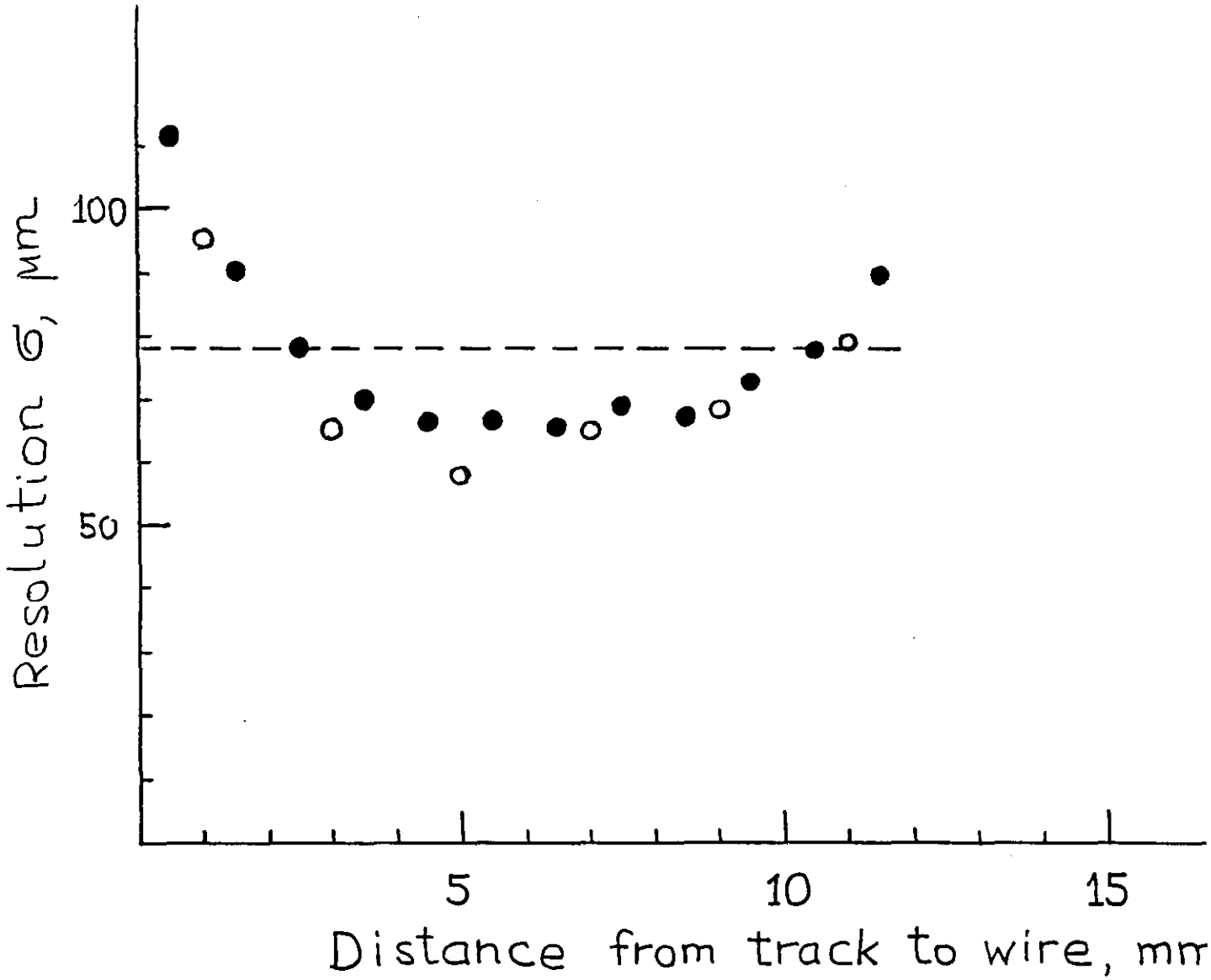

○ FILE: ARGISOB3. ALL
● FILE: ARGISOB5. ALL

tr+ ^3H_e = 1+3, 80% mode.
cosmic ray data

May 20, 1991

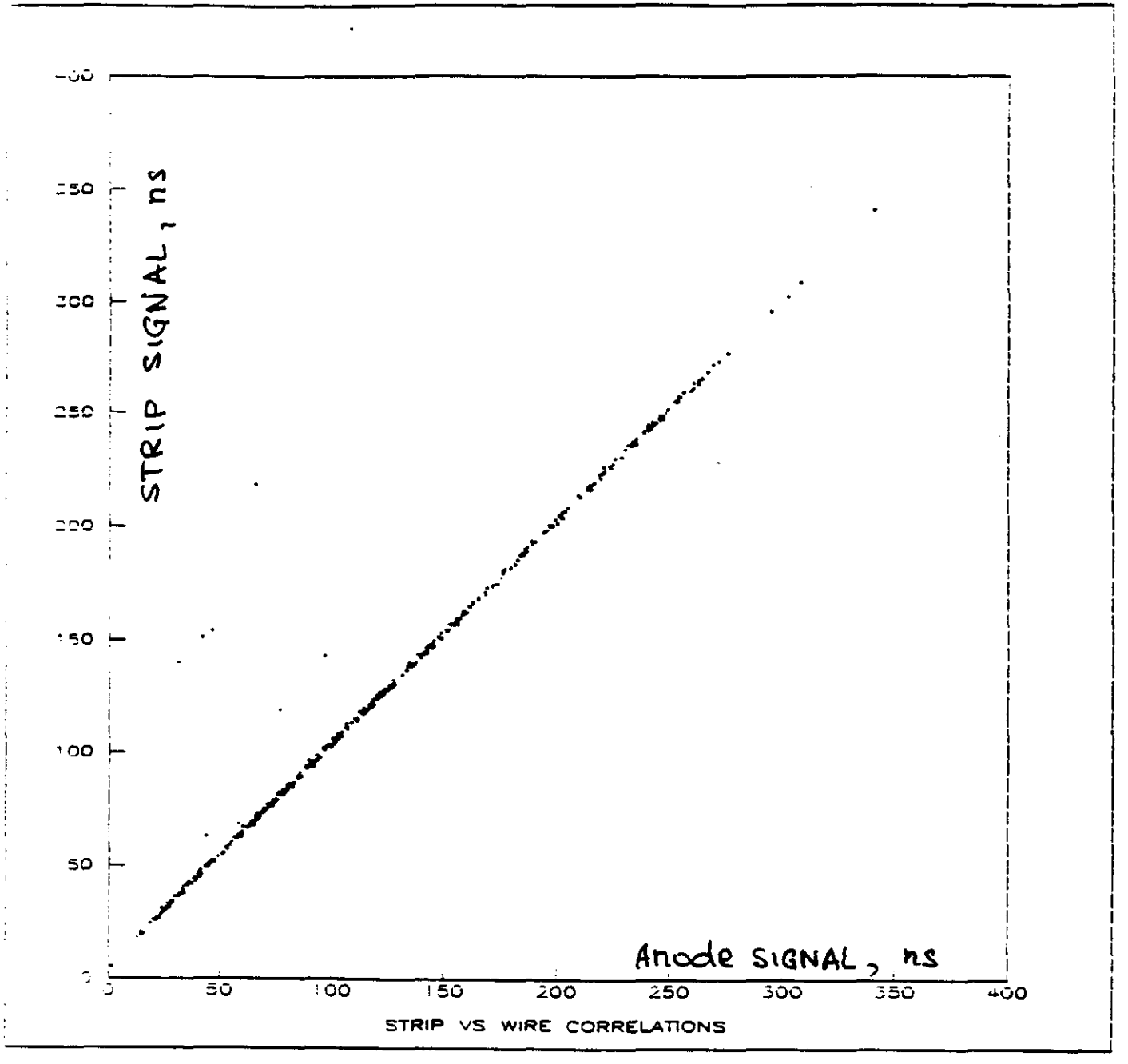

COSMIC RAYS DATA

$Ar + C_4H_{10} = 1 + 3$ SGS mode

M. MOHAMMADI
7/17/91

MUON TRACKING WORKSHOP

CENTRE JEAN MONNET, ST. GENIS-POUILLY
4 - 5 JULY 1991

ORGANIZED BY: Chris Fabjan
Ulrich Goerlach

4th July:
Chairman - F. Dydak

09h00	Registration	
09h30	Introduction	
	GENERAL ASPECTS	
09h45	Performance requirements of tracking chambers in different LHC muon systems	R. Voss
10h15	Rates and occupancies in muon chambers and trigger requirements	M. Pimia
10h35	Coffee	
	MUON TRACKING (GENERAL)	
10h50	Large area tracking techniques Overview	W. Blum
11h20	Muon tracking and triggering in the SSC LOIs	G. Bellettini
	DRIFT CHAMBERS	
11h50	Drift tubes at high and atmospheric pressure	G. Alexeev
12h15	UA1 drift chambers and their future developments	H. Reithler
12h45	lunch	

Chairman - K. Freudenreich

14h15	H1 muon chambers for the forward spectrometer	M. Ibbotson
14h40	L3 drift chambers: status and further developments	M. White
15h10	Test results on chambers with combined drift time and cathode strip readout	G. Mitselmakher
15h30	Large area drift chambers	G. Laurenti (*)
15h45	Coffee	
	CHAMBERS WITH CATHODE READOUT	
16h10	The honeycomb strip chamber	H. van der Graaf
16h40	The RPC future development	R. Santonico
17h10	Interpolating chevron pad chambers	V. Polychronakos

5th July
Chairman - S. Cittolin

	NEW CHAMBER TECHNIQUES	
09h15	The blade chamber	F. Bergsma
09h30	Development of a gaseous pixel chambers	C. Williams
09h45	free	
	MECHANICAL ASPECTS	
10h00	Mechanical stability of large chambers	J.L. Chevalley
10h20	Ultra stable chamber support systems	H. Gerwig
10h40	Coffee	
11h00	Laser alignment: L3-experience and prospects	P. Seiler
11h20	High precision survey methods	C. Lasseur
	ELECTRONICS	
11h40	Front-end electronics for muon systems	F. Bourgois
12h00	Synchronization of large read-out systems	B. Taylor
12h25	free	
12h45	Lunch	

Chairman - W. Willis

	TRIGGER/DAQ	
14h00	Trigger algorithm and electronics for an Fe toroid	S. Veneziano
14h20	Triggering with cathode strip chambers	H. van der Graaf
14h40	free	

SUMMARY DISCUSSION 15h00 - 16h00
Identification of further R&D efforts

16h00 END of WORKSHOP

(*) to be confirmed

COMPACT MUON SOLENOID

L ≃ 20 m

ø ≃ 14 m

15,000 tons

Total absorber 22λ

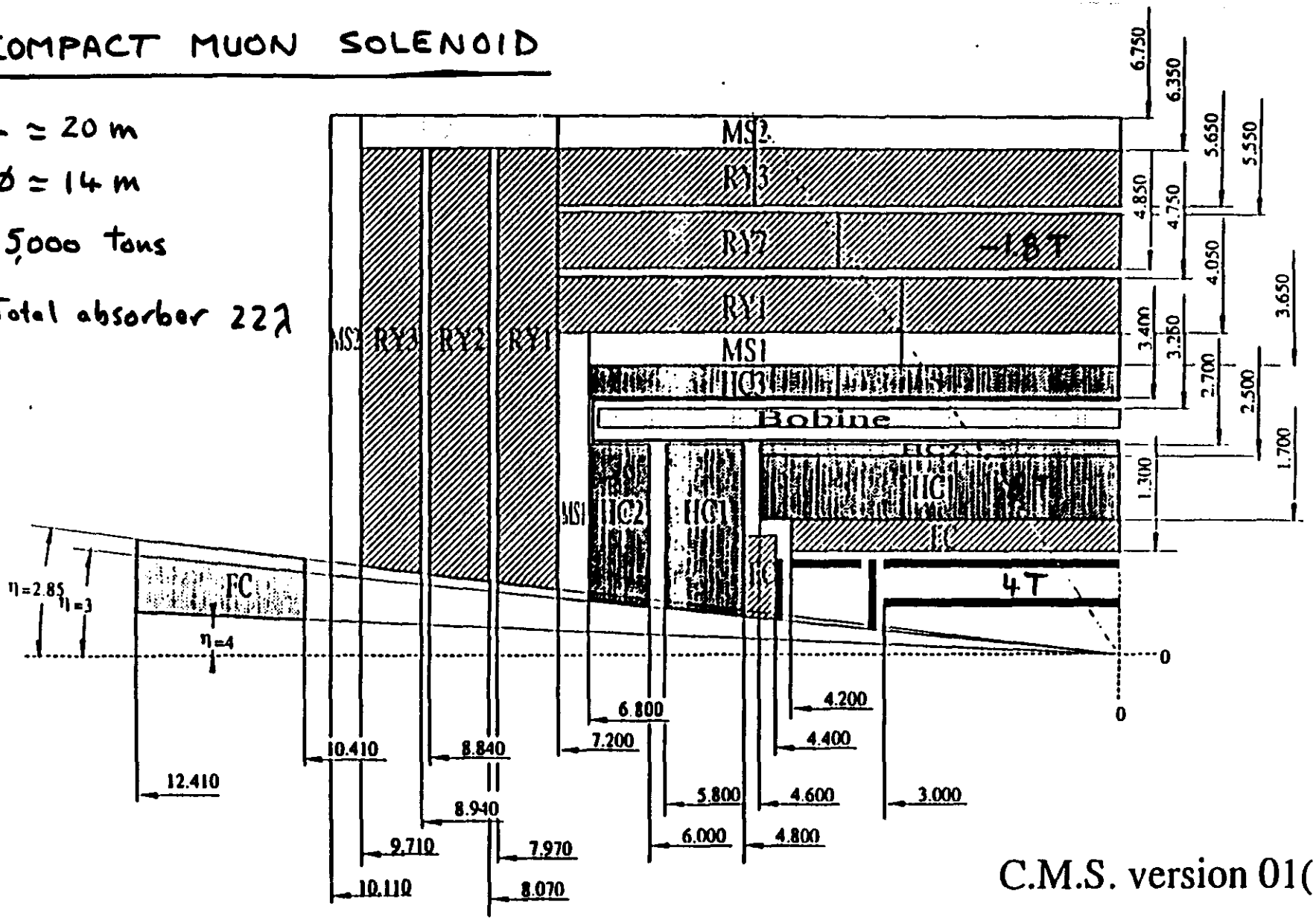

C.M.S. version 01(b)

CERN PPE 06-06-91
jl bénichou

C.M.S. Winding Mandrel Ø 6.200m.

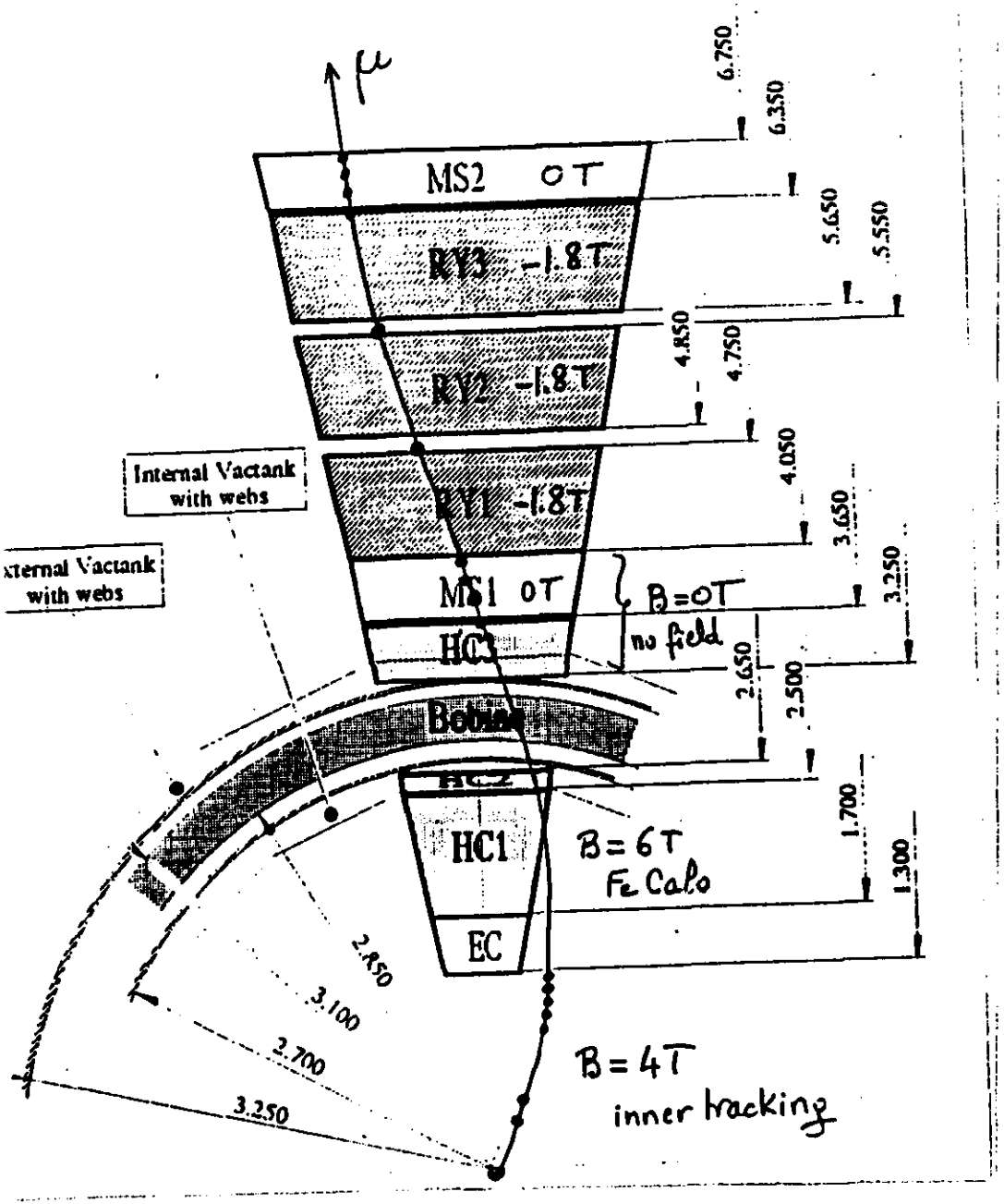

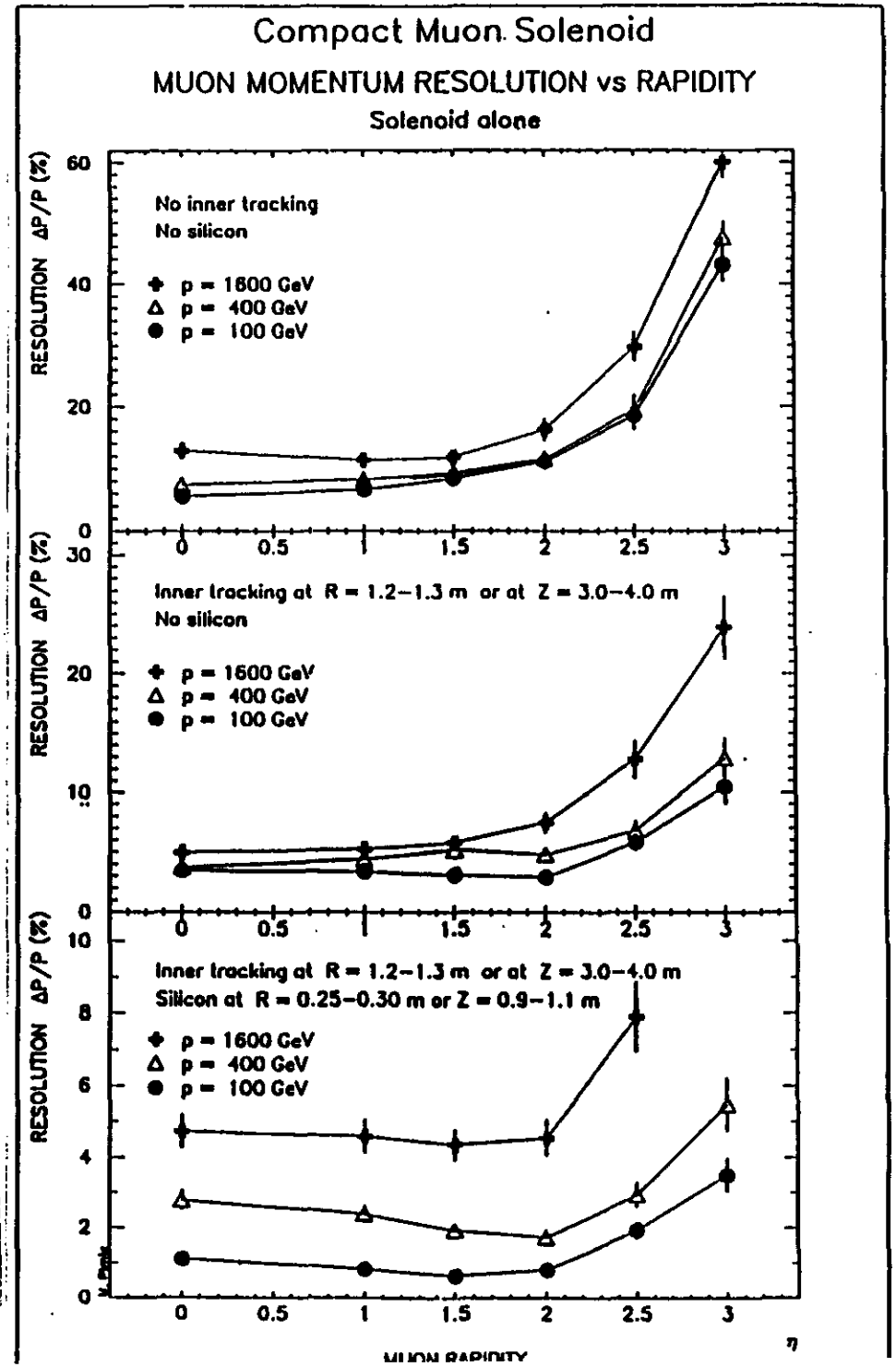

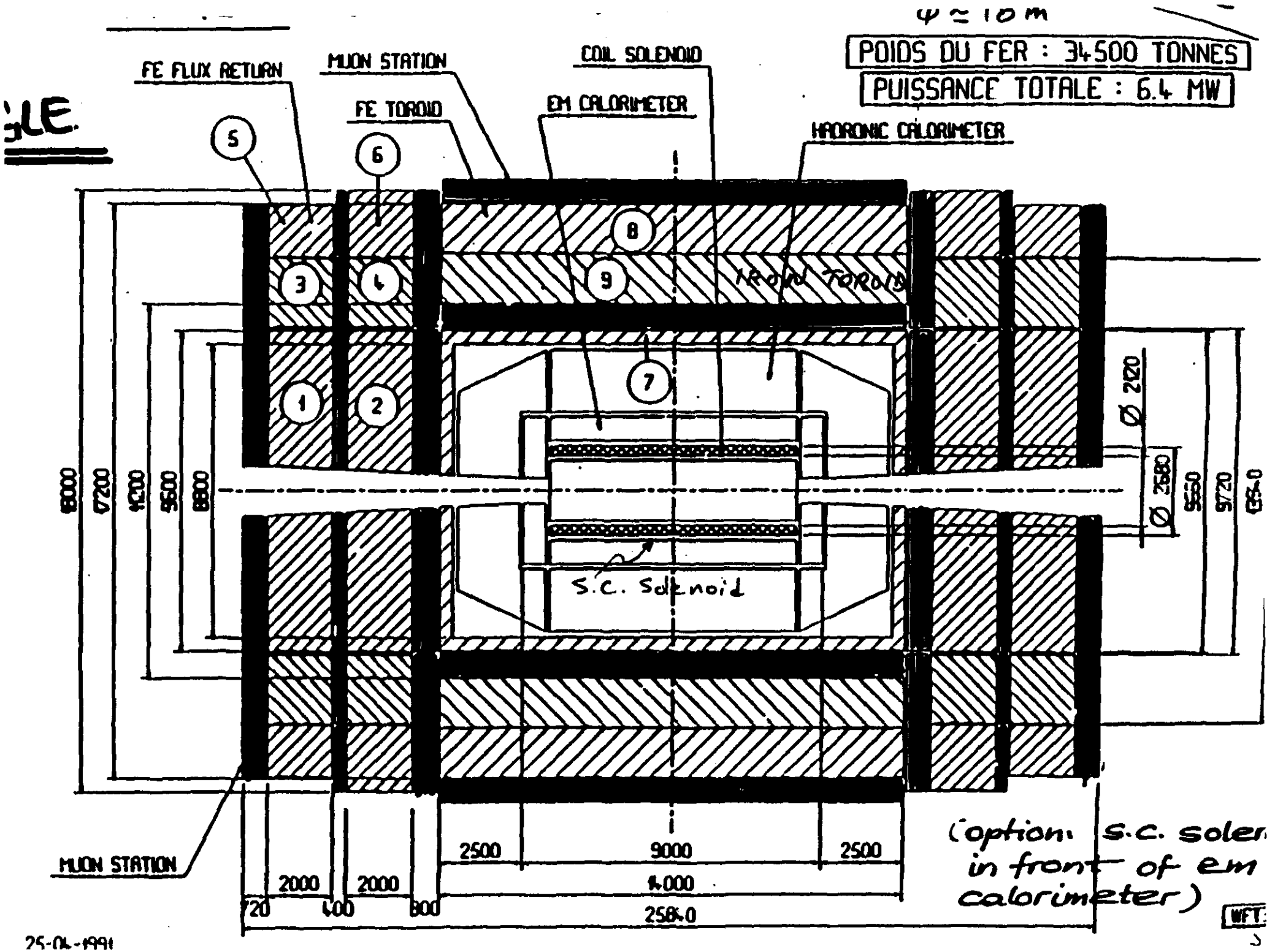
φ ≃ 10 m
POIDS DU FER : 34500 TONNES
PUISSANCE TOTALE : 6.4 MW
FE FLUX RETURN
MUON STATION
COIL SOLENOID
FE TOROID
EM CALORIMETER
HADRONIC CALORIMETER
IRON TOROID
S.C. Solenoid
MUON STATION
Ø 2120
Ø 2580
2500
9000
2500
2000
2000
720
400
800
(option: s.c. solen
in front of em
calorimeter)
25-06-1991

μ momentum resolution in the EAGLE detector

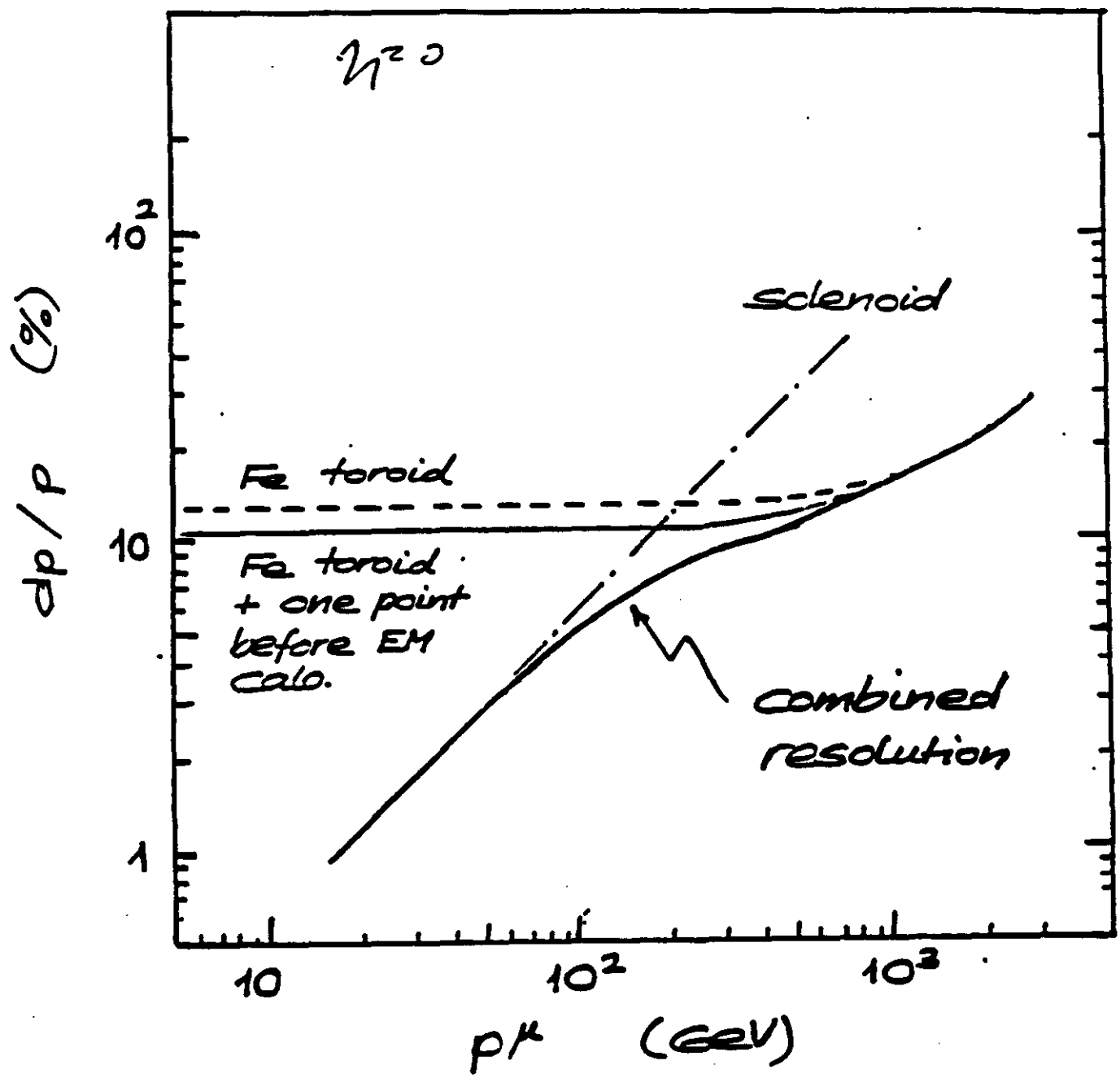

AIR CORE MAGNETS

L3+1

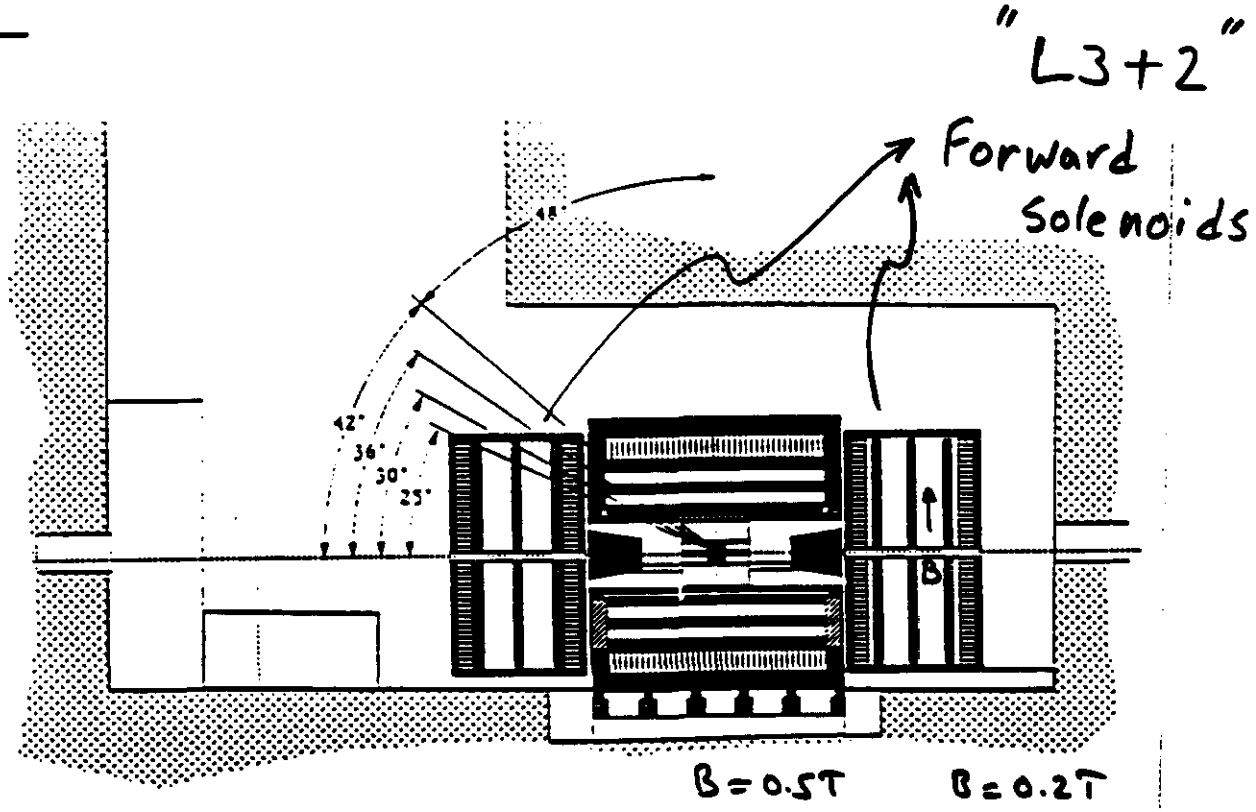

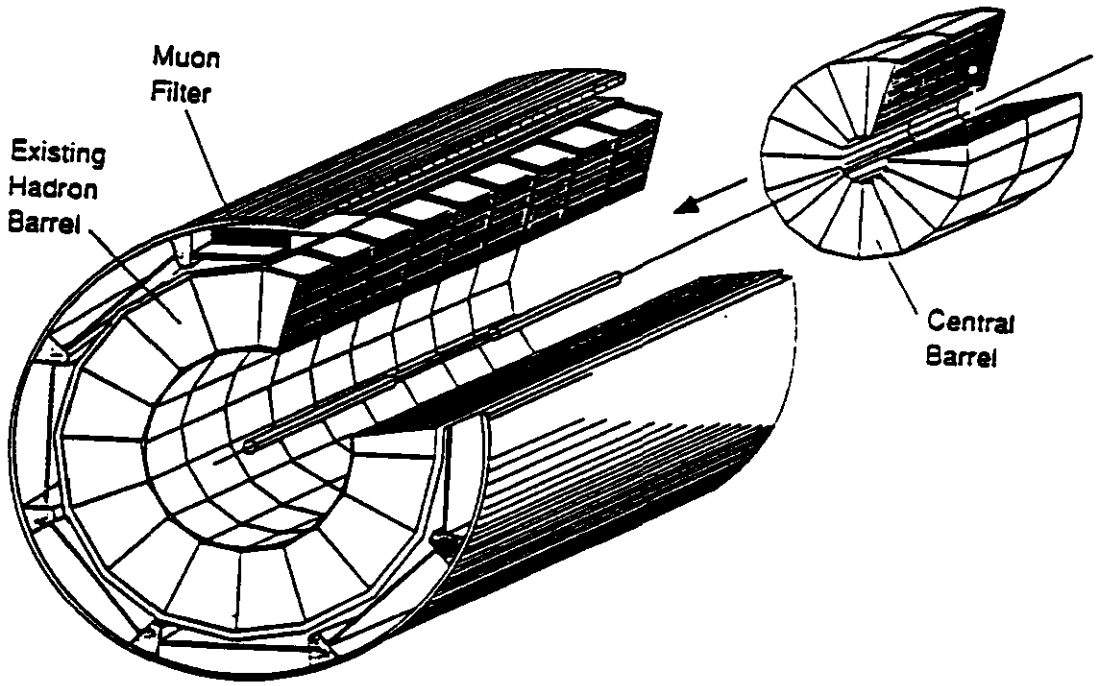

SHAPED SOLENOID

$L = 26$ m

$\phi \simeq 24$ m

$B \simeq 0.7$ T

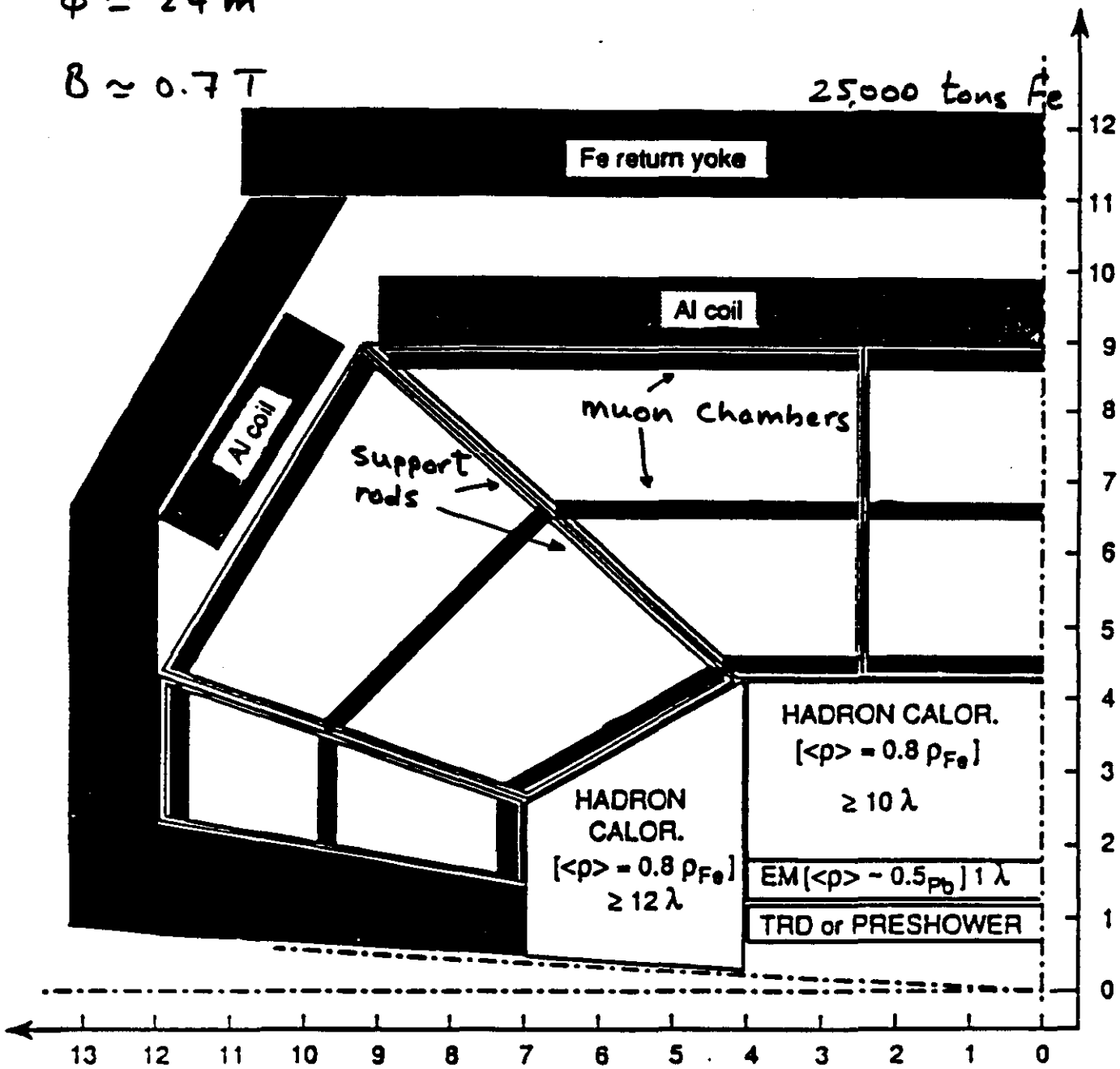

THE SUPER-CONDUCTING AIR CORE TOROID

(SACLAY DESIGN)

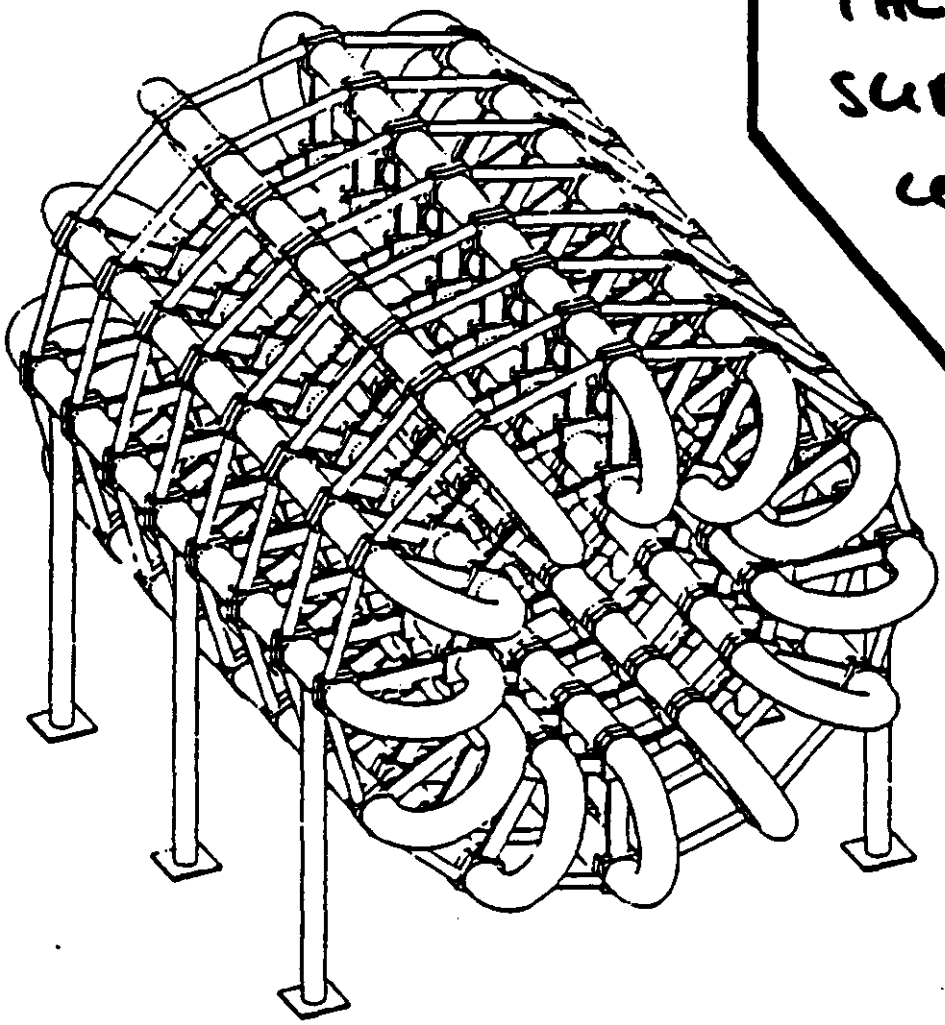

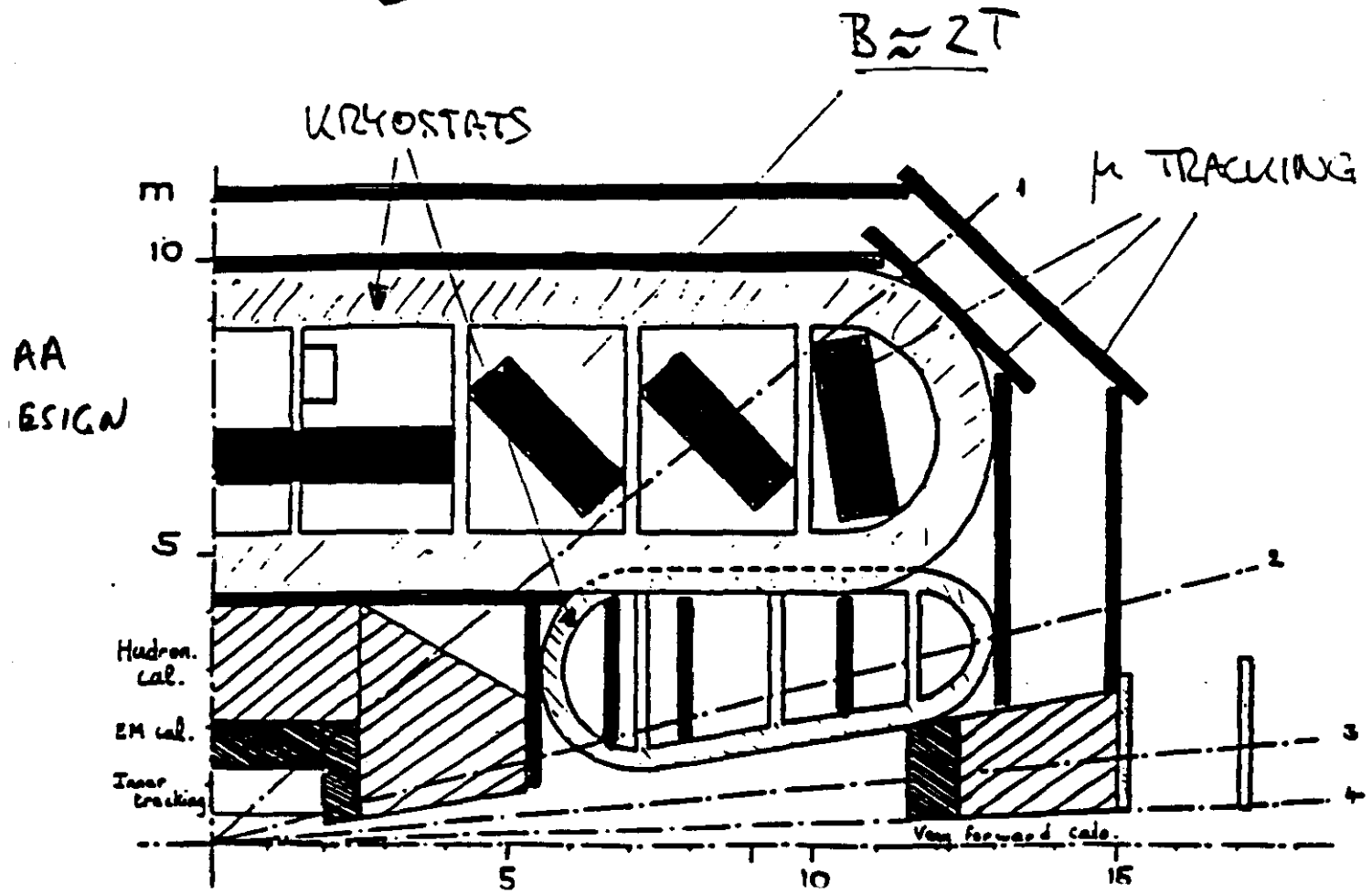

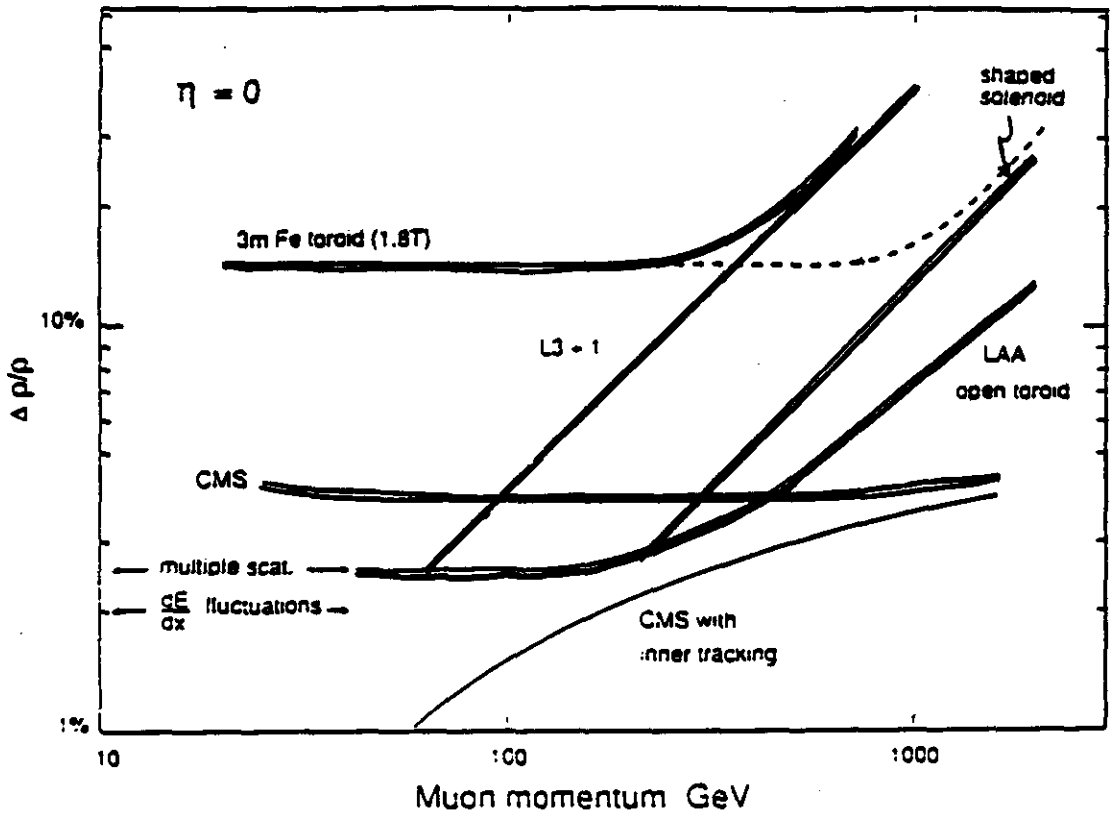

IRON MAG

AIR CORE MAG

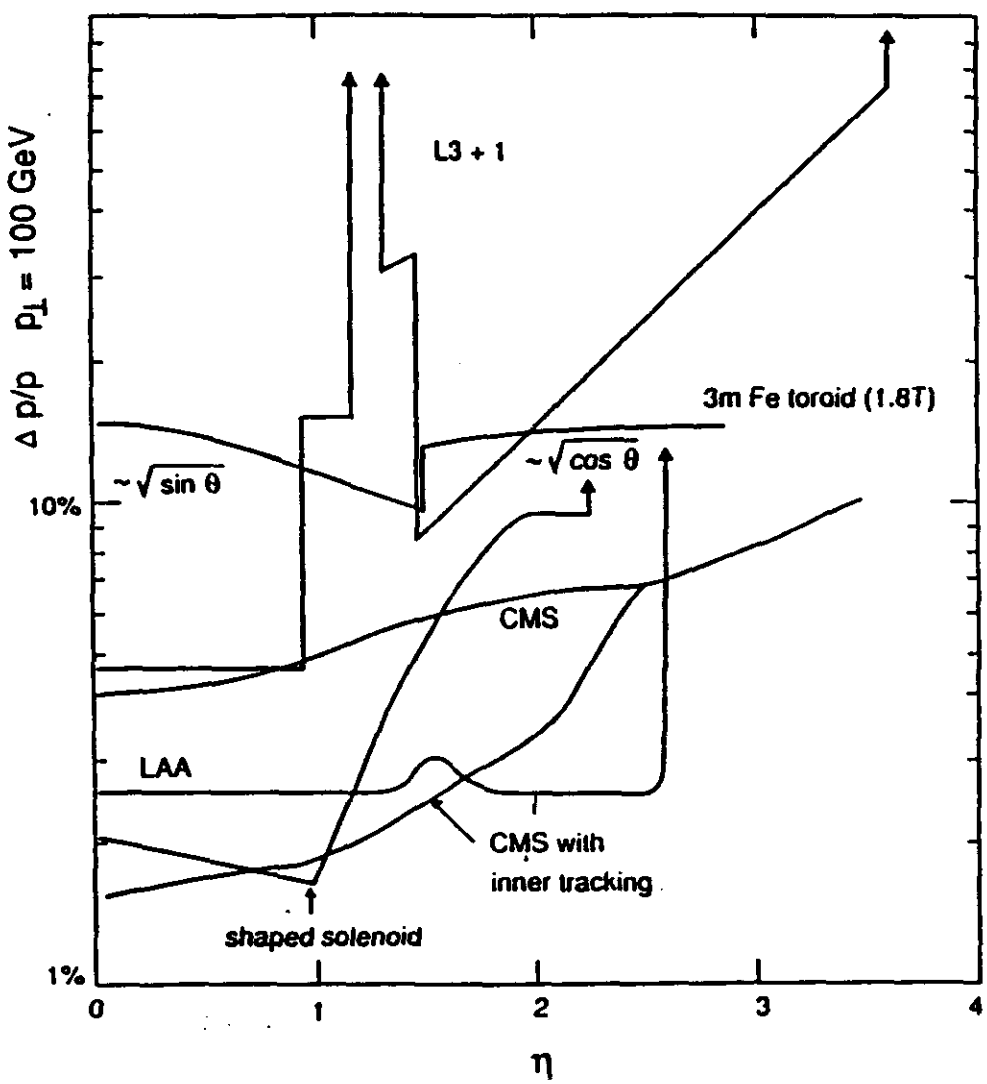

R. Voss

Basic Configurations: $\kappa = 1/p$

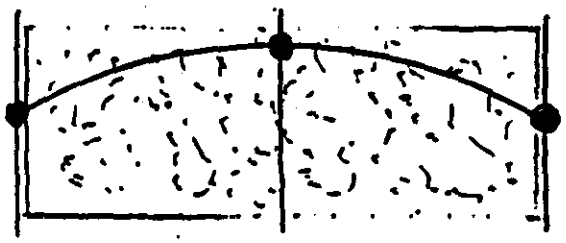

$$\left(\frac{\sigma_\kappa}{\kappa}\right)^2 = \frac{4}{3}\psi^2 + 96\,\Sigma^2$$

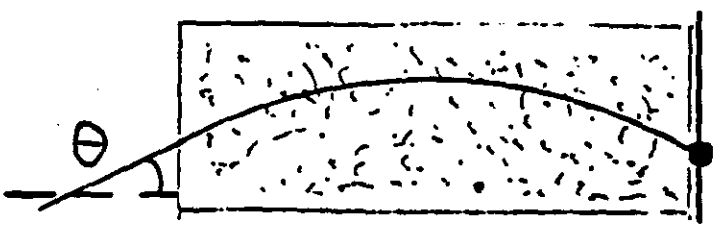

$$\left(\frac{\sigma_\kappa}{\kappa}\right)^2 = \frac{4}{3}\psi^2 + 8\,\Sigma^2 + 4\phi^2$$

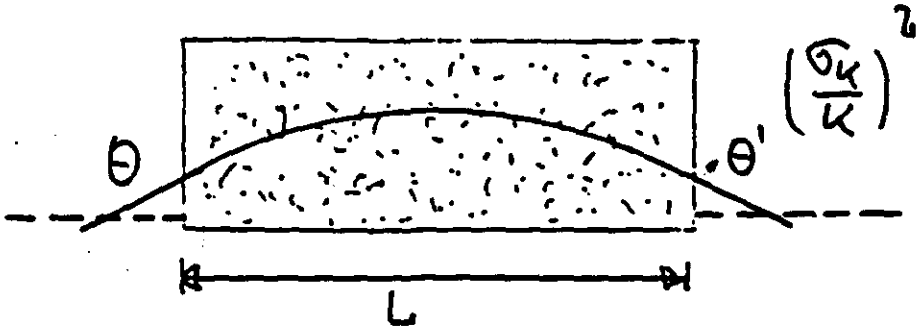

$$\left(\frac{\sigma_\kappa}{\kappa}\right)^2 = \frac{4}{3}\psi^2 + 8\phi^2$$

$$\psi^2 = \frac{1}{2}\left(\frac{20\,\mathrm{MeV}}{eBL}\right)^2 \frac{L}{L_{rad}}$$

$$\Sigma^2 = \left(\frac{\sigma}{L}\right)^2\left(\frac{p}{eBL}\right)^2 \underset{\text{AIR}}{\Longrightarrow} \frac{\sigma_\kappa}{\kappa} = \sqrt{96}\,\frac{\sigma p}{eBL^2}$$

$$\phi = \sigma_\theta^2\left(\frac{p}{eBL}\right)^2$$

e: elementary charge
L_{rad}: radiation length
σ: detector resolution
σ_θ: resolution of angular

DETECTOR RESOLUTION

R. Voss

A simple criterion for iron magnets:

We want

error: magnetic bending, multiple scattering

$$96\,\Sigma^2 < \frac{4}{3}\psi^2$$

$$\Rightarrow \quad \boxed{\sigma \lesssim 0.08 \cdot \frac{20\,\mathrm{MeV}}{p} \cdot L \sqrt{\frac{L}{L_{rad}}}}$$

independent of B!

assume: $L = 3\,\mathrm{m}$, $p = 1\,\mathrm{TeV}$:

$$\boxed{\sigma \lesssim 60\,\mu\mathrm{m}}$$

∴ Nothing prevents us from being equally (or more) ambitious for air-core magnets.

GOAL: $\sigma \simeq 50\,\mu\mathrm{m}$

OCCUPANCY

M. Pimiä

VERY LOW MEAN OCCUPANCY OF THE MUON CHAMBERS:

$|\eta| < 1.5$ 10λ, $p_\perp \gtrsim 3$ GeV, MEAN MUON RATE 200 kHz

- 200 kHz / 66 MHz → 0.003 MUONS / BEAM CROSSING
- IF 30 HITS / MUON → 0.1 HITS / BEAM CROSSING
- IF 0.1 M CHANNELS → OCCUPANCY ~ 10^{-7}

$1.5 < |\eta| < 2.5$ 20λ, $p_\perp \gtrsim 1.5$ GeV, MEAN MUON RATE 600 kHz

- 600 kHz / 66 MHz → 0.01 MUONS / BEAM CROSSING
- IF 30 HITS / MUON → 0.3 HITS / BEAM CROSSING
- IF 0.1 M CHANNELS → OCCUPANCY ~ $3 \cdot 10^{-7}$

BUT

HIGH MOMENTUM MUONS ARE ACCOMPANIED BY LOW ENERGY ELECTRONS AND PHOTONS —

RISK OF LOCAL CONFUSION

NEED DETAILED SIMULATION BECAUSE OF DEPENDENCE ON PRECISE GEOMETRY, MATERIALS AND $\bar{B}$.

EXAMPLE: AN AIR GAP (WITH $\bar{B}$) BETWEEN ABSORBER AND DETECTOR — OR SOME LIGHT MATERIAL TO ABSORB ELECTRONS AND PHOTONS?

TO BE STUDIED BY RDS

R. Voss

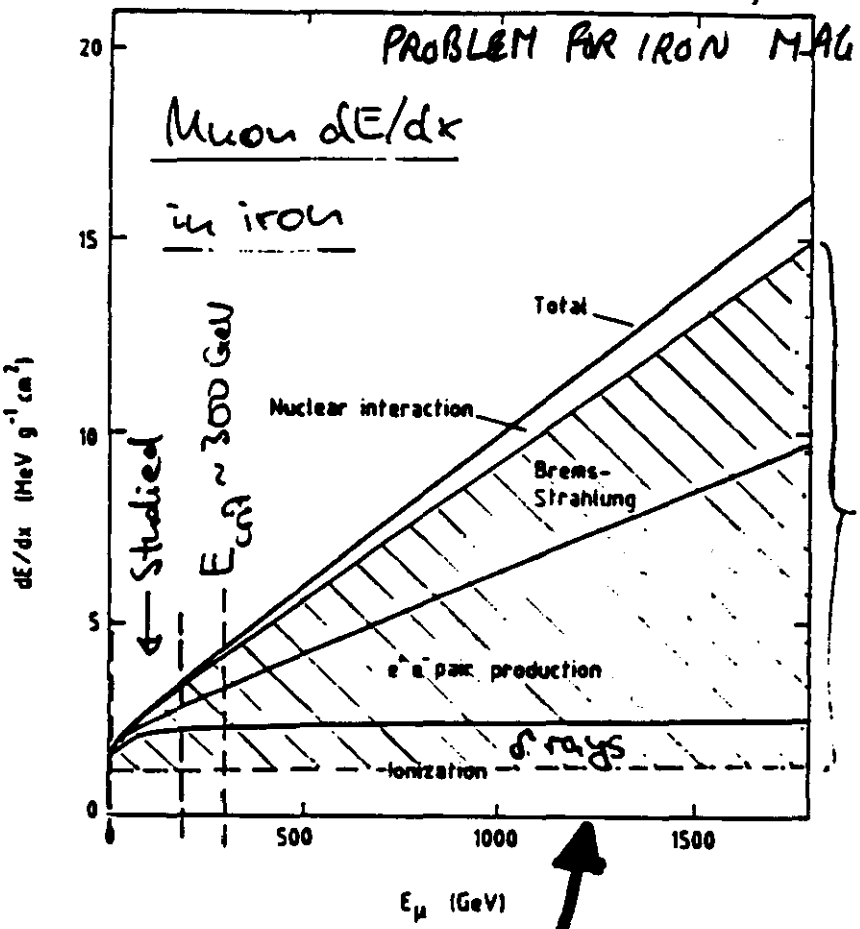

SOFT SHOWERS

NA4 Studies (~ 198[illegible]):

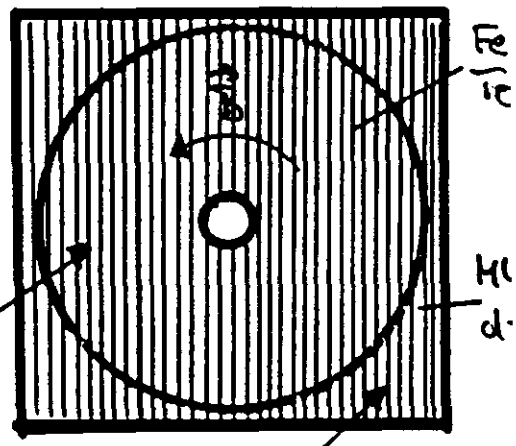

The problem:

The effect:

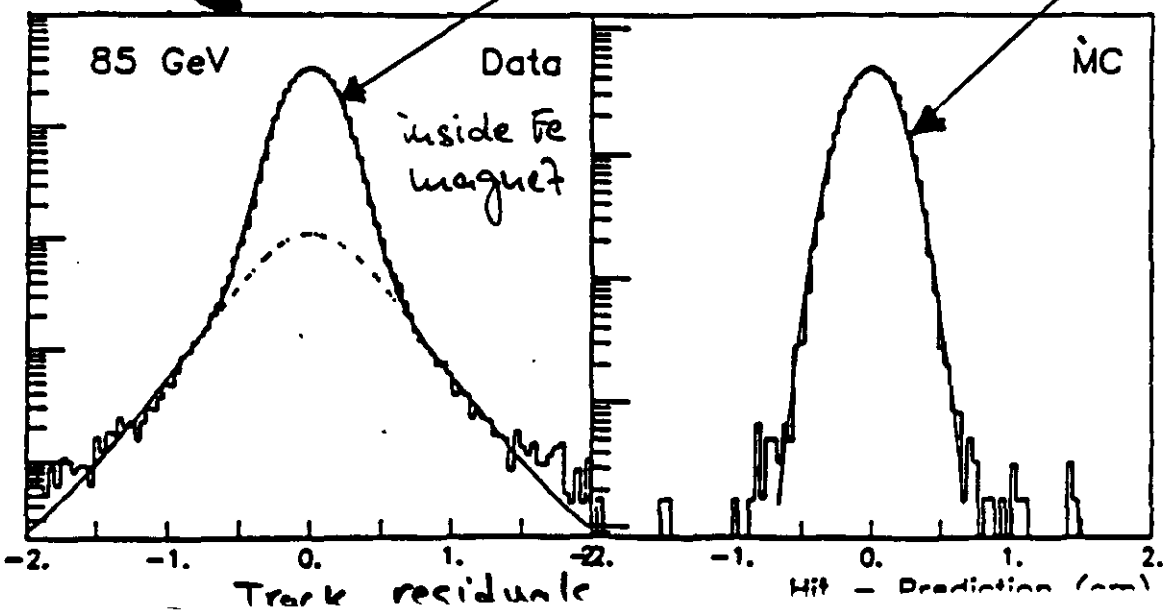

M. KIMIA

DEL PRETE + PETRIDOU
AACHEN, VOL III, 477

NUMBER OF ACCOMPANYING HITS IN A MUON DETECTOR
AFTER 2m Fe ABSORBER

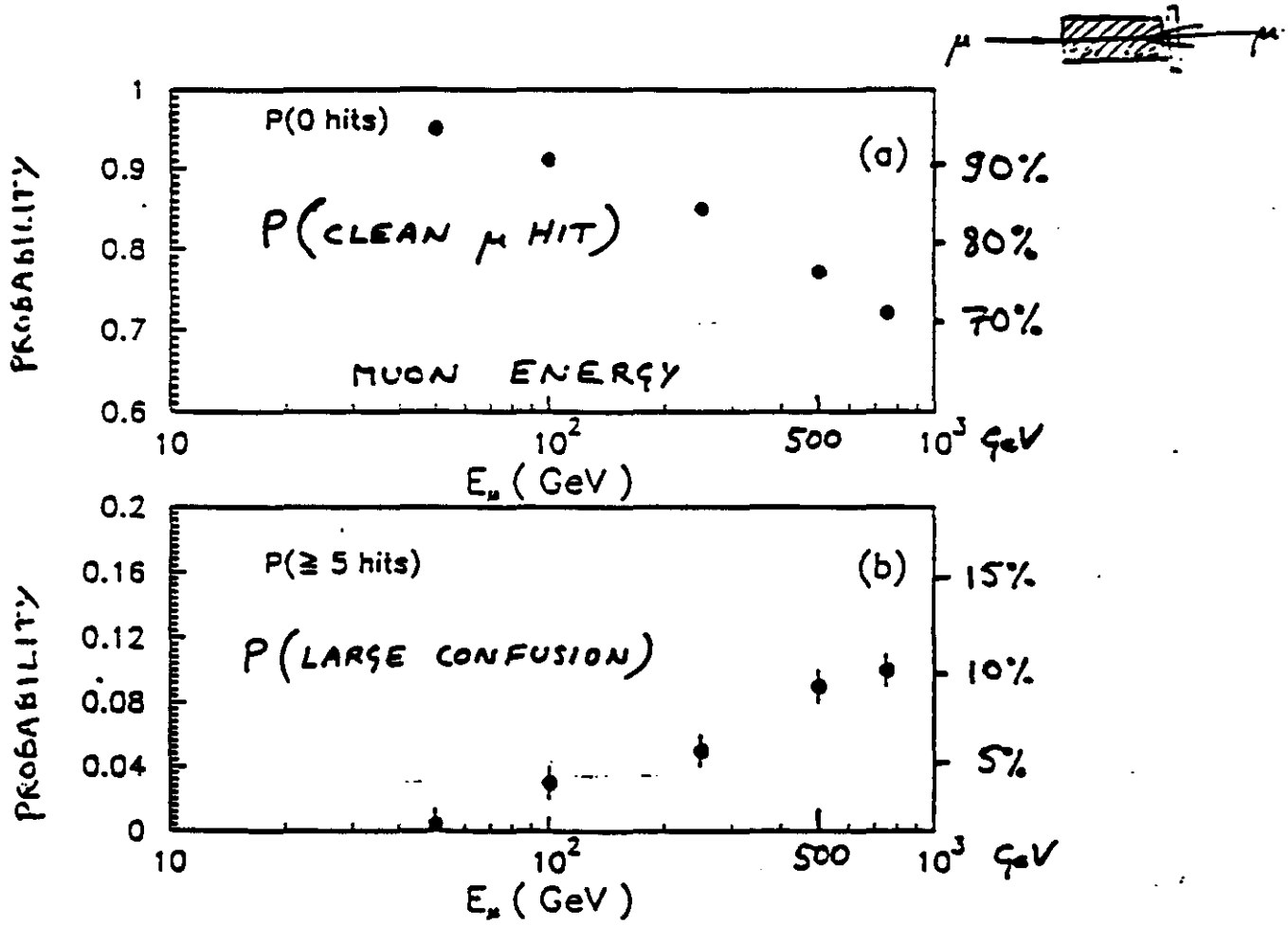

Figure 5: Probability of a clean hit in a detector after 2m of iron (a) as a function of E_μ. The probability of detecting more than 4 hits is plot in (b).

∴ NEED

→ REDUNDANCY : MANY TRACKING STATIONS

→ REDUNDANCY : MANY MEASUREMENTS AT EACH STATION

CAREFUL : THERE ARE MANY PHOTONS, TOO !
NEED DETAILED STUDY !!
(DEPENDENCE ON MATERIALS, $\vec{B}$ FIELD etc.)

TIMING :

SLOW SYSTEMS ARE POSSIBLE - ~ 1 μsec

BUT TRIGGER REQUIRES :

- FAST COLLECTION TIME — Honey Comb
- FAST CHAIN — PAD Chamber
- SECOND FAST DETECTOR — UA1 drift ch
  RPC's

MECHANICS :

MECHANICAL STABILITY OF LARGE CHAMBERS

STABLE SUPPORT SYSTEMS

ALIGNMENT

⇓

CONTROL OF SYSTEMATIC ERRORS

L* Muon Support Structures

- Truss Structure fabricated with 6061-T6 Aluminum Tubing and Investment Cast aluminum joints
- Low stress Structures for Stability, Linearity and Repeatability
- Joints are Clevis Joints (to minimize moments on truss structure) which are bolted and pinned for Repeatability and for Ease of Manufacture and Assembly.
- Muon Chambers attached to structure so that they can be moved on the structure (they contribute no significant structural rigidity to the module assembly)
- Structure/chamber design permits accurate muon chamber prealignment, long term storage and final assembly while maintaining alignment (similar to L3 procedures)
- Alternative Integrated Structure ties muon chamber structure into the support structure.
  - Integrated structure has order of magnitude less deflection for module at 90° relative to gravity.
  - System requires that internal wire plane assemblies be capable of moving laterally to maintain alignment of module wire planes.

DRAPER LABORATORY

F. Nimblett 7/17/91

L* Alignment (module)

- Local Alignment needs for L* modules quite similar to those achieved for L3 Octants. (L* Goals are 8μm for 3 layers and the ability to monitor the relative positions to 1μm ; L3 achieved 10mm for 3 layers and was able to monitor relative position to an accuracy of 0.2μm)
  - For L3, Alignments of this accuracy were only achieved through careful procedures involving numerous measurements combined with good structural models which permitted the accurate placement of the chambers on the structure to compensate for "g" loading to the specific orientation of a module. Similar procedures were anticipated for L*.
  - Ability to get an absolute measure of wire plane position relative to the respective elements of the three element straight line monitor in each of the three sense planes proved to be a critical item in achieving the ultimate accuracy of the L3 chambers.
  - Finally, it was critical design feature for L3 and L* that the structures be sufficiently stable with time to permit storage of the modules in an orientation typically different from its final orientation without them changing significantly in alignment.

DRAPER LABORATORY

L* Alignment (global)

- L* Goal for global alignment accuracy is that all tracks point to interaction point within an accuracy of 0.7mm versus an achieved value of 1.0mm for L3.
- PROBLEM (L* IS NOT EASILY RELATABLE TO L3 IN THIS AREA)
  - L3 Muon System attached to its own independent support tube making it possible to achieve good global alignment without monitors or controlled actuators.
  - L* Muon System attaches to the ID of a very large superconducting magnet for the central region and to flexible steel magnet plugs for the end cap regions.
  - Potential L* alignment problems (short list) include foundation settling, magnet settling and magnet deformations due to both the cooling down of the the superconducting coils and the forces resulting from the activation of the magnet.
  - L* global alignment to this accuracy (16 arc sec range) will probably require each module to be monitored with multiple sensors to monitor both angular and linear shifts which can be referenced to external fiducials on a real time basis.

DRAPER LABORATORY

F. Nimblett 7/17/91

Muon System 2nd Detector Structure/Alignment Needs (short term)

- A group concensus on the character of the upcoming muon detector effort.
- General agreement from the muon group on the basic layout of the muon detector sensors.
- Some limits on local and global alignment requirements based on physics needs.
- Some limits on additional structure in the path of muons to allow some design flexibility.
- A first-order cut at evaluation of the baseline magnet deformations (ID of magnet tube and magnet plug).

DRAPER LABORATORY

F. Nimblett 7/17/91

Muon System 2nd Detector Structure/Alignment Goals (short term/LOI)

- Goals presume some reasonable resolution of "Needs"
- Evaluate compatability of muon detector options with baseline structure.
- Complete conceptual designs for Structure/Sensor interfaces.
- Complete conceptual designs for Structure/Magnet interfaces.
- Complete conceptual designs to fulfill local and global alignment specifications.
- Provide figures and writeup for this section of LOI.

DRAPER LABORATORY

F. Nimblett 7/17/91

Muon System 2nd Detector Structure/Alignment Goals (long term / Design Report late 92)

- Presumes that long term goal is towards a prototype of similar size and configuration to a central region muon chamber module.
- Complete design,fabrication, assembly and preliminary evaluation of prototype support structure.
  - Muon support structure to be sufficiently generic to accomodate various muon sensor options with sensor-specificinterface hardware.
  - Prototype should include "magnet interface hardware" and prototype versions of sensors and actuators appropriate to achieve local and global alignment goals.
  - Protoype should also be capable of being oriented into any of the potential module orientations and should include sensors appropriate to evaluate the physical behaviour of the module.

DRAPER LABORATORY

F. Nimblett 7/17/91

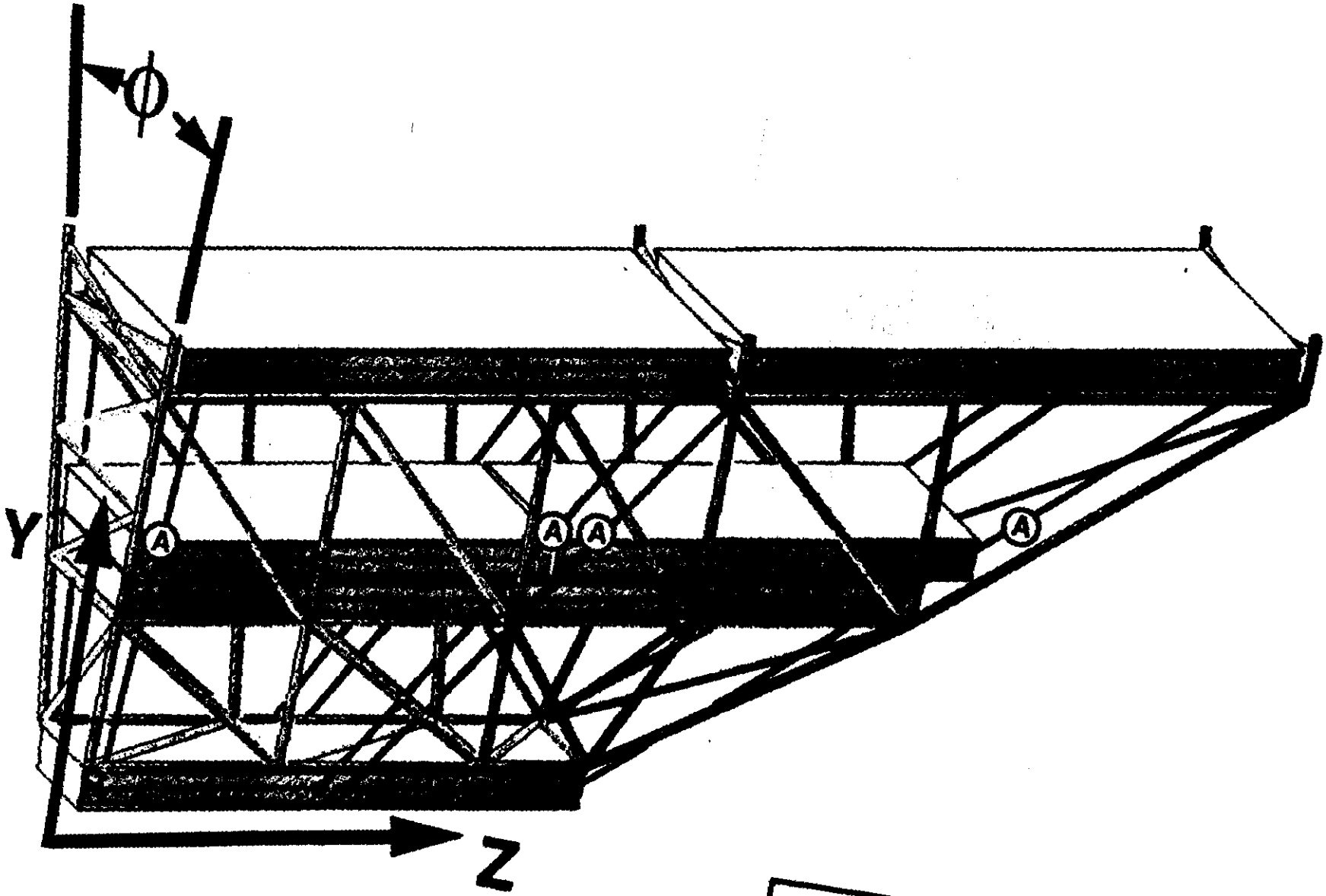

MUON CENTRAL REGION
MODULE ASSEMBLY

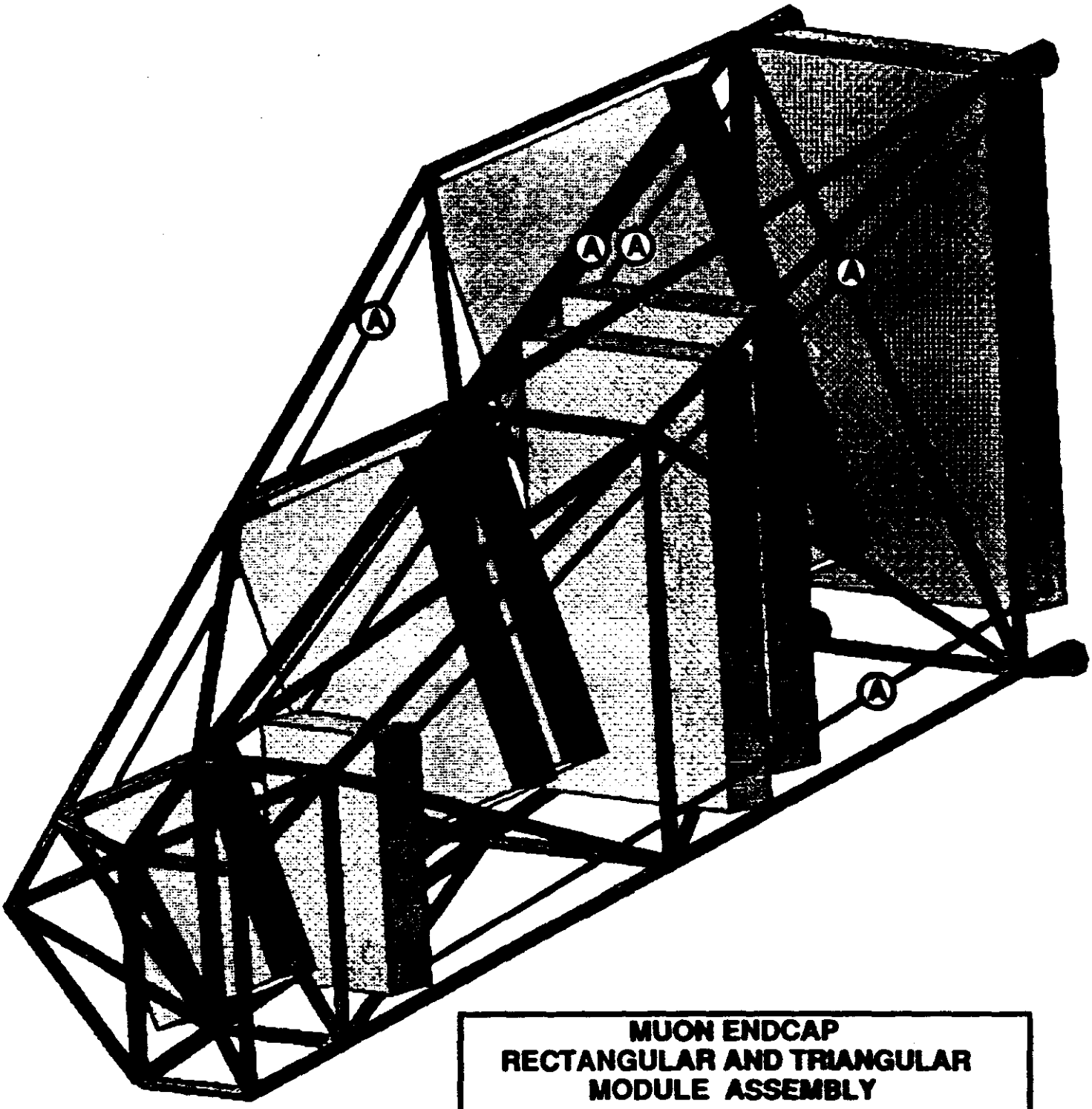

MUON ENDCAP
RECTANGULAR AND TRIANGULAR
MODULE ASSEMBLY

L* MUON STRUCTURE (TEST JOINTS)

- TEST JOINTS DESIGNED AND FABRICATED
  - CLEVIS JOINT
  - LAP JOINT (NOT TESTED)
- TESTS CONDUCTED ON CLEVIS JOINT
  - TENSION AND COMPRESSION TO 10,000 # (4 TIMES THE ANTICIPATED LOADS FOR THE CENTRAL REGION)
  - COMBINED SHEAR AND MOMENT (5,000 # AND 2,200 FT-#)
- TEST RESULTS
  - TENSION AND COMPRESSION (MAX. JOINT DEFLECTION 120 μ, MID-RANGE HYS. 6μ MAX, REPEATABILITY 0.5μ)
  - COMBINED LOADING (MAX ANGULAR DEFLECTION 2.6 MILLIRAD, MID-RANGE HYS. 0.3 MILLIRAD, REPEATABILITY 14 MICRORAD)
  - MID-RANGE HYSTERESIS BELIEVED DUE TO CLAMPING ARRANGEMENT OF MEASUREMENT SYSTEM.

DRAPER LABORATORY

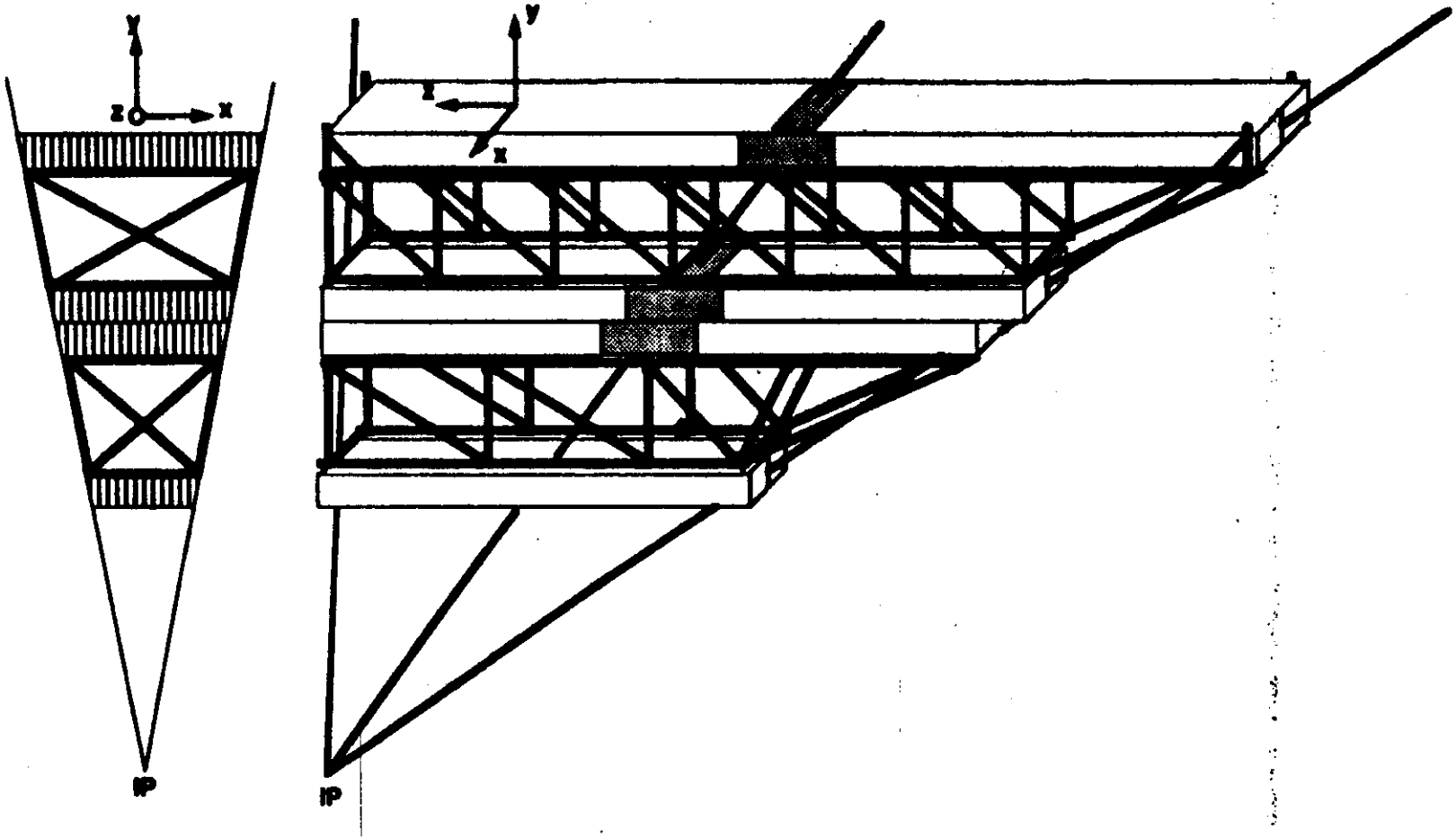

INTEGRATED TRUSS AND CHAMBER STRUCTURE

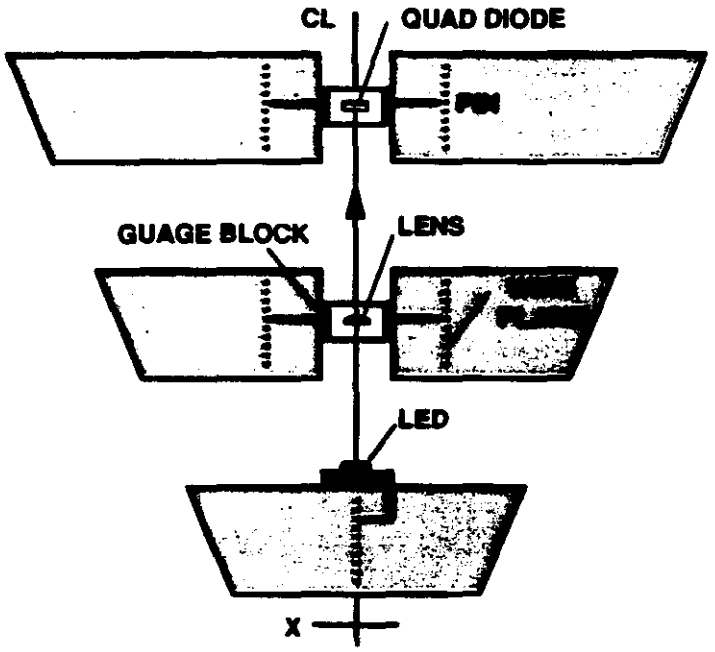

Stability of L3 Alignment for 3 Layers of Chambers

4μm

Reproduces after 1 Year

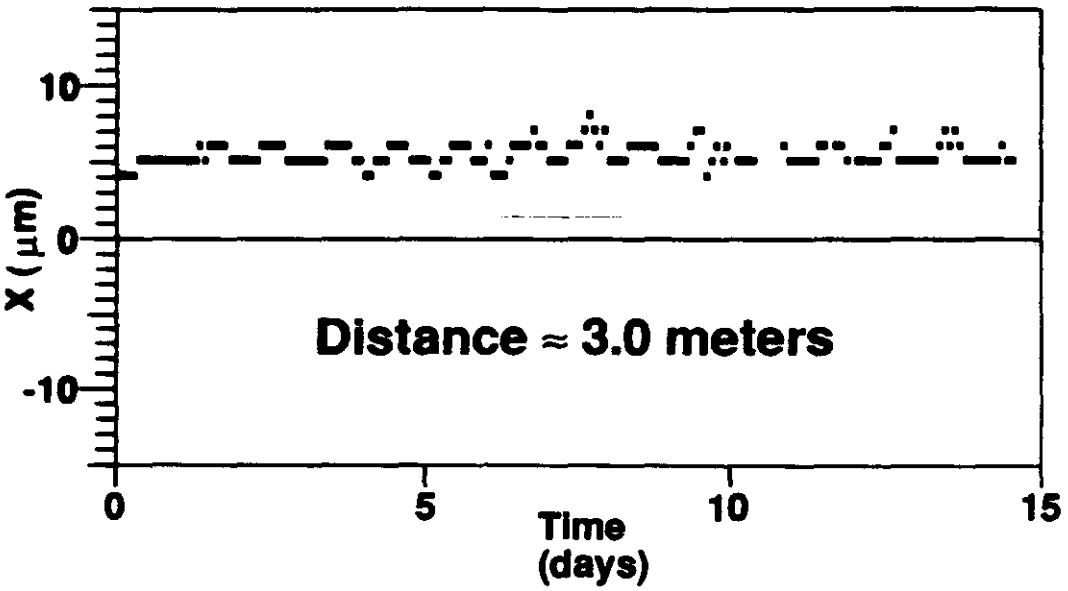

MUON ENERGY LOSS IN A SCINTILLATING FIBER CALORIMETER

Jim Branson, Hans Paar

adapted from a March 29, 1990 note

This note presents a study of the precision required in the measurement of muon bremsstrahlung inside the hadron calorimeter. We wish to measure 500 GeV muons with on the order of 4% momentum resolution. To do this we must correct for energy lost in the material between the interaction point and the muon chambers. A particular question arises if we propose to use a scintillating fiber calorimeter with only one longitudinal segment. Because of the attenuation of light in the fiber, a given energy deposit will give rise to a variable response in the light detected depending upon the longitudinal position of the brems. We have carefully calculated the effect, using a complete Monte Carlo simulating energy loss.

The effect of attenuation has been measured, in a real 2 meter long module. This has been presented by Hans Paar. The measurement was done over a range of 1.55 meters with electrons incident from the side of the module. Over this range the light output decreased by 23.9%. Extrapolating to a 2 meter thick module, we expect a variation of $\pm 17.4\%$ compared to the middle of the module. We have used this measured value for our Monte Carlo calculation. It should be pointed out, however, that the radiation resistant fiber 3HF, has been measured to have an attenuation length from 6 to 8 meters without a mirror. With a 0.85 reflective mirror the light variation for a 6 meter attenuation length is only $\pm 3.9\%$.

The far more conservative variation of $\pm 17.4\%$ was put into a Monte Carlo calculation of the energy loss of a 500 GeV muon in lead. GEANT was used for the simulation. The energy losses produced by GEANT have been checked against those calculated and measured. In our calculation, the energy loss for each small step was attenuated depending upon the position in the calorimeter at which the muon lost energy.

Figure 1 shows the energy distribution after the calorimeter for 500 GeV muons. The average energy loss is 20.4 GeV while the most probable value is about 9 GeV. There is a long tail with high energy loss. Figure 2 shows the energy measured after attenuation smearing divided by the energy lost. The effect of calorimeter energy resolution is not

included. This error is smaller than that expected for energy loss due to a single brems in the calorimeter because most muons loose energy throughout the calorimeter. Note that there are no long tails on the distribution and the resolution on the energy lost is 4.4%.

Figure 3 shows the energy in the muon chambers corrected for energy loss with smearing due to attenuation. The RMS due to smearing calculated in this region is 3.6 GeV or 0.7%, much smaller than the muon momentum resolution. It is clear from the figure that, with some small acceptance loss, a substantially better resolution can be achieved by cutting out muons with large energy deposition in the calorimeter.

Figure 4 shows the energy in the muon chambers corrected for energy loss with smearing due to attenuation and electromagnetic energy resolution of $\frac{0.13}{\sqrt{(E)}} + 0.015$. This is what we measure for 1 mm fibers. It is shown below that coarser segmentation does not compromise the measurement. The RMS is now 3.8 GeV.

Figure 5 shows the energy measured in the muon chambers corrected for energy loss with no smearing from attenuation but with energy resolution of $\frac{0.30}{\sqrt{(E)}} + 0.030$ as might be expected for the average for a standard segmented calorimeter. The RMS here is 4.3 GeV, still quite acceptable. One can see a broadening of the central peak compared to the scifi calorimeter.

Since both of the calorimeters do well enough here, the argument becomes somewhat academic, however, it might be argued that due to the segmentation of the standard calorimeter, one can only add up the large energy depositions and use an average for the rest of the muon track. Looking at the muon energy shown in figure 1, it is clear that most events will require some correction in order to approach the resolutions obtained in figures 4 and 5. For example 30 GeV below the most probable value, there is still a substantial tail. This is unlike the situation for the fully measured muons in figures 4 and 5.

Figures 6-10 repeat the same graphs for 100 GeV muons. Here the fractional error on the muon momentum is somewhat bigger but still quite acceptable. Again the scintillating fiber calorimeter is slightly better, with a contribution to the momentum resolution of 0.9%.

Figures 11 and 12 repeat figures 8 and 9 assuming the attenuation measured in the

3HF fiber. As expected the attenuation effect improves by a factor of 4, becoming 0.17% at 100 GeV.

It should be noted that we can also obtain some information about the longitudinal position of the shower by using either timing, pulse shape, or front/deep fiber information. From the above calculation it does not appear to be needed for this correction.

In summary on this important point, even without the current improvements in the fiber the situation is quite good. With the already existing fiber it should improve by a factor of four. A study of our measurement capabilities for nonisolated muon still needs to be done. Here, some say, longitudinal segmentation may buy us something. This is far from clear since the first half of the calorimeter will be contaminated by energy from the jet containing the muon. The fine transverse segmentation (for the same number of channels) coupled with the short radiation length of scintillating fiber may be as useful as longitudinal segmentation.

A quick test of the possibility of using an Alumina absorber at the back of the calorimeter was made. Figure 13 shows the muon energy after at 1.6 meter thick (density 3.9) Alumina absorber. We see a 1.8% muon momentum resolution if we simply correct for the average energy loss of 2.5 GeV. This resolution contribution, by a 5λ absorbtion length alumina block, is substantially larger than the effect of the calorimeter. If we look only at the narrow part of the peak, even this would most likely be acceptable, resulting in a small acceptance loss. The amount of space used, however, seems to be the bigest drawback to this idea.

1

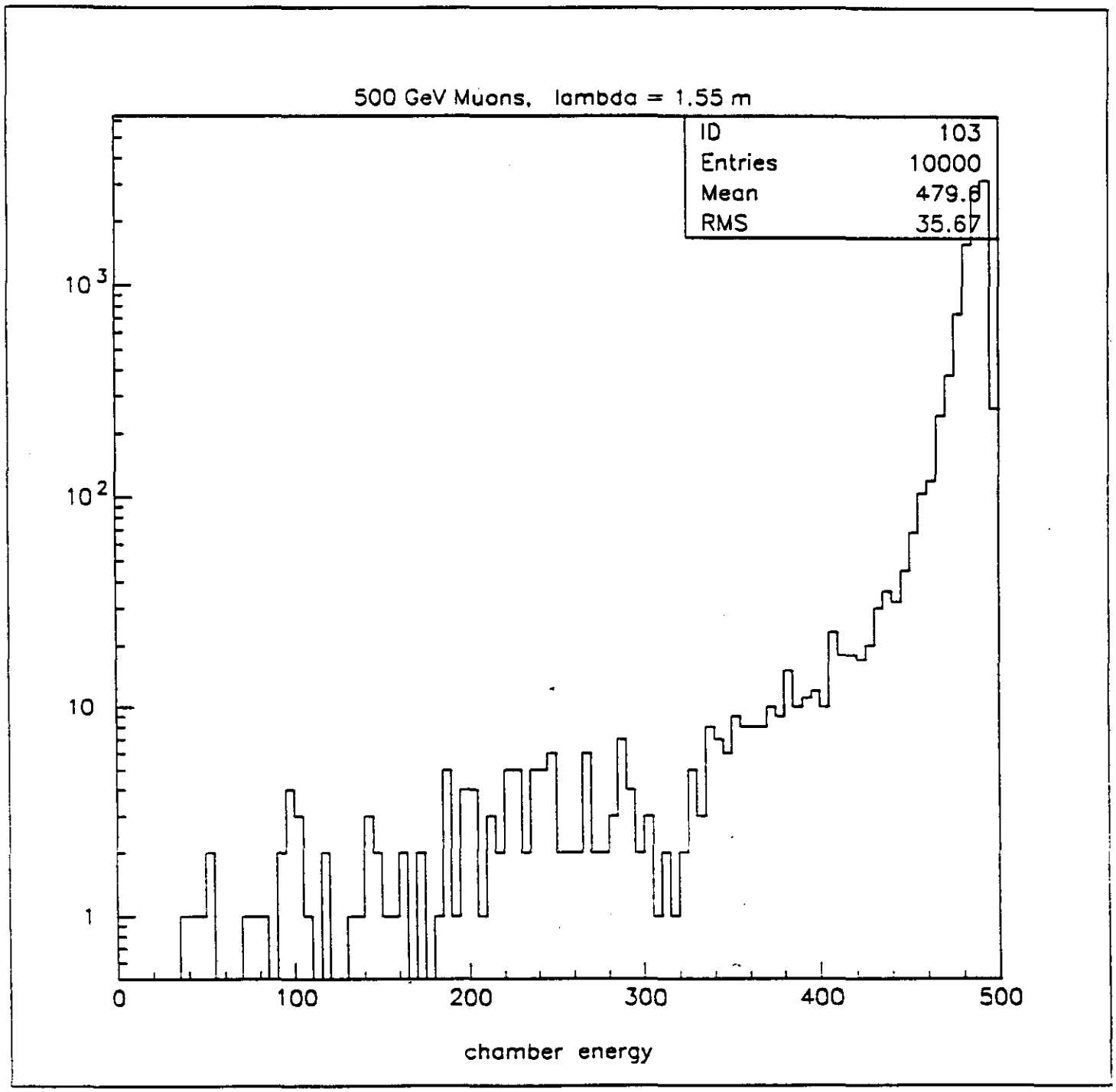
500 GeV Muons, lambda = 1.55 m
ID 103
Entries 10000
Mean 479.8
RMS 35.67
10 3
10 2
10
1
0
100
200
300
400
500
chamber energy

2

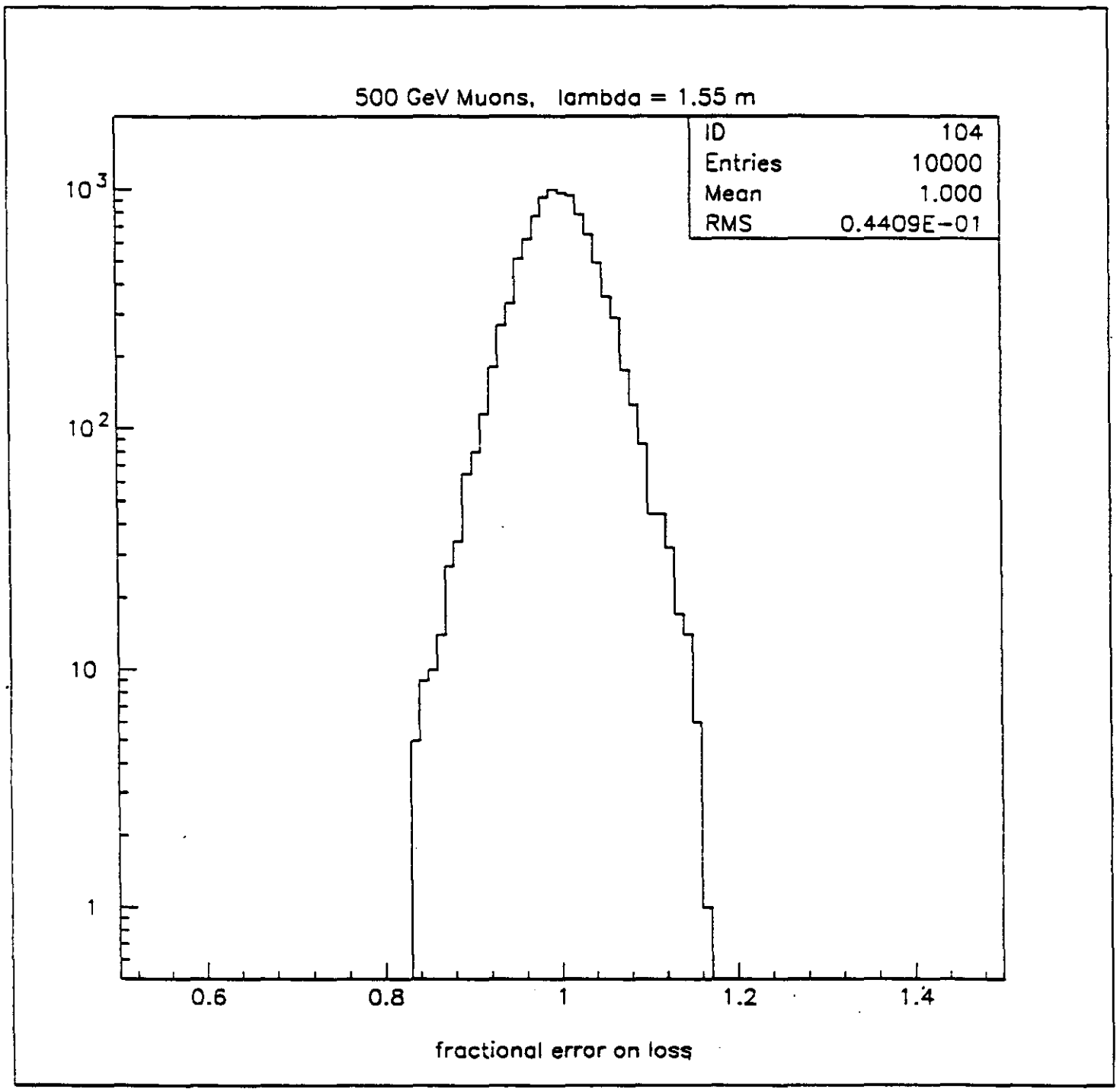
500 GeV Muons, lambda = 1.55 m
ID 104
Entries 10000
Mean 1.000
RMS 0.4409E-01
10^3
10^2
10
1
0.6
0.8
1
1.2
1.4
fractional error on loss

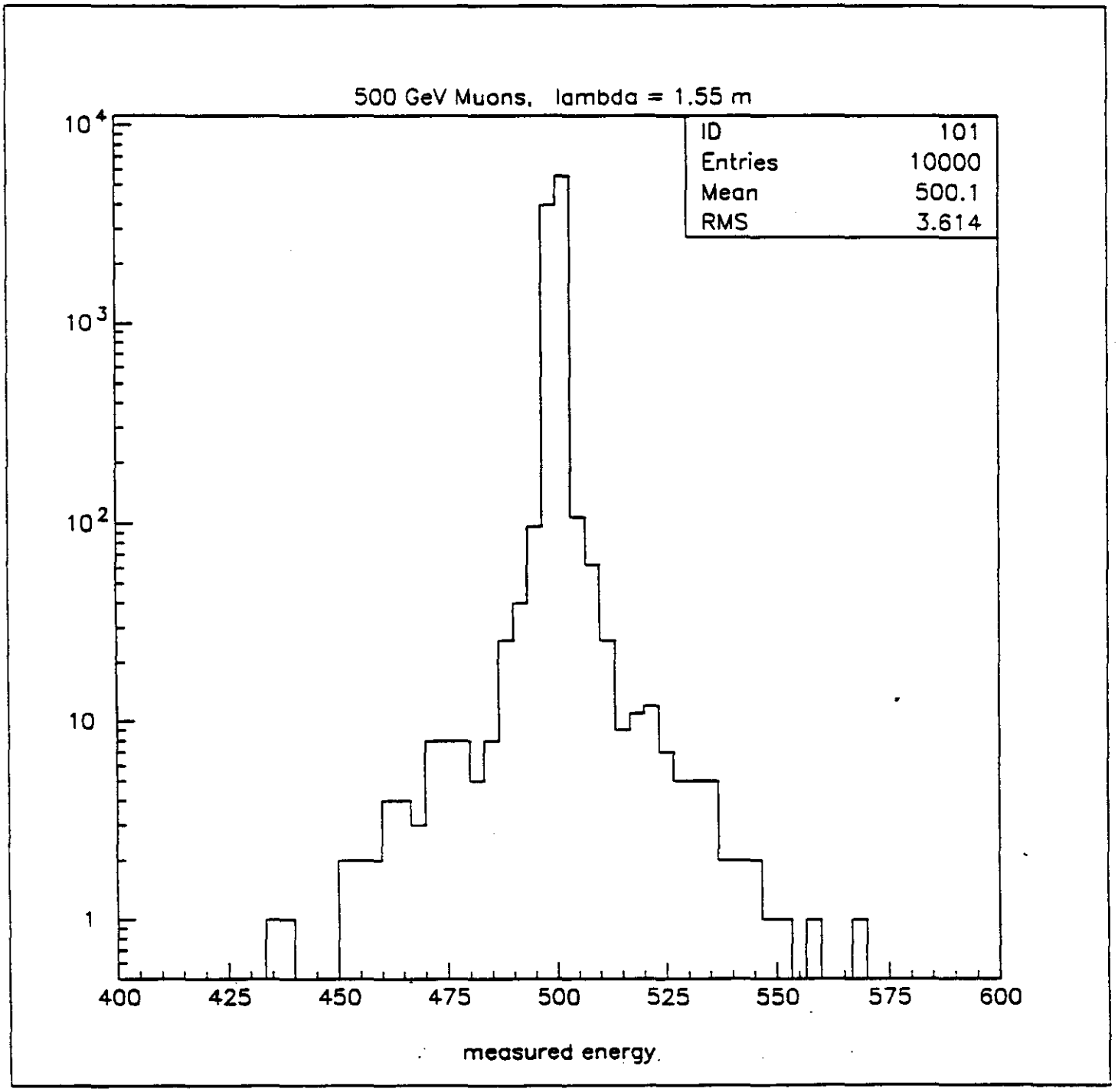
500 GeV Muons, lambda = 1.55 m
ID 101
Entries 10000
Mean 500.1
RMS 3.614
10^4
10^3
10^2
10
1
400
425
450
475
500
525
550
575
600
measured energy

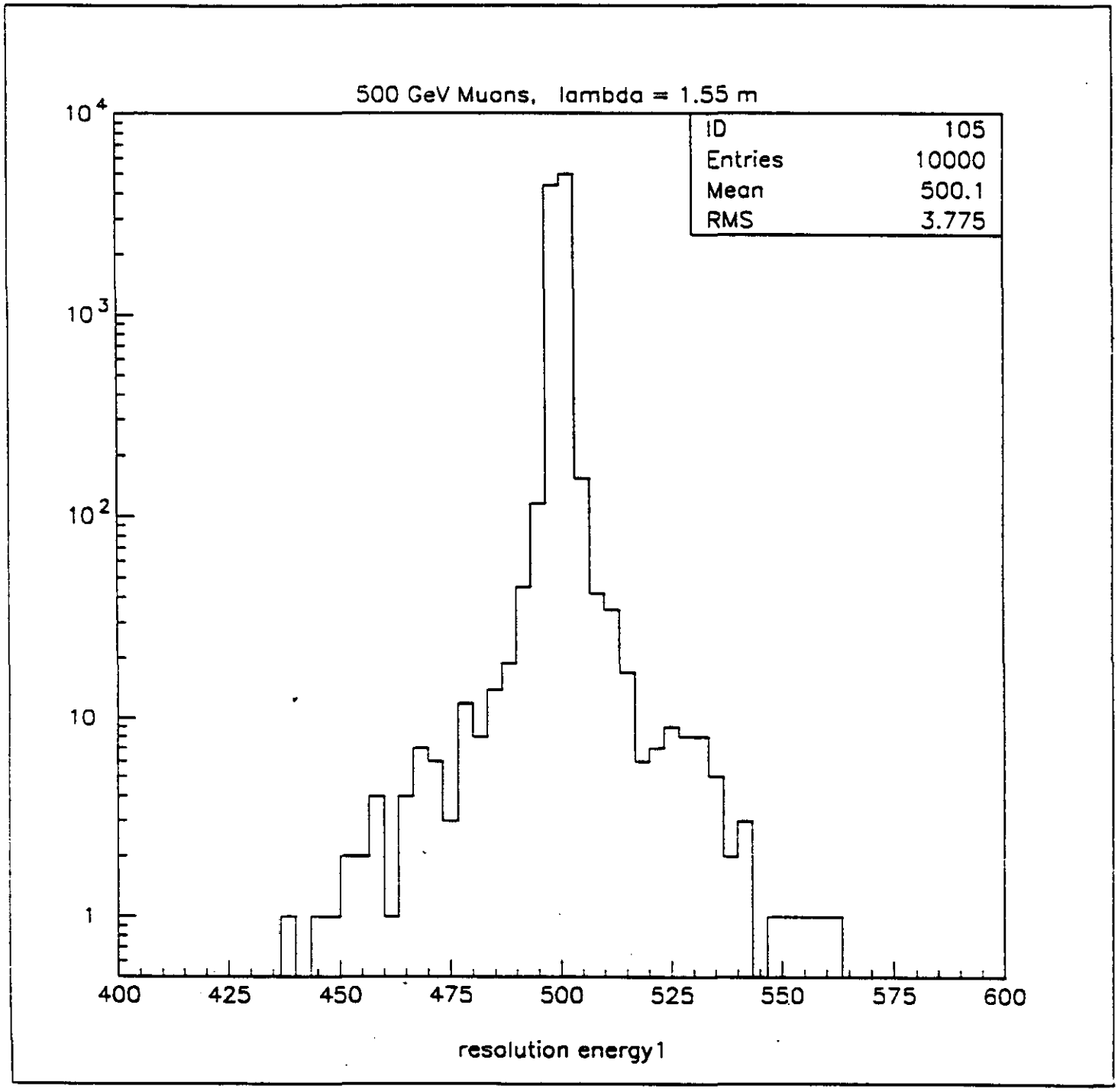
500 GeV Muons, lambda = 1.55 m
ID 105
Entries 10000
Mean 500.1
RMS 3.775
10^4
10^3
10^2
10
1
400
425
450
475
500
525
550
575
600
resolution energy1

5

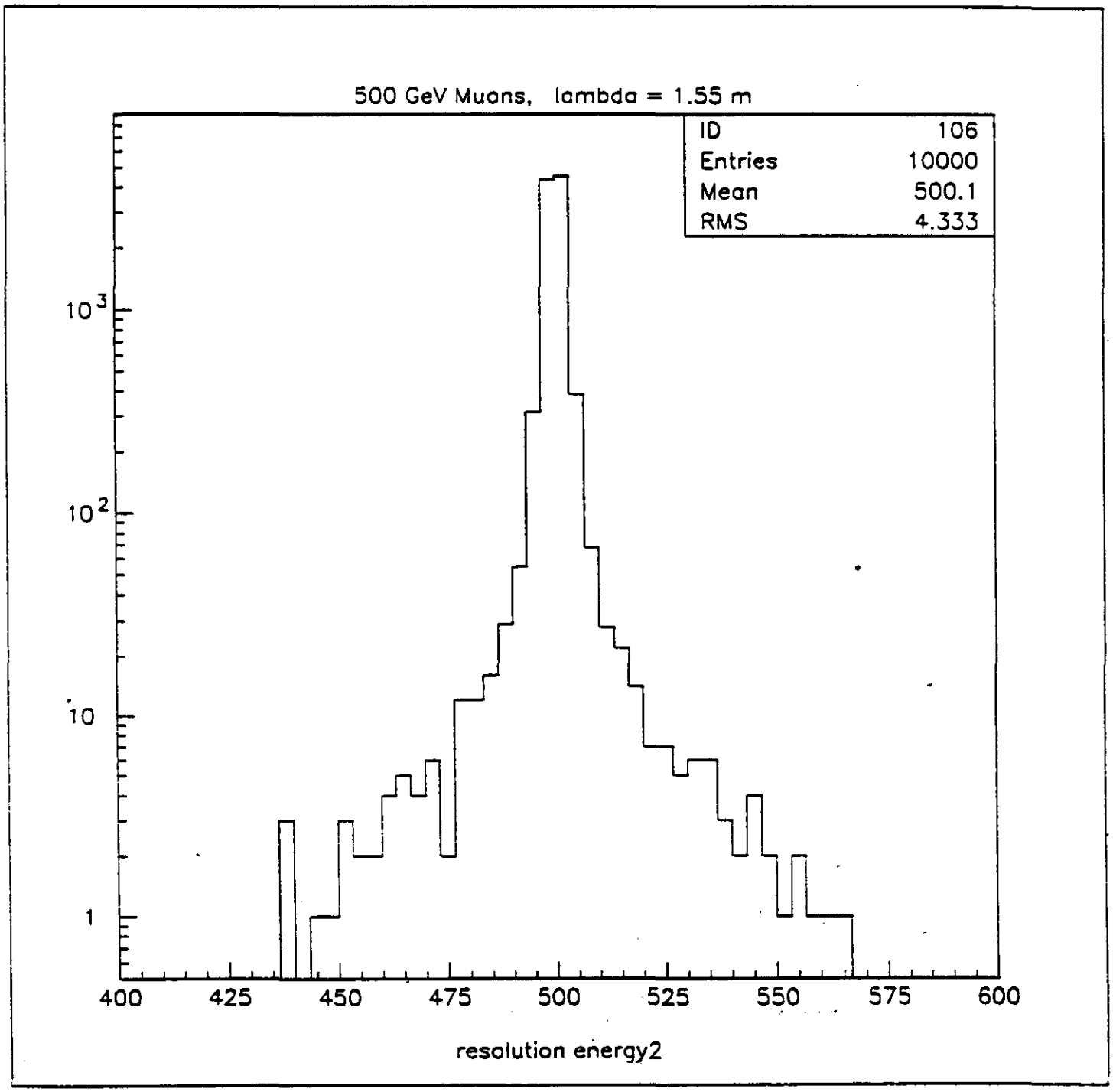
500 GeV Muons, lambda = 1.55 m
ID 106
Entries 10000
Mean 500.1
RMS 4.333
10^3
10^2
10
1
400
425
450
475
500
525
550
575
600
resolution energy2

6

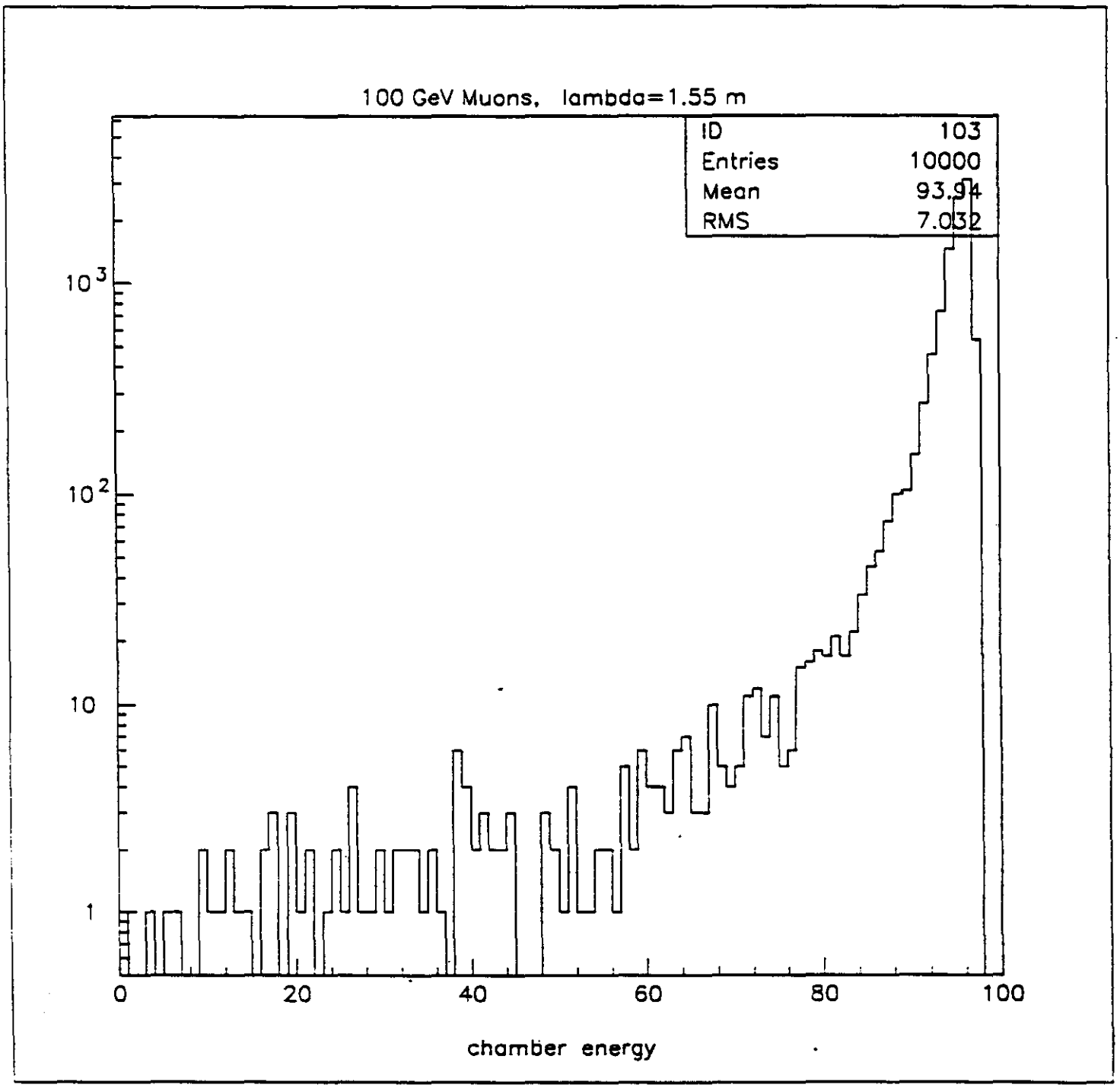
100 GeV Muons, lambda=1.55 m
ID 103
Entries 10000
Mean 93.94
RMS 7.032
10^3
10^2
10
1
0
20
40
60
80
100
chamber energy

7

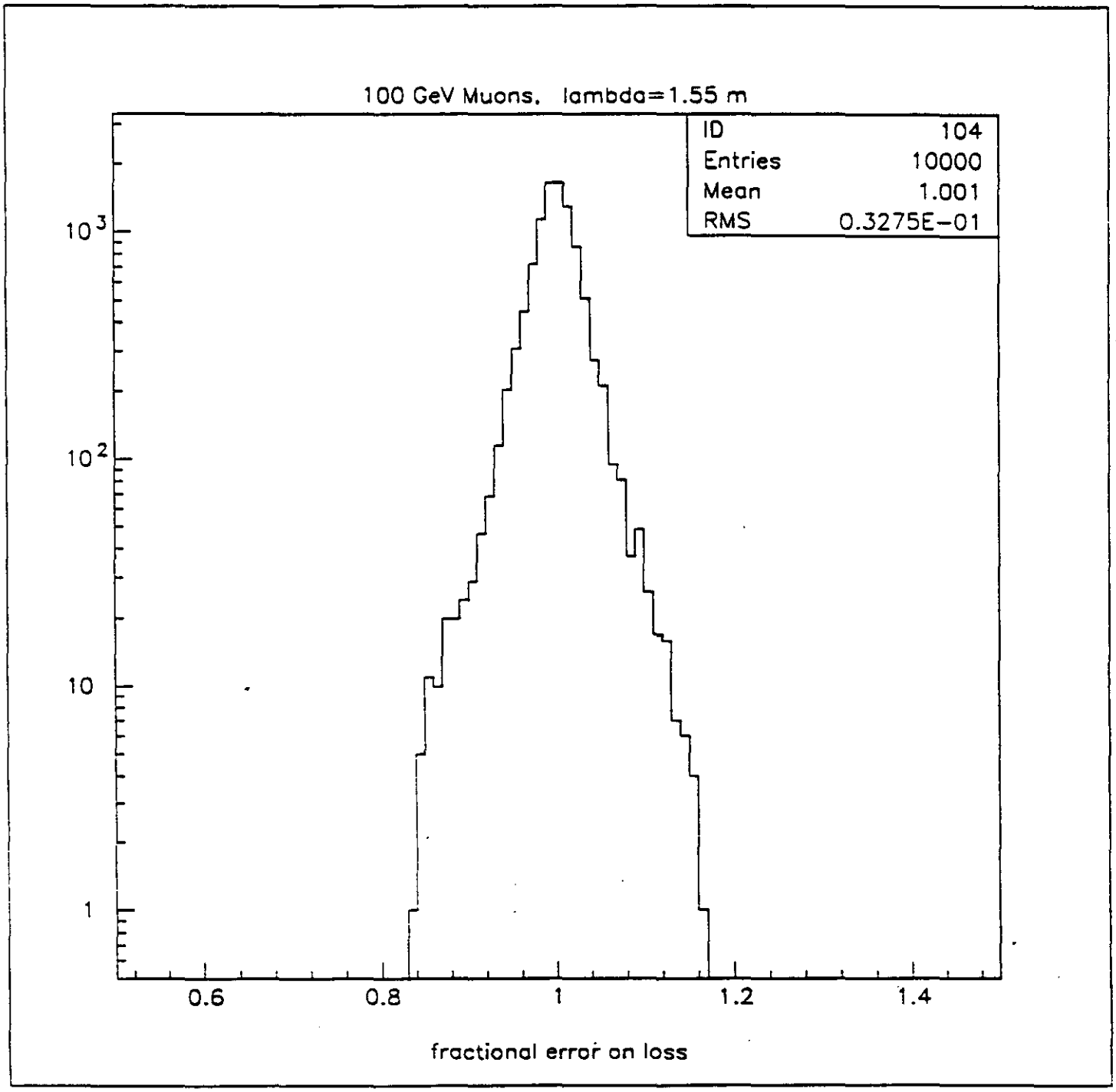
100 GeV Muons, lambda=1.55 m
ID 104
Entries 10000
Mean 1.001
RMS 0.3275E-01
10^3
10^2
10
1
0.6
0.8
1
1.2
1.4
fractional error on loss

8

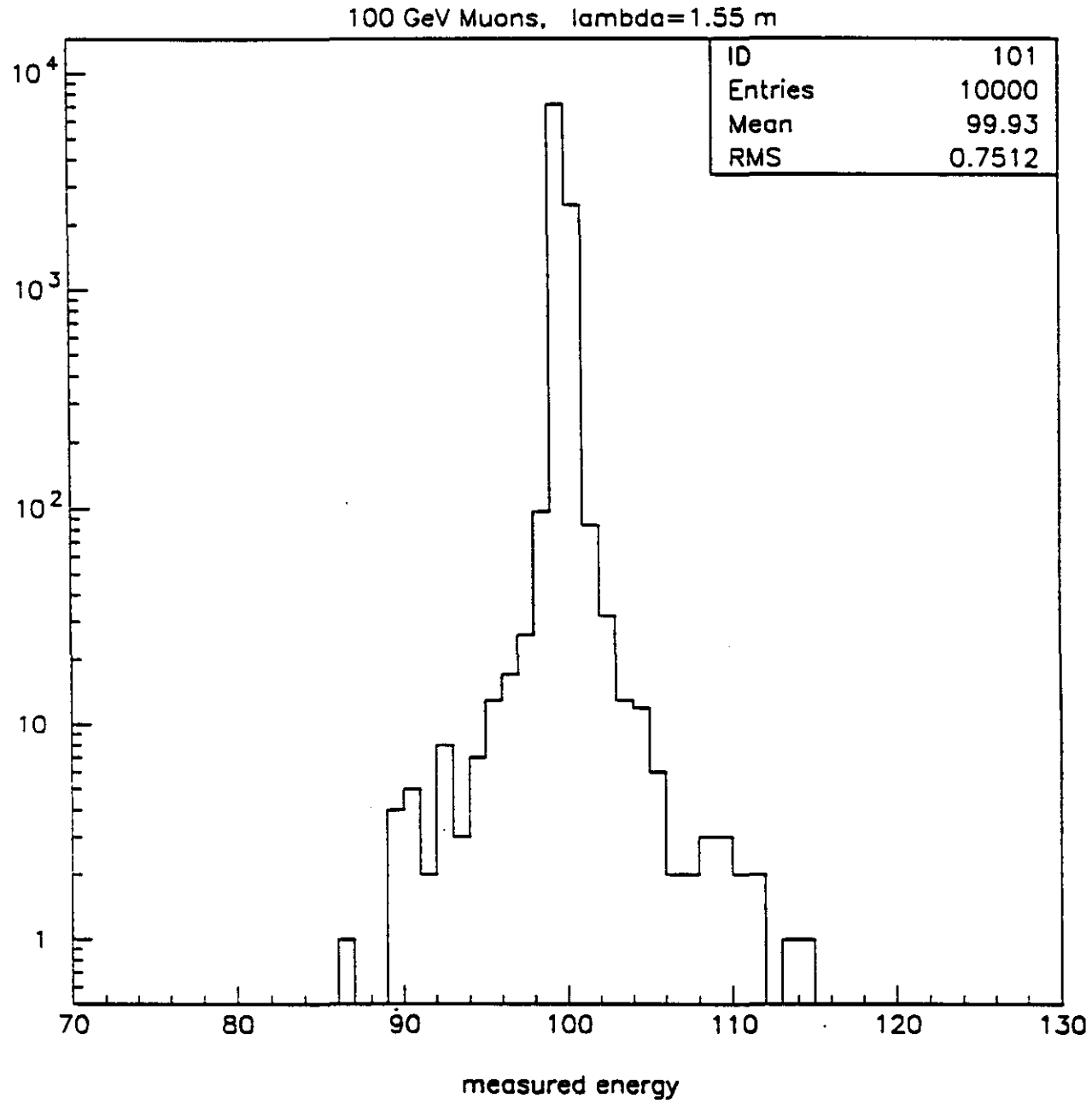
100 GeV Muons, lambda=1.55 m
ID 101
Entries 10000
Mean 99.93
RMS 0.7512
10^4
10^3
10^2
10
1
70
80
90
100
110
120
130
measured energy

9

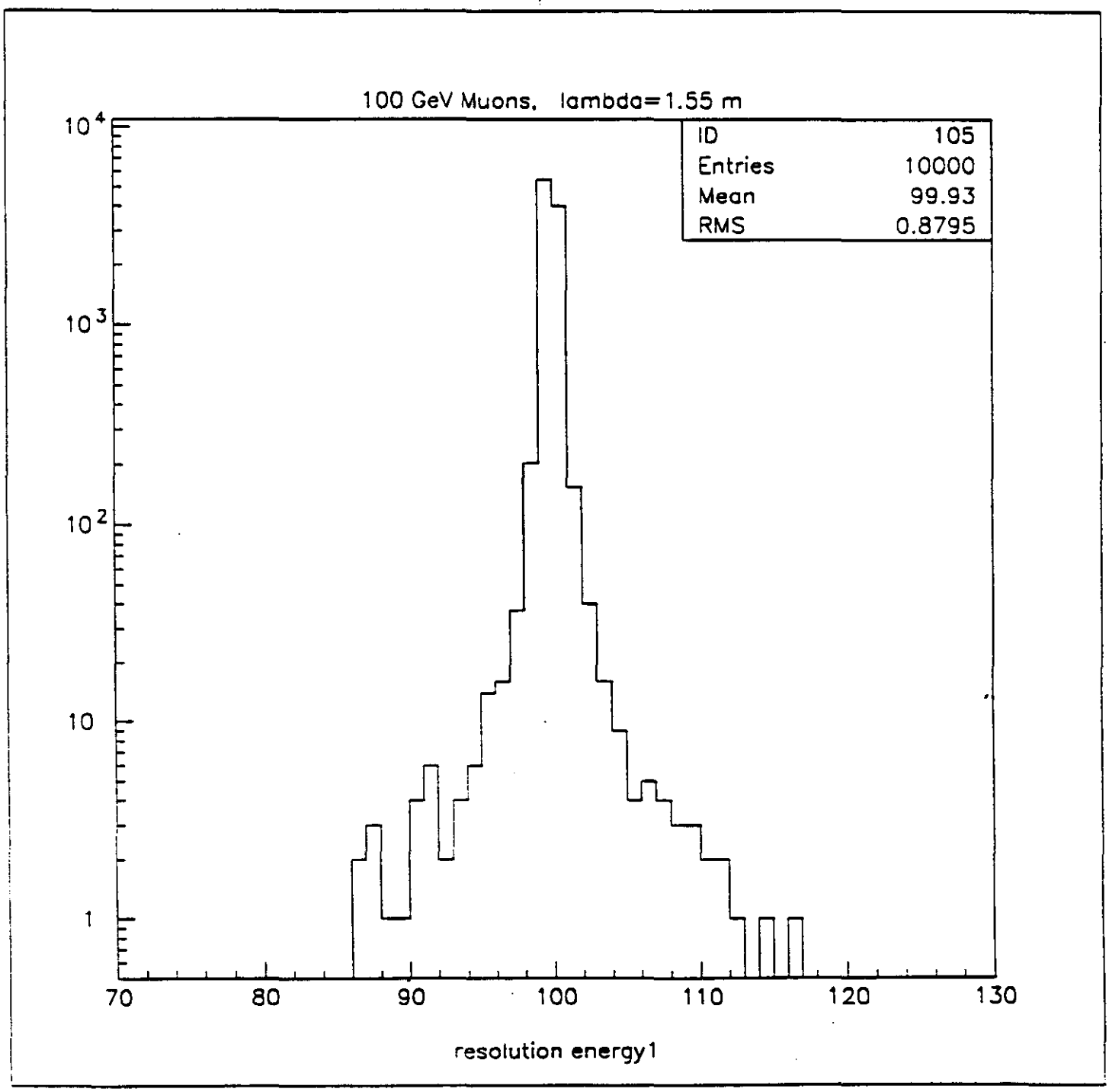
100 GeV Muons, lambda=1.55 m
ID 105
Entries 10000
Mean 99.93
RMS 0.8795
10^4
10^3
10^2
10
1
70
80
90
100
110
120
130
resolution energy1

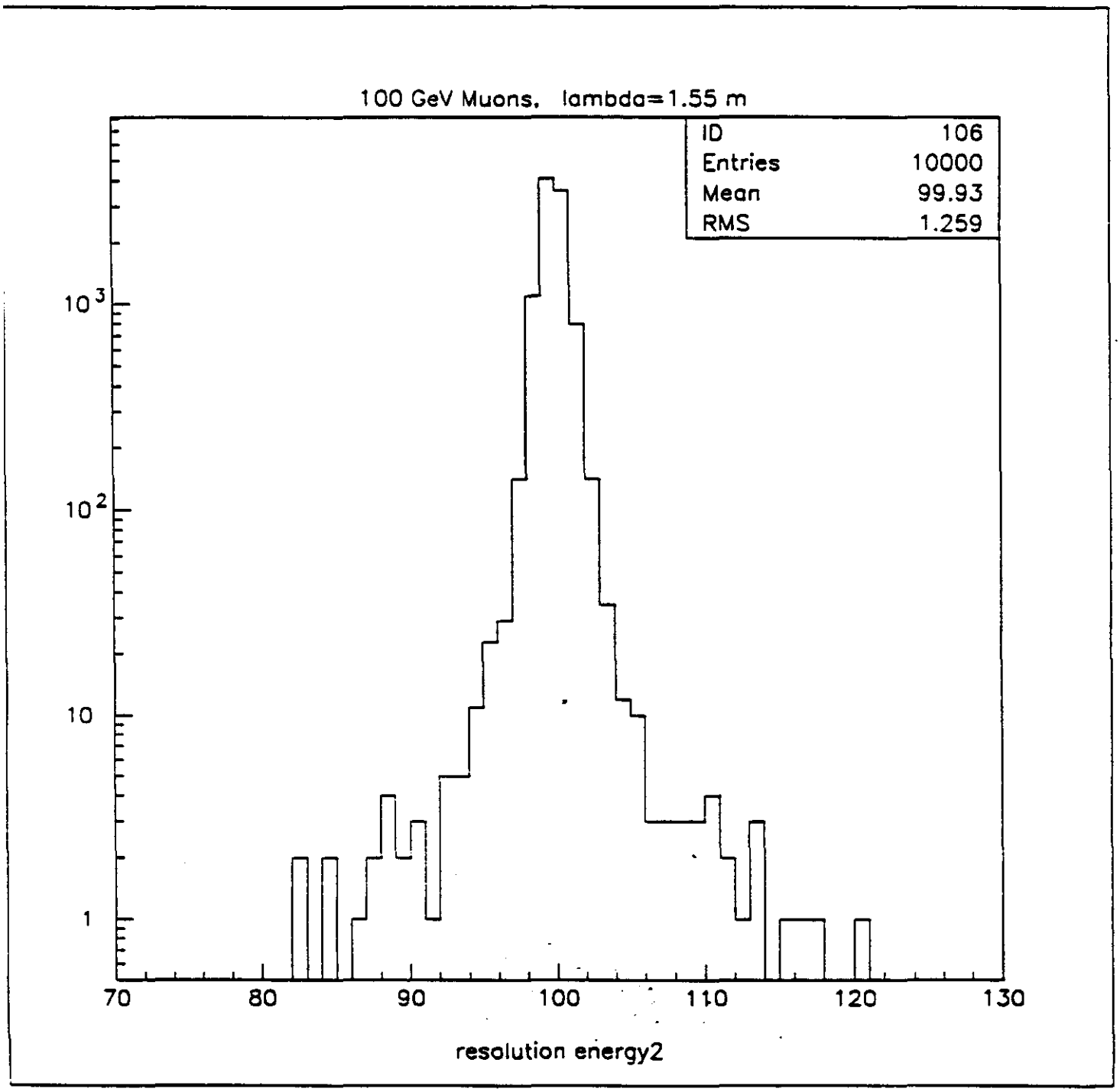
100 GeV Muons, lambda=1.55 m
ID 106
Entries 10000
Mean 99.93
RMS 1.259
10^3
10^2
10
1
70
80
90
100
110
120
130
resolution energy2

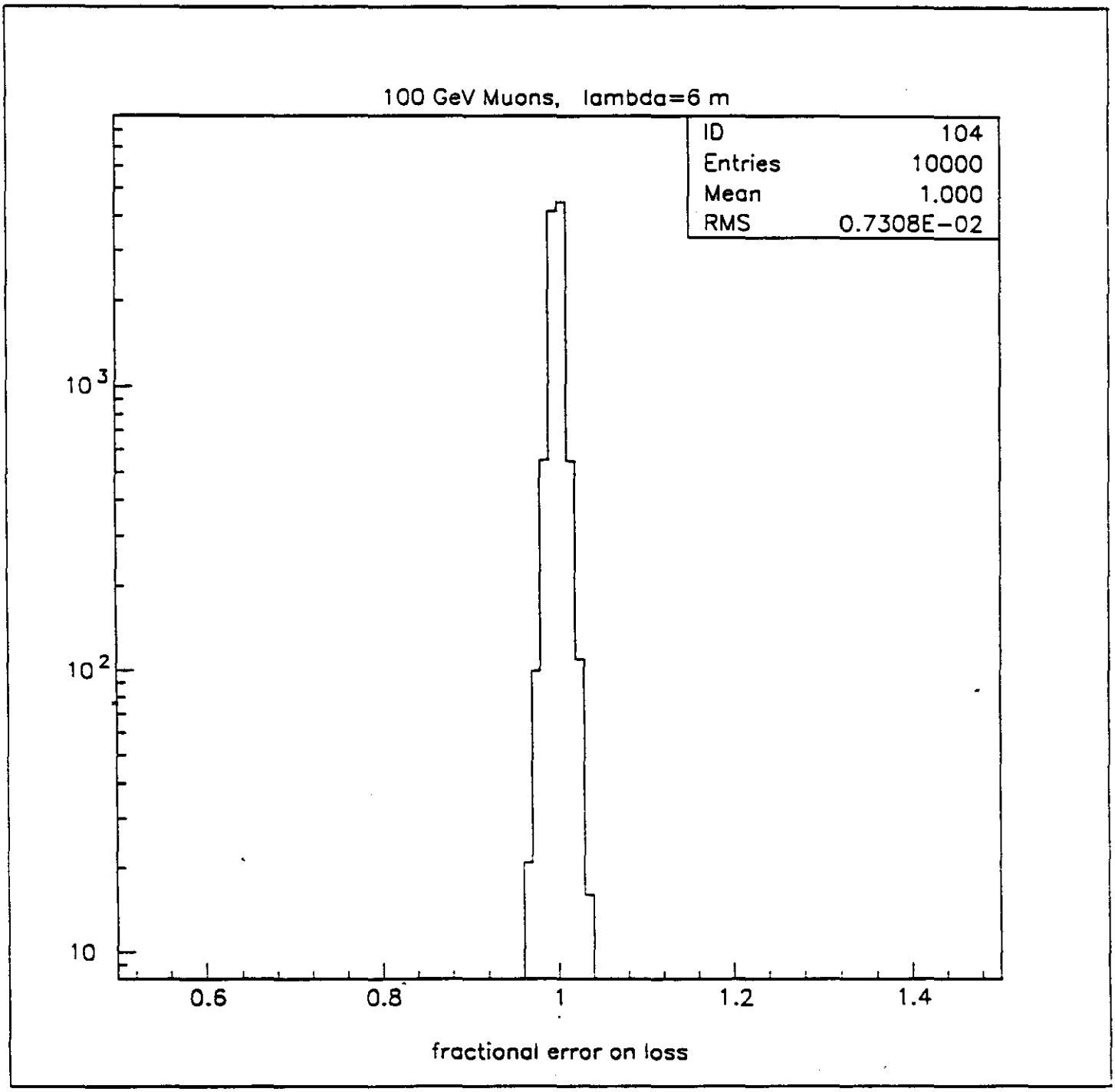
100 GeV Muons, lambda=6 m
ID 104
Entries 10000
Mean 1.000
RMS 0.7308E-02
10 3
10 2
10
0.6
0.8
1
1.2
1.4
fractional error on loss

12

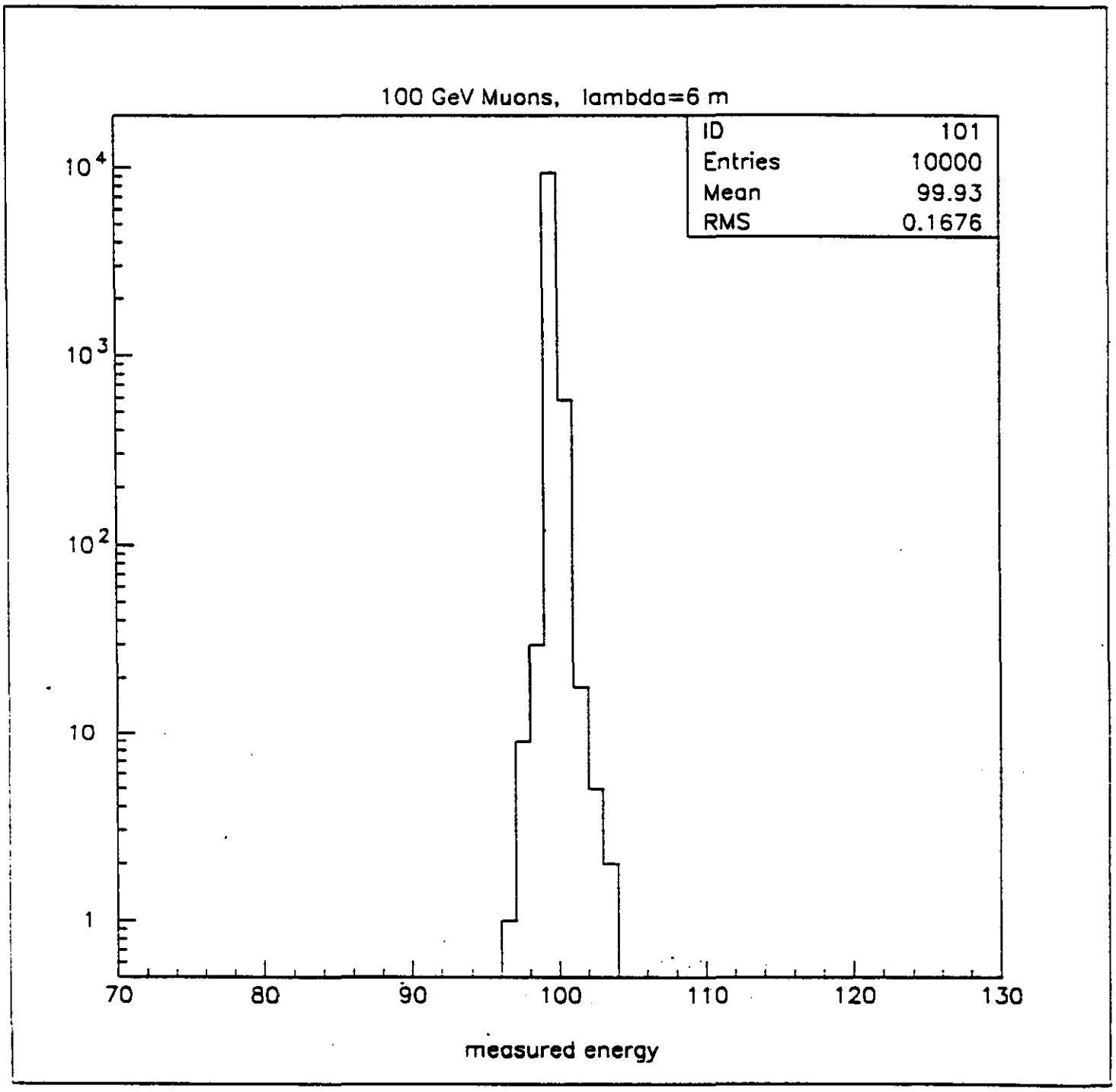
100 GeV Muons, lambda=6 m
ID 101
Entries 10000
Mean 99.93
RMS 0.1676
10^4
10^3
10^2
10
1
70
80
90
100
110
120
130
measured energy

13

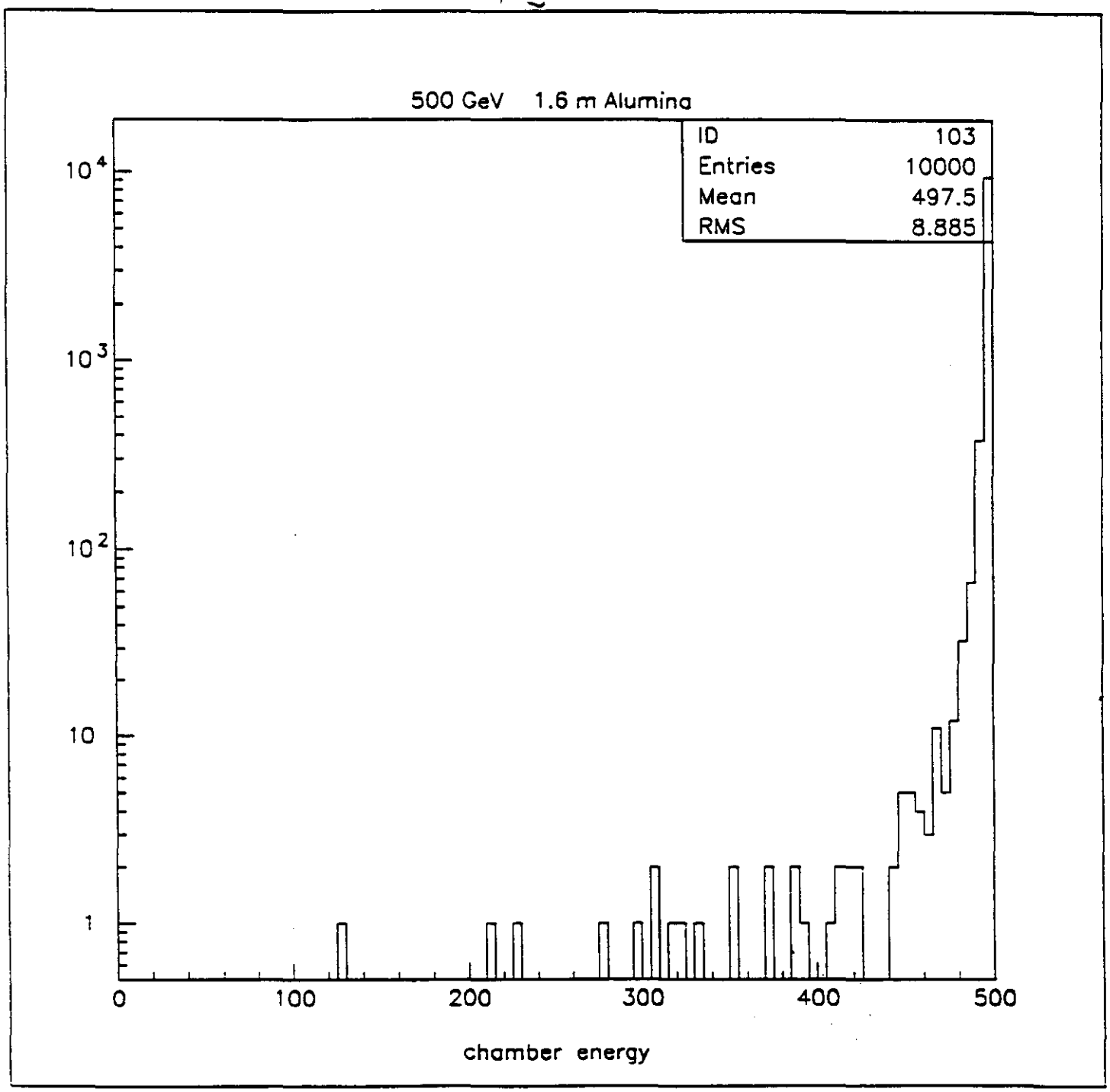
500 GeV 1.6 m Alumina
ID 103
Entries 10000
Mean 497.5
RMS 8.885
10^4
10^3
10^2
10
1
0
100
200
300
400
500
chamber energy

BOLTON

Muon trigger studies/simulation @ NEVIS

① Semi-ANALYTIC calculations of resolution required for triggering. (M. Shaevitz)

② Begin Geant based trigger studies.
(M. Seemens, S. Cannon, T. Bolton).

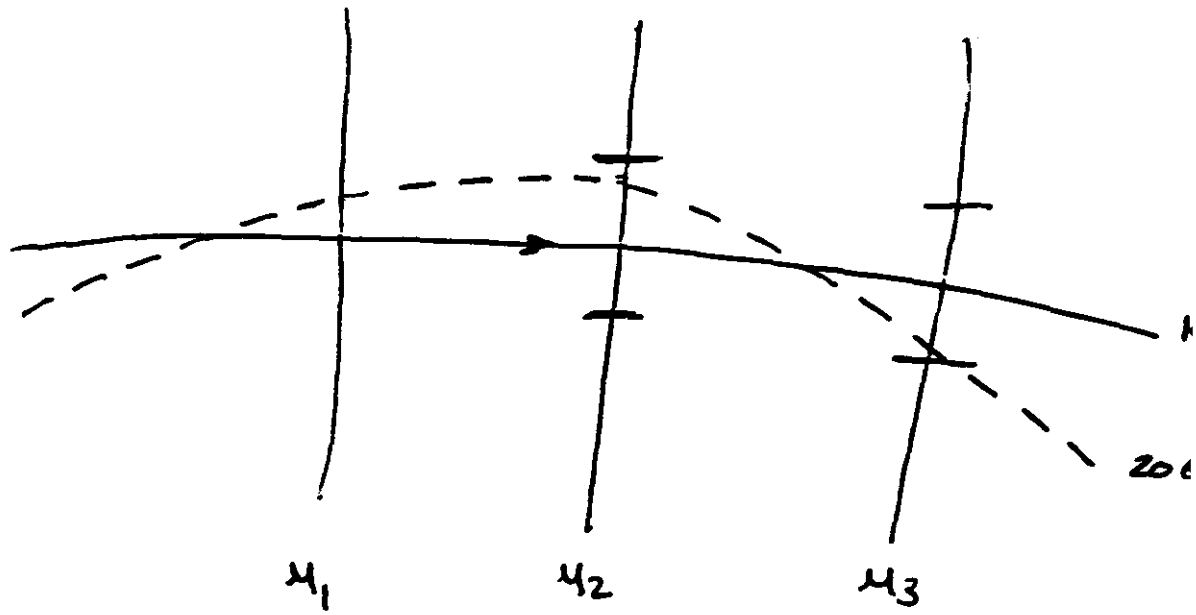

<u>Cell</u> <u>size</u> <u>studies</u> (M. Shaevitz)

- For each hit in 2nd μ layer, search a window in layer 3.

- Layer 3 window is defined by curvature of lowest desired p_T track ⊕ multiple scattering.

- Cell size determines how sharply trigger cuts out lower p_T tracks.

- At first level, layer 1 may not be useful due to punchthrough (?)

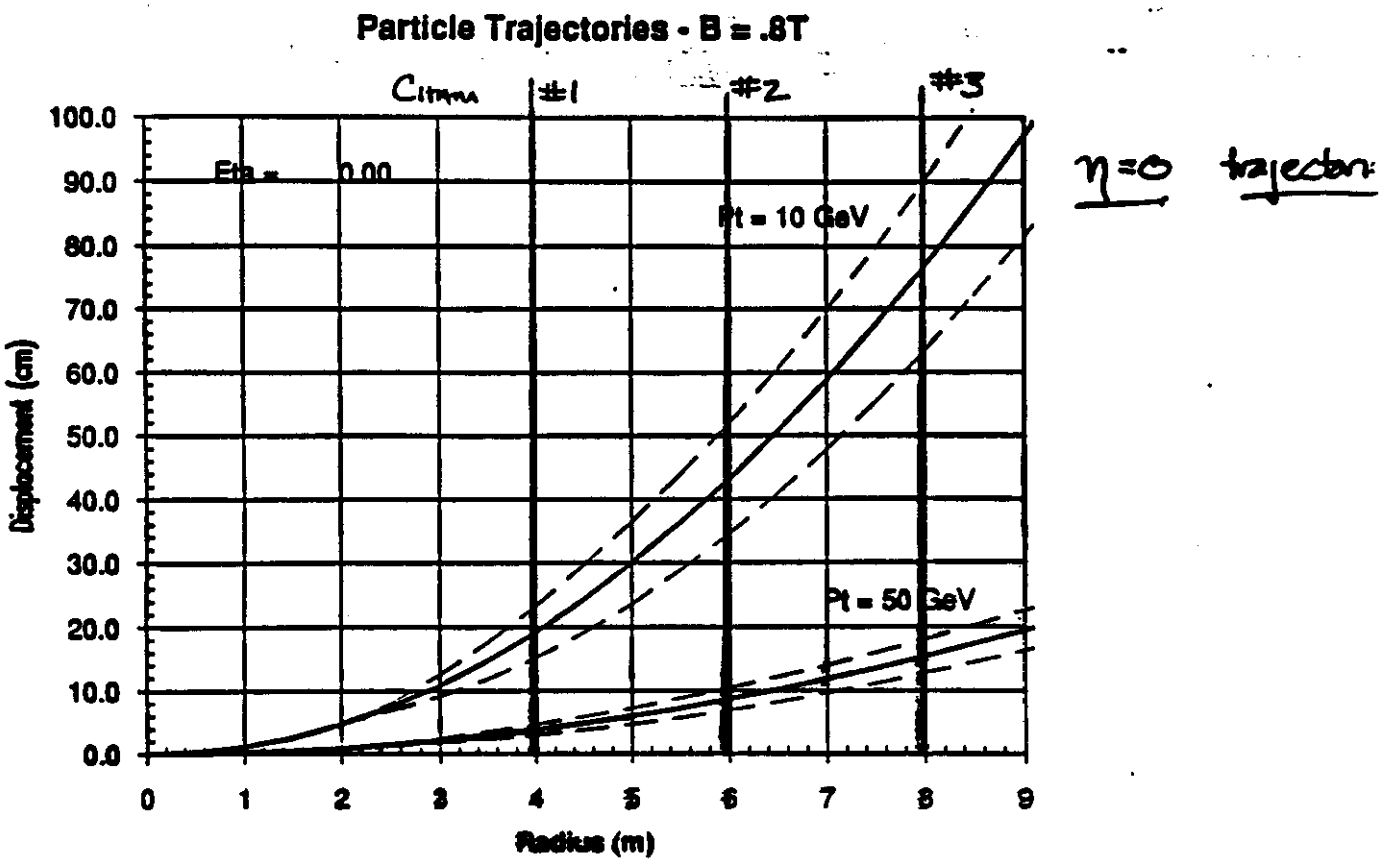
Particle Trajectories - B = .8T
Citrum
#1
#2
#3
Eta = 0.00
Pt = 10 GeV
Pt = 50 GeV
Displacement (cm)
Radius (m)
η=0 trajector

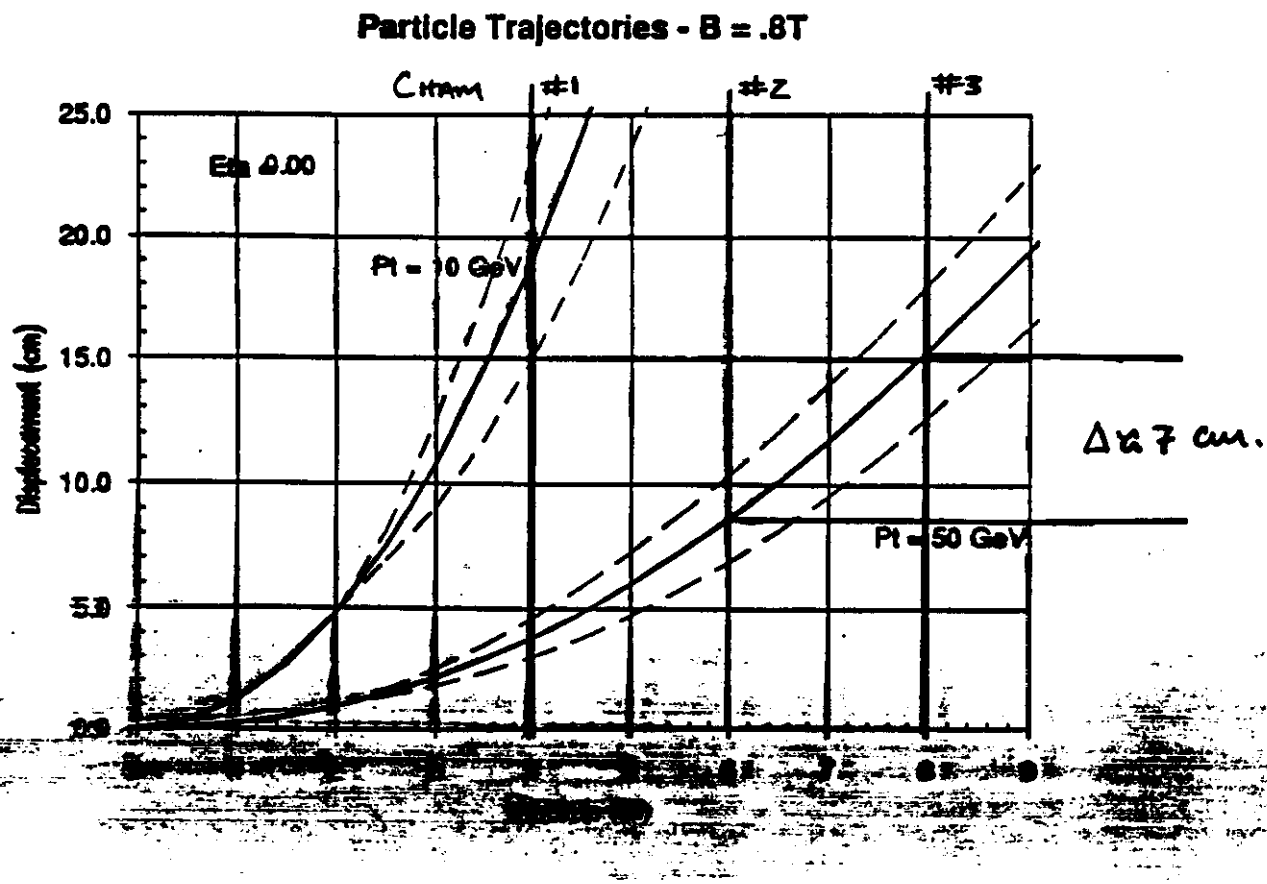
Particle Trajectories - B = .8T
Citrum
#1
#2
#3
Eta 0.00
Pt = 10 GeV
Pt = 50 GeV
Displacement (cm)
Δx ≈ 7 cm.

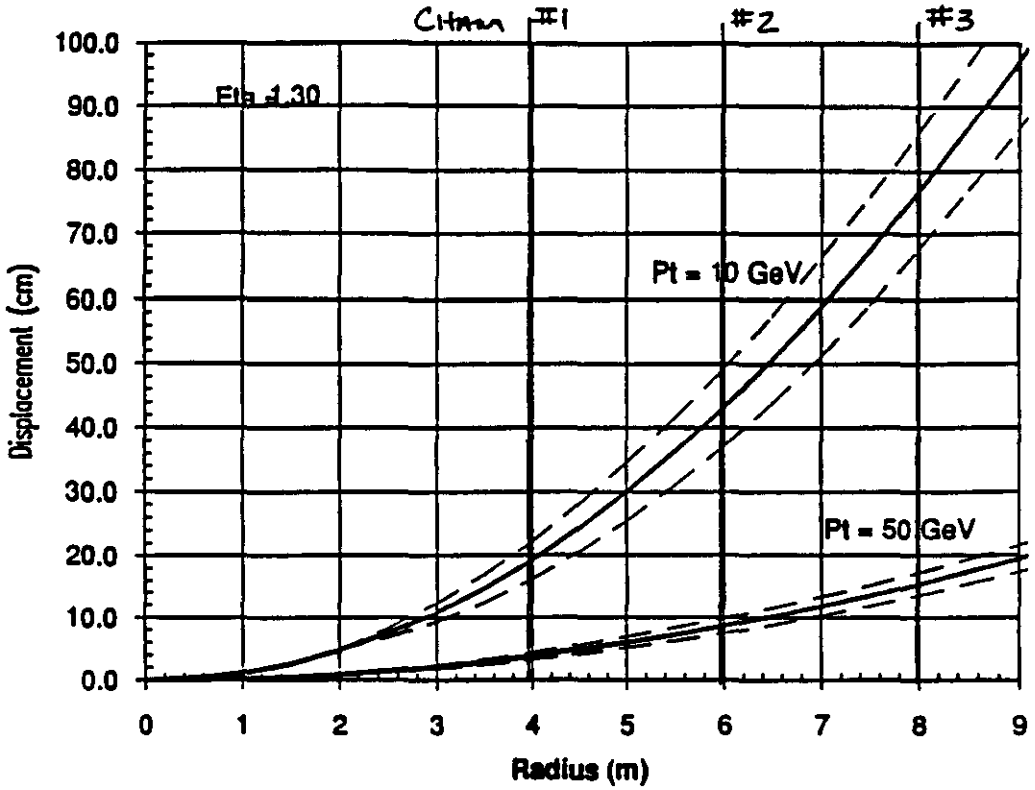

$\eta = 1.3$

→ 2-3 cm $\Delta\phi$ granularity

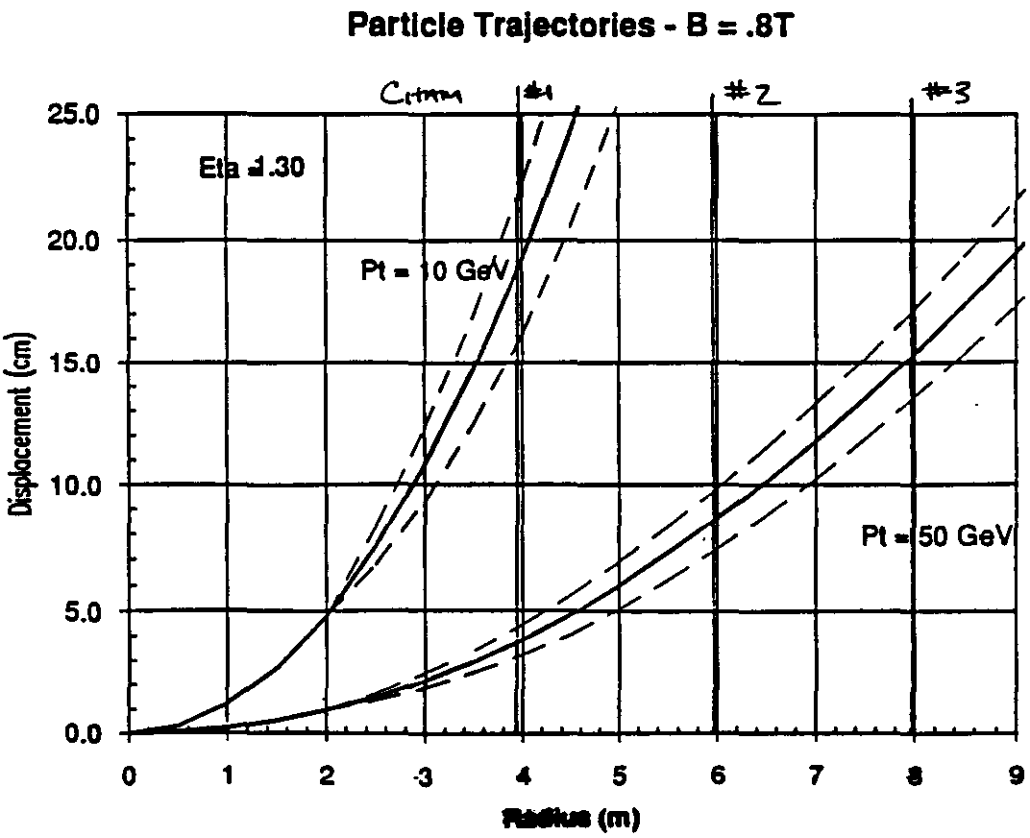

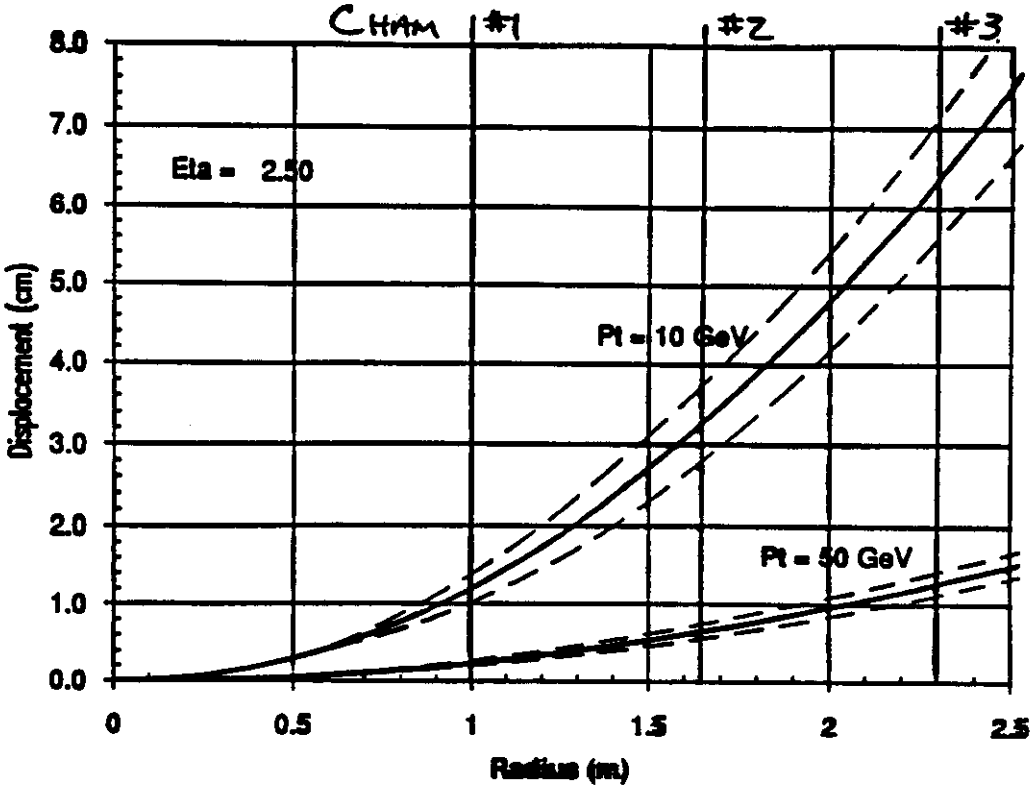
CHAM
#1
#2
#3
Eta = 2.50
Pt = 10 GeV
Pt = 50 GeV
Displacement (cm)
Radius (m)
8.0
7.0
6.0
5.0
4.0
3.0
2.0
1.0
0.0
0
0.5
1
1.5
2
2.5

$\eta = 2.5$

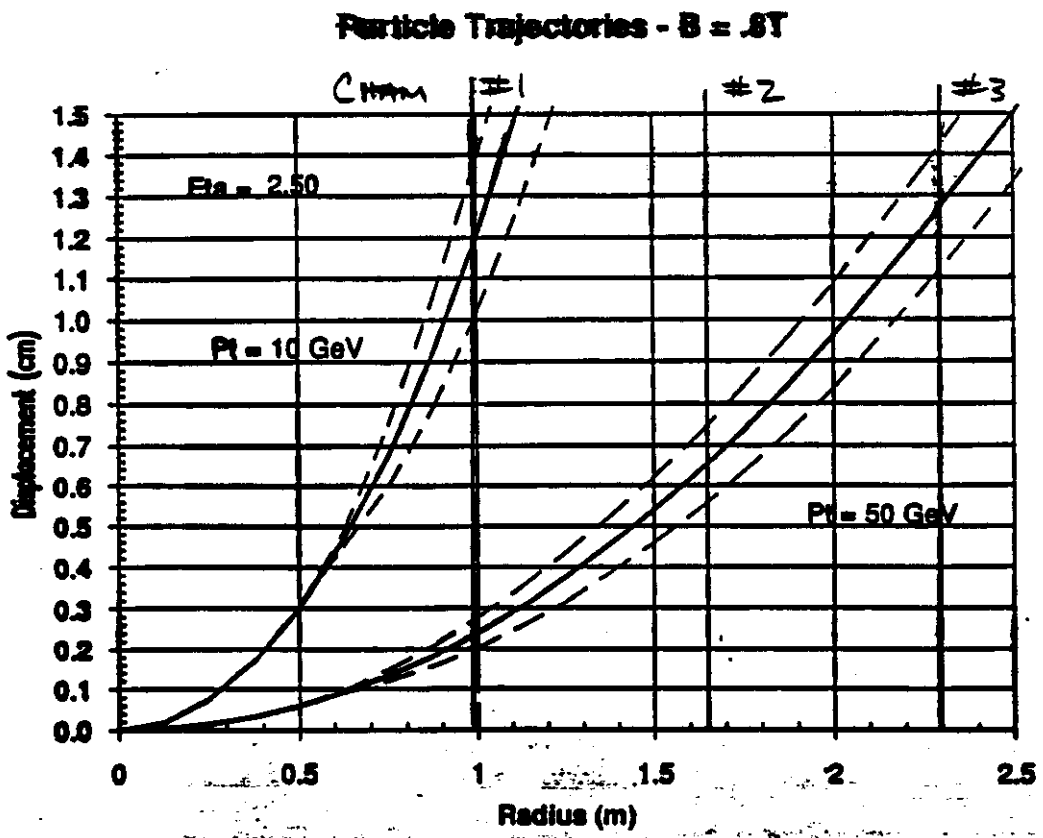
Particle Trajectories - B = .5T
CHAM
#1
#2
#3
Eta = 2.50
Pt = 10 GeV
Pt = 50 GeV
Displacement (cm)
Radius (m)
1.5
1.4
1.3
1.2
1.1
1.0
0.9
0.8
0.7
0.6
0.5
0.4
0.3
0.2
0.1
0.0
0
0.5
1
1.5
2
2.5

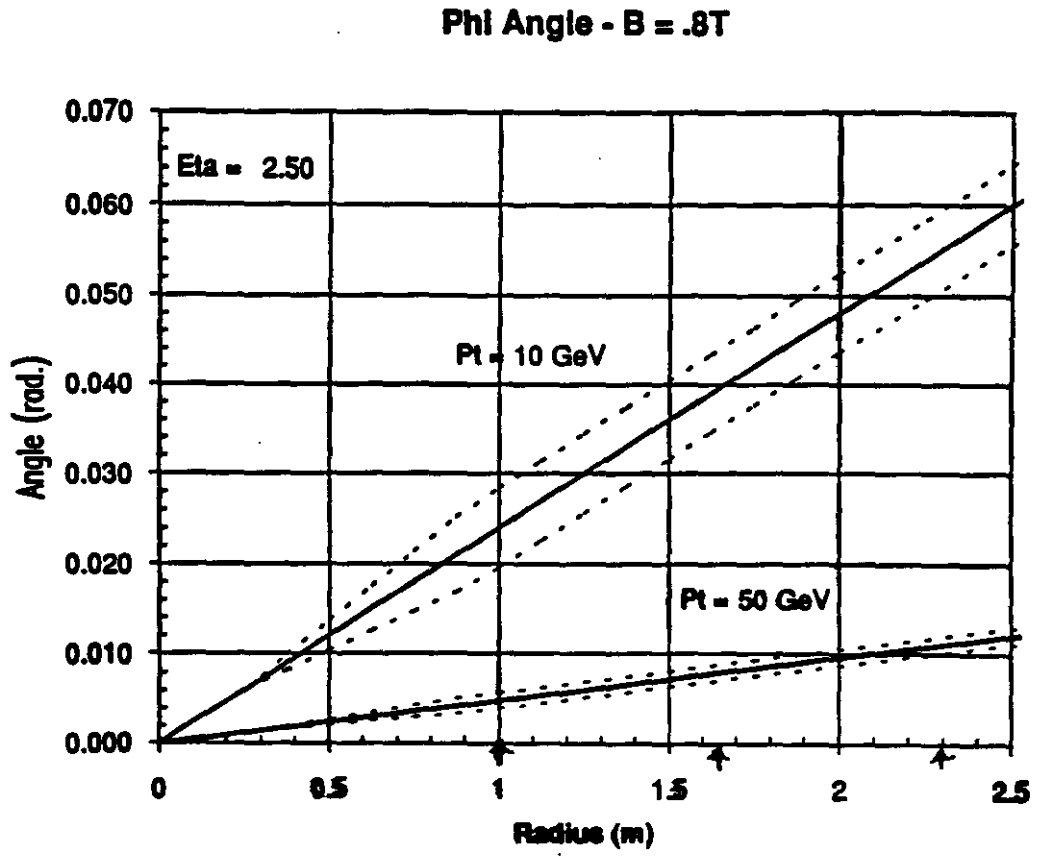

$\eta = 2.50$

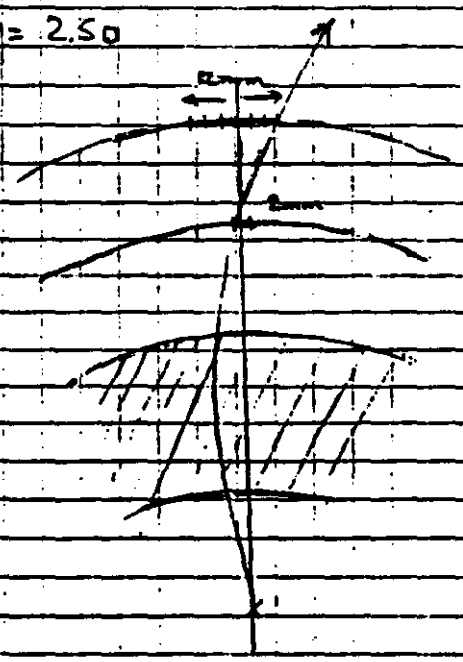

$P_\perp = 50\ GeV \Rightarrow \Delta\phi = .010$

$R_{Chamb\,3} - R_{Chamb\,2} = .65m$

$\Delta d = \Delta\phi\ .65 = 6.5mm$

2mm P_{ADS} (Phi P_{ADS})

Chamb 2 2mm P_{ADS} $\Rightarrow$ Chamb 3 12

$\theta_{max} = \frac{6+1}{650} = .011 \Rightarrow$ $P_\perp$

3mm P_{ADS}

$\theta_{max} = \frac{6+1.5}{6.50} = .012 \Rightarrow$ $P_\perp$

6mm P_{ADS}

$\theta_{max} = \frac{6+3}{650} = .014 \Rightarrow$ $P_\perp$

Conclusions:

① Triggering puts no demands on resolution in central region.

② At $\eta = 2.5$, 2-6 mm pads (or equivalent) are needed to raise trigger threshold.

Simulation Studies (M. Seemans, S. Carron, T. Bolton

① Philosophy : use as simple Geant as possible for task.

② Status : simple geometry defined using simple geometrical shapes and "average" materials.

③ Studies: Resolution
Punchthrough to layer 1
$\eta \approx 2.5$

[redacted] CFT
[redacted] HRD
[redacted] ABS
[redacted] M

PHOENIX*DETECTOR

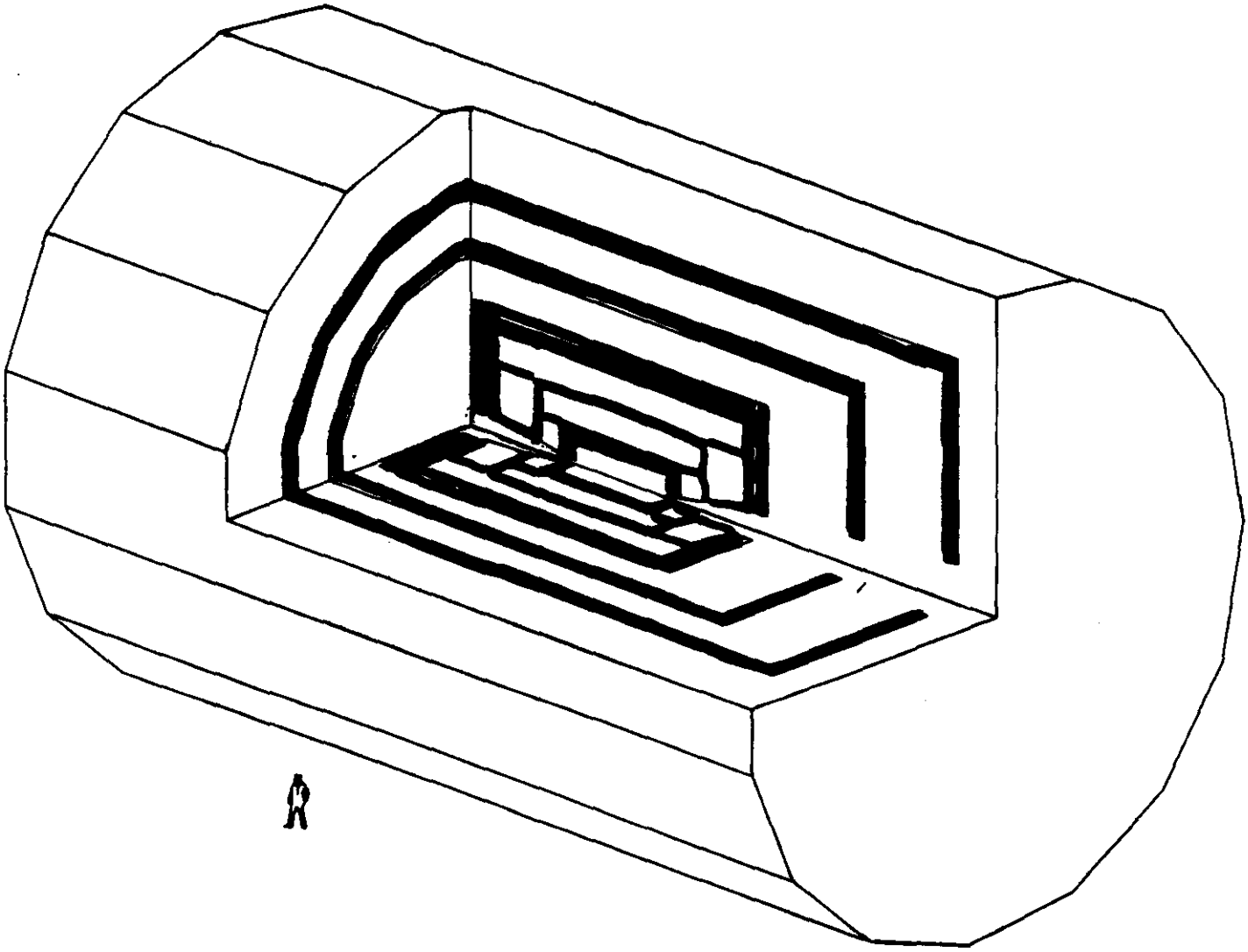

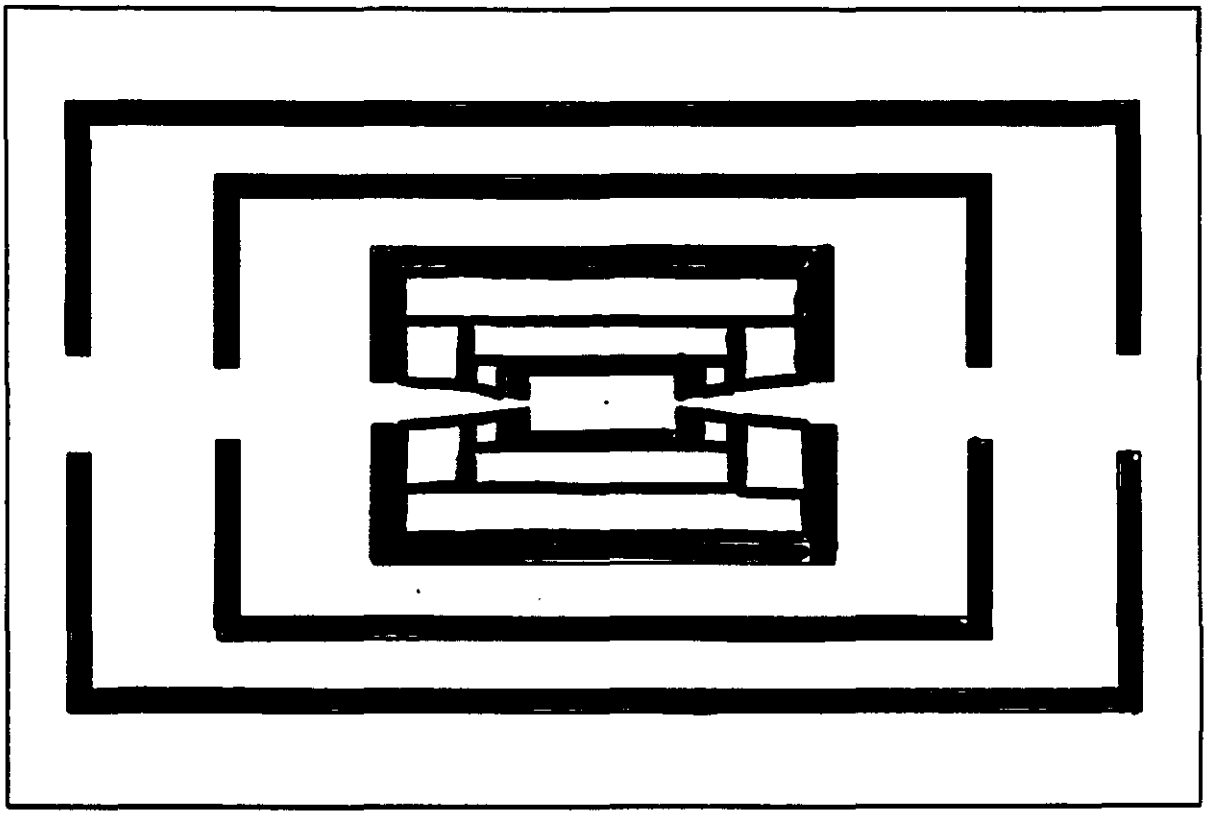

N. di Giacomo

Ray Tracing Procedure

- Build 3d Solid Model of appropriate fidelity
  - include model attributes
    material type, detector subsystem, active/passive ...
  - generate hardcopy or viewgraphs

- Determine Magnetic Field of appropriate quality
  - input analytic or numeric model of $\vec{B}$
  - from Poisson
  - from 3d finite element model (EMAS)

- Trace Rays thru 3d Solid Model
  - determine objects/materials that the rays intersect
  - determine total/differential path length of the rays
  - determine total/differential radiation and interaction lengths of the ray
  - determine calorimeter energy loss and resolution
  - upgrades: propagate track errors to determine muon resolution (Rosenson's program)

- Combine output
  - calculate bend angle ~ $0.3B_{\perp}L/p$
  - calculate multiple scattering ~ [...]/p
  - generate plots

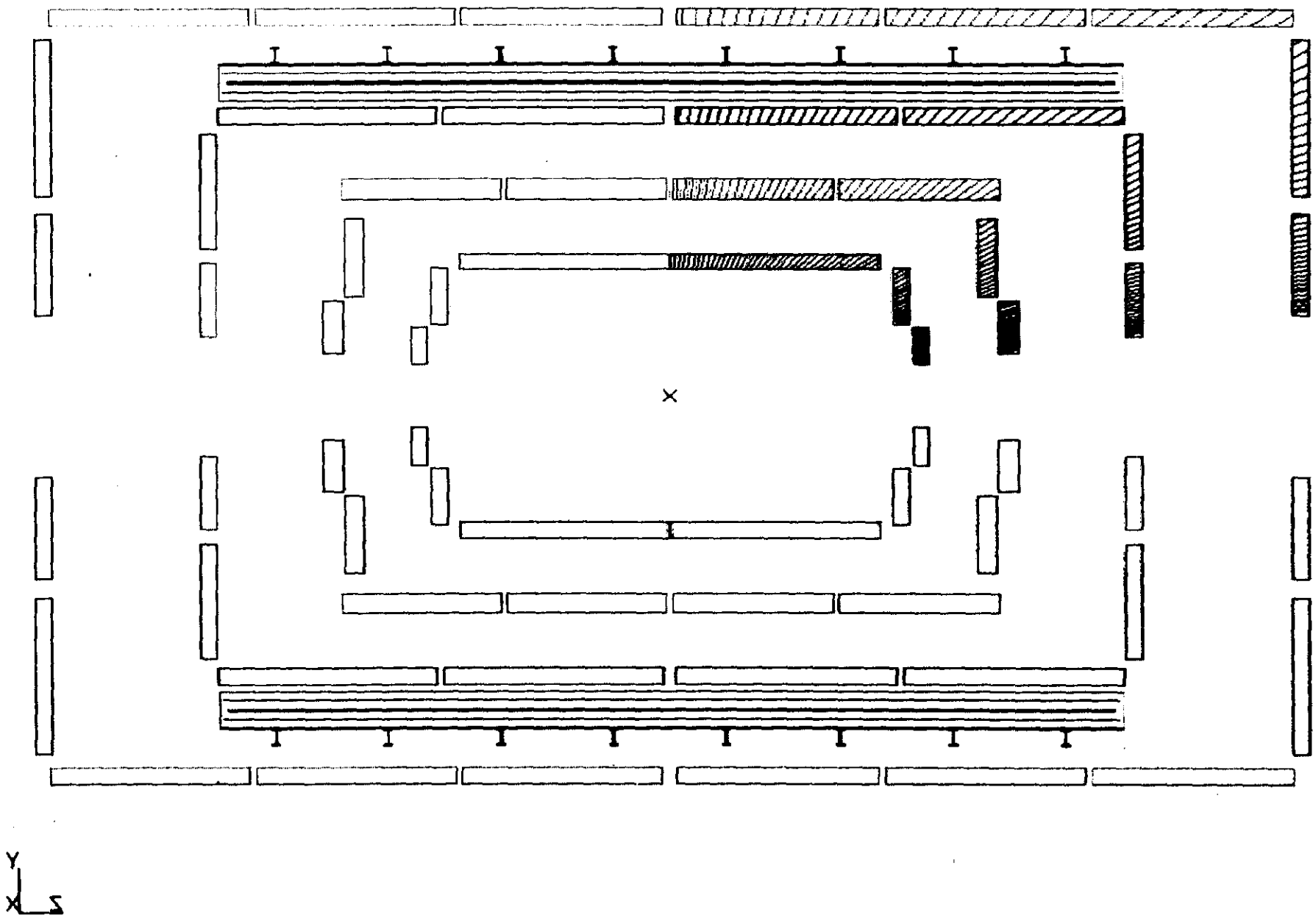
Y
X
Z

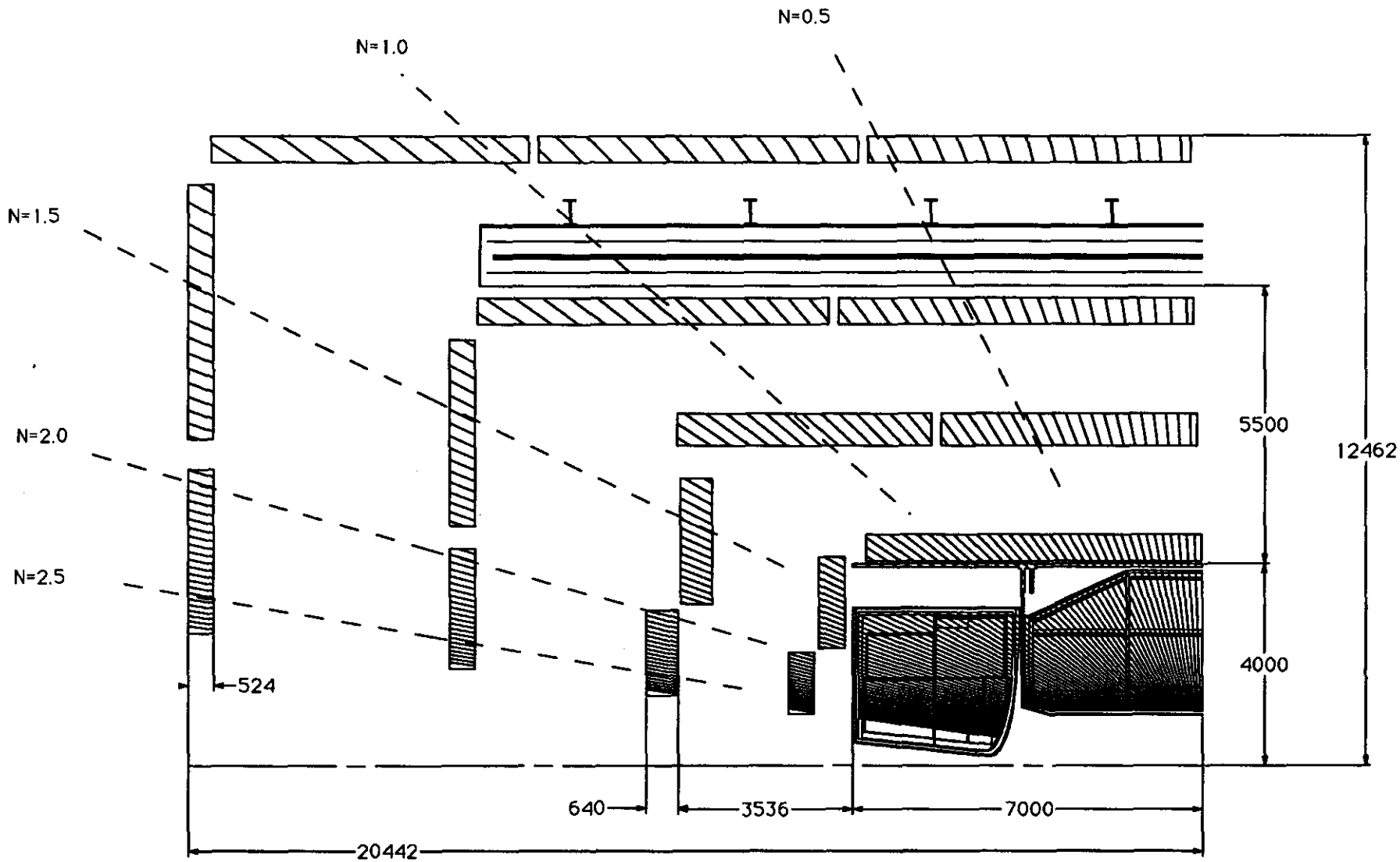
N=0.5
N=1.0
N=1.5
N=2.0
N=2.5
5500
12462
4000
524
640
3536
7000
20442

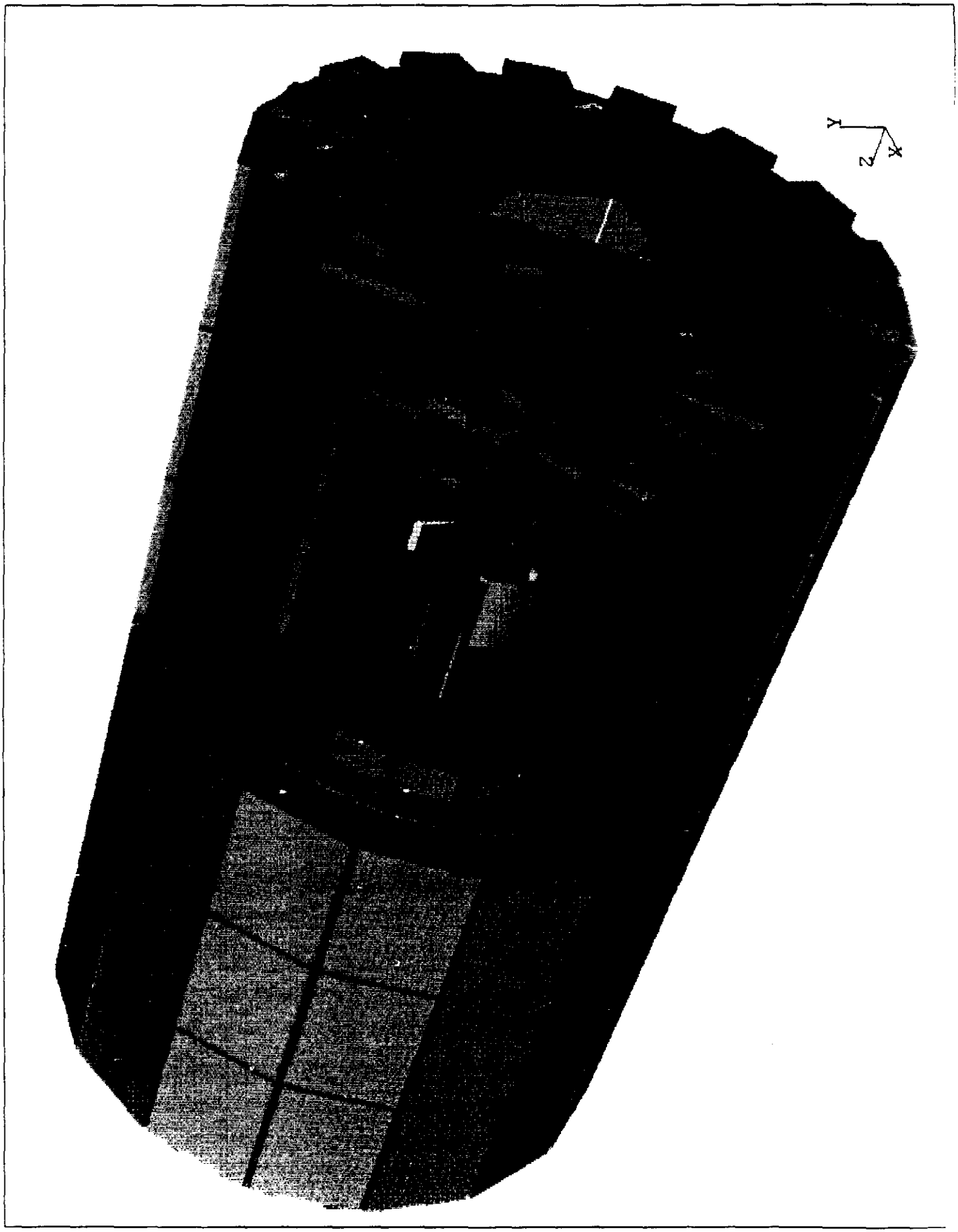
Y
Z
X

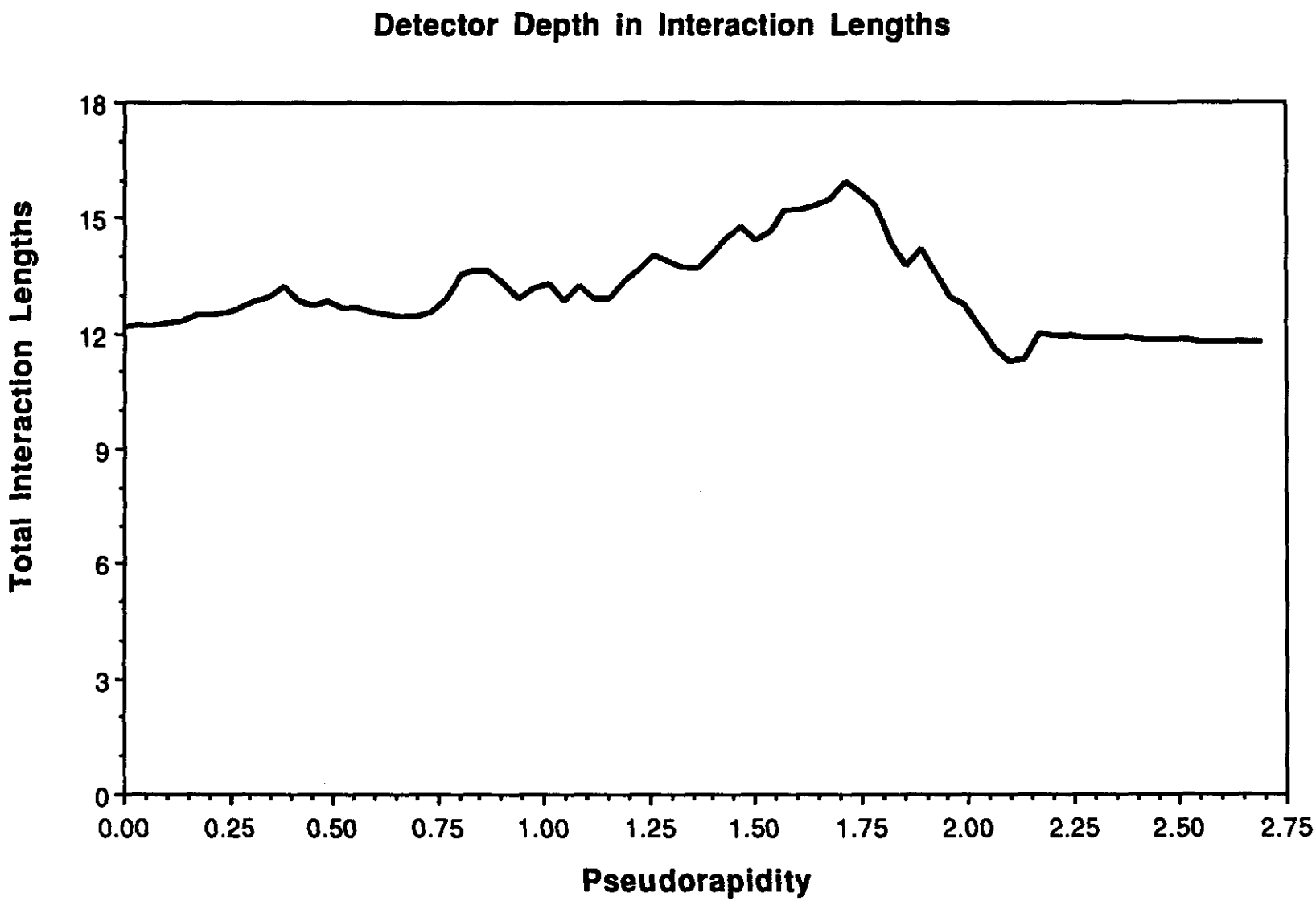
Detector Depth in Interaction Lengths
Total Interaction Lengths
18
15
12
9
6
3
0
0.00
0.25
0.50
0.75
1.00
1.25
1.50
1.75
2.00
2.25
2.50
2.75
Pseudorapidity

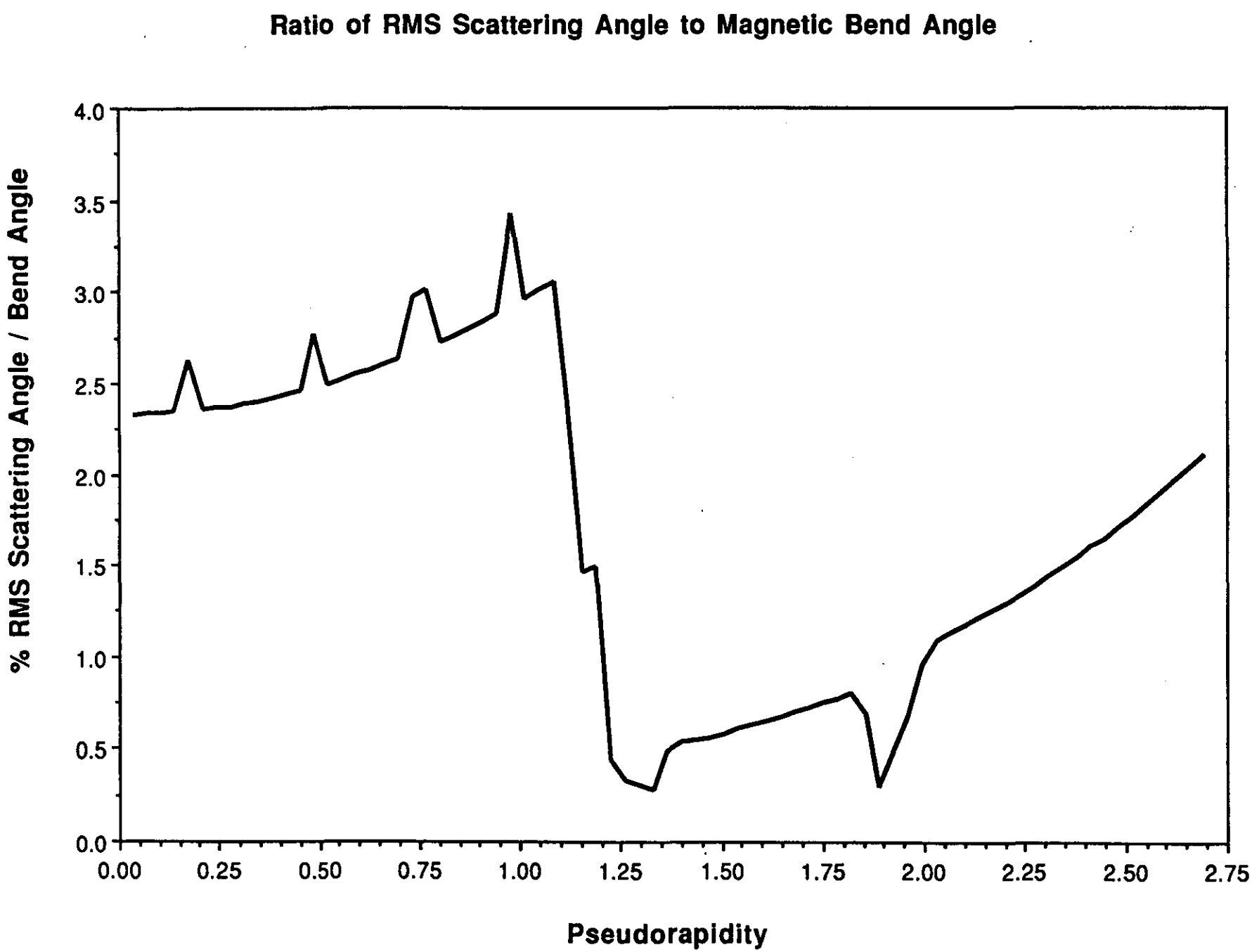
Ratio of RMS Scattering Angle to Magnetic Bend Angle
% RMS Scattering Angle / Bend Angle
4.0
3.5
3.0
2.5
2.0
1.5
1.0
0.5
0.0
0.00
0.25
0.50
0.75
1.00
1.25
1.50
1.75
2.00
2.25
2.50
2.75
Pseudorapidity

IMPROVEMENT OF MOMENTUM RESOLUTION USING MEASUREMENTS OUTSIDE THE MAGNET

LARRY ROSENSON - MIT --7/11/91

ABSTRACT

The consideration of a magnet geometry with no return iron over most of the barrel region opens the possibility of significantly improving the momentum resolution of the system at high momenta (i.e. P > 500 GeV/c) by the addition of an additional Superlayer of detectors outside of the magnet coil. It is conjectured that this will be a cost effective design approach and it is proposed that such a feature be incorporated into the engineering design studies for the magnet and muon system.

It has been decided to pursue design studies on a magnet with a superconducting coil and with no return iron in the search for economies in the design of the detector. This approach immediately suggests the possible exploitation of the more open configuration by the extension of the muon system to include measurements outside the coil. Such measurements promise improved momentum resolution due to the effectively larger sagitta that will be measured if the effective point measurement errors can be kept approximately the same as for a measurement system all contained within the field. In addition, the use of a superconducting coil will tend to keep multiple scattering effects small. It is the purpose of this note to point out that such an approach is indeed feasible and in fact, that the potential gains are large enough to justify further investigation of such configurations.

In Fig. 1 we show a schematic drawing of the muon detection system.

We initially consider a detection system composed of the first three Superlayers, among which 16 layers of detecting planes with point resolution $\sigma_0 = 150$ μm. are distributed. All three Superlayers are assumed to lie inside the magnet so only the chamber material itself will give rise to relevant multiple scattering along the track. If Superlayer #1 and Superlayer #3 are separated by L the optimal position of Superlayer #2 is at L' = L/2. We call this arrangement the 'Sagitta' configuration. The optimal distribution of the 16 planes between the three Superlayers is then $N_1 = 4$, $N_2 = 8$ and $N_3 = 4$, where N_1, N_2 and N_3 are the number of planes in Superlayers #1, #2 and #3 respectively. We assume that the chamber planes are made of material with 0.025 radiation lengths per plane, giving 0.2 radiation lengths in Superlayer

#2. The uncertainty in momentum arising from imperfect alignment is taken into account by adding in quadrature to the ith Superlayer point resolution , $\sigma_0/\sqrt{N_i}$, a term, σ_{ext} , to account for the distribution in residual misalignment between the Superlayers, and a term, $\sigma_{int}/\sqrt{N_i}$, to account for the residual misalignment of planes with respect to each other within a Superlayer . We take $\sigma_0 = 150\mu m.$, $\sigma_{ext} = 25\mu m.$ and $\sigma_{int} = 50\mu m.$ in this example. The magnetic field B is taken equal to 1.0 tesla and the measuring interval L=5 m. The momentum resolution is shown in curve a) of Figure 2 .

As a second example we consider a three layer measurement provided by the same 16 planes but now placing the third Superlayer at D = 2 m outside the magnet coil. The coil is assumed to present 4 radiation lengths to the muon track. Superlayer #2 is moved downstream from it's previous location at L' = 2.5 m to L' = 3.2 m (this would be the the optimal position if there were no multiple scattering in the coil and detectors) Again we distribute the 16 planes optimally (within roundoff) resulting in $N_1 = 4$, $N_2 = 8$ and $N_3 = 4$. We call this arrangement the 'Outside Lever Arm' configuration. The momentum resolution is shown in curve b) of Figure 2.

From Figure 2 we see that the Sagitta measurement is better at momenta well below 250 GeV/c and the Outside Lever Arm measurement is better at momenta well above 250 GeV/c. This behavior is qualitatively true for any range of values of the radiation thickness' of the coil and detector planes likely to arise in practice. The difference in performance is significant in both momentum regions and if a choice had to be made between the two approches it would have to be made on the basis of Physics priorities and prognostications which are very difficult to make at this time.

A simple redeployment of the 16 layers can give us the best features of both measurement strategies. We retain three Superlayers inside the field in the geometry of the 'Sagitta' measurement and with a sufficient number of planes to provide almost the optimal Sagitta measurement and we add a fourth layer to the system at D = 2m. outside the coil. We take as an example $N_1 = 4$, $N_2 = 7$ and $N_3 = 3$ and $N_4 = 2$. We show the resulting momentum resolution as curve c) in Figure 3. Curves a) and b) from Figure 2 are shown for reference. It is clear that with this 'Four Point Measurement' configuration we essentially completely recover the low momentum Sagitta measurement and almost completely recover the high momentum Outside Lever Arm behavior.

In Figure 4 we show the dependence of the Four Point Measurement on the radiation thickness of the coil over the range $2 \leq n_{coil} \leq 10$, where

n_{coil} is the number of radiation lengths in the coil. The relative insensitivity of the basic result to the coil thickness is an important aspect of the robustness of the Four Point Measurement as a design concept.

As is well known, the most important sensitivity of the detector system is to the quality of the alignment of the system. In particular the main effect is due to relative misalignment of the Superlayers which we have parameterized with σ_{ext}. In Figure 5 we show the variation of the Four Point Measurement momentum resolution to σ_{ext} over the range $0 \leq \sigma_{ext} \leq 100$ μm. All the other parameters have the same values as in curve c) in Figure 3. Significant degradation of the resolution occurs for $\sigma_{ext} \geq 50$ μm. A comparable sensitivity occurs also for the Sagitta strategy and is shown in Figure 6.

It is fair to ask whether one will be able to achieve the same quality of alignment for the proposed Fourth Superlayer which lies outside the magnet coil and can only with some difficulty be physically or even optically coupled to the inner three Superlayers. In Figure 7 we show the sensitivity of the resolution to variation in $\sigma_{ext\text{-}Superlayer\ \#4}$, the alignment uncertainty of the fourth Superlayer, for the range 25 μm.$\leq \sigma_{ext\text{-}Superlayer\ \#4} \leq 200$ μm. All other parameters are the same as in curve c) of Figure 3. From Figure 7 we see that as long as $\sigma_{ext\text{-}Superlayer\ \#4} \leq 100$ μm. we will not degrade the momentum resolution catastrophically.

In conclusion it appears that a significant improvement in the momentum resolution at high momenta(a factor of about 0.7) can be obtained over that achievable with a Sagitta measurement by redeploying several detector planes to the outside of the magnet. The alignment requirement of such a Superlayer must be carefully studied to see whether it presents any insuperable problems. The possible gain in resolution would seem to be large enough to strongly suggest the inclusion of this approach in the cost effectiveness optimization of the magnet/muon system.

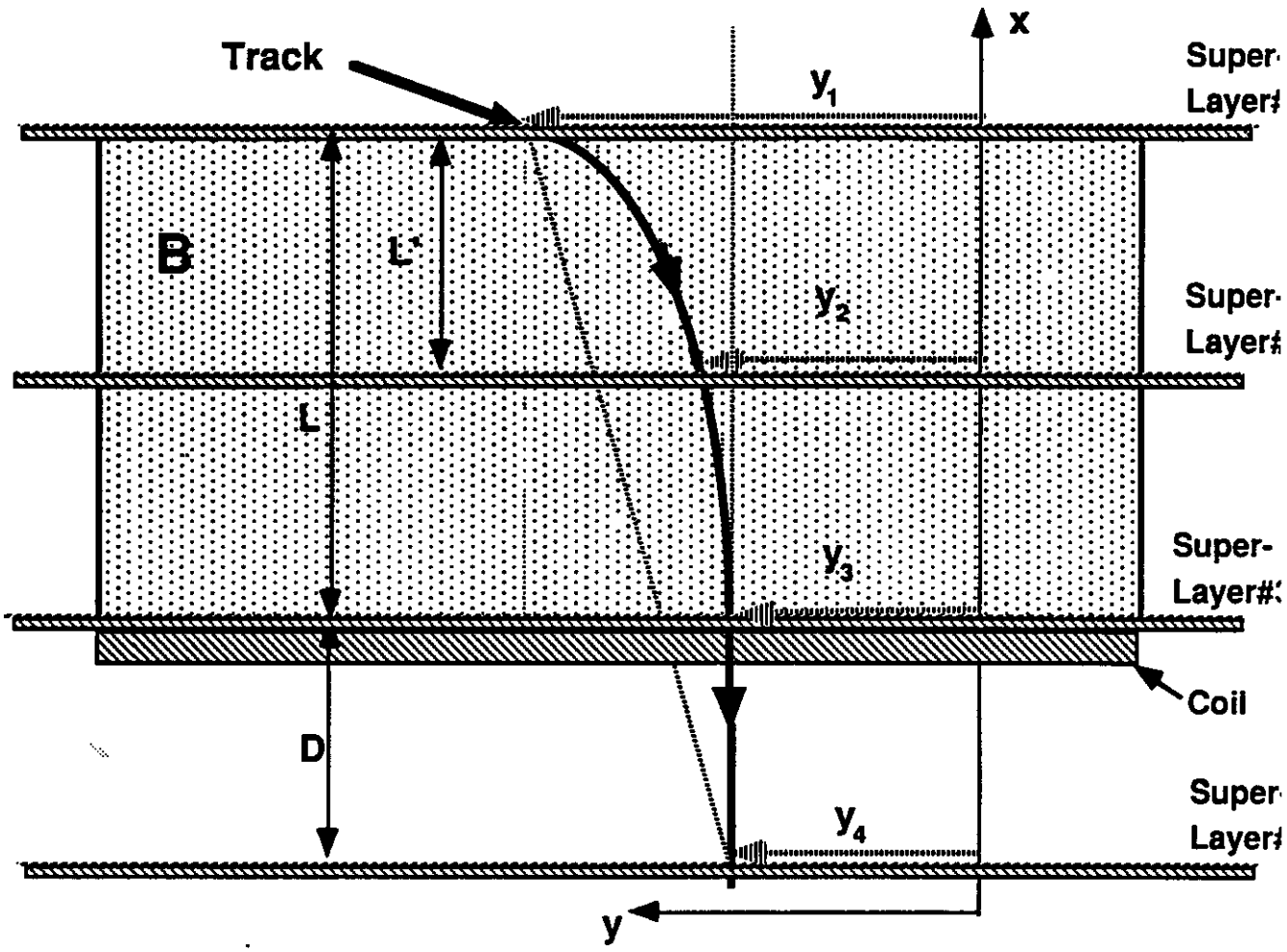

Figure 1

Schematic of the muon detection system.

In a region with uniform magnetic field, B, the track first crosses detector Superlayer #1. It then crosses Superlayer #2 at L' and Superlayer #3 at L, at which point it passes through the coil and leaves the magnetic field. An optional fourth Superlayer is located a distance D outside the coil. Measurements are made of the y_i by suitably averaging point measurements in the measurements made in the N_i planes in the ith Superlayer. The 'Sagitta' measurement may be thought of as utilizing only Superlayers #1, #2 and #3. The 'Outside Lever Arm' measurement may be thought of as utilizing only Superlayers #1, #2 and #4. The 'Four Layer ' measurement uses all four Superlayers as drawn.

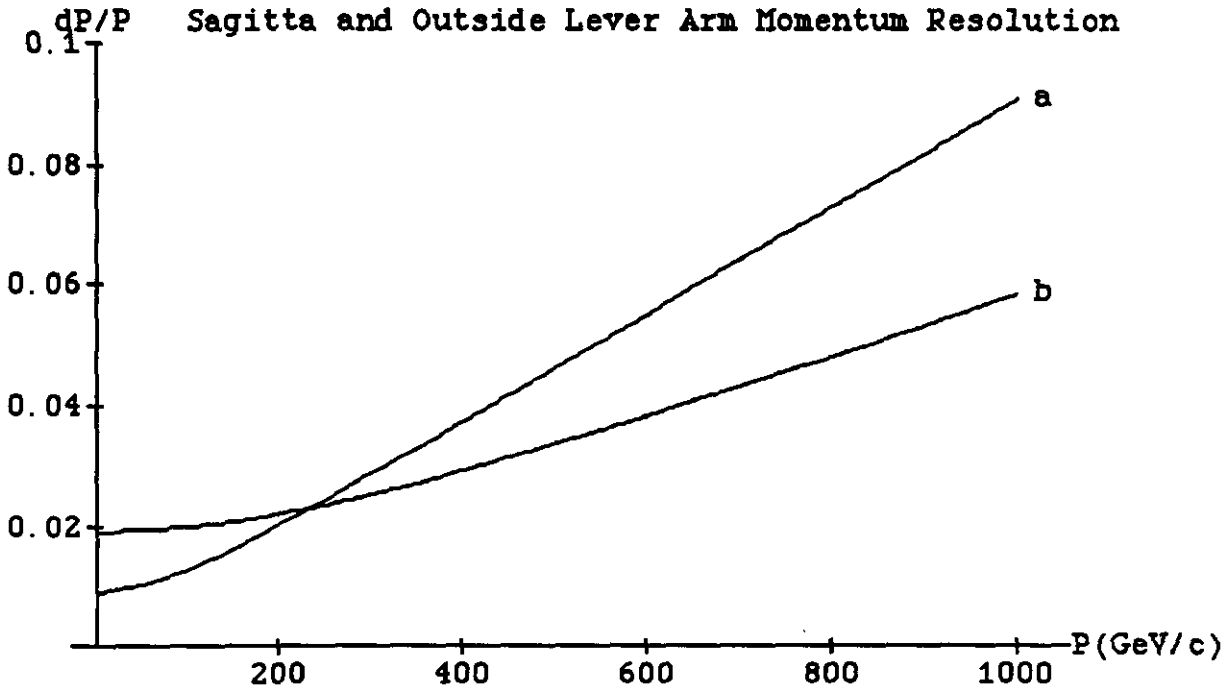

Figure 2

Momentum resolution for the Sagitta and Outside Lever Arm strategies. Curve a - Sagitta Measurement; Curve b- Outside Lever Arm. Measurement

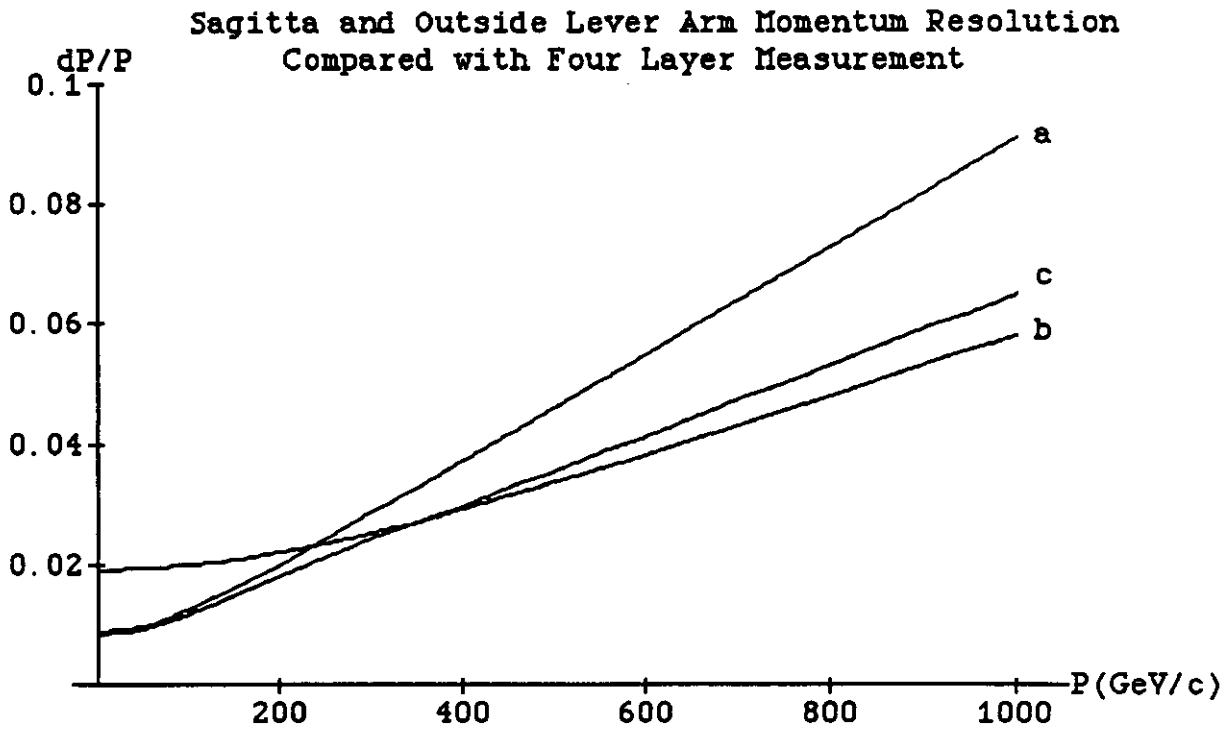

Figure 3

Comparison of Four Layer Measurement Momentum resolution with that of the Sagitta and Outside Lever Arm strategies. Curve a - Sagitta Measurement; Curve b- Outside Lever Arm.Measurement;Curve c) - Four Layer Measurement.

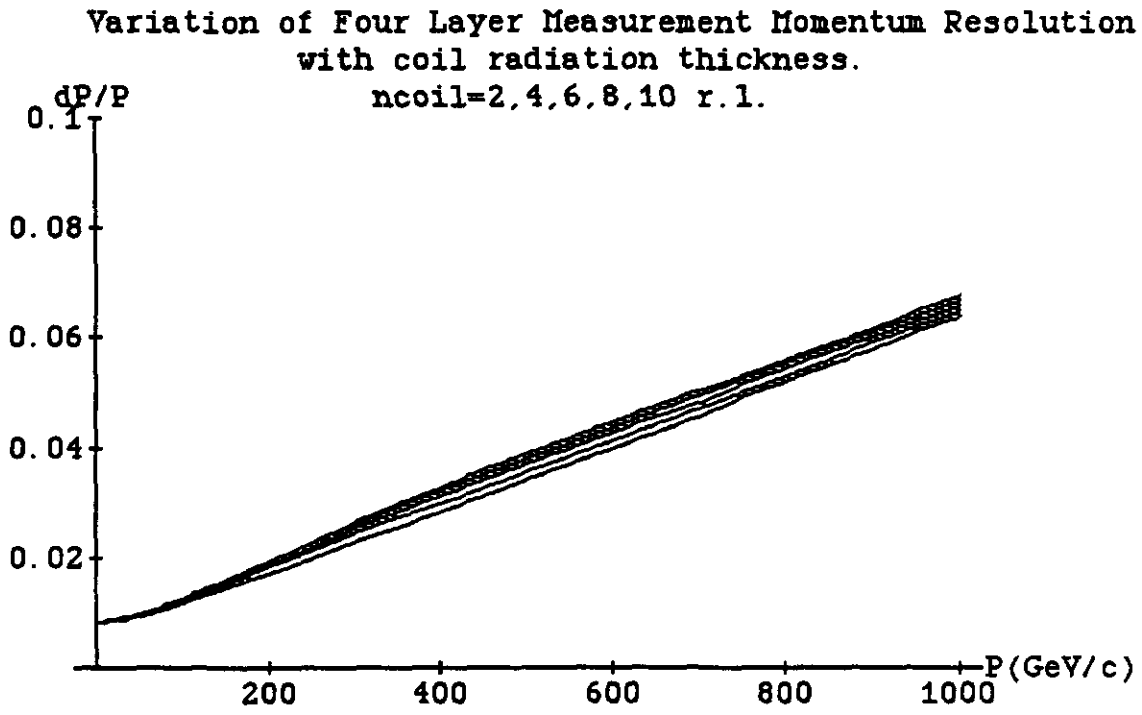

Figure 4

Variation of Four Layer Measurement Momentum Resolution with coil radiation thickness ,n_{coil} . The lowest curve corresponds to n_{coil} = 2 radiation lengths. The curves successively correspond to increments of n_{coil} = 2 radiation lengths.

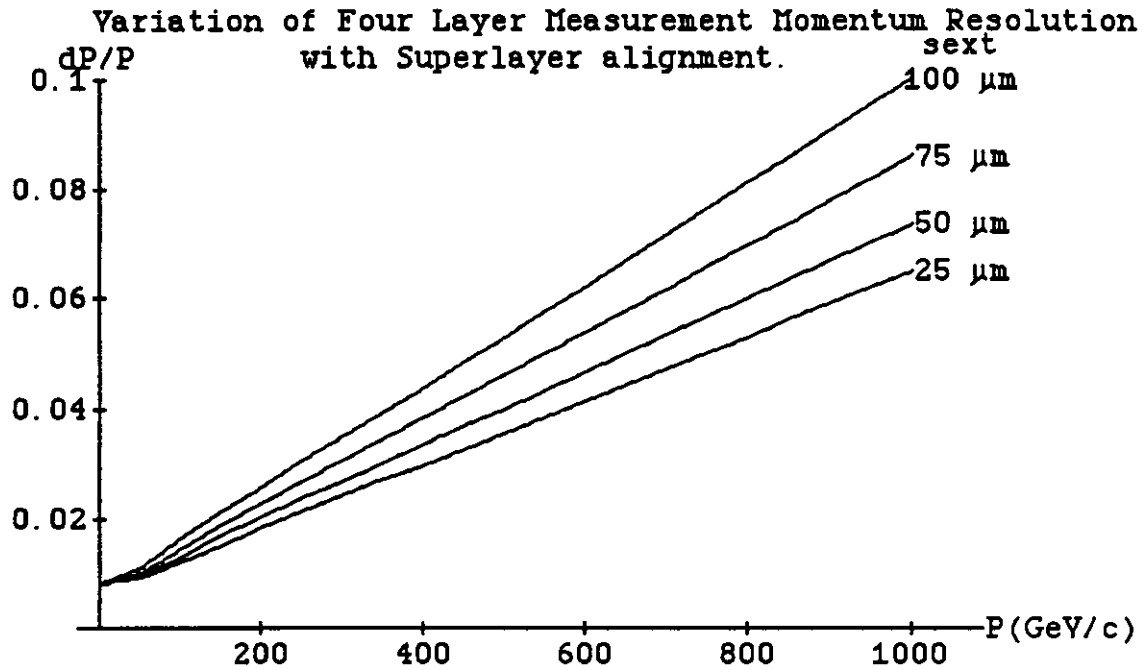

Figure 5

Variation of Four Layer Measurement Momentum Resolution with Superlayer Alignment. The nominal configuration is the lowest curve corresponding to σ_{ext} = 25µm. The successively increasing curves correspond to σ_{ext} = 50µm., σ_{ext} = 75µm.and σ_{ext} = 100µm.

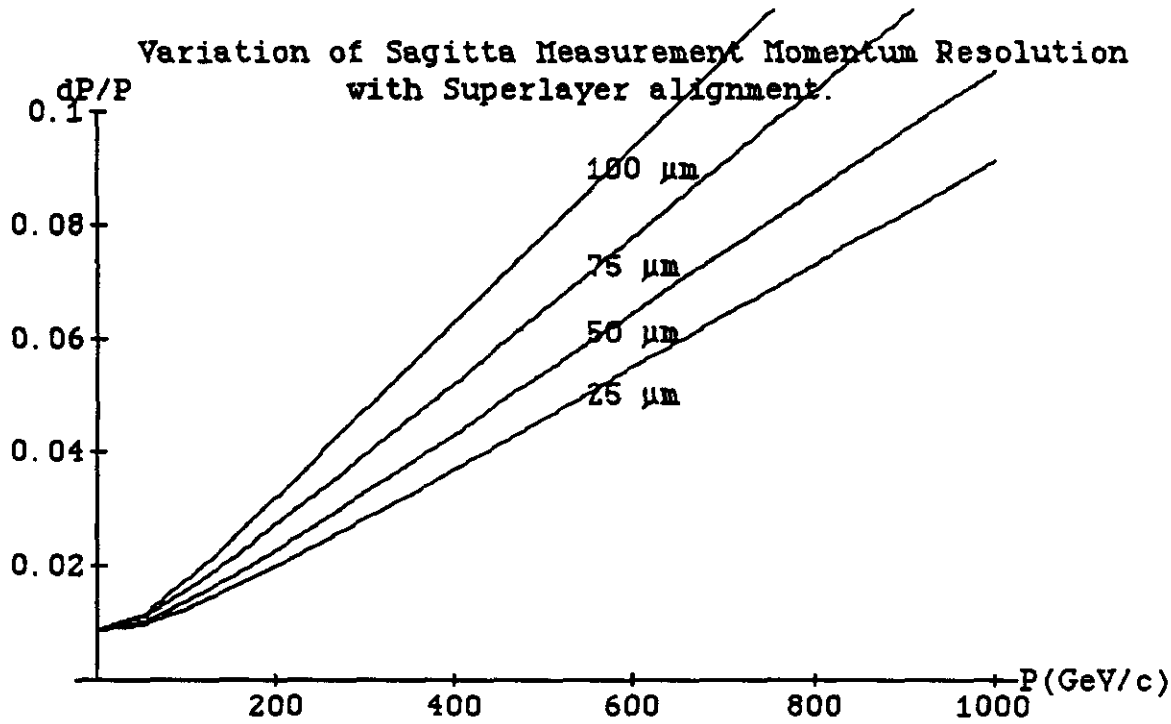

Figure 6

Variation of Sagitta Measurement Momentum Resolution with Superlayer Alignment. The nominal configuration is the lowest curve corresponding to σ_{ext} = 25µm. The successively increasing curves correspond to σ_{ext} = 50µm., σ_{ext} = 75µm.and σ_{ext} = 100µm.

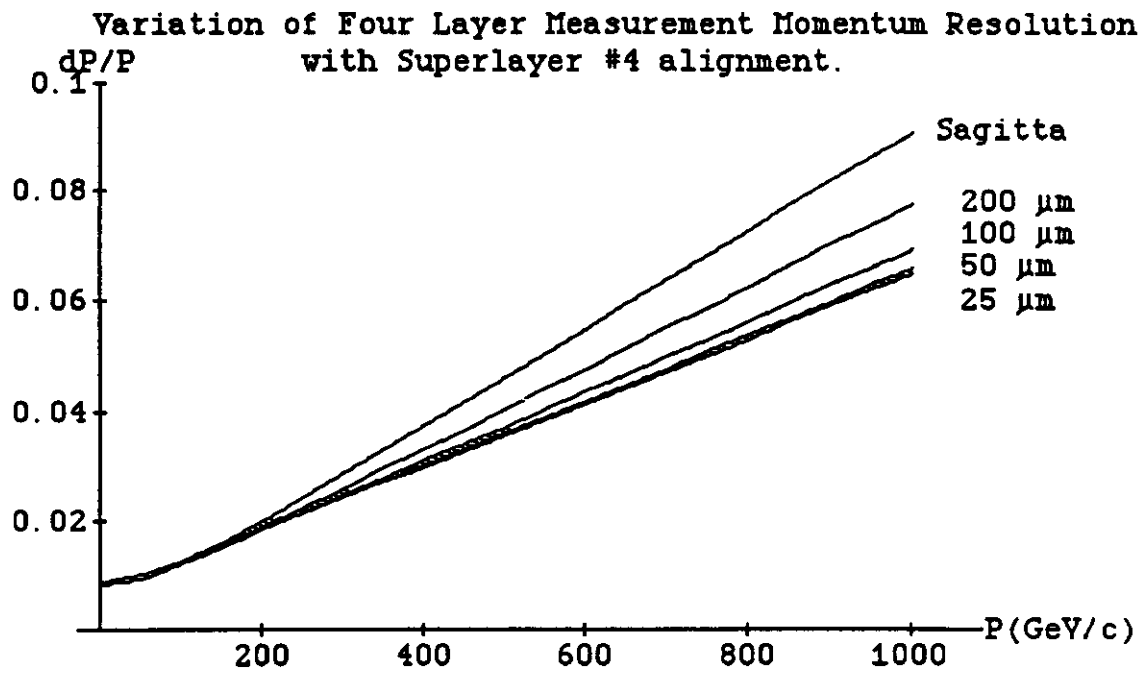

Figure 7

Variation of Four Layer Measurement Momentum Resolution with Superlayer #4 Alignment. The four lowest curves correspond to $\sigma_{ext\text{-}Superlayer\ \#4}$ ranging from 25 µm. to 200 µm. The highest curve, labeled 'Sagitta', is a reproduction of Figure 2 curve a) for comparison. It is close to the limiting resolution from the Four Point Measurement for a completely useless coordinate measurement by Superlayer.#4 and gives a scale for the degradation arising from misalignment of this Superlayer.

- Momentum Distribution of exiting particles by type

- 10 GeV/c Incident Pions

- After 10 λ

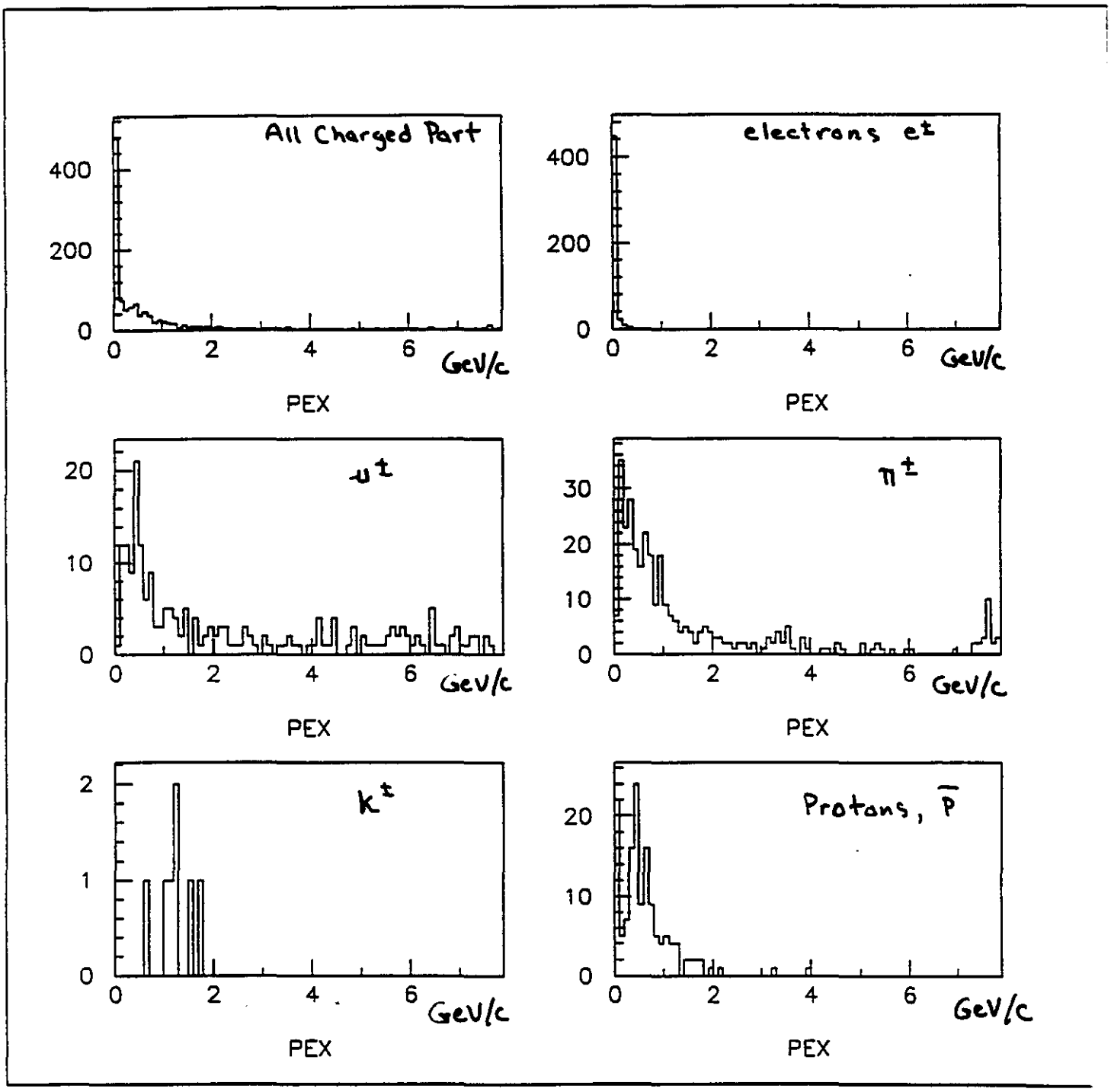

The right tool for this job is an integrated parametric cost model

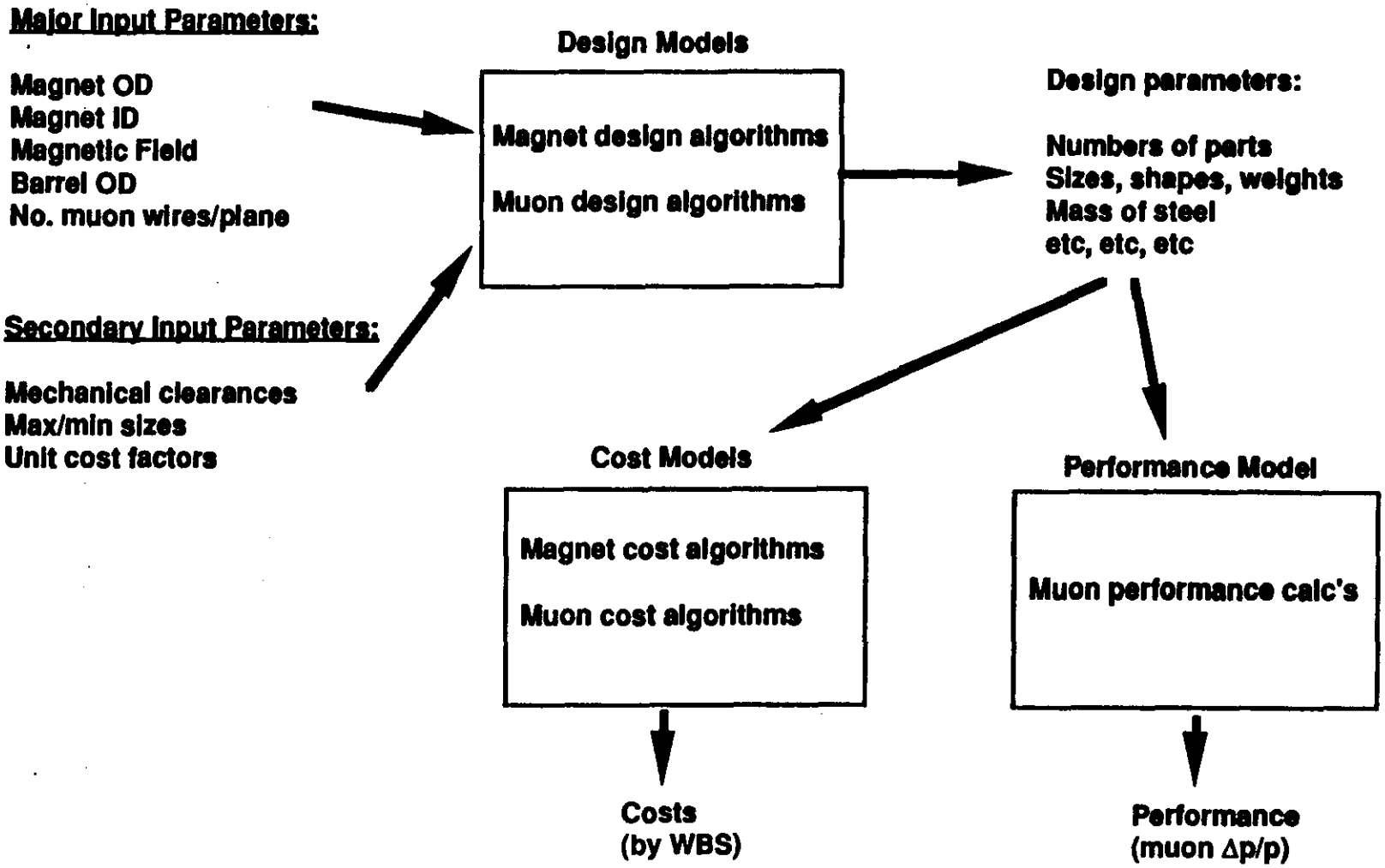

DEIS/LLNL 7/17/91

Muon/Magnet Parametric Cost Model Layout

Central Magnet	Muon-Central	Muon - Endcap outer	Muon - Endcap inner	Muon-Forward side	Muon-Forward center	Forward Magnet	Misc Items	Working area
Input param's	Input param's	Input param's	Input param's	Input param's	Input param's	Input param's	Input param's	Key input param's OD mag field No. wires etc
Output param's	Output param's	Output param's	Output param's	Output param's	Output param's	Output param's	Output param's	
design parameters (calc'd)	Performance param's, calc'c: BL2 Δp/p	Performance param's, calc'c: BL2 Δp/p	Performance param's, calc'c: BL2 Δp/p	Performance param's, calc'c: BL2 Δp/p	Performance param's, calc'c: BL2 Δp/p	design parameters (calc'd)	This column includes the tracker solenoid and project engineering costs, all assumed constant	Key output param's Δp/p min Δp/p max etc
	Design param's overall Sector Outer Middle Inner	Design param's overall Sector Outer Middle Inner	Design param's overall Sector Outer Middle Inner	Design param's overall Sector Outer Middle Inner	Design param's overall Sector Outer Middle Inner			Cost rollup (WBS lev 2)
Cost rollup (by US-format LOI WBS)	Cost rollup (by US-format LOI WBS)	Cost rollup (by US-format LOI WBS)		Cost rollup (by US-format LOI WBS)		Cost rollup (by US-format LOI WBS)	Cost rollup (by US-format LOI WBS)	
		Cost subtotal-outer EC only	Cost subtotal-inner EC only	Cost subtotal-FWD-side only	Cost subtotal-FWD-center only			
2ndary Inputs, Cost Factors	2ndary Inputs, Cost Factors	2ndary Inputs, Cost Factors		2ndary Inputs, Cost Factors		2ndary Inputs, Cost Factors		

These inputs "wired into" column inputs as req'd

These ouputs taken from column outputs

MAGNETIC-FIELD SIMULATION

POISSON, WITH "REST OF THE UNIVERSE" BOUNDARY CONDITION

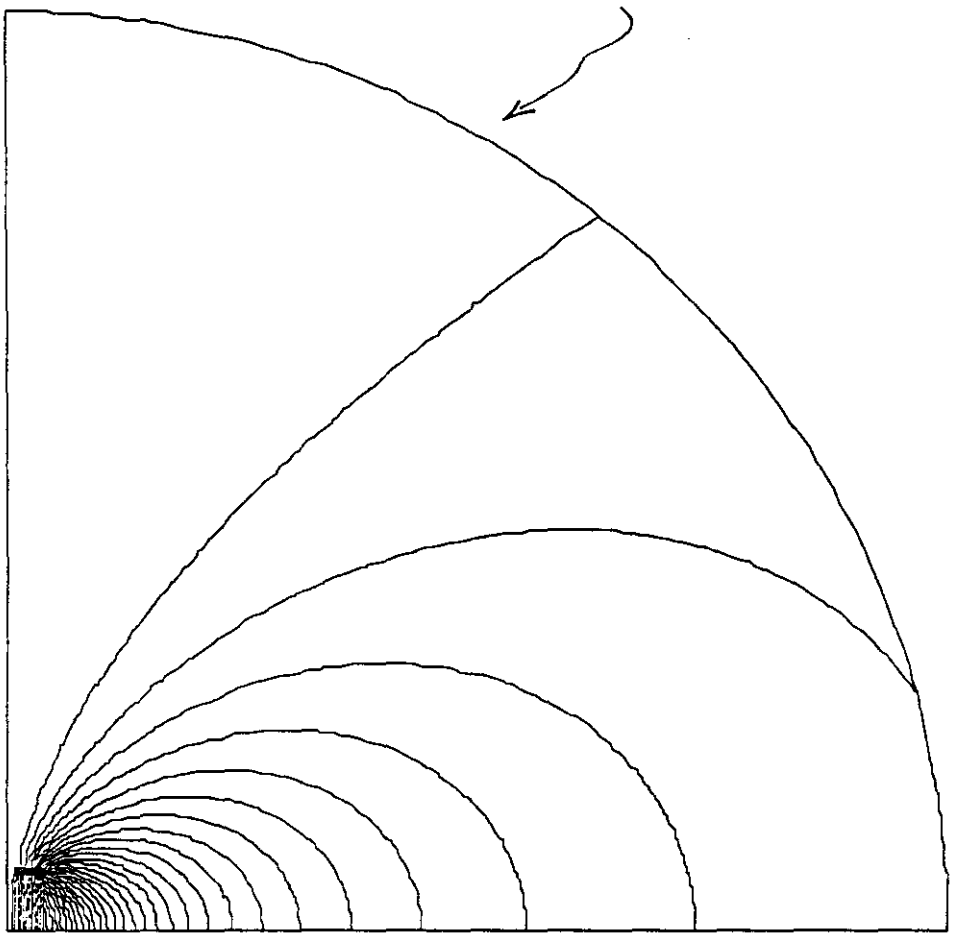

Detector 2 Stray Field, thin p

DEIS/LLNL 7/17/91

MAGNETIC-FIELD SIMULATION

BENDING POWER

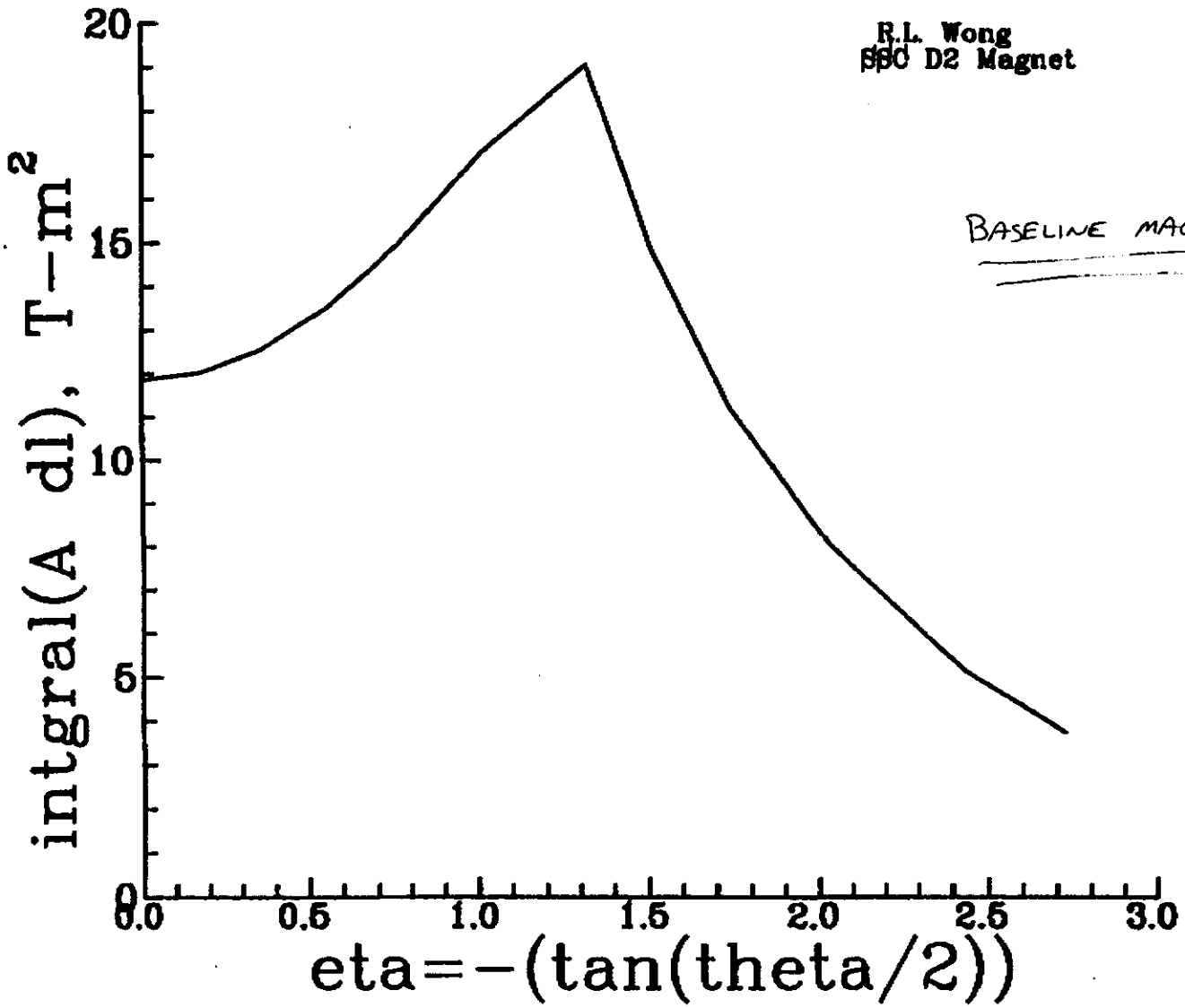

BASELINE MAGNET DESIGN

DEIS/LLNL 7/17/91

JUL 17 '91 11:47 FROM AREA TO SSC PAGE.002

Unshielded SC Magnet

Field on midplane vs radius

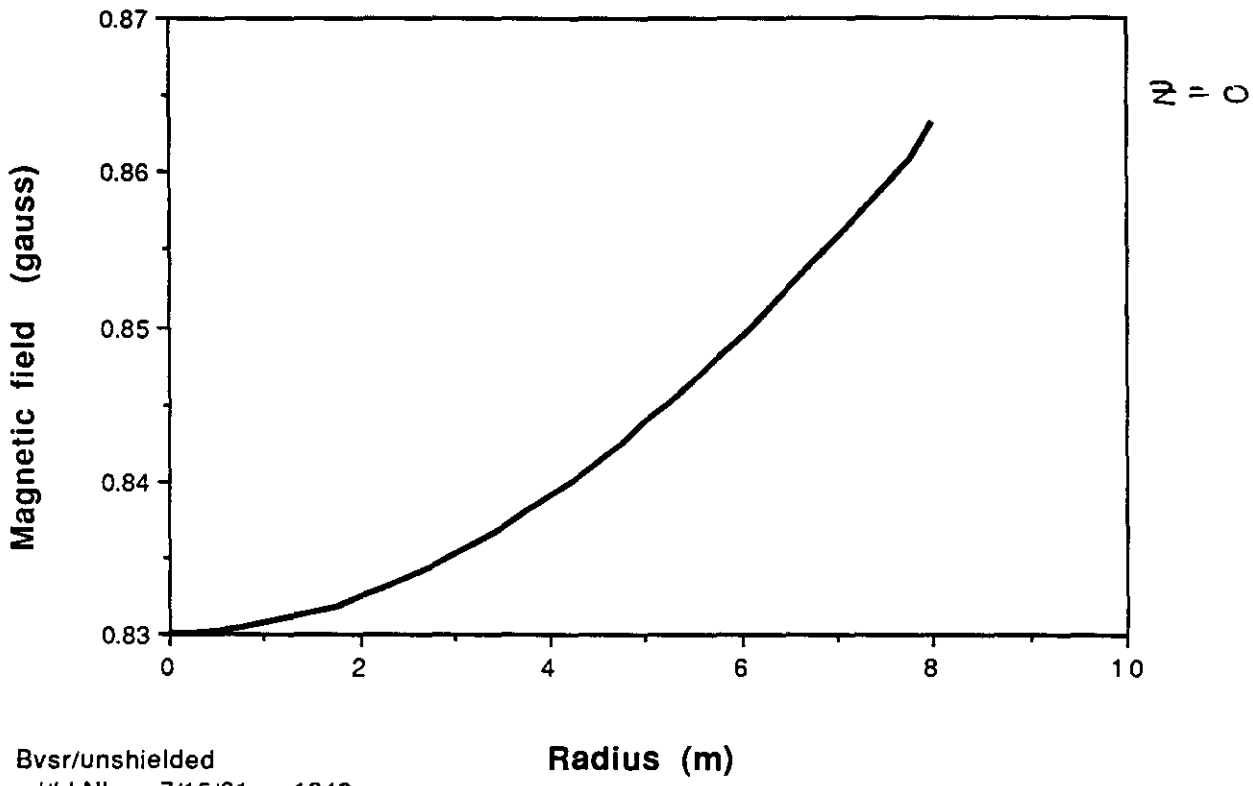

Bvsr/unshielded
gd/LLNL - 7/15/91 - 1842

→ FIELD INSIDE SOLENOID IS NOT UNIFORM, SINCE FLUX RETURNS WERE ELIMINATED.

FIELD ≈ AIR-CORE SOLENOID

DEIS/LLNL 7/17/91

MAGNET ENGINEERING AND R&D SCHEDULE

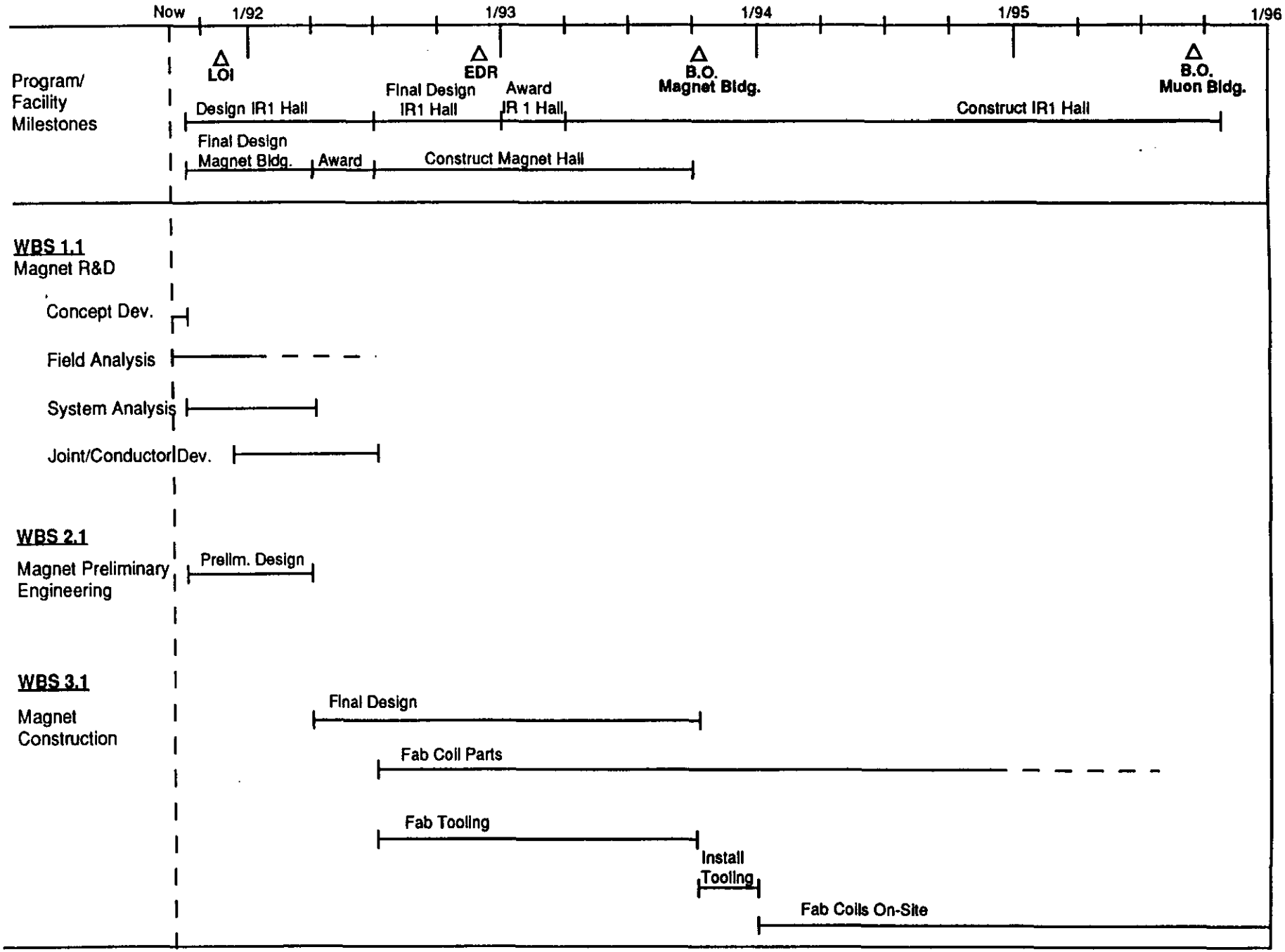

7/17/91

A FAST Subroutine to Produce Punchthrough Showers

Hadron Punchthrough ≡ Charged particles exiting Calorimeter
(P_{out} > 1MeV/c)
Hadron Induced

- GEANT has had some successful comparisons with experimental data

BUT,

- A full-scale simulation of hadron showering for Punchthrough studies on PP events ala GEANT is impractical due to CPU time limits in the Short term.

AND

- Simple parameterizations of punchthrough probabilities are NOT Sufficient to address muon ID, Pattern recognition issues.

We need a simulation (FAST) which produces 4-vectors for the outgoing punchthrough particles

But if you measure muons outside iron

Punchthru is at very low momentum

Karol Lang, Ph.D. Thesis U of Rochester UR908

E379 Data & Dan Green & Dave Hedin FNAL - PUB - 90/18

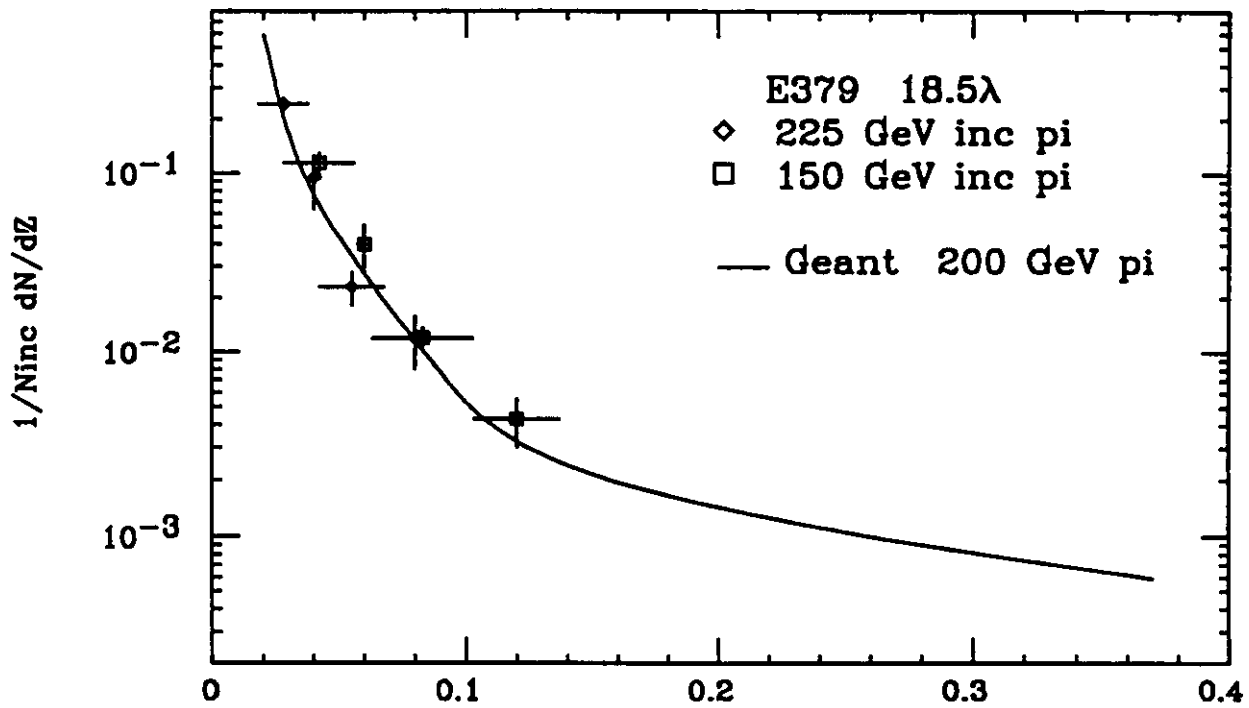

GEANT Agrees Both Ab & Spect.

$Z = P^*_{MU}/P_{IND}$

P_μ = Momentum Before Calorimeter

Can Easily reject Punchthru by Momentum Cut

Position and momentum information from PCHTHR allows for μ ID, Pattern recognition studies

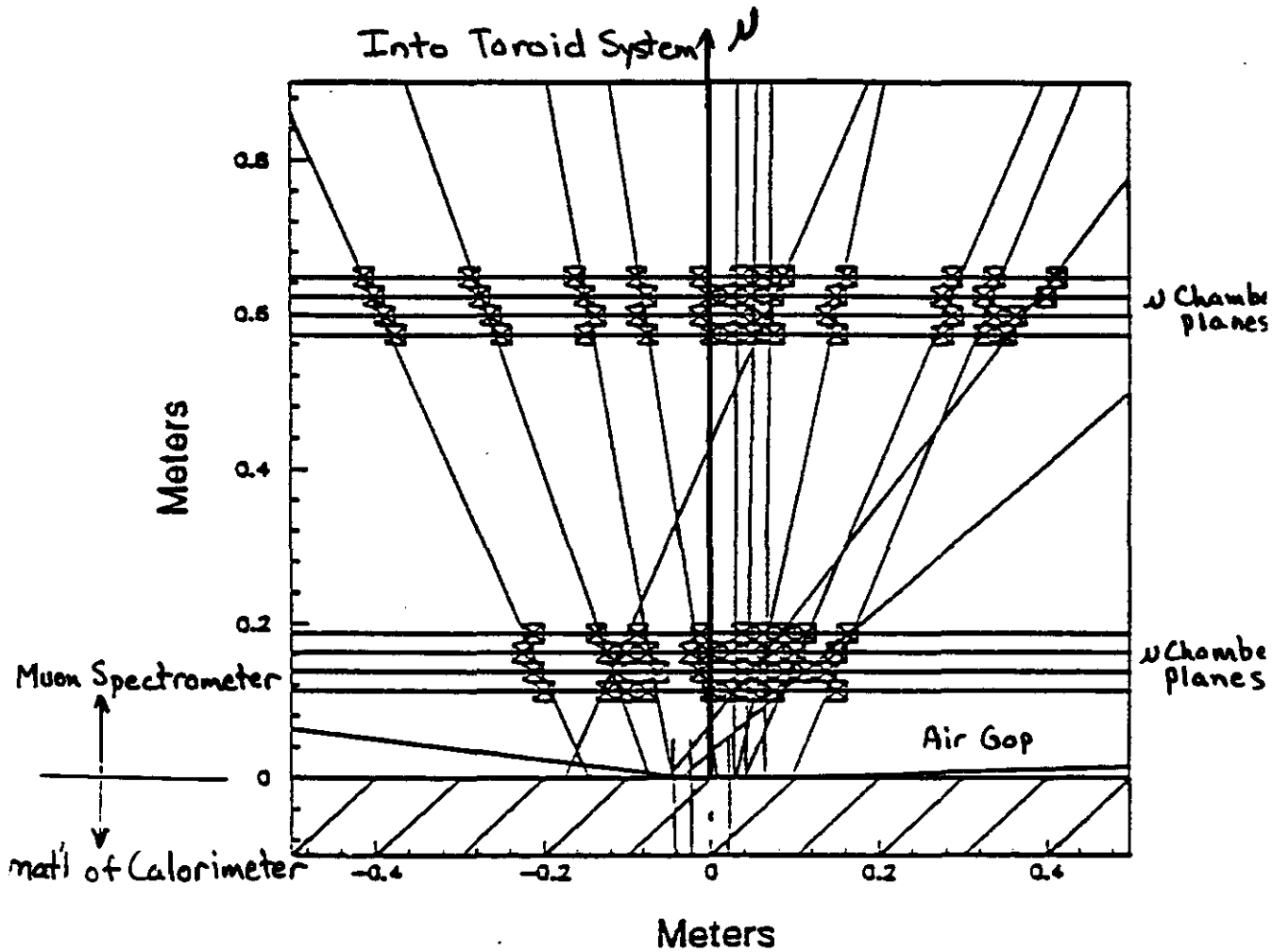

Figure 3-23 Muon track (vertical at 0) coming out of the calorimeter accompanied by the secondary particles resulting from hadronic punchthrough or muon radiation in a 250 $\frac{GeV}{c^2}$ high-p_T top event.

Towards a Fast Subroutine for Hadron Punchthro

Punchthrough Shower Profiles include:

Full GEANT Simul.

- Probability for ≥ 1 Punchthrough Particle
- Momentum Spectrum of Particles exiting Absorber
- Multiplicity Spectrum of punchthrough Particles
- Lateral Spread of Punchthrough (w.r.t. parent track pro
- Outgoing angle of Punchthrough (w.r.t. parent track dir
- ⋮

Probability Tables

⇓

Fast Subroutine (P_{INC}, Thickness) called from ISAJET analysis program, etc.

⇓

Punchthrough Background Rates

$\boxed{\text{4-vectors of outgoing particles}}$

R. McN

1. GEANT + GHEISHA

Simulation of Hadron Punchthrough

WORK in PROGRESS

GOALS

- Obtain profile of Punchthrough as function of absorber thickness & Incident momentum
- Determine Rate of Punchthrough as a function of Absorber thickness & Θ_{LAB} & P^{OUT}_{LAB}
- Ultimately Determine Optimum absorber thickness trigger thresholds, Muon ID requirements

Time

Simplified Detector Simulated by GEANT / GHEISHA

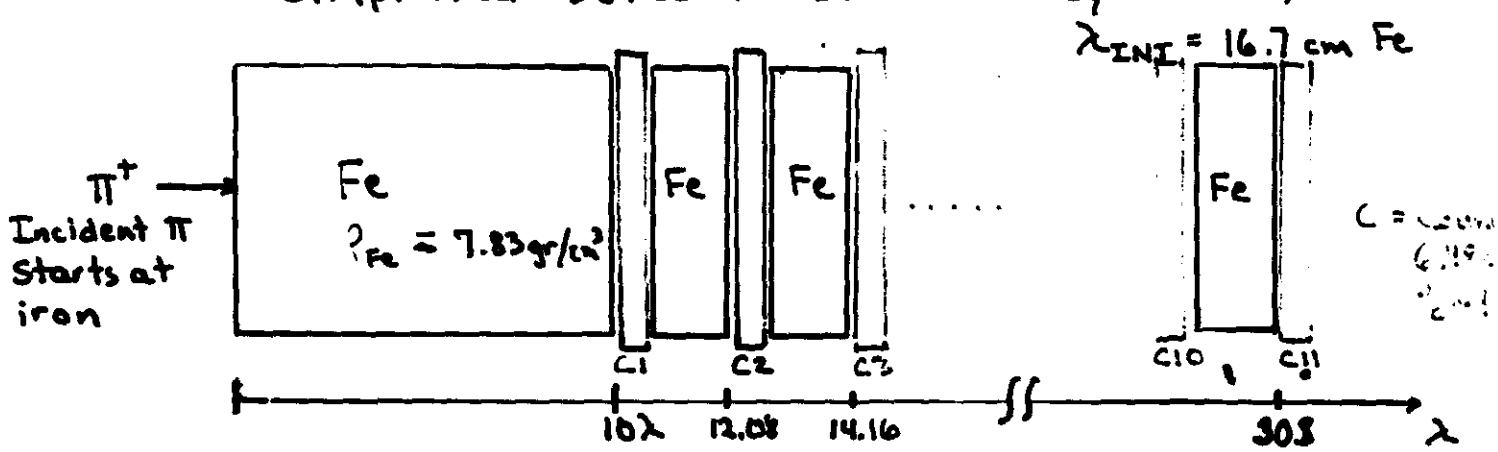

Record charged particles in counters (10, 12, 14, ···, 30λ)

$\vec{P}$, (x, y) in plane, particle type

Simulated 10, 20, 40, 100, 200, 800, 3000 GeV π^+

Charged Multiplicity of exiting shower

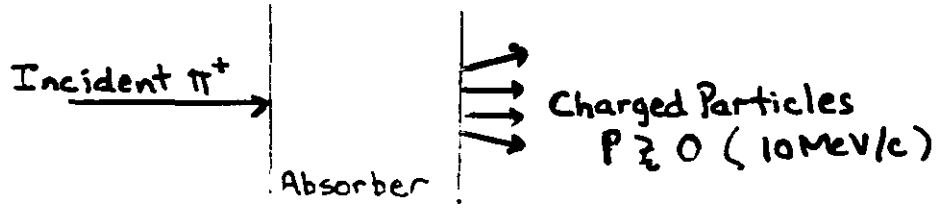

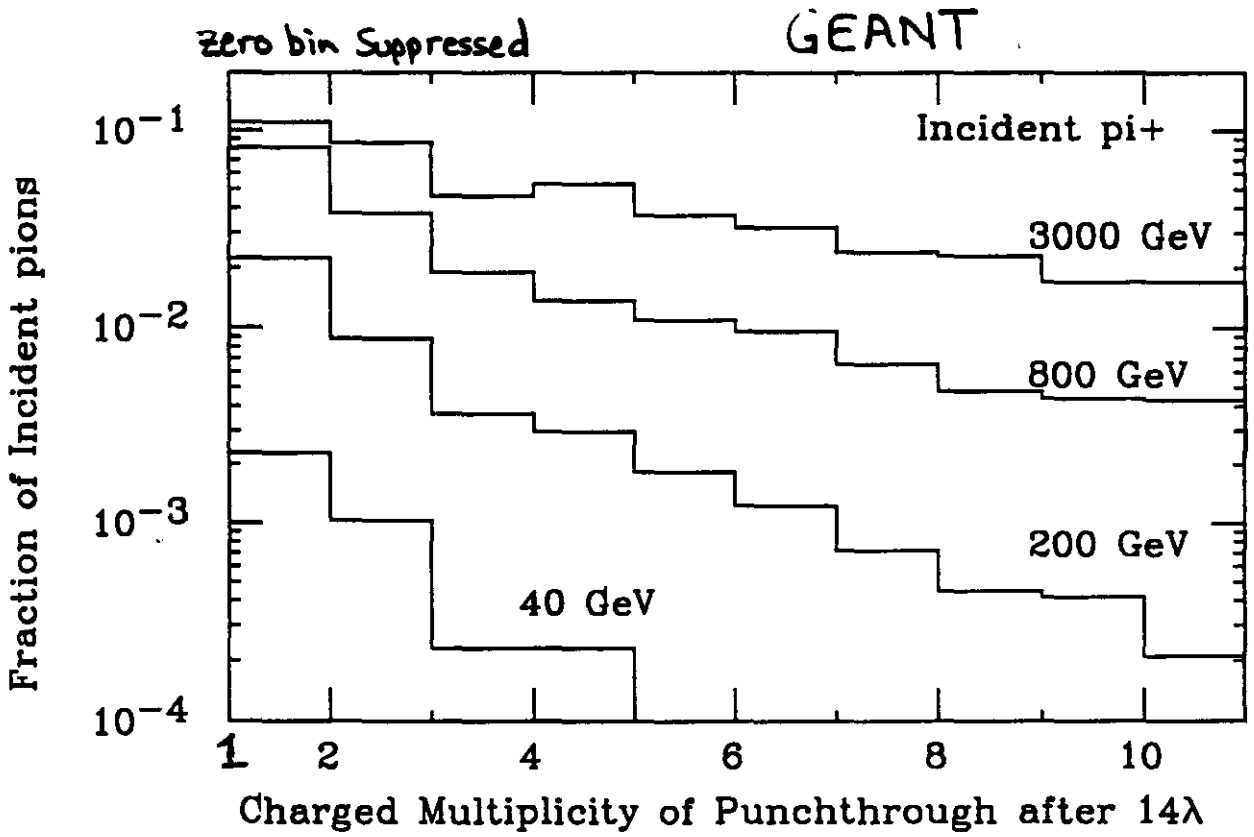

Not only does punchthrough probability increase but also Multiplicity increases with parent hadron energy (Incident)

$P_{in} = 200$
200 GeV Pions

Comparison of Leading and non-leading Charged Particle spectrum

$Z = P_{out}/P_{in}$

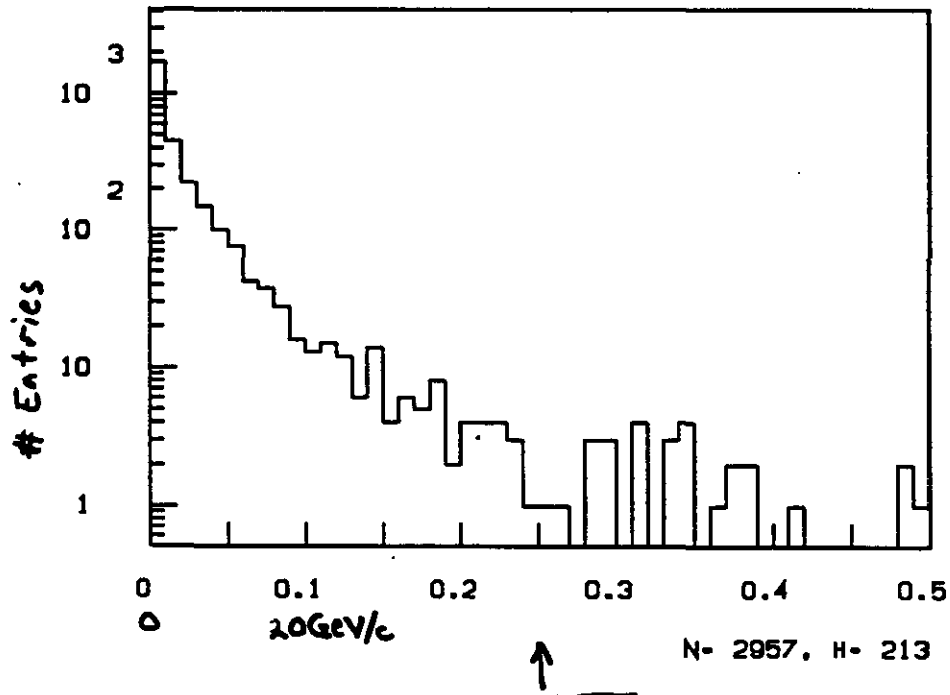

Z=Pout/Pinc of Leading Charged Part

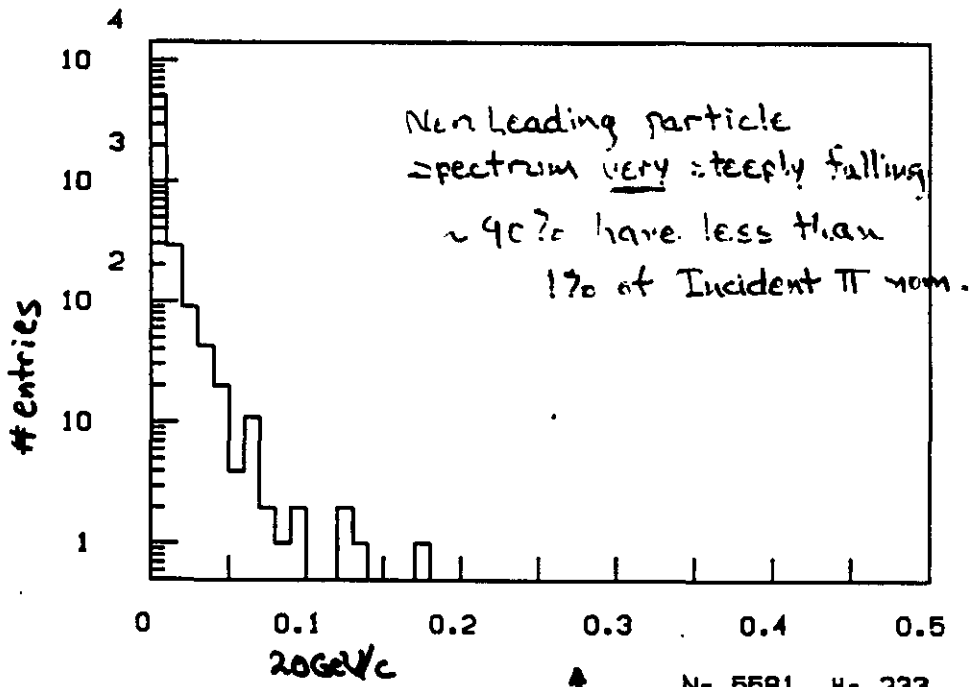

Z=Pout/Pinc of Non-Leading Charged

Spectrums after 12 Lambda

Lateral Spread of Punchthrough Shower
200 GeV/c Incident pi- GEANT Simulation

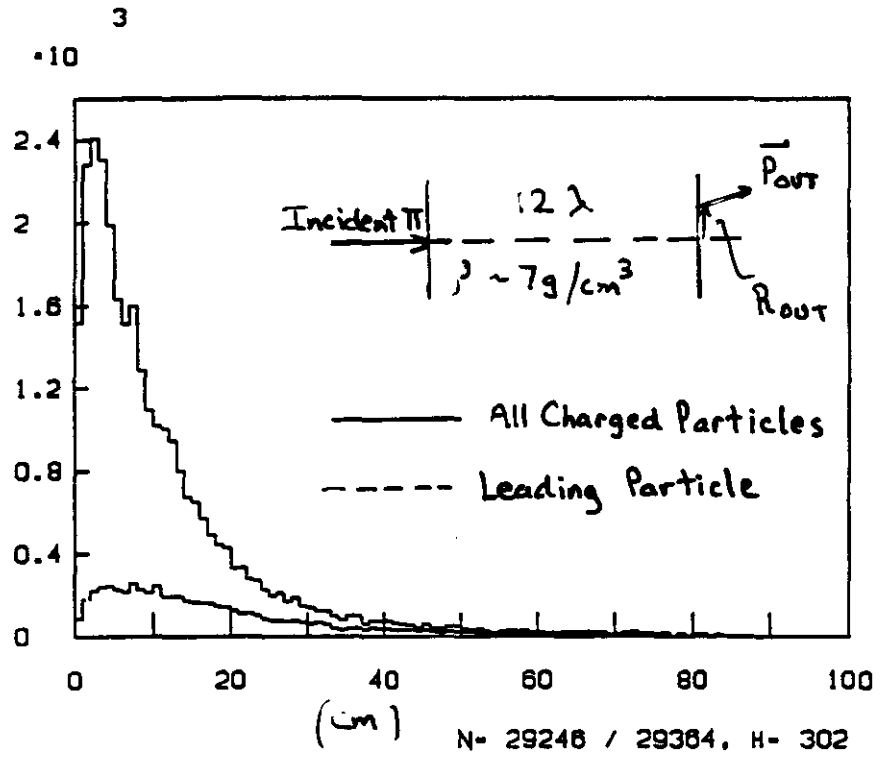

RØUT CHARGED 12L

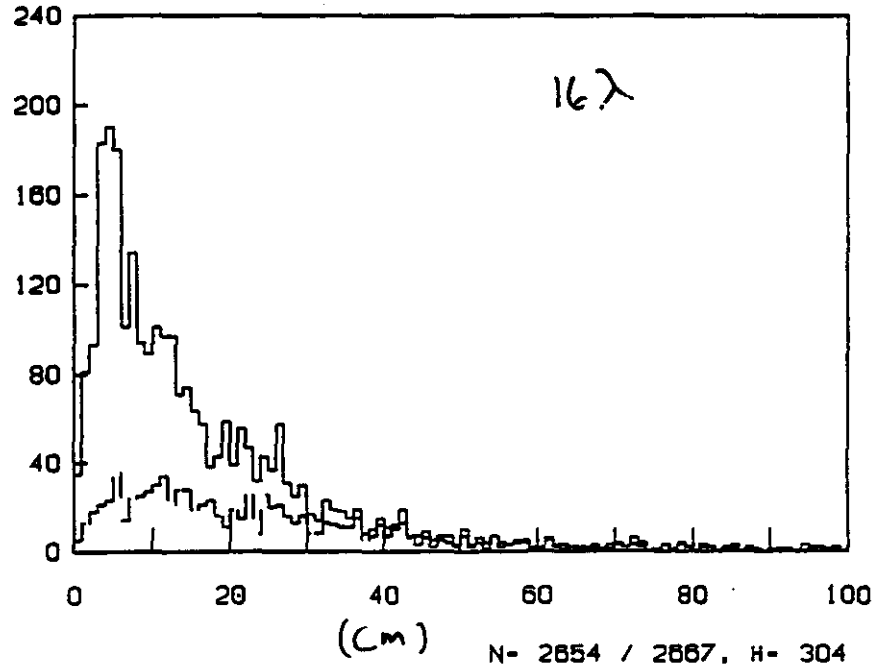

RØUT CHARGED 16L

After Iron

Outgoing angle of Punchthrough

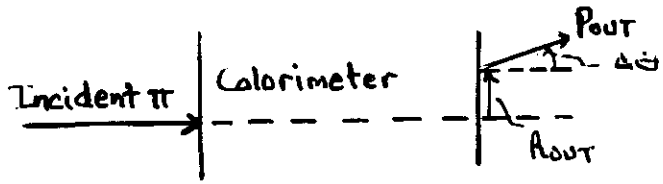

Δθ depends on $|\vec{P}_{OUT}|$

generally insensitive to

P_{INC}, Thickness of mat'l

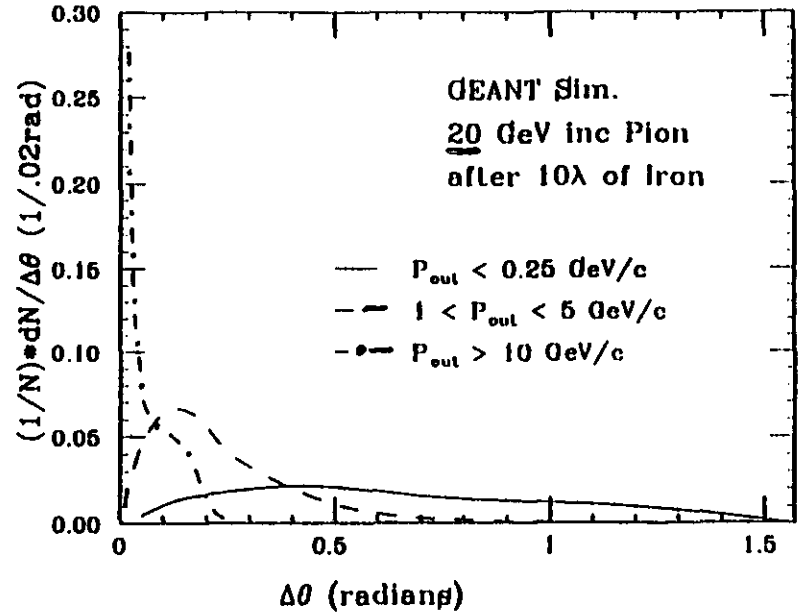

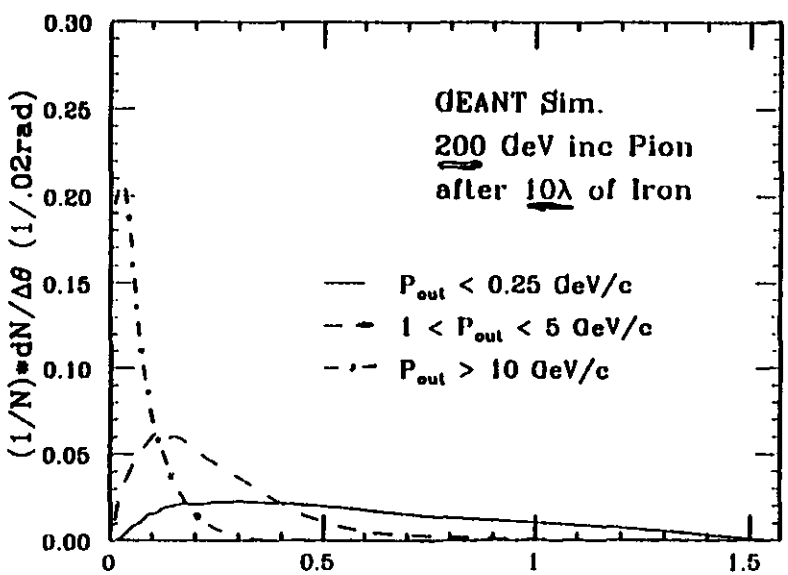

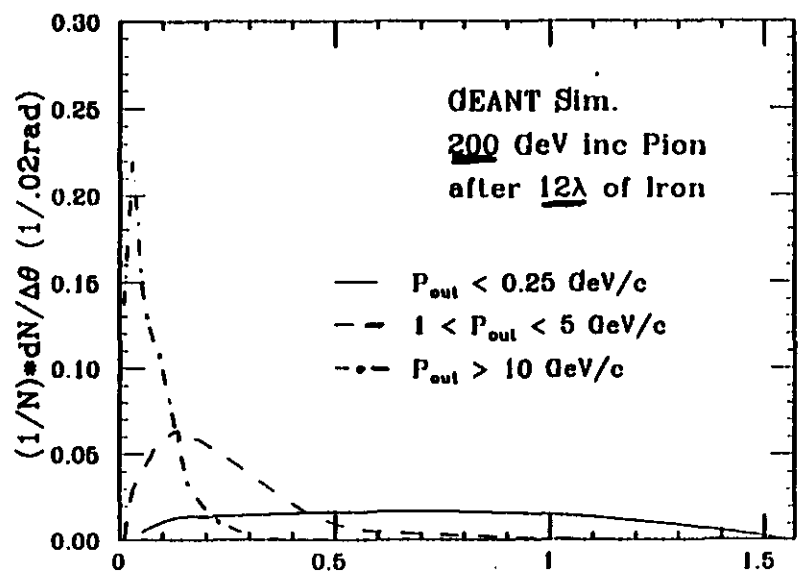

Summary - Future Work

- A subroutine exists <u>now</u> (PCHTHR) which incorporates GEANT-Produced Punchthrough Shower Profiles. It can be used for thicknesses of hadron filter from 10λ to 30λ and called from any analysis routine.

Further work is ongoing to refine and expand the PCHTHR probability tables:

- More incident momentum bins (at lower momenta)
- Include outgoing particle type $\Leftrightarrow$ correlations
- Consider more depth bins (lower depths $4-10\lambda$)
- Consider Calorimeter mat'l properties ($\rho, Z, \vec{B}, \cdots$
- ?

Preparing a NEW release of PCHTHR by Fall, 1991

```
      SUBROUTINE PCHTHR(ZCAL,IDABS,P,POUT,RO,NP,WT,NPOUT)
C-----------------------------------------------------------------------
C-                                                                     -
C-    Authors:    R. McNeil , W. Morse, and H. Ma
C-    Date:       1-Nov-1990                                           -
C-                                                                     -
C-                                                                     -
C-    Variables:                                                       -
C-      Input:                                                         -
C-              ZCAL     -    The Thickness of Material in Lambda     -
C-              IDABS    -    Particle ID of the Parent Track         -
C-              P        -    Momemtum of the Parent Track (GeV/c)    -
C-                                                                     -
C-      Output:                                                        -
C-              POUT     -    Momentum of the Puncthrough Tracks (GeV/c) -
C-              RO       -    Radius of Punchthrough from the projected -
C-                            parent track in cm (at end of Mat'l)    -
C-              NP       -    Multiplicity of Punchthrough            -
C-              WT       -    Weight (probability for the punchthrough) -
C-              NPOUT    -    Multiplicity of Punchthrough Output     -
C-----------------------------------------------------------------------
      IMPLICIT NONE

      INTEGER IDABS,MUL,NP,NPOUT
      INTEGER I,IM,IP,J,K,ILAM
      REAL POUT(9,4),RO(9),P(4),PUNCH,WT,ZCAL,PPU,TCAL,RR,PROB
      REAL THINC,PHINC,THOUTL,PHOUTL
        REAL*4 Y1,Y2,Y,XLAM,ZPF1,ZPF2,PB1,PB2
                                    CCFR
C       PUNCHTHROUGH DATA FROM NIM A245,27(1986) AND ROGER MCNEIL
        REAL ZLAM(20),ZP(11),ZPUNCH(20,11),ZPF(9),ZINTER,PPLEAD
        REAL ZFRACHI(9),ZFRACLO(9),ZFRACNL(9)
C       PROB OF HAVING LEADING ENERGY OF PUNCHTHROUGH BE LESS THAN ZPF*P
        DATA ZFRACHI/0.61,0.75,0.910,.963,.977,.985,.993,.996,.998/
        DATA ZFRACLO/0.16,0.29,0.59,0.76,0.83,0.88,0.93,0.966,0.978/  } Spectrum
        DATA ZFRACNL/0.84,0.95,0.996,0.9993,1.,1.0,1.,1.,1./            GEANT
        DATA ZPF/  0.010,0.020,0.05,0.100,0.15,0.200,0.300,0.400,0.500/
C       PROB OF ANY PUNCHTHROUGH
        DATA ZLAM/10.1,10.8,11.5,12.2,12.9,13.6,14.3,15.,15.7,16.4,17.1,
     &          17.8,18.5,19.2,20.0,22.0,24.0,26.0,28.0,30.0/,
     1ZP/0.0,4.7,7.5,15.,25.,50.,100.,200.,300.,800.,3000./
        DATA ZPUNCH/20*0.0,
     1  0.1,.07,.03,.02,.01,0.,0.,0.,0.,0.,0.,0.,0.,0.,0.,        } P_INC < 10
     &  0.,0.,0.,0.,0.,                                             Harris etal
     2  0.3,0.1,.07,.03,.01,.007,.003,0.,0.,0.,0.,0.,0.,0.,0.,
     &  0.,0.,0.,0.,0.,
     3  2.5,1.3,.7,.5,.3,.2,.1,.04,.04,.04,0.,0.,0.,0.,0.,
     &  0.,0.,0.,0.,0.,
     4  6.,3.6,2.2,1.3,.7,.5,.3,.2,.2,.2,.1,.05,0.,0.,0.,
     &  0.,0.,0.,0.,0.,
     5  14.6,9.7,6.6,4.2,2.8,2.0,1.2,1.,.8,.6,.5,.3,.3,.3,0.,        CCFR
     &  0.,0.,0.,0.,0.,                                              P_INC < 300
     6  30.,22.,15.,10.,7.,4.5,3.0,2.1,1.5,1.1,0.7,.5,.4,.2,.2,
     &  0.3,0.3,0.2,0.1,0.,
     7  54.,42.,32.,24.,18.,14.,9.4,7.1,5.0,3.6,2.9,2.3,2.1,1.7,1.0,
     &  0.8,0.5,0.4,0.4,0.3,
     8  66.,56.,44.,35.,27.,21.,14.,11.,8.,6.,4.7,3.6,3.0,2.5,2.1,
     &  1.5,1.2,0.9,0.8,0.6,
     9  70.,60.,50.,40.,30.,25.,20.,15.,11.,9.,7.,5.,4.,3.,1.8,     GEANT
     &  1.5,1.2,0.9,0.8,0.6,
```